JNC TN8400 99-033

Hydrochemical Investigation and Status of Geochemical Modeling of Groundwater Evolution at the Kamaishi In-situ Tests Site, Japan

July 1999

Tokai Works
Japan Nuclear Cycle Development Institute

JNC TN8400 99-033
July, 1999

Hydrochemical Investigation and Status of Geochemical Modeling of Groundwater Evolution at the Kamaishi In-situ Tests Site, Japan

Hiroshi Sasamoto[1], Mikazu Yui[1], Randolph C Arthur[2]

Abstract

The results of hydrochemical investigations of groundwaters in the Kurihashi granodiorite at JNC's Kamaishi *in-situ* tests site indicate that these solutions are:

- meteoric in origin,
- chemically reducing (at depths greater than a few hundreds meters),
- relatively young [residence times in the Kurihashi granodiorite generally less than about 40 years, but groundwaters older than several thousand years BP (before present) are also indicated by preliminary carbon-14 dating of samples obtained from the KH-1 borehole],
- Ca-HCO_3 type solutions near the surface, changing to Na-HCO_3 type groundwaters with increasing depth.

The evolution of groundwater compositions in the Kurihashi granodiorite is modeled assuming local equilibrium for selected mineral-fluid reactions, taking into account the rainwater origin of these solutions. Results suggest it is possible to interpret approximately the "real" groundwater chemistry (i.e., pH, Eh, total dissolved concentrations of Si, Na, Ca, K, Al, carbonate and sulfate) in the Kurihashi granodiorite if the following assumptions are adopted:

- CO_2 concentration in the gas phase contacting pore solutions in the overlying soil zone $=10^{-2}$ bar,
- minerals in the rock zone that control the solubility of respective elements in the groundwater include; chalcedony (Si), albite (Na), kaolinite (Al), calcite (Ca and carbonate), microcline (K) and pyrite (Eh and sulfate).

Discussions with international experts suggest a systematic approach utilizing reaction-path models of irreversible water-rock interactions in open systems may be needed to more realistically model groundwater evolution at the Kamaishi test site. Detailed information characterizing certain site properties (e.g., fracture mineralogy) may be required to adequately constrain such models, however.

---

1) Japan Nuclear Cycle Development Institute, Tokai Works Japan
2) Monitor Scientific, L.L.C.*, Denver, Colorado USA (**formerly QuantiSci Inc.*)

JNC TN8400 99-033
１ ９ ９ ９ 年 ７ 月

釜石原位置試験場における地下水水質の調査および地下水の地球化学モデリングに関する現状（研 究 報 告）

笹本 広[1)]，油井三和[1)]，Randolph C Arthur[2)]

要 旨

釜石鉱山における原位置試験は，主に栗橋花崗岩閃緑岩を対象として行われた。栗橋花崗閃緑岩中の地下水の地球化学的調査により，主に以下の点が明らかになった。

- 地下水の起源は，降水である。
- 深部の地下水は，還元性である。
- ほとんどの地下水にはトリチウムが検出されることから，これらの地下水の滞留時間は長くとも 40 年程度である。一方，KH-1 孔の地下水にはトリチウムが検出されず，予察的な ^{14}C年代測定から，数千年程度の年代が示唆される様な，より古い地下水が存在すると推定される。
- 比較的浅部の地下水は $Ca\text{-}HCO_3$ 型であるが，より深部になると $Na\text{-}HCO_3$ 型になるような深度方向での水質タイプの変化が認められる。

上記の様な地球化学的特性を示す栗橋花崗閃緑岩中の地下水に関して，地下水の起源と地下水－岩石反応の進展を考慮した地球化学平衡モデルをもとに，地下水水質のモデル化を試みた。その結果，土壌中での炭酸分圧の値，岩体中での以下の鉱物を平衡と仮定することで地下水の pH，Eh および主要イオン（Si，Na，Ca，K，Al，炭酸および硫酸）濃度について，実測値をほぼ近似することができた。

- 土壌中での炭酸分圧：$\log PCO_2 = -2.0$
- 岩体中での平衡鉱物：玉随（Si 濃度），アルバイト（Na 濃度），カオリナイト（Al 濃度），方解石（Ca および炭酸濃度），マイクロクリン（K 濃度），黄鉄鉱（硫酸濃度，Eh）

また，海外の専門家との議論により，釜石サイトにおける，より現実的な地下水変遷モデルを構築するためには，開放系での不可逆的な岩石－水反応に関して，反応経路モデルを用いたシステマティックなアプローチを適用することが必要であると考えられた。さらに，モデルの妥当性を示すためには，釜石サイトの地質情報に関して，より詳細なデータ（例えば，割れ目充填鉱物に関する詳細なデータ等）も必要である。

---

1) 核燃料サイクル開発機構，東海事業所

2) Monitor Scientific, L.L.C., Denver, Colorado USA

Table of Contents

List of Tables

List of Figures

List of Appendices

1. BACKGROUND

Candidate sites for the geological disposal of high level radioactive waste (HLW) have not yet been selected in Japan. The Japan Nuclear Cycle Development Institute (*JNC*[1]) has nevertheless carried out field studies to characterize the hydrogeology and hydrochemistry of several types of geologic environments that are representative of subsurface conditions in this country. These "*in-situ* tests sites" include granodioritic host rocks (Kamaishi site), granitic host rocks and overlying Tertiary sediments (Tono site), Pliocene-aged mudstones and sandstones (Horonobe site), and intercalated mudstones and volcaniclastic sediments (Mobara site – not strictly an *in-situ* tests site, but rather an area investigated as a natural analogue of engineered barrier materials). The objectives of these studies include *characterization* of actual geochemical conditions in potential repository host rocks, and *testing* of equilibrium-based geochemical models of groundwater chemistry and evolution in relation to the actual behavior of real groundwater systems. Such testing is needed to assess the reliability of groundwater evolution models supporting the H-12 performance assessment.

The results of such testing for conditions at the Kamaishi site are described in this report. The modeling approach used and results obtained are presented in Section 2. A summary of discussions between JNC staff and international experts concerning the modeling approach and interpretation of results is summarized in Section 3.

---

[1] *JNC* was established in October 1998 to carry out R&D functions formerly assigned to the Power Reactor and Nuclear Fuel Development Corporation (*PNC*)

2. GEOCHEMICAL MODELS OF GROUNDWATER EVOLUTION

2.1 Introduction

Geochemical models of groundwater evolution were used by JNC to define four types of hypothetical, or "site-generic", groundwaters considered in the H-3 performance assessment of the disposal concept for HLW in Japan (PNC, 1992). Similar models (Yui et al., 1999) are used to define site-generic groundwaters considered in the updated H-12 performance assessment.

The models are based on the assumption that equilibrium is attained among mineral-fluid and homogeneous reactions that determine the composition of the site-generic groundwaters. Equilibrium conditions may be established, for example, if the flow rate of groundwater is sufficiently slow that there is time for the solution to equilibrate with coexisting minerals. The assumption may be unrealistic, however, if the flow rate is too high, in which case the composition of the groundwater will depend on both the flow rate and the rates of one or more mineral dissolution/precipitation reactions.

The present study addresses the validity of the equilibrium assumption in JNC's groundwater evolution models by comparing model predictions with *in-situ* geochemical conditions at the Kamaishi test site. JNC carried out *in-situ* tests at this site from 1988 to 1998 as a part of a geoscientific research program (Takeda and Osawa, 1993; PNC 1998). The main objectives of this program (JNC, 1999) were to:

- understand variations in geological conditions (e.g., geology, groundwater geochemistry, mechanical properties of the host rock) as a function of increasing depth, and to
- investigate the detailed characteristics of the excavated disturbed zone (EDZ) including, hydrogeochemical properties.

To address the first objective with regard to groundwater geochemistry, JNC collected numerous groundwater samples at various depths to reveal the depth-dependency of groundwater compositions at the Kamaishi site (Sasamoto et al., 1996). With regard to the second objective, JNC conducted an investigation of redox conditions in host rocks surrounding a drift as a part of the excavation disturbance experiment carried out at this site (Sasamoto et al., 1999a). As a result of these field studies, the mineralogy of the Kurihashi granodiorite was characterized, and the inorganic, organic and isotopic composition of associated groundwaters was determined. This set of mineralogic and groundwater data is used in the present study to test the equilibrium-based geochemical models of groundwater chemistry noted above.

2.2 Geological Setting

In-situ tests at the Kamaishi site were carried out in the abandoned Kamaishi iron-copper mine. The site is located approximately 600km north of Tokyo (Figure 1). The geology of the study area consists of Paleozoic and Cretaceous sedimentary rocks, the Ganidake granodiorite and the Kurihashi granodiorite (Figure 1). The *in-situ* tests were carried out mainly at the E.L. (Elevation Level) 550m drift and E.L.250m drift, both of which lie within the Kurihashi granodiorite. The age of the Kurihashi granodiorite is about 120 Ma (Kawano and Ueda, 1969).

Fracture mapping was conducted over a portion of the E.L. 250m drift in which the *in-situ* tests were carried out. Fracture properties, such as orientation, mineralogy of fracture-filling material, and widths of alteration zones (i.e., extending into the host rock from fracture surfaces) were characterized (Sasamoto et al., 1993). The distribution of 400 fractures characterized in this study are summarized in Appendix A. Three types of fractures are distinguished based on the presence or absence of fracture fillings and alteration zones (Osawa et al., 1995):

- Type A, single fracture with fracture fillings present,
- Type B, single fracture with fracture fillings and an altered zone present, and
- Type C, multiple fractures with fracture fillings and an altered zone present (see Appendix A-3).

Type B is the predominant type of fracture in this area, comprising > 60% of the total number of fractures. Rock-forming minerals in samples obtained from the E.L.250m drift were identified by XRD analysis (Osawa et al., 1995), and include the following:

- unaltered granodiorite; quartz, plagioclase, biotite > k-feldspar, hornblende, chlorite > sericite, sphene, magnetite,
- fracture fillings; calcite, stilbite > quartz, chlorite, laumontite > plagioclase, epidote > hornblende, sericite, prehnite, and
- altered zone; quartz, plagioclase, chlorite > k-feldspar, hornblende, sericite > calcite, epidote, sphene.

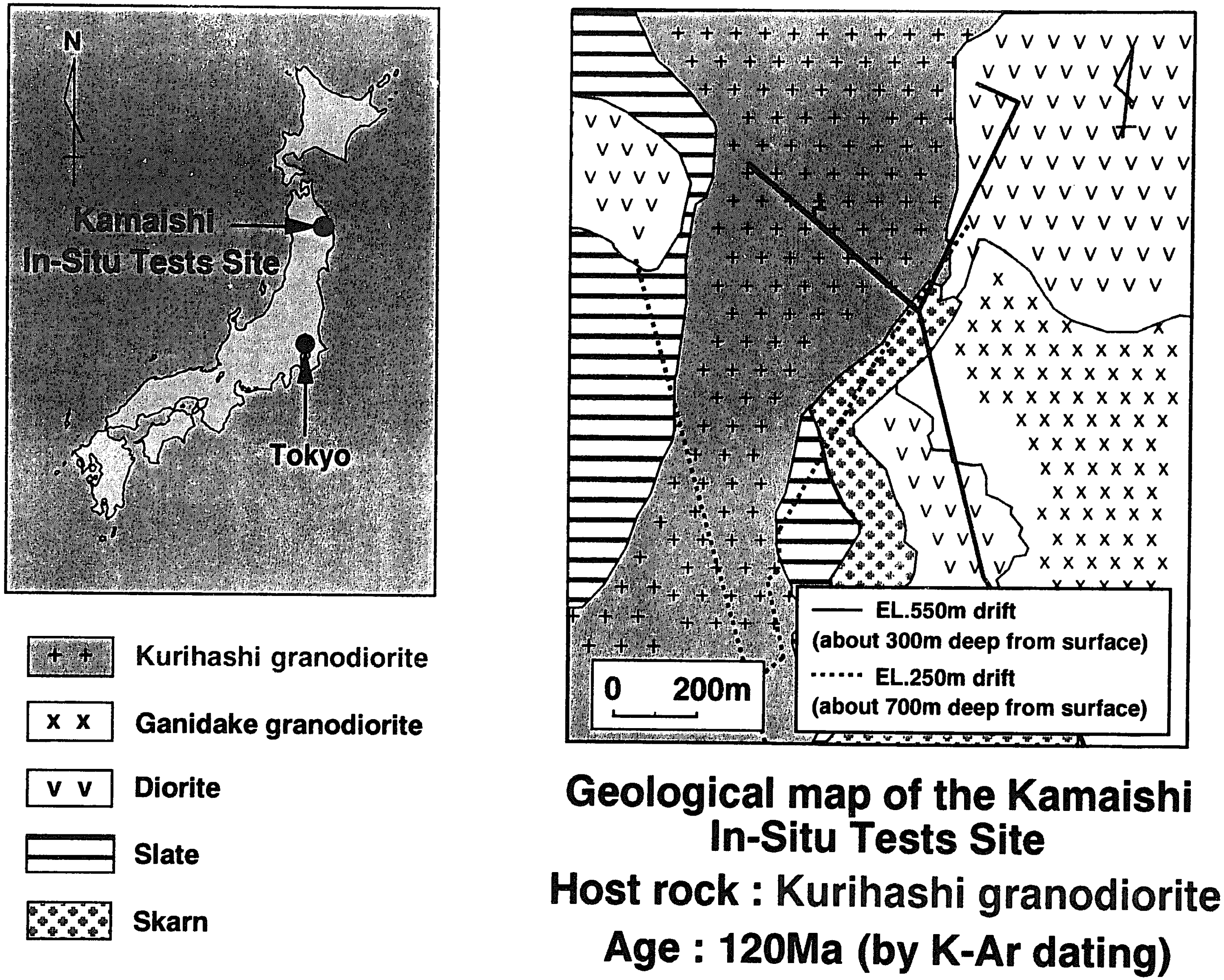

Figure 1 *: Location of the Kamaishi In-situ tests site and geology around Kamaishi mine. In-situ tests were carried out in the Kurihashi granodiorite.*

The Kamaishi mine, a scarn type iron-copper ore deposit, was mined out in 1993. The ore mineralogy included magnetite, pyrite, pyrrhotite and chalcopyrite. Other sulfide minerals (e.g., pyrite, pyrrhotite, chalcopyrite) are disseminated throughout the Kurihashi granodiorite (Hamabe and Kuwata, 1977).

2.3 Groundwater Chemistry

Hydrochemical investigations were carried out in conjunction with the *in-situ* tests at Kamaishi. The objectives of these investigations were to:

- identify the origin and age of the groundwater in the Kurihashi granodiorite,
- measure the chemical composition of groundwaters in the Kurihashi granodiorite from the surface to depths of several hundred meters, and
- interpret the geochemical evolution of groundwater in the Kurihashi granodiorite.

2.3.1 Sampling Locations

Surface water and groundwater samples were obtained from the following locations (Figure 2):

- surface water; sampled at the surface above the test area, and
- groundwater; sampled in existing drifts and boreholes

The drifts from which groundwater samples were obtained include the E.L.550m and E.L.250m drifts. The E.L.550m drift is located about 300m below the surface. Twenty two sampling locations were established in this drift (Appendix B-1). The E.L.250m drift is located about 700m below the surface. Nineteen sampling points were established in this drift (Appendix B-2). Photographs of the sampling locations and sampling method used in the E.L.250m drift are included in Appendix B-3.

The boreholes from which groundwaters were sampled include two deep boreholes: KH-1 and KG-1 (Figure 2). The KH-1 borehole was drilled to a depth of about 500m from the floor of the E.L.550m drift. The KG-1 borehole was drilled to a depth of about 800m from the ground surface.

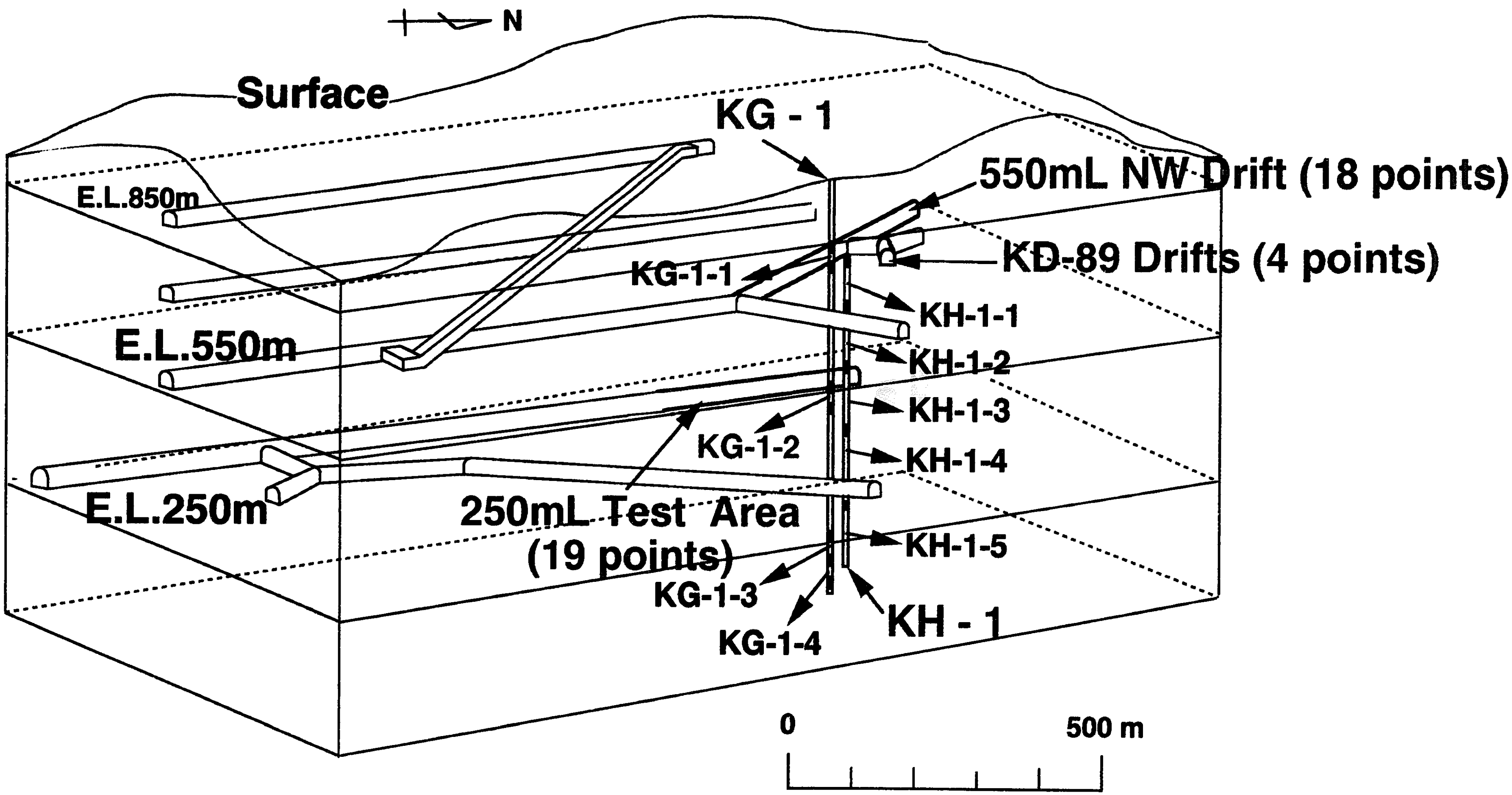

***Figure 2** : Sampling points of groundwaters in the Kurihashi granodiorite. The groundwater samples were collected at the existing dirfts (E.L.550m and E.L.250m) and boreholes (KH-1 and KG-1).*

2.3.2 Sampling Method

In the E.L.250m and E.L.550m drifts, groundwaters were sampled directly from water-bearing fractures intersecting the drift wall (Appendix B-3). Physico-chemical parameters [temperature, pH, Eh, Electrical Conductivity (EC), Dissolved Oxygen (DO)] were measured immediately after the samples were obtained. The chemical composition of the samples was analyzed later in the laboratory. In the KH-1 and KG-1 boreholes, groundwaters were sampled from packed off water-bearing fractures intersecting these boreholes. An MP system (Multiple-Piezometer monitoring system ; Black et al., 1986) was used to collect groundwater samples in the KG-1 borehole. The MP system [developed by Westbay Inc., Canada: Westbay Inc (1992); Appendix C] enables sampling of groundwaters under *in-situ* pressures from multiple sections of a borehole, which are sealed off by packers.

To account for contamination of groundwater samples by drilling fluids, which are introduced into the host rocks when the boreholes are drilled, variations in physico-chemical parameters (especially pH and EC) and solution compositions (especially Na^{+} and Ca^{2+}) were monitored in a series of batch samples taken over a period of time using a MOSDAX-2350 Probe. The physico-chemical parameters were measured immediately after sampling under an argon atmosphere (99.999%). The chemical composition of the samples was later analyzed in the laboratory.

The results of such monitoring of groundwaters sampled from section KG-1-2 [i.e., from G.L.(Ground Level) -489m to G.L.-495m] of the KG-1 borehole (Figure 2) are shown in Figures 3-1 to 3-4, for example (in Figure 3-2, the captions "Tono" and "Nittetsu" refer to laboratories in which the samples were analyzed). A lack of contamination of groundwater samples with drilling fluids is indicated when the physico-chemical parameters and composition of the samples become stable. At this time groundwaters were sampled for detailed analysis of their chemistry, gas composition and bacterial population.

2.3.3 Analytical Method

Groundwaters sampled from the E.L.250m and E.L.550m drifts, and from the KH-1 borehole, were analyzed for their chemical composition, concentrations of stable isotopes (δD, $\delta^{18}O$) and tritium concentration. Table 1 indicates the respective analytical methods, detection limits and analytical errors. Groundwaters sampled from KG-1 borehole were analyzed for chemical

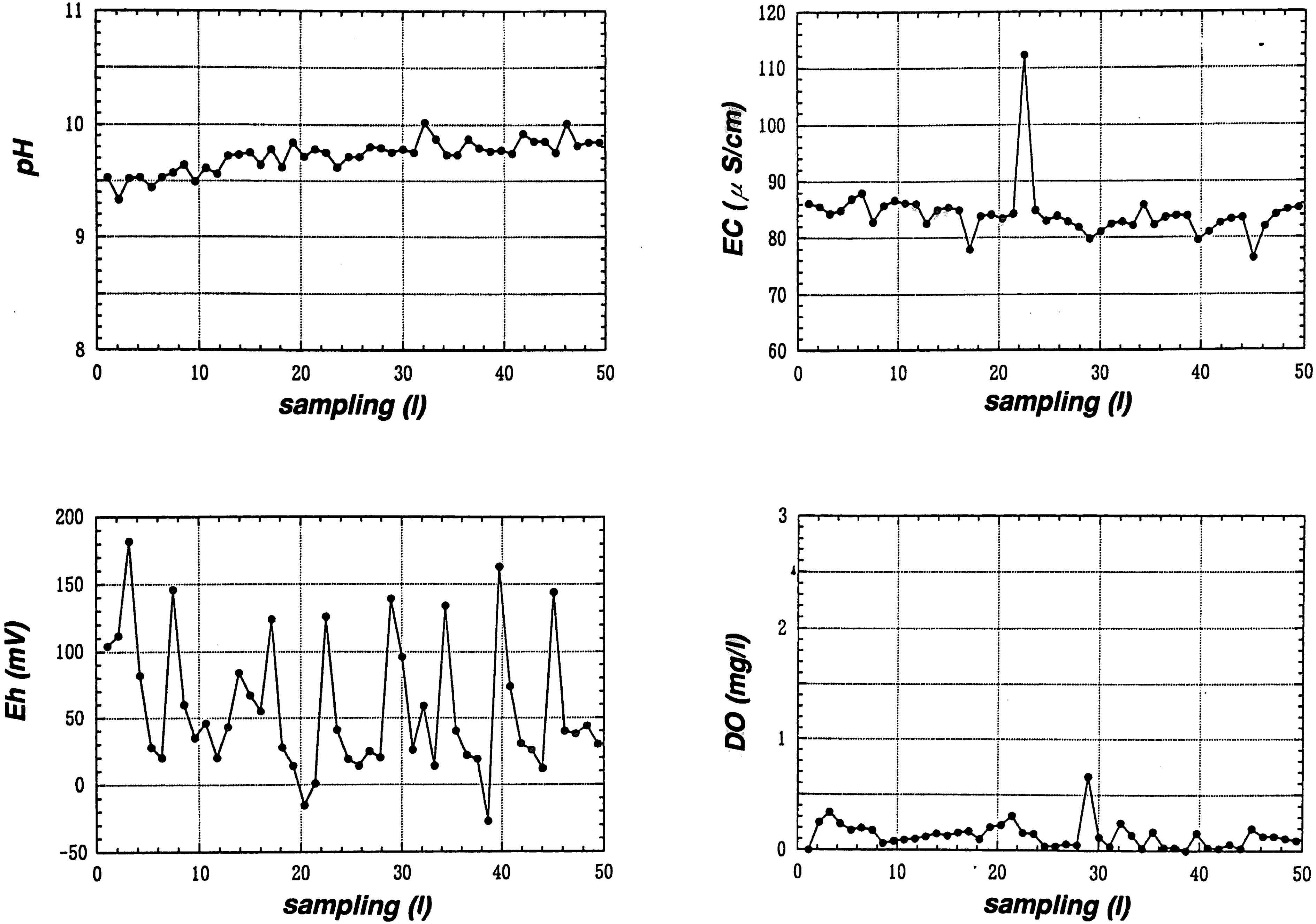

***Figure 3-1 :** Variation of physico-chemical parameters (pH, EC, Eh and DO) for sampling of KG-1-2 groundwater*

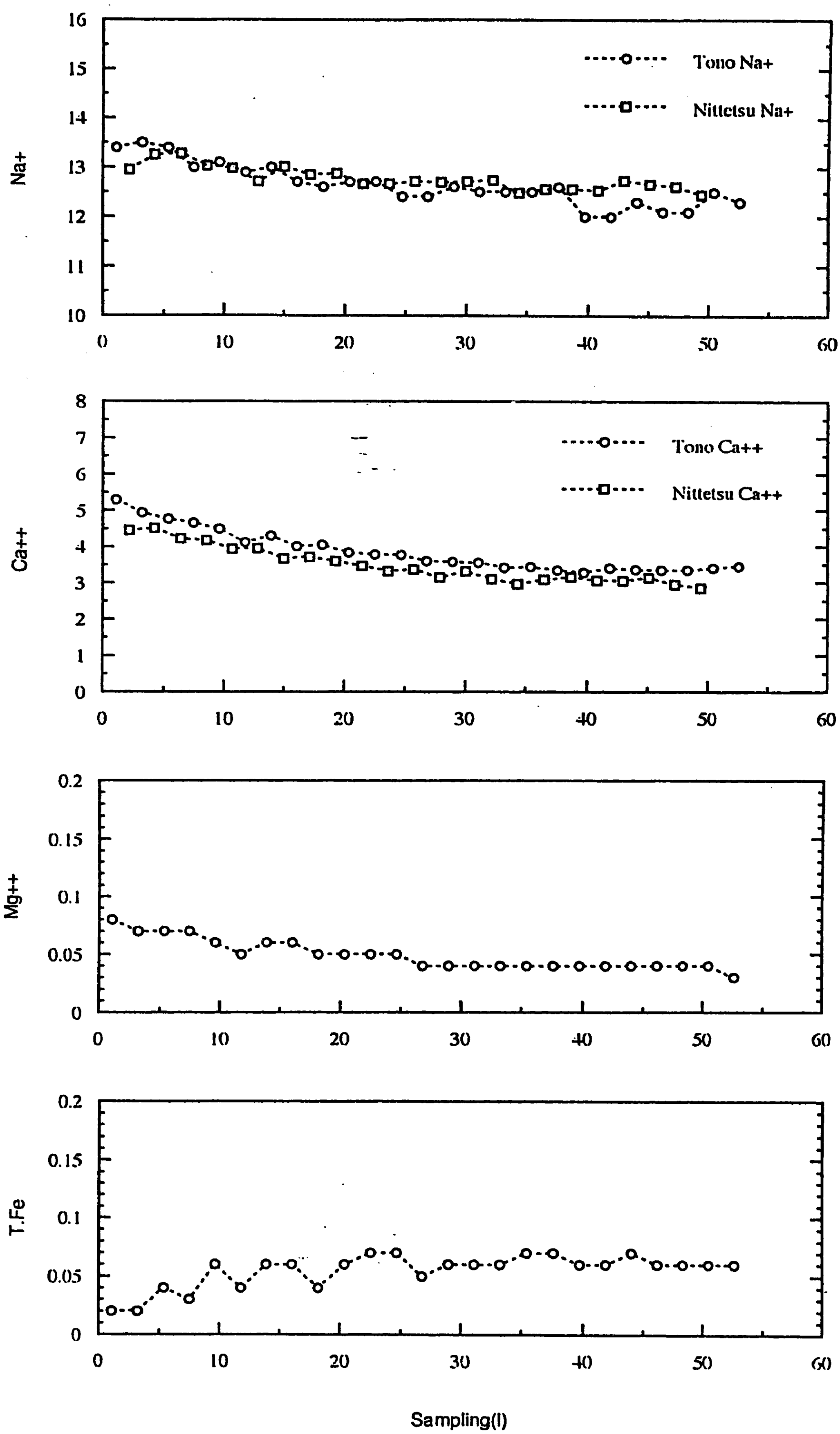

Figure 3-2 : Variation of groundwater chemical composition for sampling of KG-1-2 groundwater (1)

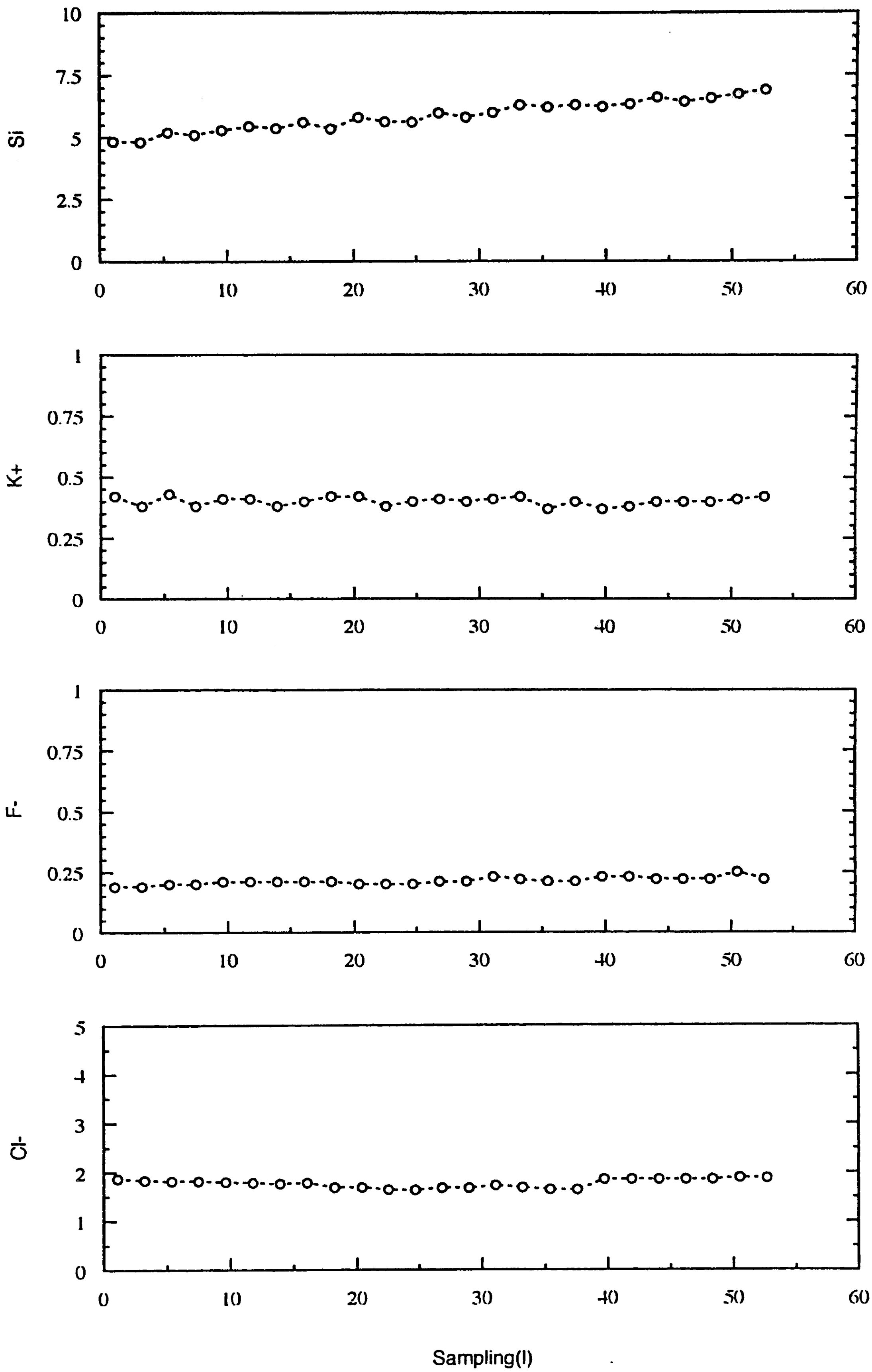

***Figure 3-3 :** Variation of groundwater chemical composition for sampling of KG-1-2 groundwater (2)*

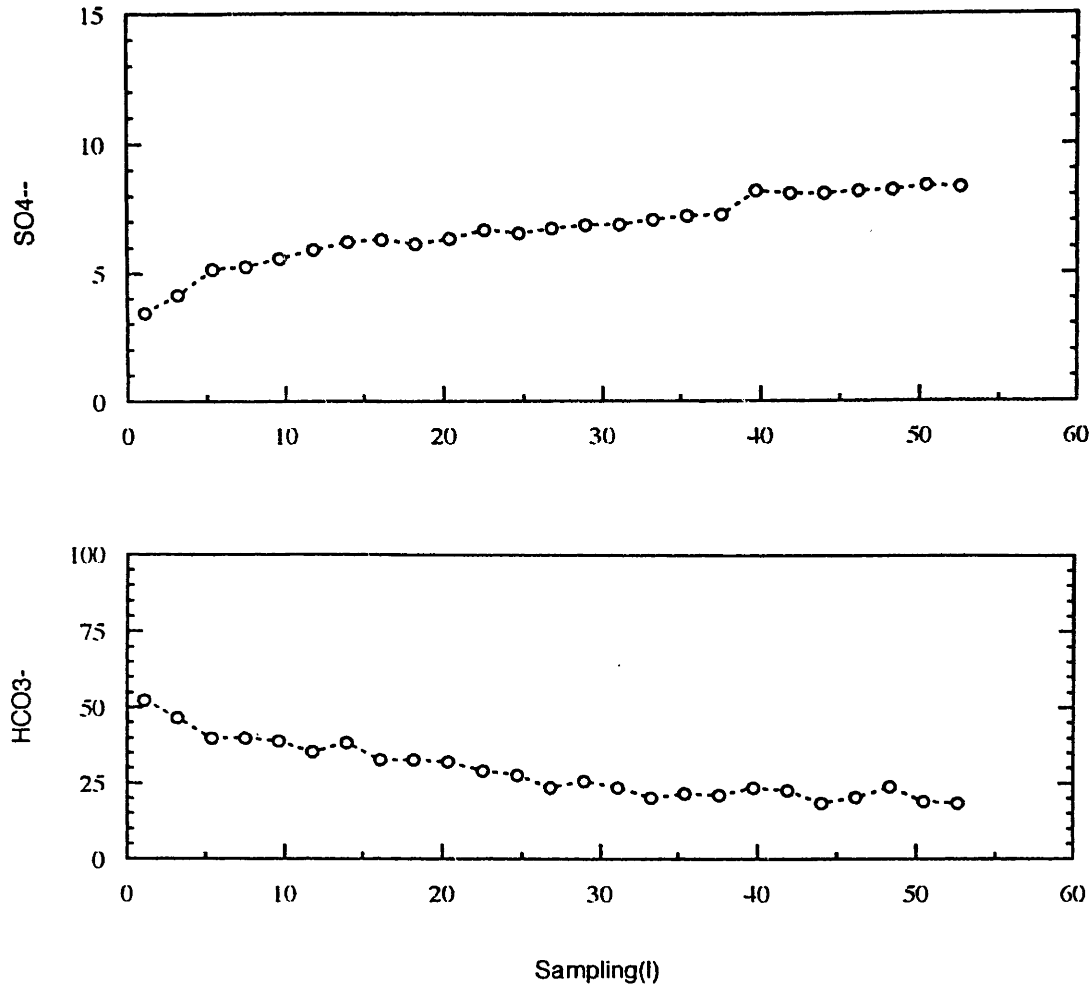

Figure 3-4 : *Variation of groundwater chemical composition for sampling of KG-1-2 groundwater (3)*

Table 1 *: Analytical method, detection limit and analytical error for the groundwater collected from existing drift and KH-1 borehole*

Items	Analytical Method	Detection Limit	Error
Temp.	Thermistor	-	±0.1℃
pH	Glass Electrode	-	±0.01
Eh	Pt Electrode	-	±5 mV
EC		-	3% in range
Na	AAS[1)]	0.01 ppm	1%
K	AAS	0.03 ppm	6%
Mg	ICP-AES[2)]	0.01 ppm	5-8 %
Ca	ICP-AES	0.01 ppm	0.4-2.3 %
Al	ICP-AES	0.1 ppm	1.5-3.5 %
Total Fe	ICP-AES	0.01 ppm	2-10 %
Fe^{2+}	Adsorption Photo	0.1 ppm	2-10 %
Si	ICP-AES (Filter)	0.1 ppm	1.3-2.8 %
Cl-	Ion Chromato	0.1 ppm	1-3 %
SO_4^{2-}	Ion Chromato	0.1 ppm	0.7-2.7 %
HCO_3^-	Calculated	-	-
CO_3^{2-}	Calculated	-	-
F-	Ion Chromato	0.05 ppm	0.30%
TOC[3)]	Infrared Adsorp	0.5 ppm	10%
IC[4)]	Infrared Adsorp		10%
δD		-	±1.5 ‰
δ^{18}O		-	±0.16 ‰
Tritium		0.3 T.U.	±0.2 T.U.

1) : AAS (Atomic Adsorption Spectroscopy)
2) : ICP- AES (Inductively Coupled Plasma - Atomic Emission Spectroscopy)
3) : TOC (Total Organic Carbon)
4) : IC (Inorganic Carbon)

** : $HCO3^-$ and CO_3^{2-} are calcuted by using the pH value of groundwater and result of IC. The detailed caluculation strategy is indicated in Appendix D* composition, stable isotope content, dissolved gases and bacterial population. Table 2 shows the respective analytical methods, detection limits and analytical errors for these samples.

Analytical results are tabulated in Tables 3-1 to 3-3, and in Table 4. As can be seen, total anion concentrations in all the samples are less than 3.0 meq/L. In such cases, groundwater analyses are considered to be reliable if the difference between the total cation concentration and total anion concentration is within ±0.2 meq/L (Friedman and Erdmann, 1982). The results of such charge-balance calculations for all the groundwater samples analyzed in this study are shown in Figure 4. As can be seen, most of the groundwater analyses are compatible with the acceptable charge-balance error of ±0.2 meq/L. These analyses were therefore accepted as being reliable.

2.3.4 Origin of the Groundwater

Figure 5 shows δD and $\delta^{18}O$ values measured in surface waters and groundwaters at the Kamaishi site. Craig (1961) notes that δD and $\delta^{18}O$ values in precipitation generally plot along a straight line in such figures, with $\delta D = 8\delta^{18}O + 10$ (referred to as the global meteoric line). Matsubaya (1985) describes two such lines ($\delta D = 8\delta^{18}O + 10$ and $\delta D = 8\delta^{18}O + 20$) and notes that δD and $\delta^{18}O$ values in samples of precipitation from Japan generally plot between them over a range of δD values from -40 to -100‰. The former line (equivalent to the global meteoric line) corresponds to the precipitation line for the Pacific Ocean side of Japan. The latter line is defined by precipitation falling on the Sea of Japan side of Japan. The δD and $\delta^{18}O$ values in samples of precipitation from Ryori (about 30 km south of Kamaishi) plot between these lines [$8\delta^{18}O + 13.59$; (IAEA, 1986)], as do most δD and $\delta^{18}O$ values measured in Kamaishi groundwaters. This suggests that Kamaishi groundwaters are meteoric in origin.

The δD and $\delta^{18}O$ values of some KH-1 groundwaters are lighter than those of other groundwaters and surface waters at Kamaishi (Figure 5). This suggests that either

- the KH-1 groundwaters are considerably older than other groundwaters at this site [e.g., several thousand years BP (before present)], and originated as rain water precipitated under colder climatic conditions than exist at present, or
- the KH-1 groundwaters are not older than other groundwaters (e.g., a few hundred years BP); they originated as rain water precipitated under climatic conditions similar to present-day conditions, but at higher altitudes than other groundwaters at this site.

***Table 2** : Analytical method, detection limit and analytical error for the groundwater collected from KG-1 borehole*

Analytical Items	Analytical Method	Detection Limit	Analytical Error (%)		
			KG-1-2 GL-489〜-495m	KG-1-3 GL-740〜-747m	KG-1-4 GL-785〜791m
Temp.	Thermistor	-	±0.1℃	±0.1℃	±0.1℃
pH	Glass Electrode	-	±0.01	±0.01	±0.01
Eh	Pt Electrode	-	±5mV	±5mV	±5mV
EC		-	3% in range	3% in range	3% in range
DO					
O2(g)	GC(TCD)/P&T	0.4	-		
N2(g)	GC(TCD)/P&T	0.5	-	1.1	1.8
H2(g)	GC(TCD)/P&T	0.03	-	4.3	5.2
He(g)	GC(TCD)/P&T	0.03	-	6.6	6.1
CH4(g)	GC(FID)/P&T	0.005	-		
CO(g)	GC(FID)/ReduceHS	0.05	-		
ΣCO2(g)	Infrared Adsorption	0.1	-	2.3	2.4
T-Si	ICP	0.1	0.38	0.53	0.73
D-Si	ICP	0.1	0.25	0.32	0.81
SiO2(T-Si)	ICP				
Na+	Atomic Adsorption	0.08	0.62	0.42	0.21
K+	Atomic Adsorption	0.05	0.43	0.67	0.66
Li+	Atomic Adsorption	0.09			
Ca++	ICP	0.04	1.40	0.65	0.24
Mg++	ICP	0.08	1.30	1.00	0.89
Sr++	ICP	0.005	0.71	1.50	0.91
Al+++	ICP	0.04	0.61	0.59	0.88
T-Mn	ICP	0.01			
D-Mn	ICP	0.01			
T-Fe	ICP	0.001	1.40	1.10	0.87
D-Fe	ICP	0.001	0.60	0.89	1.00
Fe++	Absorption Photometry	0.001	2.10	2.10	
Cl-	Ion Chromatography	0.09	0.22	0.89	0.75
F-	Ion Chromatography	0.03	2.50	0.64	1.00
Br-	Ion Chromatography	0.07			
I-	Ion Chromatography	0.06			
ΣS--	Titration	0.9			
T-P					
PO4---(P)	Absorption Photometry	0.0001	0.82	0.82	0.54
SO4--	Ion Chromatography	0.1	0.40	0.38	0.65
HCO3-	Calculated Value	-	-	-	-
CO3--	Calculated Value	-	-	-	-
T-N					
NO2-(N)		0.0001			
NO3-(N)		0.005			
NH4+(N)	Absorption Photometry	0.005	0.76	0.74	0.84
TC	-	-	-	-	-
IC	Infrared Adsorption	0.14	2.3	2.3	2.4
TOC	Infrared Adsorption	0.14	0.70	0.53	0.82
Humic acid	Fluorescent Photometry	0.5			
Fulvic acid	Fluorescent Photometry	1.0			
δD	Mass Spectrometry	-	±2‰	±2‰	±2‰
δ18-O	Mass Spectrometry	-	±0.2‰	±0.2‰	±0.2‰
3-H	Liquid Scintillation	-	±0.1	±0.1	±0.1
Total number of B.	AODC	-	-	-	-
Ferrooxidans	MPN	-	-	-	-
SRB	MPN	-	-	-	-
Methanobacterium	MPN	-	-	-	-
Nitro Reducing B.	MPN	-	-	-	-
Denitrification B.	MPN	-	-	-	-

[*Explanation of the abbreviation in Table 2*]

- *"GC(TCD)/P&T"* is abbreviation of *"Gas Chromatography (Thermal Conductivity Detector) / Purge and Trap"* method.
- *"GC(FID)/P&T"* is abbreviation of *"Gas Chromatography (Flamed Ionization Detector) / Purge and Trap"* method.
- *"ΣCO2(g)"* means same as *"IC ; Inorganic Carbon"*. The dissolved CO2(g) in groundwater is measured by infrared absorption method as IC.
- *"T-Si"* means *"Total Silica (dissolved silica + colloidal silica)"*.
- *"D-Si"* means *"Dissolved Silica"*.
- *"SiO2(T-Si)"* means converted value from *"T-Si"* as SiO2.
- *"T-Mn"* means *"Total Mangan (Mn2+ and other valence Mn)"*.
- *"D-Mn"* means *"Dissolved Mangan (mainly Mn2+)"*.
- *"T-Fe"* means *"Total Iron (Fe2+ and Fe3+)"*.
- *"D-Fe"* means *"Dissolved Iron (mainly Fe2+)"*.
- *"ΣS--"* means *"Total dissolved Sulfide (H2S, HS-, S--)"*.
- *"PO4--- (P)"* means *"Total dissolved Phosphate"*.
- *"T-N"* means *"Total dissolved Nitrogen"*.
- *"NO2-(N)"* means *"dissolved N as NO2-"*.
- *"NO3-(N)"* means *"dissolved N as NO3-"*.
- *"NH4+(N)"* means *"dissolved N as NH4+"*.
- *"δD"* and *"δ18O"* are calculated as follows :

  $\delta D = [(D/H)_{sample} / (D/H)_{SMOW}] \times 1000‰$

  $\delta 18O = [(18O/16O)_{sample} / (18O/16O)_{SMOW}] \times 1000‰$

  where, $(18O/16O)_{sample}$ and $(D/H)_{sample}$ are stable isotope ratio of oxygen and hydrogen in groundwater sample, on the other hand, $(18O/16O)_{SMOW}$ and $(D/H)_{SMOW}$ are stable isotope ratio of oxygen and hydrogen in SMOW (Standard Mean Oceanic Water).
- *"3-H"* means concentration of tritium.
- *"Total number of B"* means *"Total number of Bacteria"*.
- *"SRB"* is abbreviation of *"Sulfate Reducing Bacteria"*.
- *"MPN/ml"* means *"bacteria number measured by MPN method"*.
- *"AODC"* and *"MPN"* are abbreviation of bacteria analysis. These are the following mean, respectively.

  "AODC" : Acridine Orange stained Direct Counts method

  "MPN" : Most Probable Number method

And also, HCO_3^- and CO_3^{2-} were calculated based on the results of pH measurement and IC analysis (see Appendix D).

Table 3-1 : Results of measurement for physico-chemical parameters, chemical composition and stable-radioactive isotope of surface waters and groundwaters in the Kurihashi granodiorite (1)

Sample	Location	Altitude (m)	Date	Sampling method	Laboratory	Temp (℃)	pH	ORP (mV)	Eh (mV)	EC (μS/cm)	Na+ (ppm)	K+ (ppm)	Mg+ (ppm)	Ca+ (ppm)
S-1	surface	815	901120	Normal	Nittetsu	9.0	6.1	252	470	18.0	2.50	0.60	0.40	1.80
S-2	surface	650	901120	Normal	Nittetsu	8.5	5.8	214	432	20.5	2.70	0.50	0.30	2.70
S-3	surface	588	901120	Normal	Nittetsu	9.3	5.3	218	436	22.5	2.70	0.70	0.40	2.30
S-4	surface	800	901120	Normal	Nittetsu	9.5	6.3	260	477	25.1	2.80	0.70	0.70	3.30
Aonoki	surface	785	920831	Normal	Nittetsu	-	7.4	-	-	33.0	3.10	0.90	0.50	2.90
88W01	550m NWdrift	575	881212	Normal	Nittetsu	12.3	8.2	261	476	77.3	6.20	0.80	0.10	10.30
88W02	550m NWdrift	575	881212	Normal	Nittetsu	12.1	8.2	266	481	76.9	7.00	0.90	0.00	9.50
88W03	550m NWdrift	575	881212	Normal	Nittetsu	11.9	8.5	275	491	81.0	6.20	0.70	0.10	11.00
88W04	550m NWdrift	575	881212	Normal	Nittetsu	12.2	8.4	294	509	77.2	5.90	0.60	0.10	12.10
88W05	550m NWdrift	575	881212	Normal	Nittetsu	11.9	7.7	260	476	73.7	6.90	0.70	0.00	9.20
88W06	550m NWdrift	575	881212	Normal	Nittetsu	12.0	7.4	266	482	77.2	8.90	0.60	0.00	7.90
88W07	550m NWdrift	575	881212	Normal	Nittetsu	12.2	9.3	180	395	78.2	8.40	0.70	0.00	7.90
88W08	550m NWdrift	575	881215	Normal	Nittetsu	12.1	7.7	257	472	81.3	11.10	0.60	0.00	7.60
88W09	550m NWdrift	575	881213	Normal	Nittetsu	11.9	9.0	206	422	65.8	10.40	0.50	0.00	4.50
88W10	550m NWdrift	575	881213	Normal	Nittetsu	11.9	8.9	230	446	64.0	9.20	0.50	0.00	5.20
88W11	550m NWdrift	575	881213	Normal	Nittetsu	11.6	9.2	245	461	64.7	8.80	0.50	0.00	5.50
88W12	550m NWdrift	575	881213	Normal	Nittetsu	11.5	8.4	243	459	69.9	9.90	0.40	0.00	6.50
88W13	550m NWdrift	575	881213	Normal	Nittetsu	11.5	8.0	261	477	61.2	4.50	0.60	0.30	8.30
88W14	550m NWdrift	575	881213	Normal	Nittetsu	11.3	8.5	261	477	63.1	6.50	0.50	0.00	7.20
88W15	550m NWdrift	575	881213	Normal	Nittetsu	10.8	8.4	255	471	72.3	4.80	0.60	0.20	10.30
88W16	550m NWdrift	575	881213	Normal	Nittetsu	10.5	8.0	277	494	79.8	5.90	0.70	0.10	10.50
88W17	550m NWdrift	575	881213	Normal	Nittetsu	11.0	8.3	274	490	81.0	5.50	0.90	0.20	10.80
88W18	550m NWdrift	575	881213	Normal	Nittetsu	10.9	8.8	266	484	75.7	6.00	0.90	0.30	9.20
KD-89 891021	550m KD-89	575	891021	Normal	Nittetsu	11.6	7.7	154	370	78.2	11.10	0.70	0.10	5.00
KD-89 891130	550m KD-89	575	891130	Normal	Nittetsu	11.7	8.5	175	391	80.8	9.40	0.60	0.00	6.30
KD-89 891110	550m KD-89	575	891110	Normal	Nittetsu	11.6	8.6	184	400	92.4	9.00	1.70	0.10	6.60
KD-89 891229	550m KD-89	575	891229	Normal	Nittetsu	11.6	8.7	192	408	90.6	8.80	1.00	0.20	6.90
KH-1-1 900425	2.01-101.17	524	900425	Packer	Nittetsu	12.4	9.3	-145	70	76.2	10.50	0.60	0.00	4.10
KH-1-1 901025	2.01-101.17	524	901025	Packer	Nittetsu	12.2	8.5	-12	203	81.6	10.10	0.60	0.00	4.10
KH-1-1 910129	2.01-101.17	524	910129	Packer	Nittetsu	11.3	8.6	68	284	74.4	11.10	0.50	0.00	4.00
KH-1-1 910725	2.01-101.17	524	910725	Packer	Nittetsu	-	-	-	-	-	12.30	0.50	0.00	3.80
KH-1-1 920817	2.01-101.17	524	920817	Packer	Nittetsu	13.0	8.5	107	322	82.0	11.20	0.60	0.00	4.40
KH-1-1 940208	2.01-101.17	524	940208	Packer	Nittetsu	-	-	-	-	-	11.90	0.60	0.00	4.40
KH-1-2 900425	102.25-236.41	406	900425	Packer	Nittetsu	12.3	10.1	-137	78	112.6	16.70	0.40	0.00	2.80
KH-1-2 901025	102.25-236.41	406	901025	Packer	Nittetsu	12.1	9.1	-15	200	96.9	15.70	0.30	0.00	2.80
KH-1-2 910129	102.25-236.41	406	910129	Packer	Nittetsu	11.9	9.1	7	223	96.2	16.60	0.30	0.00	2.80
KH-1-2 910725	102.25-236.41	406	910725	Packer	Nittetsu	-	-	-	-	-	16.50	0.30	0.00	2.50
KH-1-2 920817	102.25-236.41	406	920817	Packer	Nittetsu	13.6	8.9	-33	181	96.7	15.30	0.30	0.00	3.00
KH-1-2 940208	102.25-236.41	406	940208	Packer	Nittetsu	-	-	-	-	-	16.80	0.30	0.00	3.10
KH-1-3 900425	237.49-337.14	288	900425	Packer	Nittetsu	12.4	10.2	-139	76	111.5	17.00	0.40	0.00	2.70
KH-1-3 901025	237.49-337.14	288	901025	Packer	Nittetsu	12.2	8.9	25	240	94.8	15.80	0.30	0.00	2.70
KH-1-3 910129	237.49-337.14	288	910129	Packer	Nittetsu	12.0	9.1	-18	198	95.4	15.60	0.30	0.00	2.80
KH-1-3 910725	237.49-337.14	288	910725	Packer	Nittetsu	-	-	-	-	-	16.80	0.40	0.00	2.60
KH-1-3 920817	237.49-337.14	288	920817	Packer	Nittetsu	13.3	8.6	-83	132	96.9	12.70	0.40	0.00	3.40
KH-1-3 940208	237.49-337.14	288	940208	Packer	Nittetsu	-	-	-	-	-	16.60	0.40	0.00	2.70
KH-1-4 900425	338.22-410.94	201	900425	Packer	Nittetsu	12.5	9.3	-197	18	111.1	18.70	0.60	0.00	2.40
KH-1-4 901025	338.22-410.94	201	901025	Packer	Nittetsu	12.3	8.8	-8	207	106.0	17.80	0.60	0.00	2.70
KH-1-4 910129	338.22-410.94	201	910129	Packer	Nittetsu	12.2	9.1	-57	158	95.2	18.90	0.50	0.00	2.80
KH-1-4 910725	338.22-410.94	201	910725	Packer	Nittetsu	-	-	-	-	-	18.90	0.60	0.00	2.60
KH-1-4 920817	338.22-410.94	201	920817	Packer	Nittetsu	13.2	8.8	-99	116	107.1	16.60	0.60	0.00	3.20
KH-1-4 940208	338.22-410.94	201	940208	Packer	Nittetsu	-	-	-	-	-	19.30	0.60	0.00	2.60
KH-1-5 900425	412.02-500.00	119	900425	Packer	Nittetsu	12.7	9.7	-151	64	143.9	24.50	0.80	0.00	5.70
KH-1-5 901025	412.02-500.00	119	901025	Packer	Nittetsu	12.3	9.2	-31	184	134.0	20.30	0.70	0.00	4.50
KH-1-5 910129	412.02-500.00	119	910129	Packer	Nittetsu	12.0	9.3	-98	118	128.3	21.00	0.50	0.00	4.70
KH-1-5 910725	412.02-500.00	119	910725	Packer	Nittetsu	-	-	-	-	-	20.80	0.50	0.00	4.40
KH-1-5 920817	412.02-500.00	119	920817	Packer	Nittetsu	13.1	9.0	-141	74	135.1	20.40	0.50	0.00	5.30
KH-1-5 940208	412.02-500.00	119	940208	Packer	Nittetsu	-	-	-	-	-	21.30	0.50	0.00	3.90
KG-1-1 921221	GL-222~GL-226	560	921221	MP55 (HGP-10)	Nittetsu	11.0	9.4	261	477	129.4	11.40	1.10	0.20	5.00
KG-1-2 921211	GL-489~GL-495	293	921211	MP55 (HGP-10)	Nittetsu	14.4	9.8	-390	-176	122.0	9.40	1.10	0.20	3.50
KG-1-2 941118	GL-489~GL-495	293	941118	MP55 (MOSDAX)	DOWA	13.2	10.0	127	342	81.0	11.00	0.60	0.00	6.30
KG-1-3 921126	GL-740~GL-747	41	921126	MP55 (HGP-10)	Nittetsu	17.7	10.1	-241	-30	105.6	13.70	1.20	0.10	3.70
KG-1-3 941202	GL-740~GL-747	41	941202	MP55 (MOSDAX)	DOWA	10.9	9.3	129	345	106.0	17.30	0.60	0.10	7.20
KG-1-4 950121	GL-785~GL-791	-4	950121	MP55 (MOSDAX)	DOWA	11.1	9.0	142	358	118.0	14.70	0.80	0.30	6.80
W1-9 (TK24)	250m drift	258	930901	Normal	PNC TONO	14.1	9.5	-203	11	81.6	6.70	0.20	<0.01	8.10
W1-10 (TK24)	250m drift	258	931018	Normal	Nittetsu	14.7	9.9	19	233	78.0	4.90	0.20	0.00	8.50
W1-12 (TK24)	250m drift	258	931209	Normal	PNC TONO	15.5	9.6	33	246	77.0	5.60	0.20	0.00	7.60
W1-12 (TK24)	250m drift	258	931215	Normal	Nittetsu	15.3	9.5	10	223	78.4	5.70	0.20	0.00	8.40
W1-1 (TK24)	250m drift	258	940105	Normal	Nittetsu	14.7	9.4	-83	131	78.6	5.80	0.20	0.00	8.70
W1-1 (TK24)	250m drift	258	940126	Normal	PNC TONO	-	-	-	-	-	6.20	0.10	0.00	8.30
W1-2 (TK24)	250m drift	258	940208	Normal	Nittetsu	15.4	9.6	-113	100	78.1	5.30	0.20	0.00	8.70
W1-3 (TK24)	250m drift	258	940309	Normal	Nittetsu	15.0	9.5	-210	3	78.2	5.80	0.20	0.00	8.50
W1-4 (TK24)	250m drift	258	940413	Normal	Nittetsu	15.0	9.6	-190	23	78.1	5.80	0.20	0.00	8.30
94-W1-10 (TK24)	250m drift	258	941013	Normal	Nittetsu	14.9	9.6	-313	-100	79.1	5.20	0.20	0.00	7.20
94-W1-11 (TK24)	250m drift	258	941116	Normal	Nittetsu	15.0	9.6	-255	-42	79.3	5.10	0.20	<0.02	8.30
94-W1-12 (TK24)	250m drift	258	941215	Normal	Nittetsu	15.4	9.6	-173	40	77.9	5.30	0.20	<0.02	8.20
95-W1-1 (TK24)	250m drift	258	950111	Normal	Nittetsu	15.2	9.6	-149	64	70.4	4.90	0.30	<0.02	5.90
95-W1-2 (TK24)	250m drift	258	950214	Normal	Nittetsu	15.4	9.5	-106	107	75.6	5.50	0.20	<0.02	8.40
95-W1-3 (TK24)	250m drift	258	950315	Normal	Nittetsu	15.4	9.6	-33	180	78.2	5.30	0.20	<0.02	8.20
W2-9	250m drift	258	930901	Normal	PNC TONO	15.0	8.7	109	322	77.2	10.40	0.30	0.00	5.00

Sample	Al+++ (ppm)	T.Fe (ppm)	Fe++ (ppm)	SiO2 (ppm)	Si++++ (ppm)	Cl- (ppm)	SO4-- (ppm)	HCO3- (ppm)	CO3-- (ppm)	F- (ppm)	TOC (ppm)	IC (ppm)	TC (ppm)	δD (‰)	δ18-O (‰)	3-H (T.U.)	Dissolved solid (mg/l)
S-1	-	-	-	10.50	-	1.70	-	11.60	0.00	-	-	-	-	-63.2	-9.9	7.6±0.2	-
S-2	-	-	-	9.40	-	2.60	1.90	10.40	0.00	-	-	-	-	-65.5	-9.5	7.5±0.2	30.50
S-3	-	-	-	10.00	-	3.10	2.00	10.40	0.00	-	-	-	-	-59.6	-9.4	7.6±0.2	31.60
S-4	-	-	-	12.90	-	2.50	1.70	15.20	0.00	-	-	-	-	-	-	-	39.80
Aonoki	-	-	-	14.80	-	2.40	0.20	21.00	0.00	-	-	-	-	-61.9	-10.2	7.0±0.1	45.80
88W01	-	-	-	11.60	-	2.70	6.60	32.60	0.30	-	-	-	-	-67.1	-10.7	11.6±0.2	70.90
88W02	-	-	-	11.60	-	2.50	5.80	28.70	0.20	-	-	-	-	-	-	-	66.00
88W03	-	-	-	11.30	-	2.30	6.00	34.90	0.60	-	-	-	-	-74.8	-10.5	10.7±0.2	72.50
88W04	-	-	-	11.70	-	2.60	6.30	39.10	0.40	-	-	-	-	-	-	-	78.40
88W05	-	-	-	11.40	-	2.00	6.00	33.90	0.00	-	-	-	-	-65.8	-10.6	10.2±0.2	70.10
88W06	-	-	-	11.10	-	2.20	5.70	34.50	0.00	-	-	-	-	-72	-10.7	10.4±0.2	70.90
88W07	-	-	-	10.80	-	2.10	6.70	24.50	2.20	-	-	-	-	-66.2	-10.5	8.6±0.2	61.10
88W08	-	-	-	12.20	-	1.60	5.40	40.10	0.00	-	-	-	-	-64	-10.4	9.2±0.2	78.60
88W09	-	-	-	11.40	-	1.60	4.20	26.20	1.10	-	-	-	-	-63.7	-10.6	7.9±0.2	58.80
88W10	-	-	-	12.10	-	1.50	5.50	32.10	1.10	-	-	-	-	-	-	-	66.10
88W11	-	-	-	11.80	-	1.60	5.30	21.20	1.10	-	-	-	-	-	-	-	54.70
88W12	-	-	-	10.90	-	1.50	5.30	31.20	0.30	-	-	-	-	-	-	-	64.70
88W13	-	-	-	14.00	-	1.50	5.30	27.50	0.10	-	-	-	-	-68.9	-10.4	9.0±0.2	62.00
88W14	-	-	-	13.00	-	1.60	5.00	28.30	0.40	-	-	-	-	-62.9	-10.7	10.1±0.2	62.10
88W15	-	-	-	14.10	-	2.00	5.80	32.60	0.30	-	-	-	-	-72.3	-10.7	9.1±0.2	70.40
88W16	-	-	-	13.00	-	2.00	6.50	34.10	0.10	-	-	-	-	-66.2	-10.2	13.9±0.2	72.80
88W17	-	-	-	13.00	-	2.20	6.10	40.00	0.00	-	-	-	-	-	-	-	78.70
88W18	-	-	-	12.60	-	2.40	6.20	32.40	0.90	-	-	-	-	-64.9	-10.3	13.0±0.2	70.00
KD-89 891021	-	-	-	11.50	-	2.00	7.90	32.20	0.10	-	-	-	-	-	-	-	70.50
KD-89 891130	-	-	-	10.60	-	1.80	8.90	30.50	0.40	-	-	-	-	-62.7	-10.6	8.3±0.2	68.10
KD-89 891110	-	-	-	11.90	-	1.80	8.50	32.40	0.60	-	-	-	-	-61.4	-10.4	8.9±0.2	72.00
KD-89 891229	-	-	-	11.00	-	1.80	11.30	28.70	0.60	-	-	-	-	-60.8	-10.4	9.5±0.2	69.70
																	0.00
KH-1-1 900425	-	-	-	10.50	-	2.40	6.40	28.10	2.50	-	-	-	-	-69.7	-10.5	5.6±0.1	62.60
KH-1-1 901025	-	-	-	10.90	-	2.10	7.70	27.40	0.50	-	-	-	-	-67.1	-9.9	4.3±0.1	62.90
KH-1-1 910129	-	-	-	11.10	-	2.40	9.30	22.00	0.40	-	-	-	-	-	-	-	60.40
KH-1-1 910725	-	-	-	11.00	-	2.00	7.50	-	-	-	-	-	-	-	-	-	-
KH-1-1 920817	-	-	-	10.80	-	2.10	7.30	23.00	0.50	-	-	-	-	-	-	-	59.40
KH-1-1 940208	<0.1	0.1	-	10.70	-	2.20	8.00	-	-	0.10	0.50	4.30	-	-	-	-	-
KH-1-2 900425	-	-	-	16.00	-	2.60	11.90	21.70	11.50	-	-	-	-	-76.8	-11.5	0.7±0.09	72.10
KH-1-2 901025	-	-	-	16.00	-	2.20	11.60	32.20	1.70	-	-	-	-	-76.5	-10.9	0.4±0.09	80.80
KH-1-2 910129	-	-	-	16.10	-	2.60	11.70	25.30	1.30	-	-	-	-	-	-	-	75.40
KH-1-2 910725	-	-	-	16.40	-	2.00	9.90	-	-	-	-	-	-	-	-	-	-
KH-1-2 920817	-	-	-	16.40	-	2.20	10.60	24.60	0.80	-	-	-	-	-	-	-	72.40
KH-1-2 940208	<0.1	0	-	15.10	-	2.50	9.40	-	-	0.20	0.50	3.50	4.00	-	-	-	-
KH-1-3 900425	-	-	-	14.30	-	2.50	12.50	20.10	12.60	-	-	-	-	-78.5	-11.6	0.6±0.09	69.50
KH-1-3 901025	-	-	-	15.20	-	2.20	10.20	33.30	1.10	-	-	-	-	-77.5	-10.9	<0.3	79.70
KH-1-3 910129	-	-	-	16.00	-	2.60	12.00	24.00	1.20	-	-	-	-	-	-	-	73.30
KH-1-3 910725	-	-	-	16.20	-	2.00	9.80	-	-	-	-	-	-	-	-	-	-
KH-1-3 920817	-	-	-	16.30	-	2.20	11.20	19.10	0.40	-	-	-	-	-	-	-	65.30
KH-1-3 940208	<0.1	0	-	14.80	-	2.40	9.70	-	-	0.20	0.50	3.70	4.20	-	-	-	-
KH-1-4 900425	-	-	-	10.60	-	2.40	13.00	35.60	3.20	-	-	-	-	-75.3	-11.6	1.8±0.1	83.30
KH-1-4 901025	-	-	-	18.50	-	2.20	12.80	34.50	0.90	-	-	-	-	-76.6	-11.5	0.6±0.09	89.10
KH-1-4 910129	-	-	-	18.70	-	2.60	14.20	26.60	1.40	-	-	-	-	-	-	-	84.30
KH-1-4 910725	-	-	-	18.90	-	1.90	11.80	-	-	-	-	-	-	-	-	-	-
KH-1-4 920817	-	-	-	19.00	-	2.10	13.00	25.90	0.70	-	-	-	-	-	-	-	80.40
KH-1-4 940208	<0.1	0	-	18.60	-	2.50	12.10	-	-	0.30	0.60	4.40	4.90	-	-	-	-
KH-1-5 900425	-	-	-	26.80	-	2.00	38.50	26.10	6.40	-	-	-	-	-78.5	-11.7	<0.3	124.40
KH-1-5 901025	-	-	-	26.30	-	1.90	25.80	29.50	2.00	-	-	-	-	-80.1	-11.7	<0.3	109.00
KH-1-5 910129	-	-	-	26.50	-	2.10	25.00	28.20	2.50	-	-	-	-	-	-	-	108.00
KH-1-5 910725	-	-	-	26.60	-	1.70	21.30	-	-	-	-	-	-	-	-	-	-
KH-1-5 920817	-	-	-	26.90	-	1.80	25.70	27.40	1.00	-	-	-	-	-	-	-	106.00
KH-1-5 940208	<0.1	0	-	25.40	-	2.20	21.40	-	-	0.40	0.50	3.30	3.80	-	-	-	-
KG-1-1 921221	<0.1	0.1	0.00	12.80	-	1.80	8.40	31.00	2.00	-	-	-	-	-61.1	-10.1	10.6±0.2	71.70
KG-1-2 921211	<0.1	0.2	0.00	12.40	-	2.30	5.60	23.00	4.00	-	-	-	-	-64.8	-10.6	5.3±0.1	57.50
KG-1-2 941118	0.3	0	0.00	16.30	7.60	1.90	8.90	28.40	6.90	0.20	0.40	7.00	7.40	-73	-11.1	2.8±0.1	73.40
KG-1-3 921126	<0.1	0	0.00	21.00	-	2.30	12.30	21.00	7.00	-	-	-	-	-62.1	-10.5	4.5±0.1	75.30
KG-1-3 941202	0.2	0	0.00	9.70	4.50	2.90	17.10	31.80	2.40	0.40	0.20	6.70	7.00	-73.1	-10.6	3.4±0.1	86.70
KG-1-4 950121	0.1	0	-	16.65	3.10	3.50	8.60	45.70	1.60	0.00	0.80	9.30	10.10	-67.5	-10.1	4.7±0.1	87.10
W1-9 (TK24)	<0.1	<0.02	-	16.10	7.50	2.00	7.30	15.40	1.81	0.10	1.00	3.40	4.40	-	-	-	-
W1-10 (TK24)	<0.1	<0.01	<0.01	14.50	6.80	1.80	12.70	11.40	2.80	<0.05	0.70	2.80	3.50	-69.5	-11.1	4.8±0.1	54.00
W1-12 (TK24)	<0.1	<0.02	-	15.60	7.30	2.20	13.50	10.64	1.52	0.10	1.50	2.40	3.90	-	-	-	44.70
W1-12 (TK24)	<0.1	0	<0.01	16.30	7.60	2.00	12.90	14.50	1.70	<0.05	0.50	3.20	3.70	-67.5	-10.8	6.6±0.4	60.00
W1-1 (TK24)	<0.1	0	<0.01	16.90	7.90	2.00	12.80	9.80	0.90	<0.05	0.70	2.10	2.80	-69.7	-11	5.2±0.3	56.20
W1-1 (TK24)	<0.1	<0.02	-	15.20	7.10	2.20	13.70	-	-	0.10	0.70	2.60	3.30	-	-	-	-
W1-2 (TK24)	<0.1	0	<0.01	16.90	7.90	2.40	12.70	10.20	1.50	0.10	0.80	2.30	3.10	-69.5	-10.5	5.8±0.3	56.40
W1-3 (TK24)	<0.1	<0.01	<0.01	16.70	7.80	2.10	12.70	10.90	1.30	0.10	0.60	2.40	3.00	-68.6	-10.8	5.2±0.3	56.90
W1-4 (TK24)	0.1	<0.01	<0.01	15.40	7.20	2.00	12.80	10.20	1.50	0.10	0.80	2.30	3.10	-78	-10.7	4.9±0.1	54.70
94-W1-10 (TK24)	<0.1	<0.3	<0.05	16.50	7.70	1.80	11.80	18.70	2.70	0.30	1.00	4.20	5.20	-66.2	-10.5	5.3±0.1	61.40
94-W1-11 (TK24)	<0.1	0.4	<0.05	16.50	7.70	1.80	11.60	19.30	2.80	0.20	0.90	4.40	5.30	-69.5	-10.9	5.3±0.1	-
94-W1-12 (TK24)	<0.1	<0.3	<0.05	14.80	6.90	1.60	11.80	21.50	3.10	0.30	0.60	4.90	5.40	-68.5	-10.7	5.4±0.1	-
95-W1-1 (TK24)	<0.1	<0.3	<0.05	15.50	7.20	2.00	12.80	12.30	1.80	<0.1	0.40	2.80	3.20	-69.7	-10.6	4.9±0.1	-
95-W1-2 (TK24)	<0.1	<0.3	<0.05	16.00	7.50	2.00	13.30	26.20	3.10	0.30	0.40	5.80	6.20	-70.2	-10.9	4.5±0.1	-
95-W1-3 (TK24)	<0.1	<0.3	<0.05	15.10	7.10	2.10	13.40	23.10	3.30	<0.1	0.40	5.20	5.60	-70.1	-10.9	5.2±0.1	-
W2-9	<0.1	<0.02	-	12.70	5.90	1.80	4.90	28.50	0.50	0.10	0.70	5.70	6.40	-	-	-	63.60

Table 3-2 : Results of measurements for physico-chemical parameters, chemical composition and stable-radioactive isotope of surface waters and groundwaters in the Kurihashi granodiorite (2)

Sample	Location	Altitude (m)	Date	Sampling method	Laboratory	Temp (℃)	pH	ORP (mV)	Eh (mV)	EC (μS/cm)	Na+ (ppm)	K+ (ppm)	Mg+ (ppm)	Ca+ (ppm)	Al+++ (ppm)	T.Fe (ppm)	Fe++ (ppm)	SiO2 (ppm)	Si++++ (ppm)	Cl- (ppm)	SO4-- (ppm)	HCO3- (ppm)	CO3-- (ppm)	F- (ppm)	TOC (ppm)	IC (ppm)	TC (ppm)	δD (‰)	δ18-O (‰)	3-H (T.U.)	Dissolved solid (mg/l)
W3-9	250m drift	258	930901	Normal	PNC TONO	14.2	9.0	87	3273	79.2	9.50	0.20	<0.01	6.00	<0.1	<0.02	-	11.90	5.60	1.70	4.00	27.50	1.00	0.40	1.00	5.60	6.60	-	-	-	60.81
W3-10	250m drift	258	931018	Normal	Nittetsu	15.2	9.7	128	341	76.9	9.90	0.20	0.00	6.20	<0.1	<0.01	<0.01	10.50	4.90	1.70	9.00	18.80	3.50	<0.05	1.50	4.40	5.90	-70.6	-10.8	10.0±0.2	56.30
W3-12	250m drift	258	931209	Normal	PNC TONO	15.3	9.1	151	364	75.1	8.40	0.30	<0.01	5.70	<0.1	<0.02	-	11.80	5.50	2.00	9.60			0.10	1.30	2.40	3.70	-	-	-	37.81
W3-12	250m drift	258	931215	Normal	Nittetsu	15.2	9.2	146	359	76.7	9.10	0.20	0.00	5.80	<0.1	<0.01	<0.01	12.40	5.80	1.80	9.00	23.50	1.30	<0.05	0.60	4.90	5.50	-64.9	-11	11.0±0.4	61.80
W3-1	250m drift	258	940105	Normal	Nittetsu	14.8	9.2	156	369	76.9	9.30	0.20	0.00	6.10	<0.1	<0.01	<0.01	12.80	6.00	1.70	8.60	20.10	1.20	<0.05	0.50	4.20	4.70	-70.9	-10.9	11.5±0.4	58.80
W3-1	250m drift	258	940126	Normal	PNC TONO	-	-	-	-	-	9.70	0.30	0.10	6.30	<0.1	<0.02	-	12.10	5.60	2.00	9.40	-	-	0.10	0.40	4.00	4.40	-	-	-	-
W3-2	250m drift	258	940208	Normal	Nittetsu	15.6	9.2	161	374	76.3	9.70	0.20	0.00	6.20	<0.1	<0.01	<0.01	12.60	5.90	1.90	8.60	22.10	1.30	0.10	1.00	4.60	5.60	-67.6	-10.5	10.6±0.4	61.30
W3-3	250m drift	258	940309	Normal	Nittetsu	15.1	9.2	85	298	77.8	9.40	0.20	0.00	6.00	<0.1	<0.01	<0.01	12.40	5.80	1.90	9.30	24.00	1.40	0.10	0.60	5.00	5.60	-68	-10.7	11.9±0.4	63.20
W3-4	250m drift	258	940413	Normal	Nittetsu	15.2	9.4	76	289	78.3	9.50	0.20	0.00	5.80	0.1	<0.01	<0.01	11.30	5.30	1.90	9.40	20.90	1.90	0.10	0.90	4.50	5.40	-68.2	-10.6	9.6±0.2	59.00
94-W3-10	250m drift	258	941013	Normal	Nittetsu	14.9	9.3	80	293	79.3	8.90	0.40	<0.02	5.30	<0.1	<0.3	<0.05	12.50	5.80	1.50	8.60	27.10	2.00	0.30	1.00	5.70	6.80	-64.6	-10.4	9.8±0.2	64.32
94-W3-11	250m drift	258	941116	Normal	Nittetsu	15.0	9.2	59	272	79.7	8.20	0.30	<0.02	6.10	<0.1	<0.3	<0.05	12.50	5.80	1.50	8.60	21.80	1.30	0.10	0.80	4.60	5.30	-68.4	-10.7	11.1±0.2	59.02
94-W3-12	250m drift	258	941215	Normal	Nittetsu	15.2	9.1	139	352	77.4	8.10	0.30	<0.02	6.00	<0.1	<0.3	<0.05	11.50	5.40	1.40	8.30	23.40	1.10	0.30	0.80	4.80	5.70	-66.8	-10.9	10.5±0.2	59.02
95-W3-1	250m drift	258	950111	Normal	Nittetsu	15.0	9.4	136	349	75.9	7.90	0.30	<0.02	5.90	<0.1	<0.3	<0.05	11.80	5.50	1.70	9.00	16.30	1.50	0.30	1.70	3.50	5.20	-68.4	-10.6	9.4±0.1	52.92
95-W3-2	250m drift	258	950214	Normal	Nittetsu	15.4	9.3	128	341	76.2	8.30	0.20	<0.02	6.20	<0.1	<0.3	<0.05	11.20	5.20	1.70	9.10	30.20	2.20	0.30	0.50	6.40	6.90	-68.8	-10.7	10.1±0.1	66.92
95-W3-3	250m drift	258	950315	Normal	Nittetsu	15.5	9.2	155	368	77.9	8.50	0.20	<0.02	6.00	<0.1	<0.3	0.40	11.40	5.30	1.90	9.90	30.10	1.70	0.40	0.50	6.30	6.70	-69.8	-10.8	10.5±0.2	68.02
95-W3-4	250m drift	258	950412	Normal	PNC TONO	15.1	9.5	119	332	78.4	9.50	0.30	<0.01	6.20	<0.1	<0.02	-	12.21	5.70	2.00	10.00	18.14	2.13	0.10	5.20	4.00	9.20	-	-	-	58.37
95-W3-5	250m drift	258	950517	Normal	PNC TONO	15.3	9.4	151	364	78.6	9.40	0.20	<0.01	6.10	<0.1	<0.02	-	12.00	5.60	1.80	9.30	21.36	1.96	0.10	2.70	4.60	7.10	-	-	-	60.17
W4-9	250m drift	258	930901	Normal	PNC TONO	14.2	8.2	136	350	75.9	9.40	0.20	<0.01	6.30	<0.1	<0.02	-	11.90	5.50	1.80	4.40	26.30	0.40	0.10	1.30	5.30	6.60	-	-	-	60.31
W4-1	250m drift	258	940126	Normal	PNC TONO	-	-	-	-	-	9.40	0.30	0.00	6.70	<0.1	<0.02	-	11.50	5.40	1.90	9.50	-	-	0.10	0.60	5.20	5.80	-	-	-	-
W5-9	250m drift	258	930901	Normal	PNC TONO	14.1	8.6	118	332	76.2	9.90	0.20	<0.01	6.20	<0.1	<0.02	-	12.70	5.90	1.80	4.60	26.70	0.40	0.10	1.20	5.40	6.50	-	-	-	62.11
W5-10	250m drift	258	931018	Normal	Nittetsu	15.0	9.7	125	338	76.1	7.90	0.20	0.00	6.30	<0.1	<0.01	<0.01	11.10	5.20	1.70	8.90	19.30	3.50	<0.05	0.70	4.50	5.20	-67.8	-10.8	9.6±0.2	55.40
W5-12	250m drift	258	931209	Normal	PNC TONO	15.6	8.7	187	400	73.2	8.80	0.30	<0.01	6.10	<0.1	<0.02	-	11.60	5.40	1.90	9.30	20.90	0.40	0.10	1.20	4.20	5.50	-	-	-	58.91
W5-12	250m drift	258	931215	Normal	Nittetsu	15.2	8.4	177	390	77.6	8.60	0.20	0.00	6.60	<0.1	0	<0.01	12.40	5.80	1.80	8.70	27.00	0.40	<0.05	0.50	5.40	5.90	-65.4	-10.9	12.4±0.4	65.30
W5-1	250m drift	258	940105	Normal	Nittetsu	14.7	8.7	181	395	79.9	8.90	0.20	0.00	6.50	0.1	0	<0.01	12.20	5.70	1.70	8.60	23.90	0.40	<0.05	1.00	4.80	5.80	-67.5	-10.7	11.8±0.4	62.00
W5-1	250m drift	258	940126	Normal	PNC TONO	-	-	-	-	-	9.50	0.30	0.00	6.70	<0.1	<0.02	-	11.40	5.30	2.00	9.50	-	-	0.10	0.80	4.90	5.70	-	-	-	-
W5-2	250m drift	258	940208	Normal	Nittetsu	15.7	8.7	183	396	77.6	8.60	0.20	0.00	6.80	<0.1	0	<0.01	12.60	5.90	1.90	8.70	26.90	0.50	0.10	1.20	5.40	6.60	-67.6	-10.6	10.9±0.4	65.70
W5-3	250m drift	258	940309	Normal	Nittetsu	15.3	8.0	159	372	77.4	8.80	0.20	0.00	6.40	<0.1	<0.01	<0.01	12.40	5.80	1.90	9.00	28.50	0.40	0.10	0.60	5.70	6.30	-68.8	-10.7	13.5±0.4	67.20
W5-4	250m drift	258	940413	Normal	Nittetsu	15.6	9.1	116	329	77.4	9.20	0.20	0.00	6.20	0.1	0	<0.01	11.80	5.50	1.90	9.20	22.80	1.10	0.10	0.90	4.70	5.60	-68.7	-10.6	10.4±0.2	61.30
W6-9	250m drift	258	930901	Normal	PNC TONO	14.0	9.0	93	307	76.7	10.90	0.20	<0.01	6.00	<0.1	<0.02	-	11.30	5.30	1.90	9.30	26.50	0.90	0.10	0.90	5.40	6.30	-	-	-	66.11
W7-9	250m drift	258	930901	Normal	PNC TONO	14.0	9.4	-1	213	83.1	10.60	0.20	<0.01	5.00	<0.1	<0.02	-	11.90	5.60	2.00	10.30	25.20	2.30	0.10	1.70	5.40	7.10	-	-	-	65.21
W7-12	250m drift	258	931209	Normal	PNC TONO	15.3	9.6	145	358	77.0	10.50	0.30	<0.01	5.00	<0.1	<0.02	-	12.30	5.80	2.00	10.40	17.30	2.50	0.10	1.40	3.90	5.30	-	-	-	57.81
W7-1	250m drift	258	940126	Normal	PNC TONO	-	-	-	-	-	11.30	0.20	<0.01	5.00	<0.1	<0.02	-	12.70	5.90	2.00	9.10	-	-	0.10	0.90	3.40	4.30	-	-	-	-
W8-9	250m drift	258	930901	Normal	PNC TONO	13.9	9.6	-9	205	77.1	9.60	0.20	<0.01	5.60	<0.1	<0.02	-	12.30	5.70	2.00	9.10	22.30	3.20	0.10	0.80	5.00	5.90	-	-	-	61.11
W8-10	250m drift	258	931018	Normal	Nittetsu	14.9	9.6	118	331	75.3	5.70	0.20	0.00	5.80	<0.1	<0.01	<0.01	10.90	5.10	1.60	8.40	19.50	2.80	<0.05	0.70	4.40	5.10	-69.2	-10.7	11.6±0.2	52.10
W8-12	250m drift	258	931209	Normal	PNC TONO	15.6	9.5	125	338	74.6	6.00	0.30	<0.01	5.20	<0.1	<0.02	-	12.20	5.70	2.00	9.00	17.20	2.00	0.10	0.30	3.80	4.10	-	-	-	51.91
W8-12	250m drift	258	931215	Normal	Nittetsu	15.6	9.5	96	309	76.1	8.90	0.20	0.00	6.00	<0.1	0	<0.01	13.00	6.10	1.80	8.20	19.50	2.30	<0.05	0.50	4.30	4.80	-64.8	-10.6	10.7±0.4	57.60
W8-1	250m drift	258	940105	Normal	Nittetsu	15.3	9.5	79	292	77.2	9.00	0.20	0.00	6.00	<0.1	0	<0.01	13.30	6.20	1.80	8.30	17.70	2.10	<0.05	0.50	3.90	4.40	-67.3	-10.9	9.9±0.4	56.30
W8-1	250m drift	258	940126	Normal	PNC TONO	-	-	-	-	-	9.70	0.20	<0.01	5.80	<0.1	<0.02	-	12.30	5.70	2.00	10.80	-	-	0.10	0.50	3.50	4.00	-	-	-	-
W8-2	250m drift	258	940203	Normal	PNC TONO	-	-	-	-	-	8.90	0.30	<0.01	5.80	<0.1	<0.02	-	11.70	5.50	1.90	8.80	-	-	0.10	1.10	4.00	5.10	-	-	-	-
W8-2	250m drift	258	940208	Normal	Nittetsu	15.4	9.5	137	350	76.1	8.60	0.20	0.00	6.10	<0.1	0	<0.01	13.50	6.30	1.90	8.20	18.10	2.10	0.10	1.90	4.00	5.90	-67.9	-10.7	12.9±0.4	56.60
W8-3	250m drift	.258	940309	Normal	Nittetsu	15.3	9.4	78	291	76.2	8.80	0.20	0.00	5.90	<0.1	<0.01	<0.01	12.80	6.00	1.80	8.40	20.40	1.90	0.10	0.70	4.40	5.10	-69.5	-10.8	11.8±0.4	58.30
W8-4	250m drift	258	940413	Normal	Nittetsu	15.1	9.6	115	328	77.1	9.30	0.20	0.00	5.60	<0.1	0	<0.01	12.20	5.70	1.80	8.70	16.40	2.30	0.10	2.40	3.70	6.10	-	-	10.4±0.2	54.20
W9-9	250m drift	258	930902	Normal	PNC TONO	14.3	9.9	-85	129	78.4	10.80	0.20	<0.01	4.30	<0.1	<0.02	-	15.10	7.00	2.10	10.10	18.90	4.00	0.10	0.90	4.50	5.40	-	-	-	61.51
W9-12	250m drift	258	931209	Normal	PNC TONO	15.8	9.7	126	339	77.3	10.50	0.30	<0.01	4.30	<0.1	<0.02	-	14.90	7.00	2.10	10.00	13.30	2.40	0.10	1.30	3.10	4.40	-	-	-	55.41
W9-1	250m drift	258	940126	Normal	PNC TONO	-	-	-	-		11.60	0.30	<0.01	4.50	<0.1	<0.02	-	14.80	6.90	2.10	10.20	-	-	0.10	0.30	3.70	4.00	-	-	-	-
W10-9	250m drift	258	930902	Normal	PNC TONO	14.4	9.5	-43	171	78.9	10.70	0.20	<0.01	4.70	<0.1	<0.02	-	12.10	5.60	2.00	10.30	24.40	2.90	0.10	1.10	5.40	6.50	-	-	-	64.41
W10-10	250m drift	258	931018	Normal	Nittetsu	14.9	9.5	131	344	84.9	11.00	0.20	0.00	4.60	<0.1	<0.01	<0.01	10.90	5.10	1.60	9.60	21.30	2.50	<0.05	1.40	4.70	6.10	-68.5	-10.7	9.2±0.1	59.20
W10-12	250m drift	258	931209	Normal	PNC TONO	15.9	9.5	137	350	78.6	10.60	0.30	<0.01	4.50	<0.1	<0.02	-	12.20	5.70	2.10	10.20	16.30	1.90	0.10	1.50	3.60	5.10	-	-	-	56.21
W10-12	250m drift	258	931215	Normal	Nittetsu	15.3	9.8	129	342	81.0	10.80	0.20	0.00	4.80	<0.1	0	<0.01	13.30	6.20	1.80	9.60	16.70	3.50	<0.05	1.60	4.00	5.60	-65.6	-10.9	10.9±0.4	57.20
W10-1	250m drift	258	940105	Normal	Nittetsu	15.4	9.2	120	333	79.5	10.90	0.20	0.00	4.80	0.1	0	<0.01	13.30	6.20	1.80	9.40	18.70	1.10	<0.05	0.70	3.90	4.60	-66.7	-10.8	11.2±0.4	59.10
W10-1	250m drift	258	940126	Normal	PNC TONO	-	-	-	-	-	11.70	0.20	<0.01	4.60	<0.1	<0.02	-	12.20	5.70	2.00	10.40	-	-	0.10	0.30	3.90	4.20	-	-	-	-
W10-2	250m drift	258	940208	Normal	Nittetsu	15.7	9.6	128	341	79.1	10.50	0.20	0.00	4.90	<0.1	<0.01	<0.01	13.70	6.40	1.90	9.20	17.30	2.50	0.10	1.10	3.90	5.00	-68.1	-10.5	10.1±0.4	57.70
W10-3	250m drift	258	940309	Normal	Nittetsu	15.4	9.0	94	307	79.5	10.80	0.20	0.00	4.70	<0.1	<0.01	<0.01	12.80	6.00	2.00	9.80	22.10	0.80	0.10	0.50	4.50	5.00	-67.8	-10.7	11.2±0.4	62.40
W10-4	250m drift	258	940413	Normal	Nittetsu	15.6	9.7	62	275	81.1	11.60	0.20	0.00	4.40	0.1	<0.01	<0.01	12.20	5.70	1.80	10.40	15.80	2.90	0.10	0.60	3.70	4.30	-68.6	-10.7	8.5±0.1	56.40
94-W10-10	250m drift	258	941013	Normal	Nittetsu	15.4	9.5	69	282	83.7	9.80	0.30	<0.02	3.90	<0.1	<0.3	<0.05	13.40	6.30	1.50	9.80	23.70	2.80	0.70	1.10	5.20	6.30	-65.4	-10.5	8.8±0.1	62.42
94-W10-11	250m drift	258	941116	Normal	Nittetsu	15.6	9.3	61	274	81.3	10.10	0.30	<0.02	4.60	<0.1	0.4	<0.05	13.10	6.10	1.60	9.70	20.30	1.50	0.40	0.90	4.30	5.20	-68.5	-10.9	9.8±0.2	59.72
94-W10-12	250m drift	258	941215	Normal	Nittetsu	15.7	8.9	117	330	80.6	11.00	0.20	<0.02	4.40	<0.1	<0.3	<0.05	12.40	5.80	1.50	9.60	22.80	0.70	0.30	0.60	4.60	5.20	-67.7	-10.8	9.1±0.2	61.92
95-W10-1	250m drift	258	950111	Normal	Nittetsu	15.3	9.6	129	342	80.8	9.70	0.20	<0.02	4.20	<0.1	<0.3	<0.05	12.70	5.90	1.80	10.00	19.20	2.80	<0.1	0.60	4.30	4.90	-68.5	-10.8	8.8±0.1	57.82
95-W10-2	250m drift	258	950214	Normal	Nittetsu	15.8	9.5	128	341	80.9	10.00	0.20	<0.02	4.60	<0.1	<0.3	<0.05	13.10	6.10	1.70	10.60	31.80	3.70	0.30	0.40	7.00	7.40	-69.6	-10.7	9.1±0.2	72.02
95-W10-3	250m drift	258	950315	Normal	Nittetsu	15.6	9.3	157	370	81.6	10.30	0.20	<0.02	4.40	<0.1	<0.3	<0.05	12.80	6.00	1.90	11.30	30.10	2.20	0.20	0.50	6.40	6.90	-70.4	-10.9	9.2±0.2	71.02
W11-9	250m drift	258	930902	Normal	PNC TONO	14.5	10.0	-50	164	83.8	15.10	0.30	<0.01	2.60	<0.1	<0.02	-	16.80	7.90	2.20	13.90	19.60	5.20	0.10	1.40	4.50	5.80	-	-	-	70.51
W11-10	250m drift	258	931018	Normal	Nittetsu	15.2	9.7	140	353	88.3	14.40	0.20	0.00	2.70	<0.1	<0.01	<0.01	15.80	7.40	1.60	6.70	18.40	3.40	<0.05	1.40	4.30	5.70	-70.1	-10.8	6.8±0.1	59.80
W11-12	250m drift	258	931209	Normal	PNC TONO	15.5	9.4	163	376	80.2	13.40	0.40	<0.01	2.60	<0.1	<0.02	-	16.80	7.80	2.00	7.10	21.70	2.60	0.10	1.00	4.80	5.80	-	-	-	64.01
W11-12	250m drift	258	931215	Normal	Nittetsu	15.2	9.3	131	344	83.4	13.90	0.30	0.00	2.90	<0.1	0	0.00	18.00	8.40	1.80	6.40	23.10	1.70	0.10	0.70	4.90	5.60	-66.8	-11	7.9±0.4	66.40
W11-1	250m drift	258	940105	Normal	Nittetsu	15.1	9.7	132	345	82.8	14.60	0.30	0.00	2.90	<0.1	<0.01	<0.01	18.40	8.60	1.80	6.30	21.40	3.90	<0.05	0.80	5.00	5.80	-69.3	-10.9	8.0±0.4	65.70
W11-1	250m drift	258	940126	Normal	PNC TONO	-	-	-	-	-	14.90	0.30	<0.01	2.80	<0.1	<0.02	-	17.10	8.00	2.10	7.00	-	-	0.10	0.60	5.30	5.90	-	-	-	-
W11-2	250m drift	258	940208	Normal	Nittetsu	15.7	9.5	153	366	81.1	13.50	0.30	0.00	2.90	<0.1	<0.01	<0.01	18.60	8.70	2.00	5.90	24.90	2.90	0.10	1.40	5.50	6.90	-71.1	-10.8	8.0±0.4	68.10
W11-3	250m drift	258	940309	Normal	Nittetsu	15.3	8.5	138	351	79.5	14.30	0.30	0.00	2.90	<0.1	0	<0.01	17.80	8.30	2.00	6.20	33.00	0.50	0.10	1.20	6.60	7.80	-	-10.9	8.4±0.4	76.50
W11-4	250m drift	258	940413	Normal	Nittetsu	15.2	9.6	91	304	81.8	14.80	0.30	0.00	2.60	0.1	0	<0.01	16.90	7.90	1.80	6.60	26.20	3.70	<0.05	0.80	5.90	6.70	-70.7	-10.9	6.9±0.1	69.20
W12-9	250m drift	258	930902	Normal	PNC TONO	14.4	9.0	48	262	79.4	14.10	0.30	<0.01	2.60	<0.1	<0.02	-	15.20	7.10	2.20	10.70	25.40	0.90	0.10	2.70	5.20	7.80	-	-	-	70.51
W12-1	250m drift	258	940126	Normal	PNC TONO	-	-	-	-	-	14.50	0.40	<0.01	2.70	<0.1	<0.02	-	15.40	7.20	1.90	4.70	-	-	0.10	0.80	4.20	5.00	-	-	-	-
W13-9	250m drift	258	930902	Normal	PNC TONO	14.6	9.8	49	263	74.5	13.50	0.30	<0.01	2.60	<0.1	<0.02	-	13.00	6.10	2.00	9.80	21.90	4.70	0.10	1.40	5.30	6.60	-	-	-	63.11
W13-1	250m drift	258	940126	Normal	PNC TONO	-	-	-	-	-	14.80	0.20	<0.01	2.70	<0.1	<0.02	-	13.40	6.20	1.80	4.20	-	-	0.10	0.30	3.90	4.20	-	-	-	-

Table 3-3 : Results of measurements for physico-chemical parameters, chemical composition and stable-radioactive isotope of surface waters and groundwaters in the Kurihashi granodiorite (3)

Sample	Location	Altitude (m)	Date	Sampling mathod	Laboratory	Temp (℃)	pH	ORP (mV)	Eh (mV)	EC (μS/cm)	Na+ (ppm)	K+ (ppm)	Mg+ (ppm)	Ca+ (ppm)	Al+++ (ppm)	T.Fe (ppm)	Fe++ (ppm)	SiO2 (ppm)	Si++++ (ppm)	Cl- (ppm)	SO4-- (ppm)	HCO3- (ppm)	CO3-- (ppm)	F- (ppm)	TOC (ppm)	IC (ppm)	TC (ppm)	δD (‰)	δ18-O (‰)	3-H (T.U.)	Dissolved solid (mg/l)
W14-9	250m drift	258	930902	Normal	PNC TONO	14.4	9.6	58	272	76.4	13.50	0.20	<0.01	2.90	<0.1	<0.02	-	12.80	6.00	2.00	9.60	27.40	3.90	0.10	1.10	6.20	7.30	-	-	-	68.41
W14-10	250m drift	258	931018	Normal	Nittetsu	15.1	8.4	152	365	76.2	15.30	0.20	0.00	3.90	<0.1	<0.01	<0.01	12.80	6.00	1.50	3.90	23.50	0.30	<0.05	1.00	4.70	5.70	-69.6	-10.7	10.5±0.2	61.10
W14-12	250m drift	258	931209	Normal	PNC TONO	15.9	9.6	138	351	76.6	11.70	0.30	<0.01	2.70	<0.1	<0.02	-	12.50	5.90	1.80	4.50			0.10	0.80	4.20	5.00	-	-	-	33.51
W14-12	250m drift	258	931215	Normal	Nittetsu	15.4	9.9	113	326	79.7	12.20	0.20	0.00	3.10	<0.1	0	<0.01	13.30	6.20	1.60	4.00	18.70	4.50	<0.05	0.60	4.60	5.20	-64	-10.8	12.7±0.4	53.10
W14-1	250m drift	258	940105	Normal	Nittetsu	15.8	9.9	97	310	78.3	12.70	0.20	0.00	3.10	<0.1	0	<0.01	13.50	6.30	1.60	4.00	17.90	4.30	<0.05	0.60	4.40	5.00	-67.8	-10.7	12.1±0.4	53.00
W14-1	250m drift	258	940126	Normal	PNC TONO	-	-	-	-	-	14.10	0.20	<0.01	2.80	<0.1	<0.02	-	12.40	5.80	1.80	4.60	-	-	0.10	0.40	3.60	4.00	-	-	-	-
W14-2	250m drift	258	940208	Normal	Nittetsu	15.7	9.9	126	339	77.3	12.10	0.20	0.00	3.20	<0.1	<0.01	<0.01	13.70	6.40	1.70	3.80	16.30	4.00	0.10	0.70	4.00	4.70	-67.7	-10.7	9.0±0.4	51.00
W14-3	250m drift	258	940309	Normal	Nittetsu	15.2	9.8	108	321	76.5	12.80	0.20	0.00	3.00	<0.1	<0.01	<0.01	13.30	6.20	1.70	3.90	20.50	4.30	0.10	0.50	4.90	5.40	-67.7	-10.7	12.6±0.4	55.40
W14-4	250m drift	258	940413	Normal	Nittetsu	15.2	9.9	31	244	78.7	13.00	0.20	0.00	2.80	0.1	<0.01	<0.01	12.20	5.70	1.60	4.30	16.70	4.10	<0.05	0.70	4.10	4.80	-70.7	-10.6	11.1±0.2	50.80
94-W14-10	250m drift	258	941013	Normal	Nittetsu	15.3	9.8	53	266	78.0	11.10	0.30	<0.02	2.40	<0.1	<0.3	<0.05	12.60	5.90	1.40	4.40	27.10	5.80	0.70	1.10	6.50	7.60	-64.9	-10.5	10.9±0.2	59.32
94-W14-11	250m drift	258	941116	Normal	Nittetsu	15.2	9.8	33	246	77.1	11.00	0.30	<0.02	2.90	<0.1	<0.3	<0.05	12.90	6.00	1.50	4.40	20.10	4.30	0.20	0.80	4.80	5.70	-68	-10.7	10.1±0.2	53.12
94-W14-12	250m drift	258	941215	Normal	Nittetsu	15.4	9.7	116	329	75.6	11.30	0.30	<0.02	2.80	<0.1	<0.3	<0.05	11.80	5.50	1.30	4.00	30.20	5.50	0.20	0.90	7.10	8.00	-67.5	-10.7	11.3±0.2	61.72
95-W14-1	250m drift	258	950111	Normal	Nittetsu	15.2	9.9	119	332	77.9	10.90	0.30	<0.02	2.70	<0.1	<0.3	<0.05	12.40	5.80	1.70	4.40	19.60	4.70	0.10	0.60	4.80	5.40	-67.5	-10.8	9.8±0.1	52.02
95-W14-2	250m drift	258	950214	Normal	Nittetsu	15.7	9.8	100	313	76.7	11.40	0.30	<0.02	3.00	<0.1	<0.3	<0.05	12.20	5.70	1.60	4.30	31.90	6.80	0.10	0.50	7.60	8.10	-69.5	-10.5	11.1±0.2	64.72
95-W14-3	250m drift	258	950315	Normal	Nittetsu	15.5	9.8	136	349	77.5	11.30	0.20	<0.02	2.80	<0.1	<0.3	<0.05	12.60	5.90	1.80	4.90	32.00	6.80	0.20	0.40	7.70	8.10	-71.1	-10.8	11.6±0.2	65.62
W15-9	250m drift	258	930902	Normal	PNC TONO	14.5	9.9	62	276	77.7	13.20	0.20	<0.01	2.80	<0.1	<0.02	-	12.10	5.60	1.70	3.30	21.40	5.20	0.10	0.60	5.50	6.10	-	-	-	54.71
W15-1	250m drift	258	940126	Normal	PNC TONO	-	-	-	-	-	13.50	0.20	<0.01	2.70	<0.1	<0.02	-	13.10	6.10	1.90	4.80	-	-	0.10	0.20	3.90	4.10	-	-	-	-
																															0.00
W16-9	250m drift	258	930902	Normal	PNC TONO	14.5	10.0	65	279	75.4	12.40	0.30	<0.01	3.30	<0.1	<0.02	-	11.60	5.40	1.70	3.30	22.00	5.80	0.10	0.60	5.50	6.10	-	-	-	54.61
W16-10	250m drift	258	931018	Normal	Nittetsu	15.0	9.8	79	292	74.9	9.10	0.30	0.00	3.20	<0.1	<0.01	<0.01	10.10	4.70	1.20	2.80	18.40	3.90	<0.05	0.90	4.40	5.30	-69.5	-10.8	8.7±0.1	45.10
W16-12	250m drift	258	931209	Normal	PNC TONO	16.3	9.6	99	311	75.8	10.40	0.40	<0.01	3.00	<0.1	<0.02	-	11.50	5.40	1.70	3.00			0.00	1.00	4.20	5.20	-	-	-	30.01
W16-12	250m drift	258	931215	Normal	Nittetsu	16.1	9.8	55	267	75.2	11.50	0.30	0.00	3.50	0.1	<0.01	<0.01	12.40	5.80	1.60	2.70	19.60	4.20	<0.05	0.50	4.70	5.20	-66	-10.9	10.7±0.4	51.60
W16-1	250m drift	258	940105	Normal	Nittetsu	15.8	9.9	102	315	75.8	12.00	0.20	0.00	3.50	0.1	0	<0.01	12.60	5.90	1.50	2.60	19.10	4.60	<0.05	1.00	4.70	5.70	-67.1	-10.8	9.5±0.4	51.50
W16-1	250m drift	258	940126	Normal	PNC TONO	-	-	-	-	-	9.80	0.30	<0.01	3.20	<0.1	<0.02	-	11.50	5.40	1.70	3.00	-	-	0.10	0.70	3.60	4.30	-	-	-	-
W16-2	250m drift	258	940208	Normal	Nittetsu	15.9	9.9	119	332	76.0	11.00	0.30	0.00	3.60	<0.1	<0.01	<0.01	12.80	6.00	1.60	2.30	18.70	4.50	<0.05	0.50	4.60	5.10	-67.3	-10.6	9.0±0.4	50.30
W16-3	250m drift	258	940309	Normal	Nittetsu	15.3	9.7	5	218	75.2	11.80	0.30	0.00	3.40	<0.1	<0.01	<0.01	12.20	5.70	1.80	2.50	20.10	3.70	<0.05	0.50	4.70	5.20	-67.6	-10.6	10.7±0.4	52.10
W16-4	250m drift	258	940413	Normal	Nittetsu	15.4	9.8	30	243	74.5	11.50	0.30	0.00	3.20	0.1	<0.01	<0.01	11.10	5.20	1.60	2.50	17.10	3.60	<0.05	1.10	4.10	5.20	-69.1	-10.6	7.9±0.1	47.30
94-W16-10	250m drift	258	941013	Normal	Nittetsu	15.5	9.8	45	258	62.7	10.30	0.40	<0.02	2.80	<0.1	<0.3	<0.05	11.90	5.60	1.40	2.60	27.80	5.90	0.50	1.10	6.70	7.70	-64.2	-10.4	7.8±0.1	57.22
94-W16-11	250m drift	258	941116	Normal	Nittetsu	15.3	9.8	27	240	75.2	10.30	0.40	<0.02	3.10	<0.1	<0.3	0.30	11.90	5.60	1.50	1.50	19.30	4.10	0.20	0.60	4.60	5.20	-67.8	-10.6	8.3±0.1	48.02
94-W16-12	250m drift	258	941215	Normal	Nittetsu	15.5	9.8	93	306	74.6	10.20	0.30	<0.02	3.20	<0.1	<0.3	0.10	11.30	5.30	1.20	2.30	19.30	4.10	0.20	0.50	4.60	5.10	-66.5	-10.6	8.7±0.1	47.82
95-W16-1	250m drift	258	950111	Normal	Nittetsu	15.4	9.9	128	341	75.5	10.00	0.30	<0.02	3.00	<0.1	<0.3	0.10	11.60	5.40	1.60	2.80	19.70	4.80	0.10	0.60	4.80	5.40	-68.7	-10.6	8.5±0.1	49.02
95-W16-2	250m drift	258	950214	Normal	Nittetsu	15.8	9.8	98	311	79.6	10.30	0.30	<0.02	3.30	<0.1	<0.3	0.20	11.50	5.40	1.50	2.70	33.10	7.00	<0.1	0.40	7.90	8.40	-69.5	-10.5	8.6±0.1	62.72
95-W16-3	250m drift	258	950315	Normal	Nittetsu	15.8	9.8	134	347	75.2	10.70	0.20	<0.02	3.10	<0.1	<0.3	0.30	11.60	5.40	1.70	3.00	32.00	6.80	<0.1	0.40	7.70	8.10	-69.1	-10.8	9.2±0.2	62.32
95-W16-4	250m drift	258	950412	Normal	PNC TONO	15.4	9.9	119	332	76.8	12.10	0.30	<0.01	3.20	<0.1	<0.02	-	11.57	5.40	1.80	3.10	20.71	5.01	0.00	3.90	4.00	7.90	-	-	-	52.79
95-W16-5	250m drift	258	950517	Normal	PNC TONO	15.5	9.7	120	333	75.1	11.90	0.30	<0.01	3.30	<0.1	<0.02	-	11.79	5.50	1.60	2.90	33.10	7.03	0.00	1.50	5.90	7.40	-	-	-	64.90
W17-9	250m drift	258	930902	Normal	PNC TONO	15.5	10.5	-305	-92	117.9	19.00	0.10	<0.01	2.70	<0.1	<0.02	-	25.50	11.90	2.00	11.40	15.80	7.30	0.40	1.00	4.60	5.60	-	-	-	76.51
W17-1	250m drift	258	940126	Normal	PNC TONO	-	-	-	-	-	20.90	0.10	<0.01	2.60	<0.1	<0.02	-	26.00	12.10	2.00	10.30	-	-	0.40	0.50	2.00	2.50	-	-	-	-
W18-9	250m drift	258	930902	Normal	PNC TONO	14.8	10.0	-10	203	83.6	12.90	0.10	<0.01	2.60	<0.1	<0.02	-	12.30	5.70	1.80	5.50	27.00	7.10	0.10	1.10	6.70	7.80	-	-	-	62.21
W18-10	250m drift	258	931018	Normal	Nittetsu	15.4	9.9	125	338	83.6	15.30	0.10	0.00	2.70	<0.1	<0.01	<0.01	11.10	5.20	1.60	5.10	21.60	5.20	<0.05	1.60	5.30	6.90	-67.9	-10.7	8.4±0.1	57.50
W18-12	250m drift	258	931209	Normal	PNC TONO	16.0	9.8	185	398	86.5	13.60	0.20	0.00	2.50	<0.1	<0.02	-	12.30	5.70	1.80	5.40			0.10	1.40	4.60	6.00	-	-	-	35.80
W18-12	250m drift	258	931215	Normal	Nittetsu	15.5	9.7	105	318	85.1	14.10	0.10	0.00	2.70	0.2	<0.01	<0.01	13.00	6.10	1.70	4.80	20.10	3.70	<0.05	1.00	4.70	5.70	-64.8	-10.9	10.7±0.4	86.50
W18-1	250m drift	258	940105	Normal	Nittetsu	15.7	9.7	123	336	84.9	14.40	0.10	0.00	2.70	0.2	0	<0.01	13.30	6.20	1.60	4.80	21.40	3.90	<0.05	0.90	5.00	5.90	-68.1	-10.9	9.9±0.4	58.30
W18-1	250m drift	258	940126	Normal	PNC TONO	-	-	-	-	-	15.70	0.10	0.00	2.60	<0.1	<0.02	-	12.30	5.80	1.90	5.50	-	-	0.10	0.50	4.40	4.90	-	-	-	-
W18-2	250m drift	258	940208	Normal	Nittetsu	15.9	9.6	154	367	83.4	13.90	0.10	0.00	2.80	<0.1	0	<0.01	13.90	6.50	1.70	4.70	20.40	2.90	0.10	0.80	4.60	5.40	-68	-10.7	10.5±0.4	57.50
W18-3	250m drift	258	940309	Normal	Nittetsu	15.6	9.7	47	260	83.4	14.40	0.10	0.00	2.70	0.1	<0.01	<0.01	13.30	6.20	1.70	4.80	21.80	4.00	0.10	0.60	5.10	5.70	-68.9	-10.7	7.2±0.4	58.80
W18-4	250m drift	258	940413	Normal	Nittetsu	15.7	9.8	52	265	84.3	14.50	0.10	0.00	2.40	0.2	<0.01	<0.01	11.80	5.50	1.70	5.20	18.40	3.90	0.10	1.40	4.40	5.80	-69	-10.7	8.8±0.2	54.10
W19-1	250m drift	258	940126	Normal	PNC TONO	-	-	-	-	-	13.10	0.20	<0.01	3.90	<0.1	<0.02	-	17.10	8.00	2.30	9.10	-	-	0.20	0.60	3.00	3.60	-	-	-	-
W20-10	550m drift	575	931018	Normal	Nittetsu	11.4	9.1	22	238	81.1	4.50	0.30	0.00	10.60	<0.1	<0.01	<0.01	9.20	4.30	1.90	6.90	33.00	15.20	<0.05	0.90	6.80	7.70	-69.7	-10.7	6.4±0.1	66.40
W20-12	550m drift	575	931215	Normal	Nittetsu	12.1	8.4	22	238	82.0	5.40	0.30	0.10	10.70	<0.1	0	<0.01	11.50	5.40	2.00	6.90	29.00	0.40	<0.05	0.50	5.80	6.30	-70.5	-10.9	7.8±0.4	65.90
W20-1	550m drift	575	940105	Normal	Nittetsu	11.5	8.9	153	369	81.8	5.60	0.30	0.10	10.70	<0.1	0	<0.01	11.80	5.50	2.00	6.90	31.60	0.90	<0.05	0.90	6.40	7.30	-67.5	-11	6.7±0.4	69.00
W20-2	550m drift	575	940208	Normal	Nittetsu	12.2	8.8	169	384	81.5	5.10	0.40	0.10	11.20	<0.1	<0.01	<0.01	12.00	5.60	2.20	6.60	32.80	0.70	0.10	1.30	6.60	7.90	-68.9	-10.9	6.5±0.4	70.40
W20-3	550m drift	575	940309	Normal	Nittetsu	11.7	8.7	123	339	81.8	5.50	0.40	0.10	10.50	<0.1	<0.01	<0.01	12.00	5.60	2.10	6.70	31.90	0.60	<0.05	0.60	6.40	7.00	-67.9	-10.7	7.8±0.4	69.20
W20-4	550m drift	575	940413	Normal	Nittetsu	11.7	9.0	80	296	81.7	5.20	0.30	0.10	10.90	0.1	<0.01	<0.01	10.70	5.00	2.10	7.10	31.40	1.10	<0.05	0.60	6.40	7.00	-68.7	-10.7	6.2±0.1	67.80
94-W20-10	550m drift	575	941013	Normal	Nittetsu	11.9	8.0	183	399	83.5	5.00	0.50	0.10	9.30	<0.1	0.3	<0.05	11.10	5.20	1.80	6.30	38.00	0.50	<0.1	1.70	7.60	9.20	-65.2	-10.6	6.8±0.1	72.10
94-W20-11	550m drift	575	941116	Normal	Nittetsu	11.6	8.0	113	329	84.7	4.60	0.40	0.10	10.30	<0.1	0.2	<0.05	11.00	5.10	1.80	7.30	35.30	0.50	0.20	0.90	7.10	8.00	-68.3	-10.6	5.7±0.1	70.80
94-W20-12	550m drift	575	941215	Normal	Nittetsu	11.8	8.4	160	376	81.9	4.90	0.40	0.10	10.60	<0.1	<0.3	<0.05	10.60	5.00	1.60	6.30	22.60	0.30	0.10	0.60	4.50	5.10	-66.8	-10.8	7.2±0.1	57.10
95-W20-1	550m drift	575	950111	Normal	Nittetsu	11.7	8.0	203	419	63.1	4.70	0.40	0.10	10.30	<0.1	<0.3	<0.05	10.80	5.00	2.00	7.00	36.80	0.50	0.30	0.60	7.40	7.90	-68	-10.9	6.8±0.1	72.10
95-W20-2	550m drift	575	950214	Normal	Nittetsu	12.1	7.9	161	376	82.8	4.90	0.40	0.10	10.80	<0.1	<0.3	0.10	11.20	5.20	1.90	7.00	35.60	0.50	0.10	0.50	7.10	7.60	-69.3	-10.6	6.5±0.1	71.90
95-W20-3	550m drift	575	950315	Normal	Nittetsu	12.0	7.7	193	409	83.3	5.00	0.30	0.10	10.40	<0.1	<0.3	<0.05	10.60	5.00	2.20	7.50	39.40	0.60	<0.1	0.50	7.90	8.30	-69.2	-10.9	7.4±0.1	75.50

Note : Sampling Method

a) Normal : The groundwater was sampled directly from the inflowing fracture in the drift.

b) Packer : The groundwater was sampled from the packed-off section in KH-1 borehole.

c) MP55 (HGP10) : The groundwater was sampled by using MP system and HGP-10 system.

d) MP55 (MOSDAX) : The groundwater was sampled by using MP system and MOSDAX probe.

***Table 4** : Results of measurements for physico-chemical parameter, chemical composition, gases, bacteria population in groundwater, collected from KG-1 borehole*

		MOSDAX-2531		
Analytical Items	Unit	KG-1-2 GL-489~-495m 1994.11.18	KG-1-3 GL-740~747m 1994.12.2	KG-1-4 Gl-785~-791m 1995.1.21
Temp.	(℃)	13.2	10.9	11.1
pH	-	9.97	9.33	8.95
Eh	(mV)	342	345	358
EC	(μS/cm)	81	106	118
DO	(ppm)	0.2	0.1	0.0
O2(g)	(mg/l)	-	N.D.	N.D.
N2(g)	(mg/l)	-	45.6	43.2
H2(g)	(mg/l)	-	0.092	0.094
He(g)	(mg/l)	-	0.047	0.052
CH4(g)	(μg/l)	-	N.D.	N.D.
CO(g)	(mg/l)	-	N.D.	N.D.
ΣCO2(g)	(mg/l)	-	6.74	9.32
T-Si	(mg/l)	7.62	4.53	3.11
D-Si	(mg/l)	7.30	4.00	2.99
SiO2(T-Si)	(mg/l)	16.30	9.69	6.65
Na+	(mg/l)	11.0	17.3	14.7
K+	(mg/l)	0.62	0.56	0.77
Li+	(mg/l)	<0.09	<0.09	<0.09
Ca++	(mg/l)	6.29	7.21	6.8
Mg++	(mg/l)	0.00	0.10	0.34
Sr++	(mg/l)	0.011	0.009	0.009
Al+++	(mg/l)	0.311	0.168	0.121
T-Mn	(mg/l)	<0.01	<0.01	<0.01
D-Mn	(mg/l)	<0.01	<0.01	<0.01
T-Fe	(mg/l)	0.002	0.004	0.004
D-Fe	(mg/l)	0.001	0.003	0.001
Fe++	(mg/l)	0.002	0.002	-
Cl-	(mg/l)	1.86	2.93	3.51
F-	(mg/l)	0.19	0.35	0.01
Br-	(mg/l)			
I-	(mg/l)	<0.07	<0.07	<0.07
ΣS--	(mg/l)	<0.9	<0.9	<0.9
T-P	(mg-P/l)			
PO4---(P)	(mg-P/l)	0.021	0.018	0.009
SO4--	(mg/l)	8.93	17.1	8.57
HCO3-	(mg/l)	28.40	31.81	45.67
CO3--	(mg/l)	6.88	2.36	1.61
T-N	(mg-N/l)			
NO2-(N)	(mg-N/l)	<0.005	<0.005	0.032
NO3-(N)	(mg-N/l)	<0.005	<0.005	<0.005
NH4+(N)	(mg-N/l)	0.062	0.044	0.011
TC	(mg/l)	7.39	6.97	10.14
IC	(mg/l)	6.97	6.74	9.32
TOC	(mg/l)	0.42	0.23	0.82
Humic acid	(mg/l)	<0.5	<0.5	<0.5
Fluvic acid	(mg/l)	<1.0	<1.0	<1.0
δD	‰	-73	-73.1	-67.5
δ18-O	‰	-11.1	-10.6	-10.1
3-H	T.U.	2.8±0.1	3.4±0.1	4.7±0.1
Total number of B.	(cells/ml)	7.5E+05	9.2E+05	-
Ferrooxidans	(MPN/ml)	N.D.	N.D.	-
SRB	(MPN/ml)	1.8E+03	8.9E+01	-
Methanobacterium	(MPN/ml)	N.D.	N.D.	-
Nitro Reducing B.	(MPN/ml)	2.8E+01	1.5E+03	-
Denitrification B.	(MPN/ml)	2.0E+00	1.3E+05	-

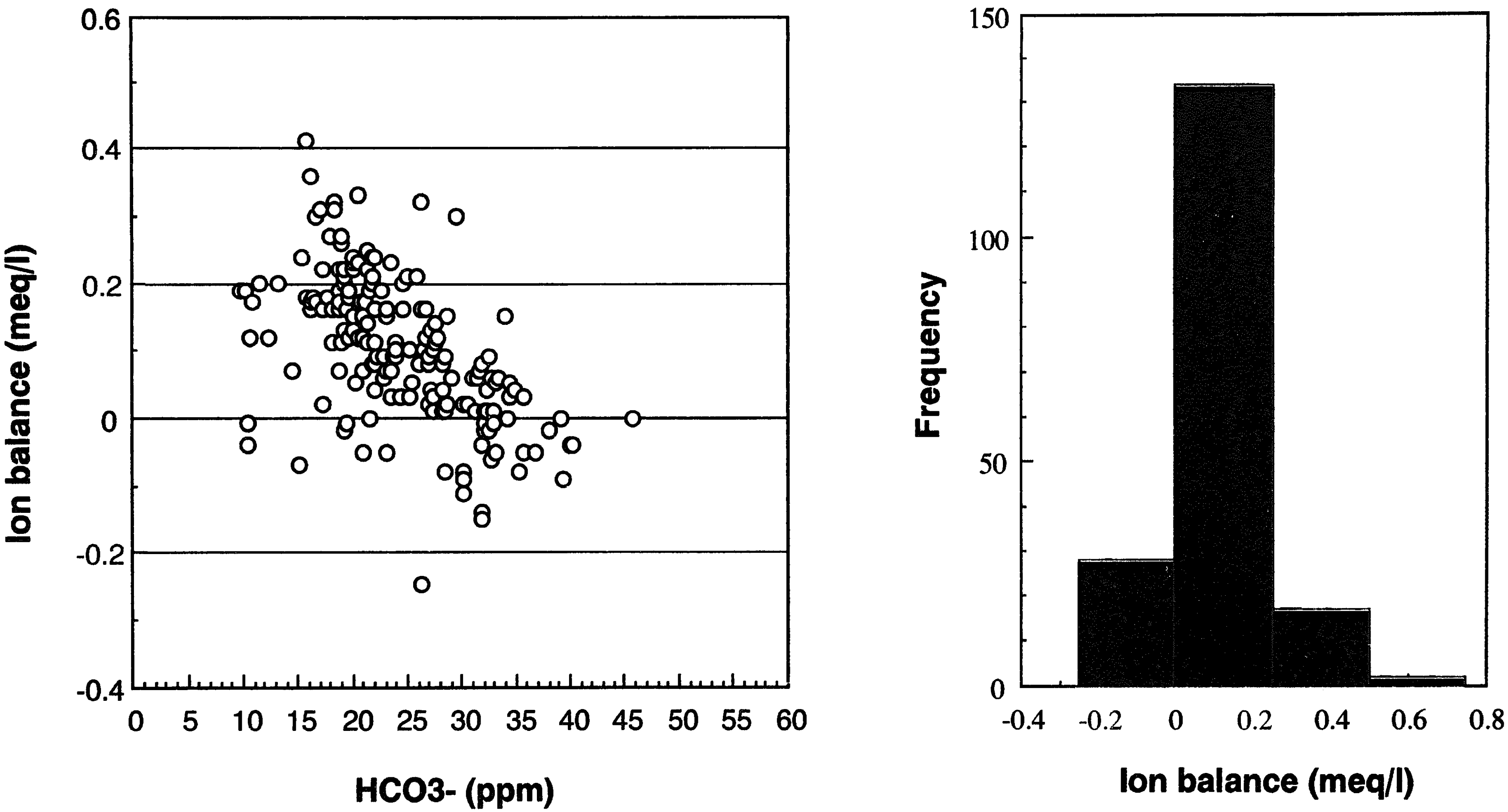

***Figure 4** : Results of charge balance calculation for all groundwater samples in the Kurihashi granodiorite. The charge balance for reliability is determined according to the criterion recommended by Friedman and Erdmann (1982).*

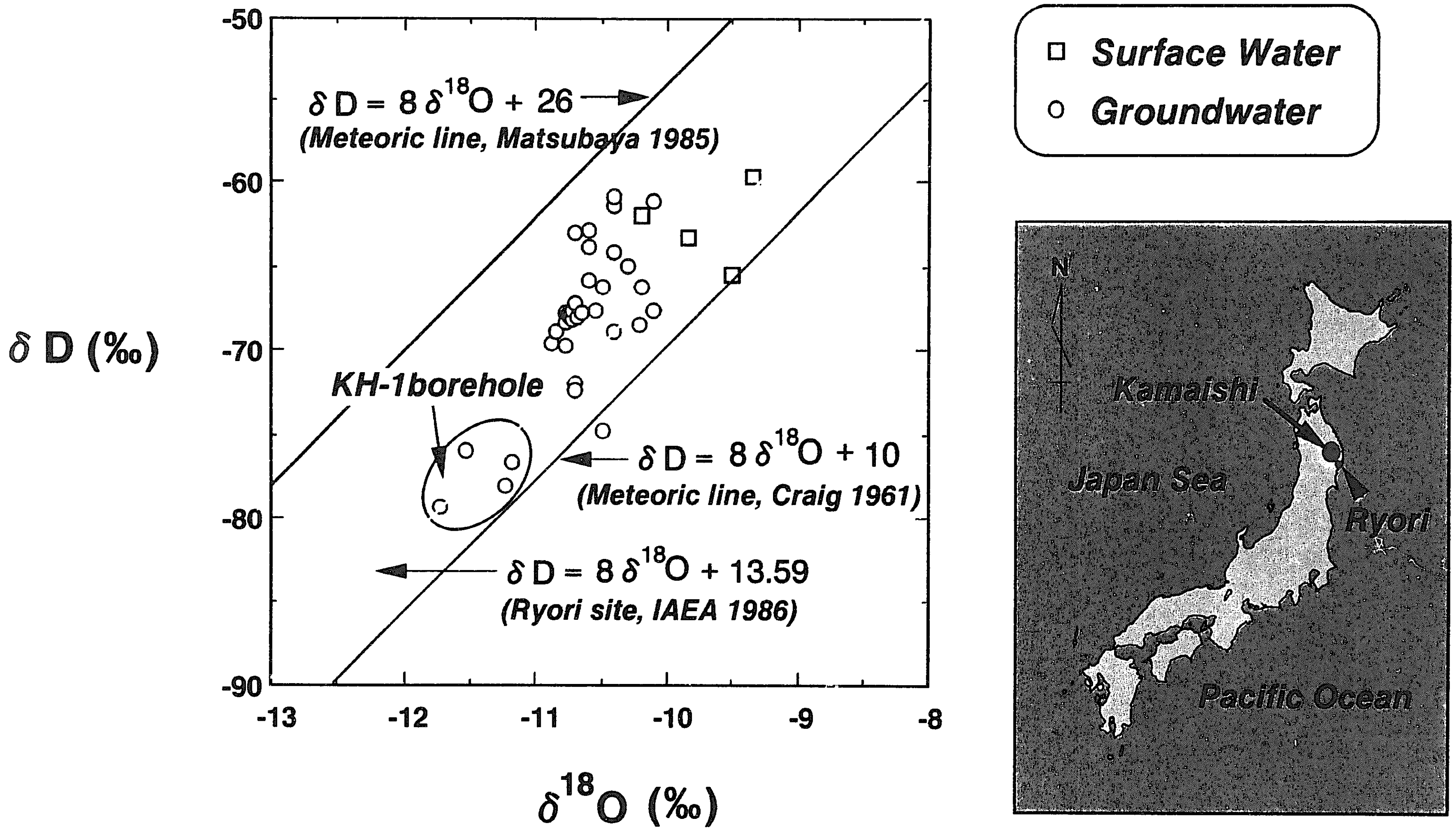

Figure 5 *: Deutrium and 18-oxygen content of the surface waters and groundwaters in the Kurihashi granodiorite. The global meteoric water line (Craig, 1961) and two local meteoric water lines (Matsubaya, 1985 and IAEA, 1986) are drawn.*

2.3.5 Age of the Groundwater

Tritium concentrations in surface waters and groundwaters at Kamaishi are shown in Figure 6. The concentrations in most groundwaters are greater than 1 T.U. (Tritium Unit), indicating that these solutions were recharged after 1953 (see below). Tritium concentrations in samples from the KH-1 borehole (except the section between 0 to 100m below the E.L.550m drift), however, are less than 1 T.U., indicating that these solutions may have been recharged before 1953.

The residence time of groundwater in the host rocks at Kamaishi can be calculated based on the half-life of tritium (12.3 years). This isotope is produced naturally in the atmosphere by the interaction of cosmic rays with nitrogen and oxygen. The most important source of modern tritium, however, is from atmospheric testing of nuclear weapons, which took place between 1952 and 1969 (Drever, 1988). Natural concentrations of tritium in rain water around Japan is about 10 T.U. (e.g., Ii et al, 1997). Tritium in groundwater is not significantly affected by chemical processes.

The most important use of tritium in groundwater studies is in distinguishing between water that entered an aquifer prior to 1953 (pre-bomb water) and water that was in contact with the atmosphere after 1953 (Drever, 1988). If it is assumed that groundwaters do not mix after recharge (piston flow), their residence time in the subsurface can be estimated as follows:

$$C = Co\, e^{-\lambda t}$$

$$ln\, C = ln\, Co\, e^{-\lambda t} = ln\, Co - \lambda t$$

$$-\lambda t = ln\, C - ln\, Co$$

$$= ln\, (C / Co)$$

$$t = -1 / \lambda \cdot ln\, (C / Co)$$

$$where,\ T = ln2 / \lambda = 0.693 / \lambda$$

$$\lambda = 0.693 / 12.3 = 5.634\, E\text{-}2$$

where, C refers to the tritium concentration in groundwater, Co stands for the tritium concentration in rain water, t represents the residence time and T denotes tritium's half-life. Assuming as noted above that Co = 10 T.U. and C = 1 T.U. (i.e., below the detection limit by normal procedures),

$$t = -1 / 5.634\, E\text{-}2 \cdot ln\, (1 / 10)$$

$$= (2.303 / 5.634) \cdot 10^2$$

$$= 40.88$$

According to the above calculation, if tritium concentrations in groundwater are less than 1 T.U., the residence time of the groundwater is greater than 40 years. Tritium concentrations in

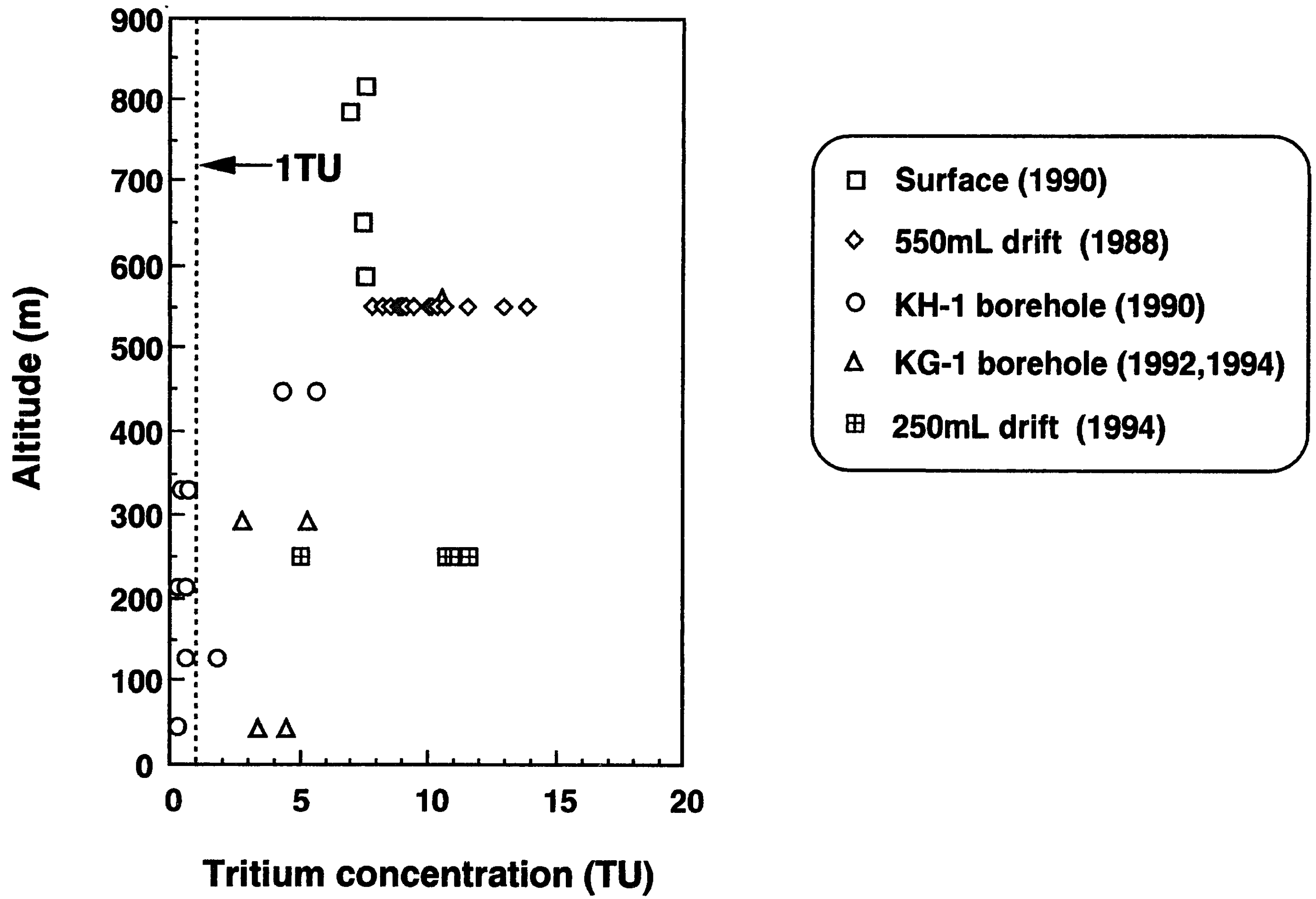

Figure 6 : Tritium concentration of the surface waters and groundwaters with each altitude. The tritium concentration is less than 1 T.U. in the almost groundwater samples collected from KH-1 borehole (except the section of KH-1-1),

many of the groundwater samples collected at the Kamaishi site are greater than 1 T.U., but tritium was not detected in samples from the KH-1 borehole. The residence time of groundwaters sampled from this borehole should therefore be greater than 40 years.

This conclusion is supported by preliminary carbon-14 dating of groundwaters collected from the lower part of the KH-1 borehole (i.e., where tritium concentrations are below detection in samples from the KH-1-2, KH-1-3 and KH-1-5 sampling locations, see Figure 2). The carbon-14 dates suggest that the age of these groundwaters ranges from 1,450 to 3,030 years BP (JNC, 1999). If these preliminary results are correct, the lighter δD and $\delta^{18}O$ values in KH-1 groundwaters may be attributed to colder climatic conditions than exist at the present time (see section 2.3.4).

2.3.6 Variation of Groundwater Chemistry with Depth

Figures 7 to 10 depict vertical variations in groundwater chemistry within the Kurihashi granodiorite. These results suggest:

- the pH varies from weakly acid-neutral (pH = 5.3-7.4) to weakly alkaline (pH = 8.2-10.5) with increasing depth,
- SiO_2 and Na^+ concentrations tend to increase with increasing depth,
- Ca^{2+} and carbonate (i.e., HCO_3^- + CO_3^{2-}) concentrations in groundwaters from the E.L.550m drift are greater than in groundwaters from the E.L.250m drift,
- SO_4^{2-} concentrations in groundwaters between the E.L.550m and E.L.250m drifts are similar, and
- electrical conductivity (EC) and total dissolved solids (TDS) tend to increase with increasing depth.

A Piper plot referring to groundwaters in the Kurihashi granodiorite is shown in Figure 11. As can be seen, these solutions change from Ca-HCO_3 type (E.L.550m) to Na-HCO_3 type waters (E.L.250m) with increasing depth.

2.3.7 State of Groundwater Equilibrium in the Kurihashi Granodiorite

2.3.7.1 Stability Diagrams

Mineral stability diagrams for the Na_2O-Al_2O_3-SiO_2-H_2O and CaO-Al_2O_3-SiO_2-H_2O systems at

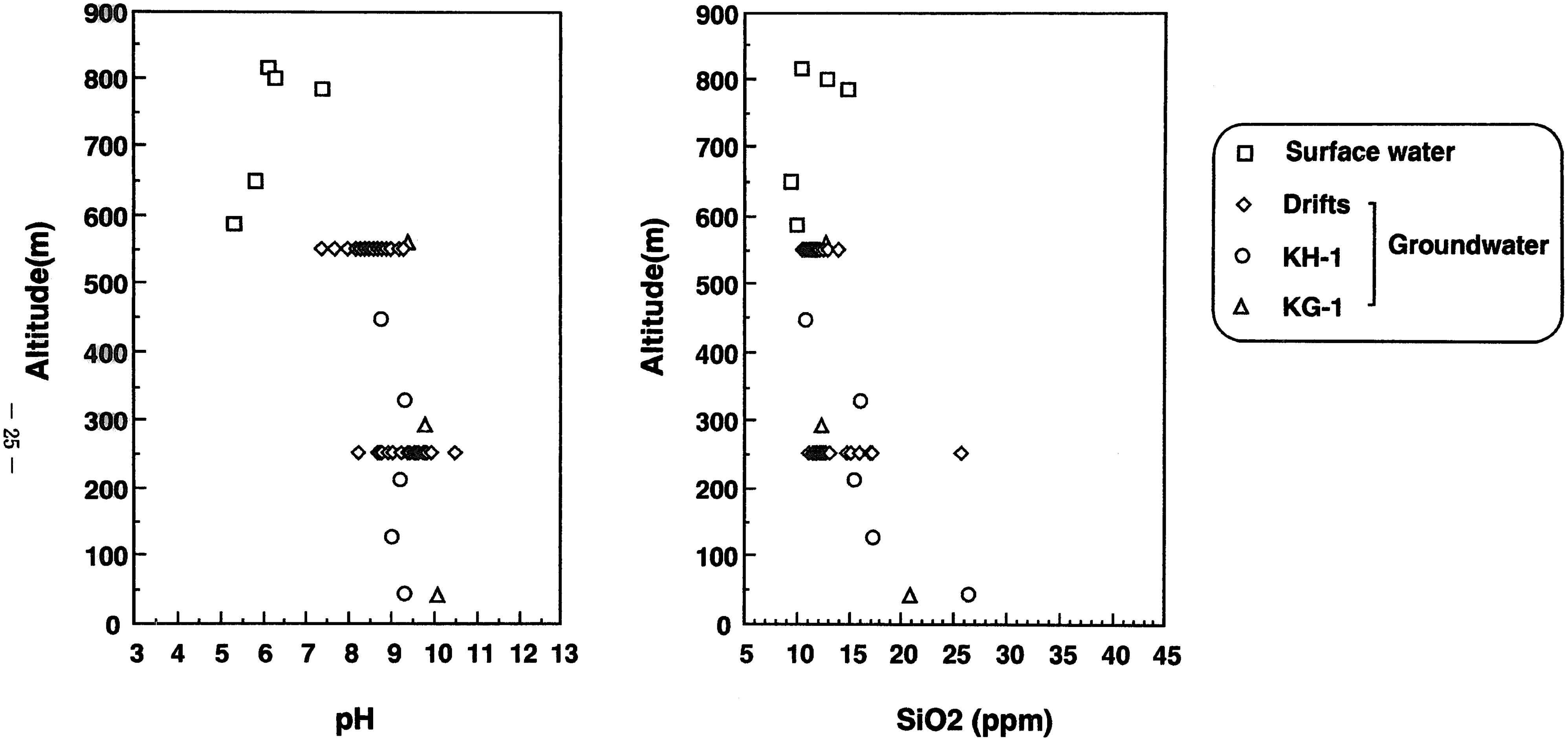

***Figure 7** : Variation of pH and SiO2 concentration for the surface waters and groundwaters with depth in the Kurihashi granodiorite.*

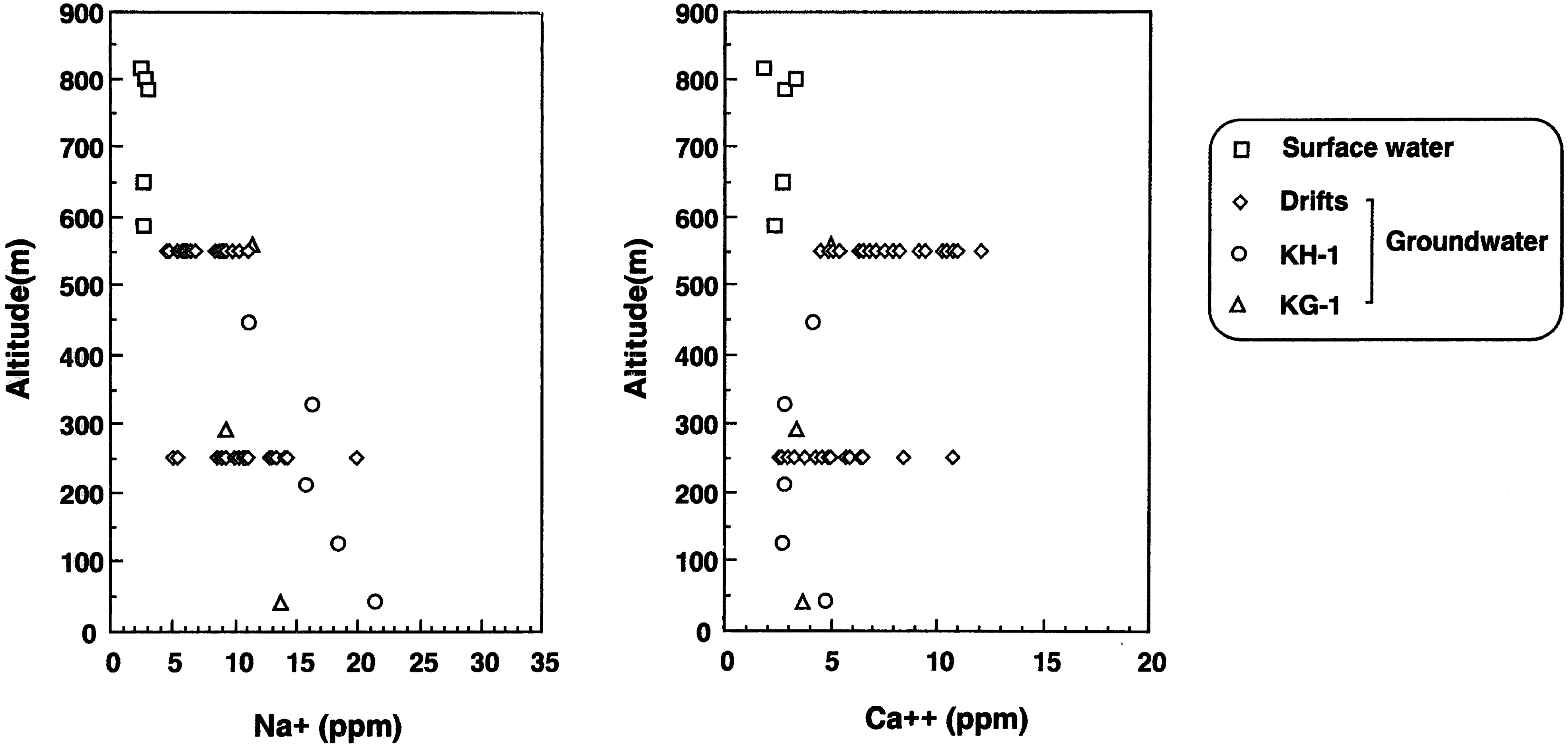

Figure 8 : *Variation of Na and Ca concentration for the surface waters and groundwaters with depth in the Kurihashi granodiorite.*

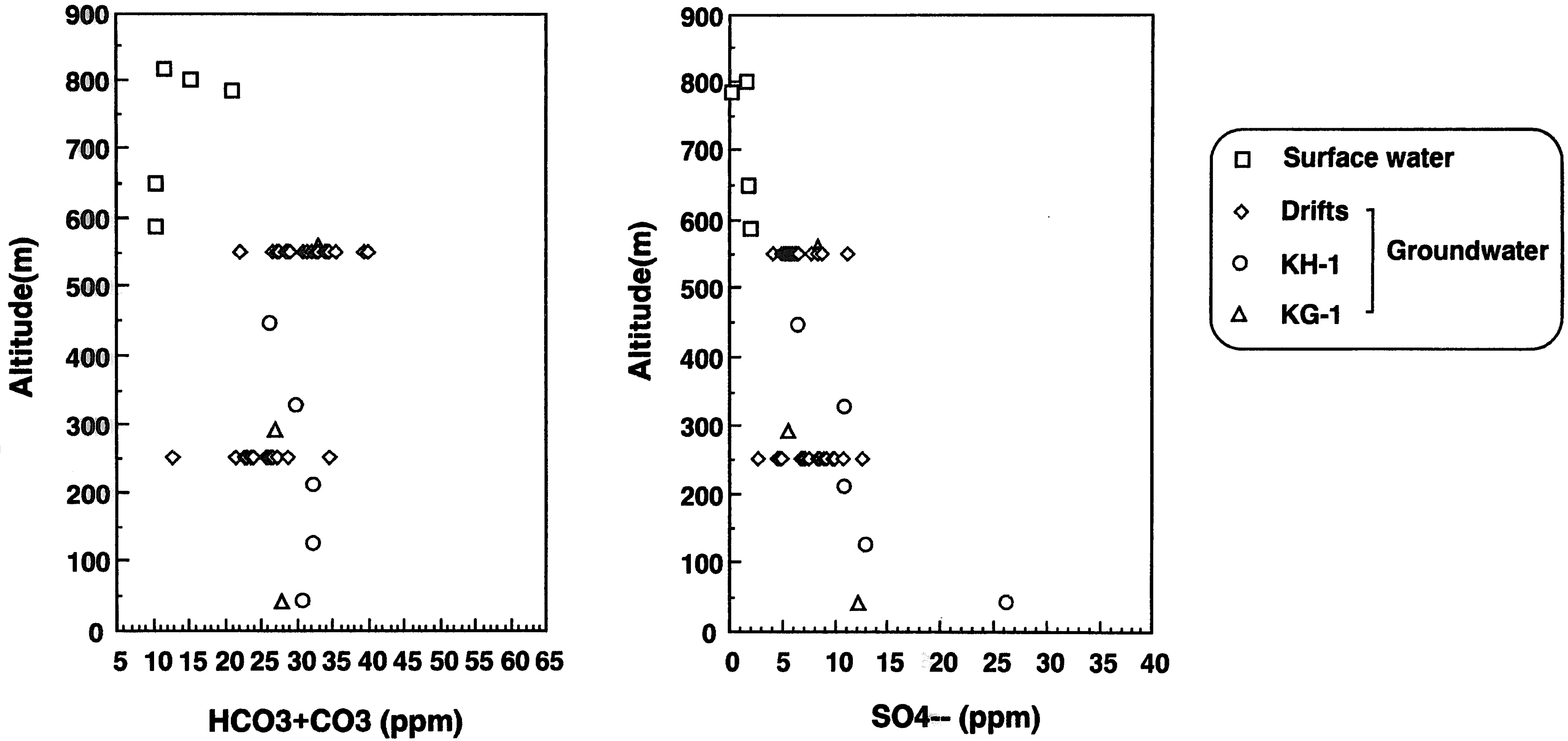

***Figure 9** : Variation of carbonate and sulfate concentration for the surface waters and groundwaters with depth in the Kurihashi granodiorite.*

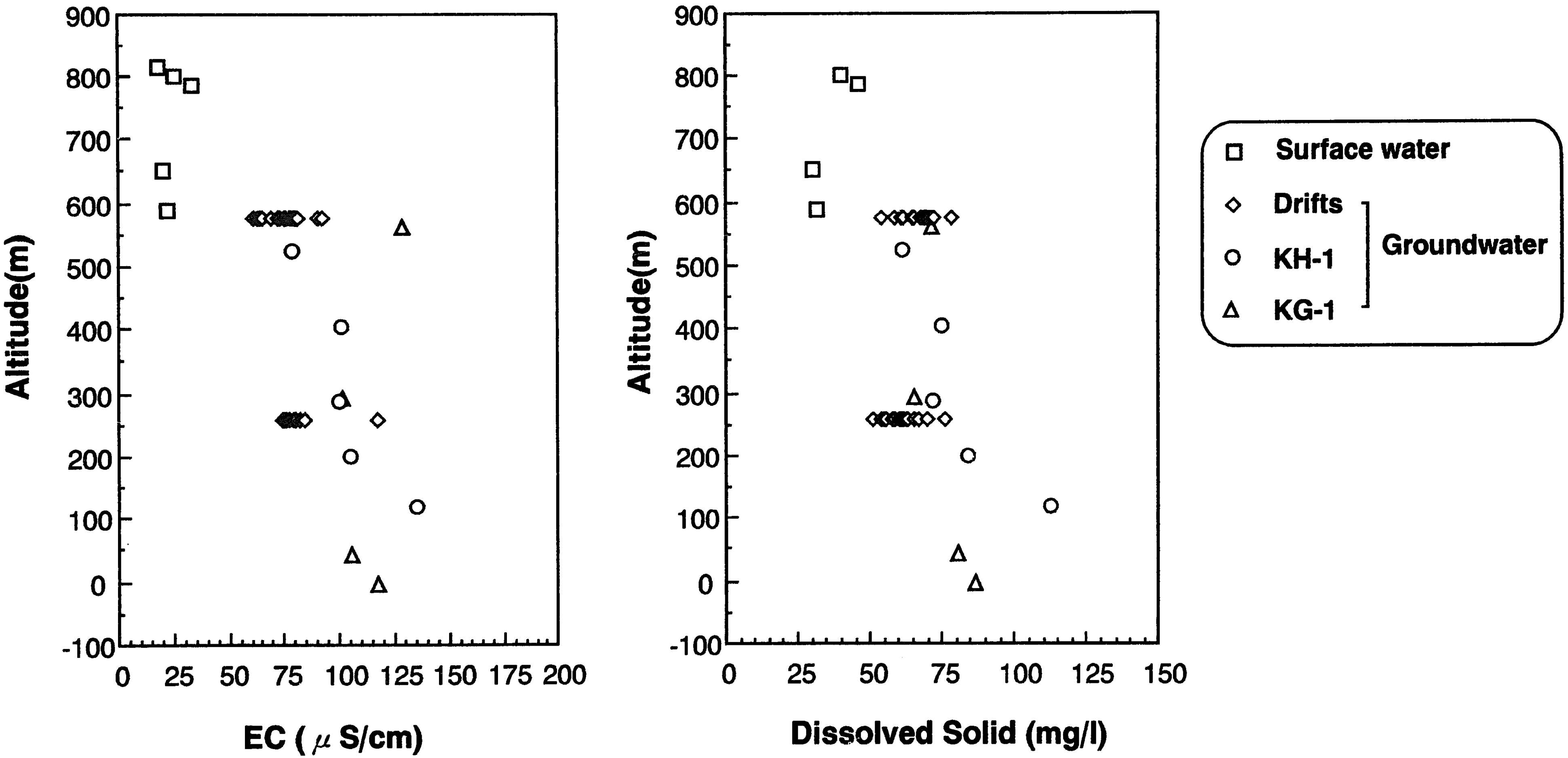

***Figure 10** : Variation of EC and dissolved solid for the surface waters and groundwaters with depth in the Kurihashi granodiorite.*

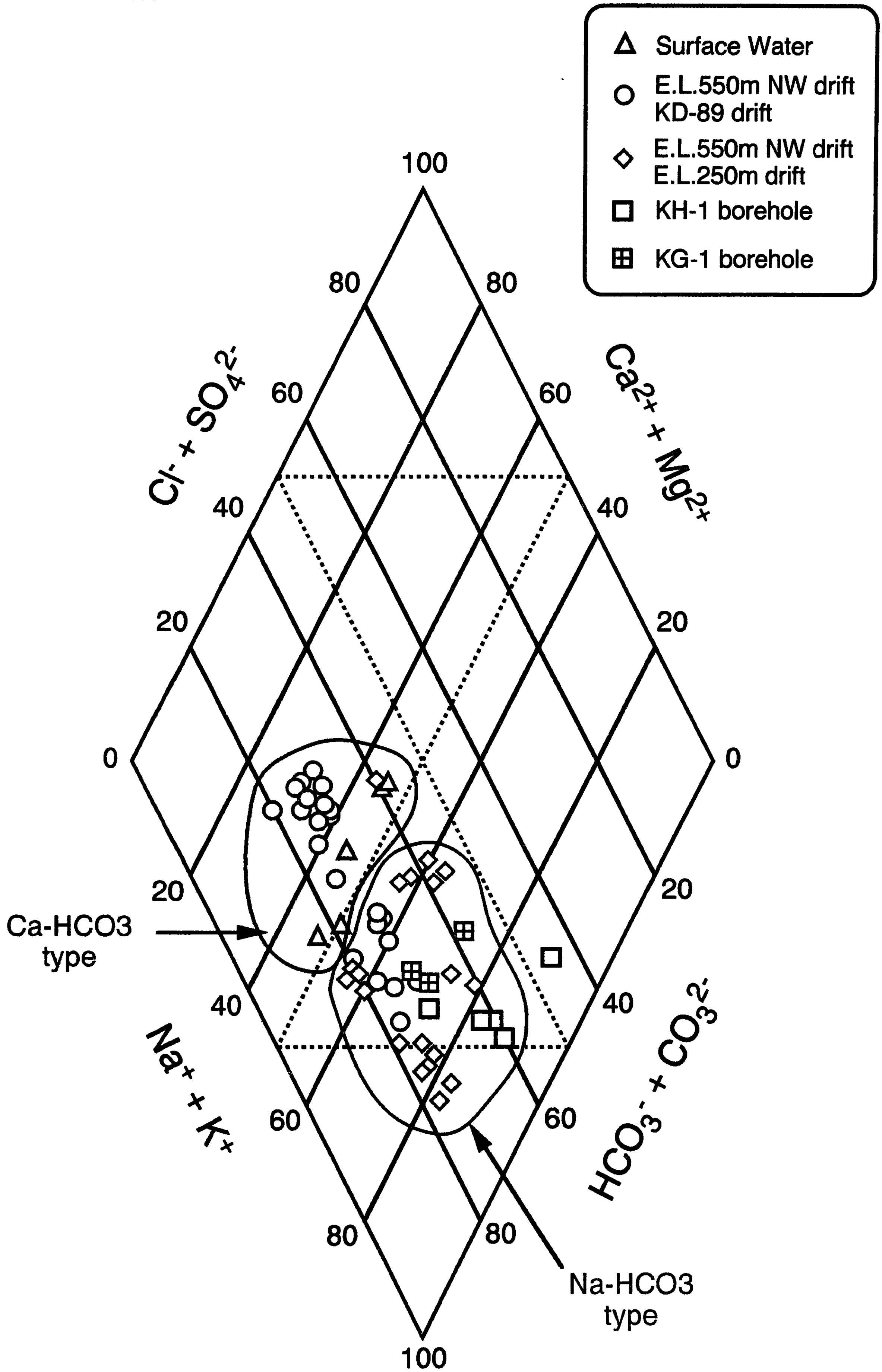

Figure 11 : Piper plot of the chemical composition of the surface waters and groundwaters in the Kurihashi granodiorite.

25°C are shown in Figure 12. These diagrams were drawn using thermodynamic data from Stumm and Morgan (1981). Symbols refer to the compositions of Kamaishi groundwaters represented in terms of the activities and activity ratios shown on X and Y axes. As can be seen, trends among these data suggest that Kamaishi groundwaters equilibrate initially with kaolinite, and later with albite and anorthite. Feldspar, which is a common rock-forming mineral in the Kurihashi granodiorite, is a solid-solution mineral whose endmember components are stoichiometrically equivalent to albite ($NaAlSi_3O_8$) and anorthite ($CaAl_2Si_2O_8$). For the Na_2O-Al_2O_3-SiO_2-H_2O system, surface waters and shallow groundwaters (Ca-HCO_3 type) plot within the stability field of kaolinite, suggesting that these waters equilibrate with kaolinite as albite continues to dissolve irreversibly. This causes the Na^+ concentration and pH to increase. Deeper groundwaters (predominantly Na-HCO_3 type) plot near the stability boundary of albite and kaolinite, suggesting that the concentration of Na^+ and pH in these solutions are controlled by equilibrium with these two minerals. Other deep groundwaters plot within the stability field of albite. Equilibration of these deep groundwaters with albite thus appears to control Na^+ concentrations in these solutions. Similar trends for the CaO-Al_2O_3-SiO_2-H_2O system (Figure 12) suggest Kamaishi groundwaters equilibrate initially with kaolinite, then with anorthite-kaolinite, and finally with anorthite as they migrate from the surface to deeper regions of the Kurihashi granodiorite.

2.3.7.2 Saturation Indices of Minerals

A useful test of the equilibrium status of mineral-groundwater reactions can be obtained by calculating the Saturation Index (SI) for each reaction of interest. The SI (dimensionless) is given by log (IAP/K), where IAP denotes the Ion Activity Product and K refers to the solubility product (i.e., equilibrium constant) for the reaction. Equilibrium is indicated when SI = 0. If SI > 0, then the groundwater composition is supersaturated with respect to equilibrium conditions (i.e., precipitation is required to achieve equilibrium), and if SI < 0, then the groundwater composition is undersaturated with respect to equilibrium conditions (dissolution is required to achieve equilibrium).

Figures 13-1 to 13-3 indicate saturation indices for several minerals in the Kurihashi granodiorite that could react with groundwaters at the Kamaishi site that were calculated using EQ3NR (Wolery, 1983) and its supporting thermodynamic database, DATA0.3245R54. The hatched zones in the figures, centered on SI = 0, refer to equilibrium conditions evaluated in this study, taking into account uncertainties that are inherent in such calculations. These uncertainties arise from both uncertainties in thermodynamic data and other uncertainties

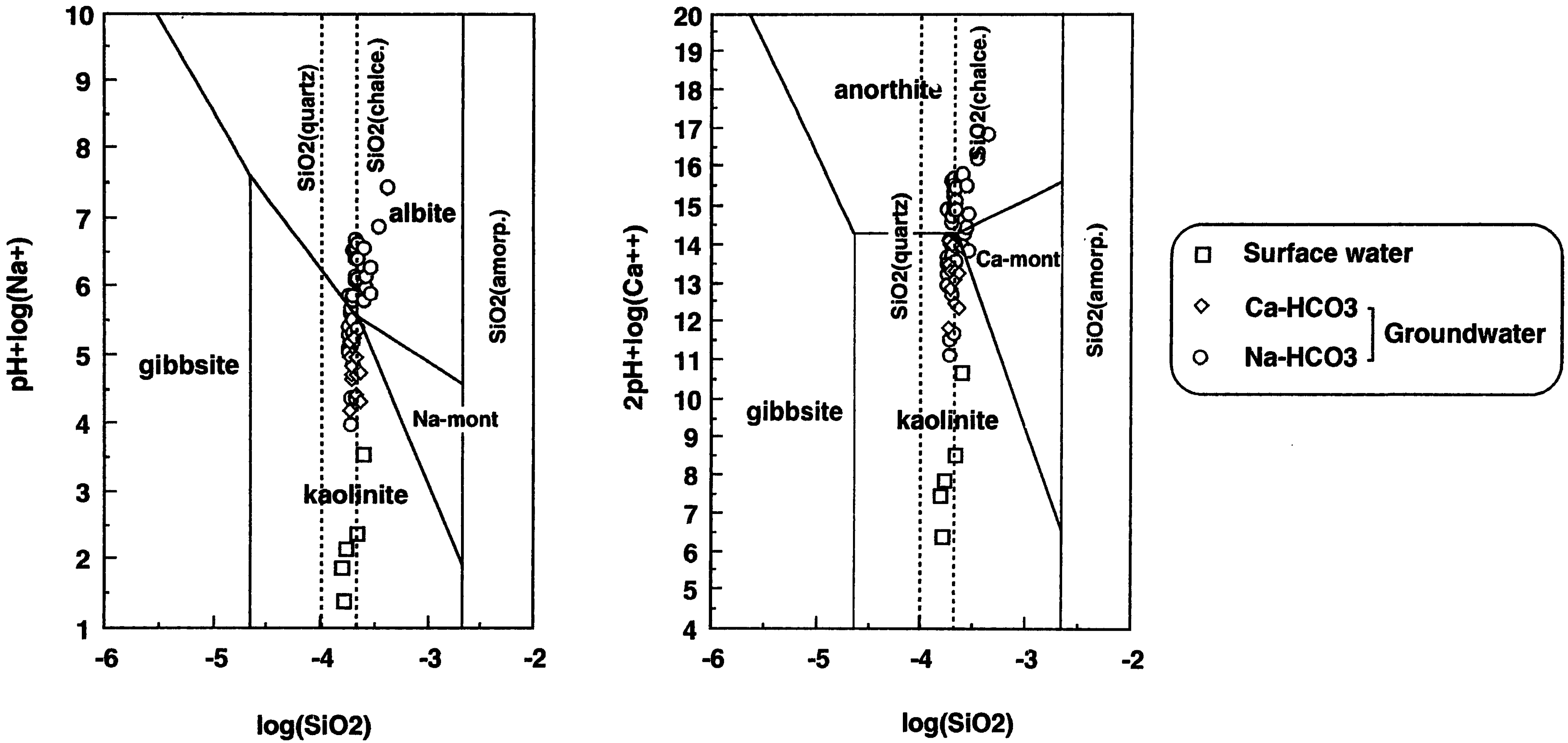

Figure 12 : Stabiliy diagram for Na2O-Al2O3-SiO2-H2O system and CaO-Al2O3-SiO2-H2O system at 25℃, 1 bar with plotted chemical analysis of Kamaishi groundwaters and surface waters. The thermodynamic data used are derived from Stumm and Morgan (1981).

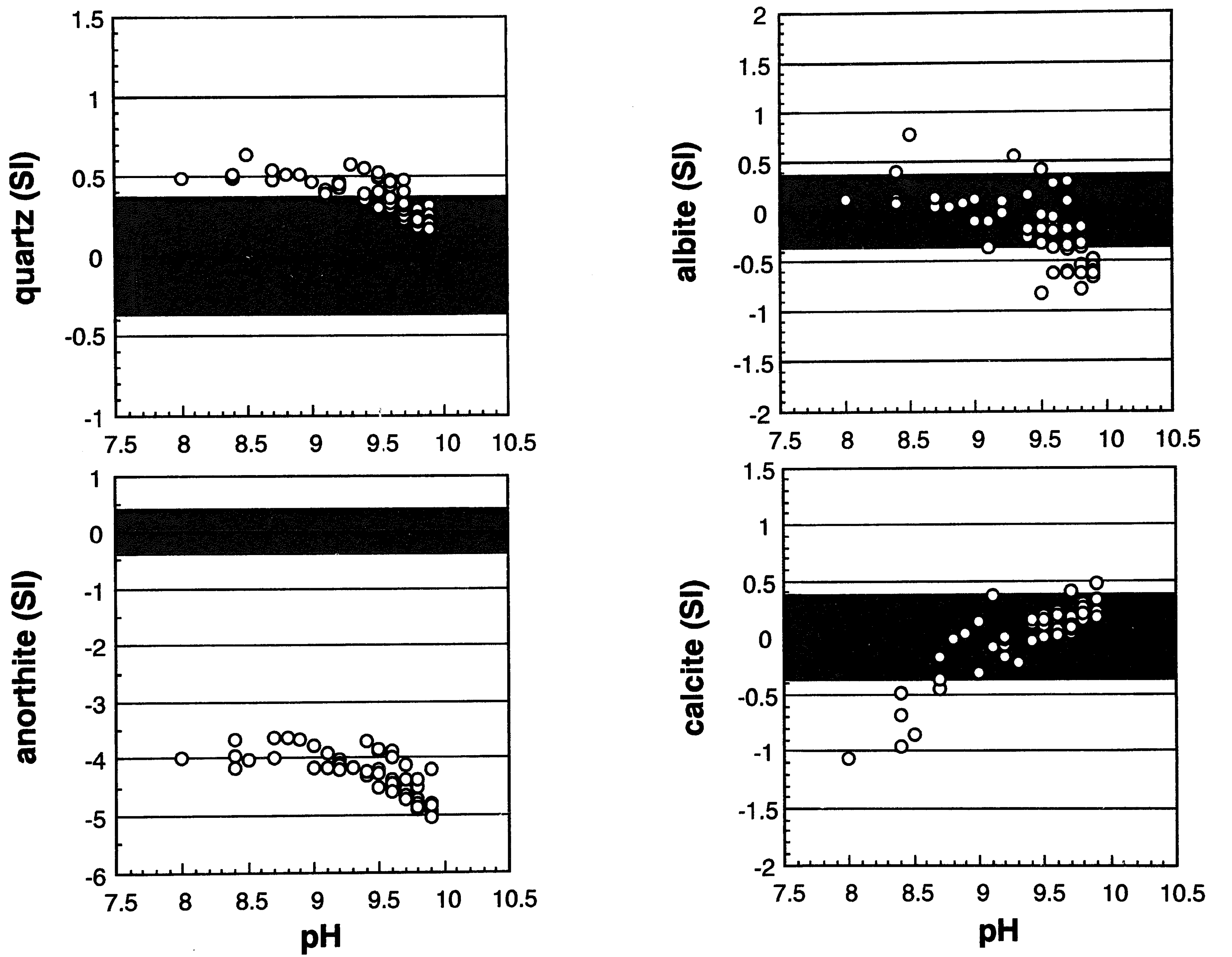

Figure 13-1 : Saturation Index calculated by EQ3NR for constituent minerals of Kurihashi Granodiorite [1]

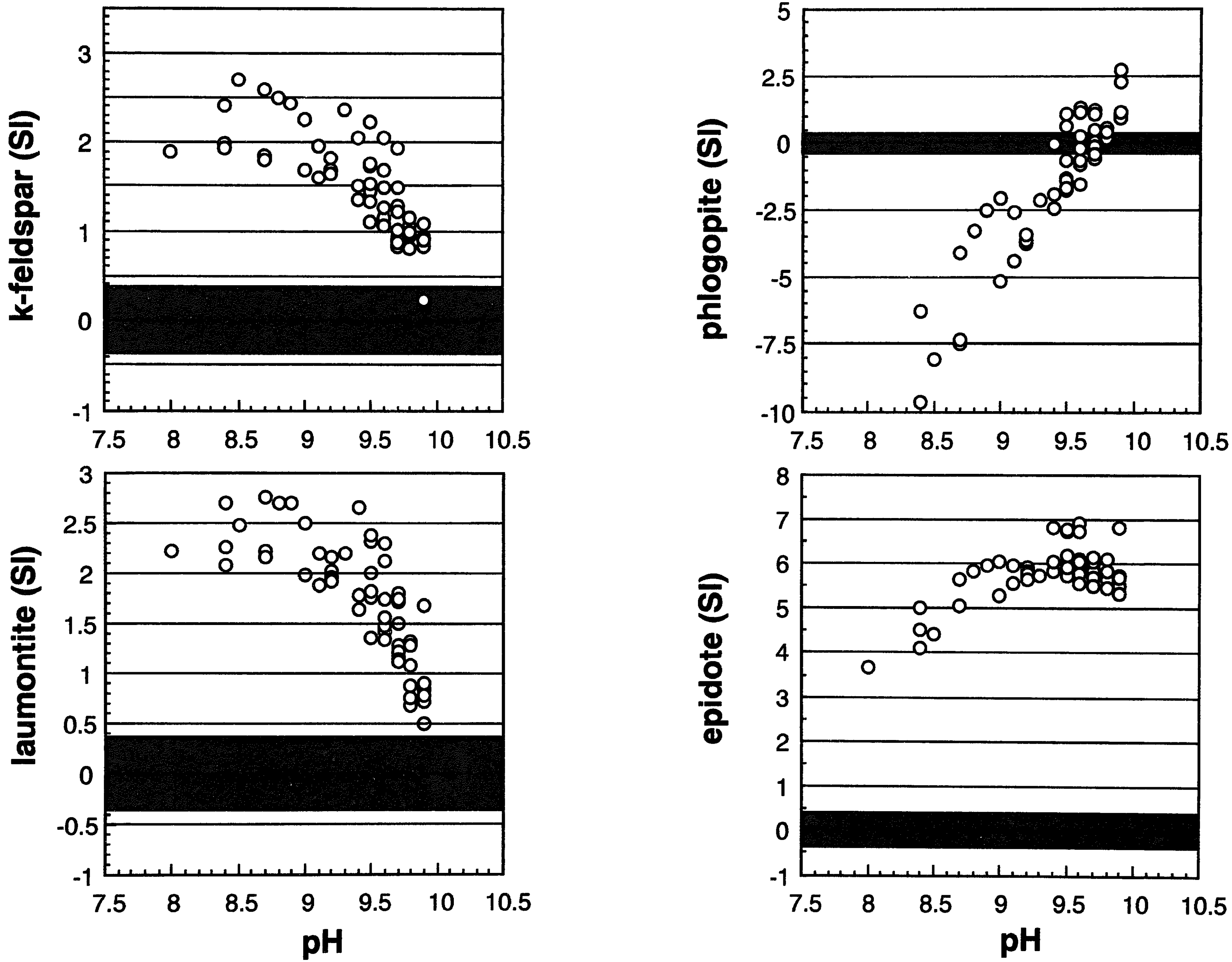

***Figure 13-2** : Saturation Index calculated by EQ3NR for constituent minerals of Kurihashi Granodiorite [2]*

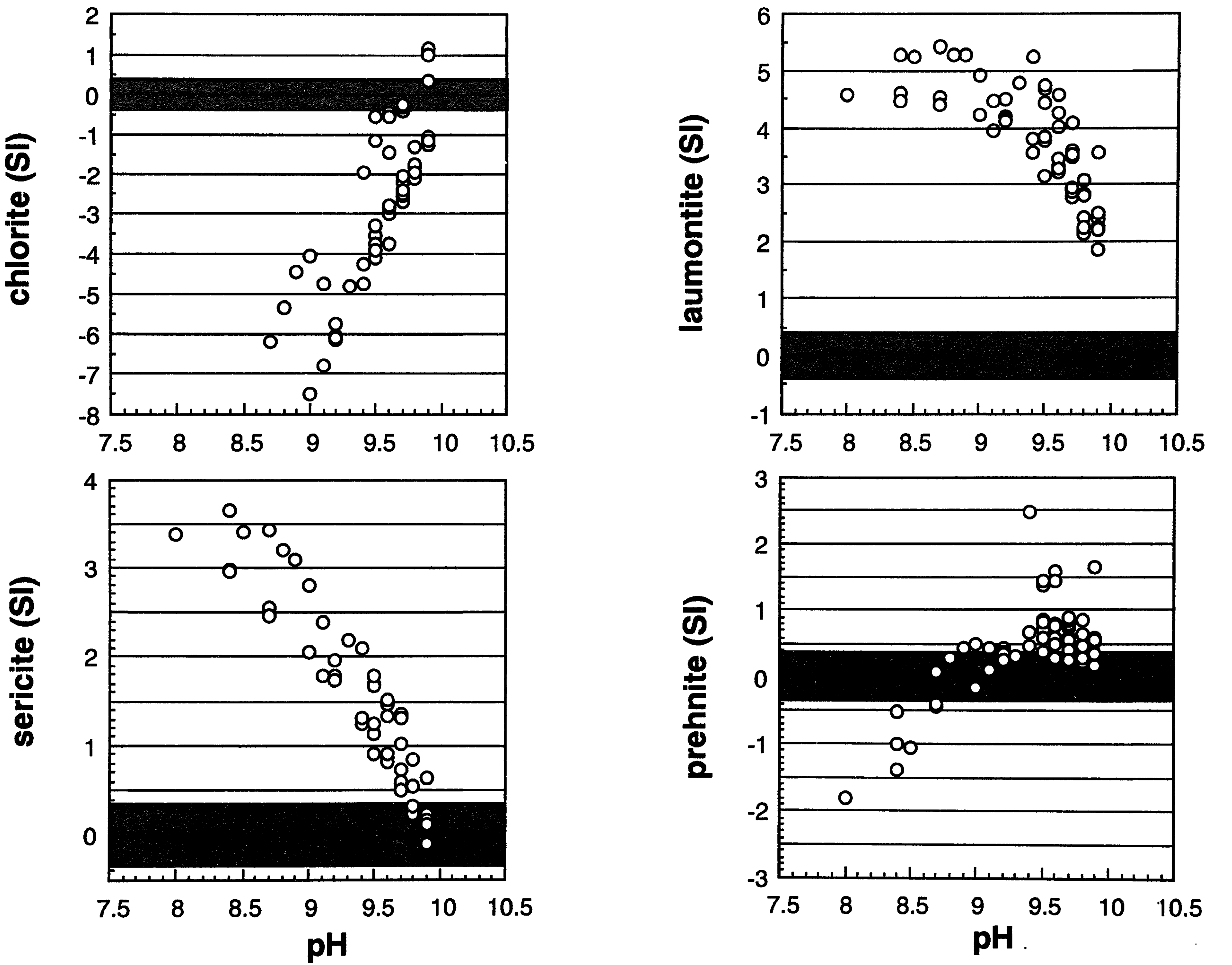

***Figure 13-3** : Saturation Index calculated by EQ3NR for constituent minerals of Kurihashi Granodiorite [3]*

associated with chemical analyses of groundwater samples. Uncertainty limits on saturation indices in the range of ±0.1 to ±1 are probably not unreasonable (Wolery, 1983), and a value of ±0.37 is probably realistic for many of the common rock-forming minerals (Paces, 1972; T. Wolery, *pers. comm.*). Thus as a first approximation, a calculated saturation index in the range 0.37 to -0.37 is taken in the present study to indicate that the respective mineral is in equilibrium with the groundwater, given the uncertainties noted above.

The results of the SI calculations shown in Figures 13-1 to 13-3 are summarized as follows:

- Quartz (SiO_2); Kamaishi groundwaters are close to saturation when the pH is greater than about 9, but slightly oversaturated when pH < 9 [most groundwaters are saturated with respect to chalcedony (SI between -0.167 and 0.465, averaging 0.1213)],
- Albite ($NaAlSi_3O_8$); most groundwaters are close to saturation when pH is in the range 8 to 10, but some groundwaters are undersaturated when pH > 9.5,
- Anorthite ($CaAl_2Si_2O_8$); groundwaters are undersaturated over the pH range 8 to 10,
- Calcite ($CaCO_3$); groundwaters are undersaturated when pH < 8.5, but saturated when pH > 8.5,
- K-feldspar ($KAlSi_3O_8$); most groundwaters are oversaturated in the pH range 8 to 10,
- Phlogopite [$K_2Mg_6(Si_6Al_2)O_{20}(OH)_4$]; the SI increases from pH 8 to pH 10, and groundwaters are near saturation when pH = 9.5,
- Laumontite ($CaAl_2Si_4O_{12}\cdot 4H_2O$); groundwaters are oversaturated in the pH range 8 to 10, but approach saturation with increasing pH,
- Epidote [$Ca_2Al_2Fe^{3+}Si_3O_{12}(OH)$]; groundwaters are undersaturated in the pH range 8 to 10,
- Chlorite [Clinochlore-14a, $Mg_5Al_2Si_3O_{10}(OH)_8$]; The SI of chlorite increases with increasing pH between pH 8 and pH 10, and are close to saturation near pH = 9.5,
- Stilbite [$CaAl_2Si_7O_{11}(OH)_{14}$]; groundwaters are undersaturated over the pH range 8 to 10,
- Sericite [$K_{0.6}Mg_{0.25}Al_{2.3}Si_{3.5}O_{10}(OH)_2$]; the SI of sericite decreases between pH 8 and pH 10. The groundwaters are close to saturation near pH 10, and
- Prehnite [$Ca_2Al_2Si_3O_{10}(OH)_2$]; groundwaters are undersaturated below pH 8.5, but most groundwaters are saturated when pH > 8.5.

Dolomite and gypsum have not been identified in the Kurihashi granodiorite, and this is consistent with saturation indices calculated for these minerals [i.e., SI for dolomite = -0.473 to -3.883, averaging -1.408); SI for gypsum = -3.279 to -4.398, averaging -3.716)].

2.3.8 Redox Conditions in Groundwaters of the Kurihashi Granodiorite

The redox conditions of groundwaters are generally controlled by water-rock interactions, but chemical equilibrium may not be attained among all the minerals present and the groundwaters (Wikberg, 1988). It is also difficult to obtain reproducible, drift-free Eh measurements in the field because groundwater samples are easily contaminated by atmospheric oxygen. To obtain stable physico-chemical measurements (especially Eh) in groundwater samples from the Kurihashi granodiorite, we used a continuous monitoring system (Figure 14). The monitoring point is located in the TK-24 borehole, which was drilled 20 years ago from the floor of the E.L. 250m drift as part of mining activities. A packer was installed near the entrance of the borehole to prevent contact of the groundwater with the ambient atmosphere (Figure 14). After a period of continuous monitoring (about 1 month), stable measurements were obtained. The results are summarized as follows:

Temp = 16°C,
pH = 9.0,
Eh (Pt electrode, *vs.*SHE) = -244 mV,
Eh (Au electrode, *vs.*SHE) = -245 mV,
EC = 104μS/cm, and
DO ≈ 0.01 mg/L (2 February, 1996)

Continuous monitoring of TK-24 groundwaters for temperature, EC and DO from 2 February 1996 to 24 December 1997 revealed little change in these parameters. In contrast, the pH varied from 9.0 to 9.8, and Eh ranged from -240mV to -320mV, during this monitoring period. Despite these variations, it is clear that the TK-24 groundwaters are reducing, and it is reasonable to assume more generally that deep groundwaters in the Kurihashi granodiorite are also reducing.

The redox state of groundwaters in the Kurihashi granodiorite has also been investigated as part of companion studies on the microbiological characteristics of these solutions (Aoki et al., 1997; Sasamoto et al., 1996). Sasamoto et al. (1996) measured the Eh of groundwaters in the KG-1 borehole using an HGP-10 *in-situ* sensor (Hydro-Geochemical and Piezometric logger system for deep boreholes, developed by Shimizu Corporation; Shimada et al., 1990). The measured Eh of groundwaters from the KG-1-2 (GL -489 to -495m sampling interval) was -176 mV (Au electrode, *vs.*SHE). Sulfate-reducing bacteria (SRB) were found in these samples, and identified as the type Desulfovibrio (Sasamoto et al., 1996). Fukunaga et al. (1995) carried

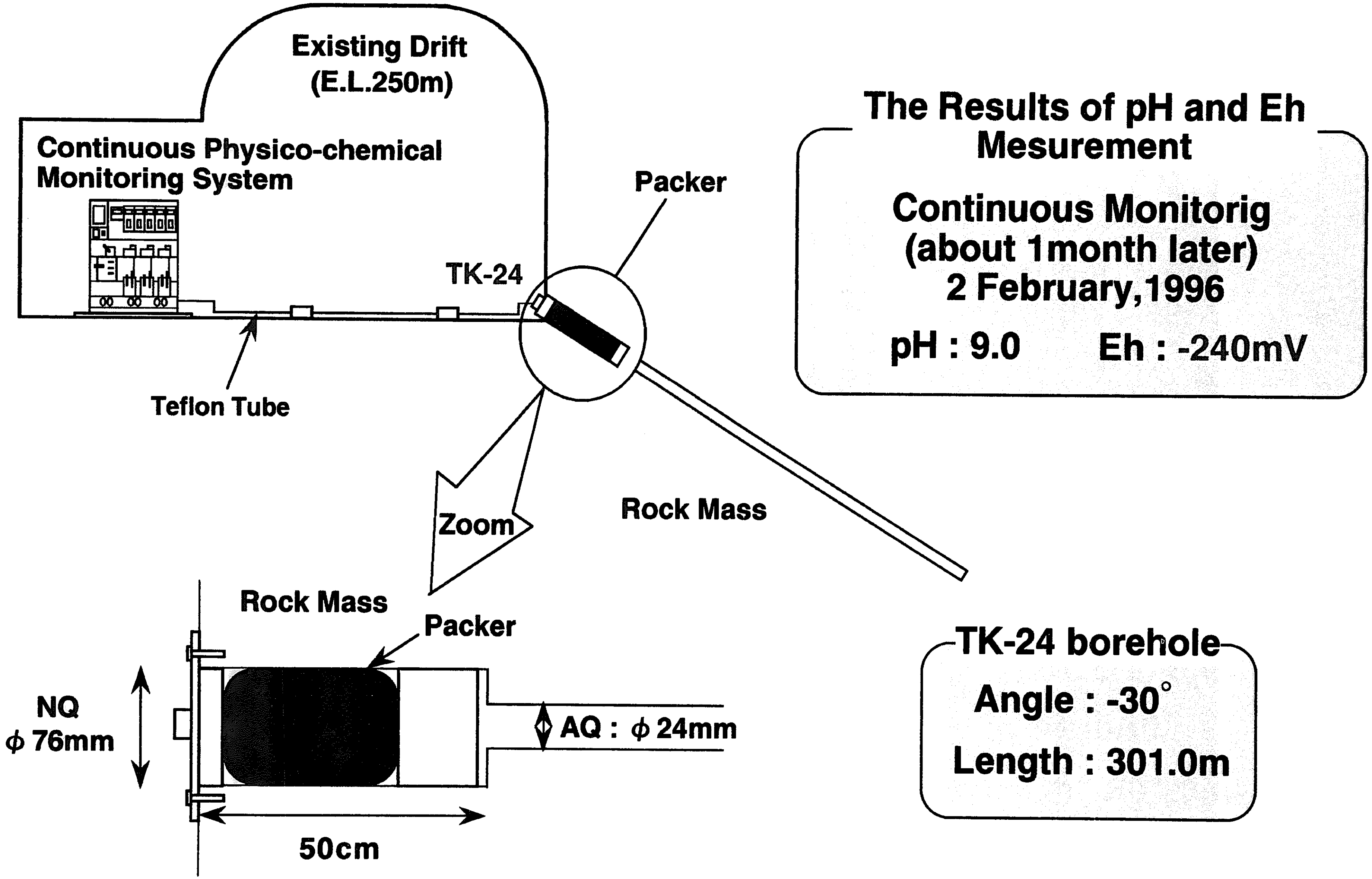

***Figure 14** : Layout of single packer system and continuous physico-chemical parameters monitoring system of groundwater at TK-24 borehole in the Kurihashi granodiorite.*

out laboratory experiments to ascertain the possible range of pH and Eh conditions required to sustain sulfate-reducing bacteria (Figure 15). The SRB considered in these experiments were the Desulfovibrio type identified in KG-1-2 groundwaters. The experiments were carried out at 35°C, which is higher than the actual groundwater temperature (approximately 13°C), but this difference in temperature probably has little impact on the SRB activity. The Eh estimated from SRB activities observed in the experiments (Figure 15) is between -300 to -400 mV (*vs*.SHE), if it assumed that the pH is equal to the value measured in KG-1-2 groundwaters (pH = 9.97). This is slightly lower than the *in-situ* measurements noted above, but both results indicate that deep groundwaters in the Kurihashi granodiorite are reducing.

2.4 Hydraulic Conditions

Pore water pressures were measured by JNC as a function of depth in the KG-1 borehole. Fujita et al. (1994) found that the distribution of pore water pressures with increasing depth does not correspond to hydrostatic conditions, although pressures do gradually increase as depth increases (Figure 16). The apparent disturbance of hydraulic conditions may affect groundwater chemistry, but this has not been determined conclusively at the Kamaishi site. It is nevertheless important to bear this in mind because the disturbance in hydraulic conditions may have caused the groundwater flow rate from the surface to the sub-surface to increase. If so, this may affect assumptions noted below in the equilibrium-based geochemical models.

2.5 Groundwater Evolution Modeling

Models of groundwater evolution at the Stripa site in Sweden, which is a granitic system at low temperatures (10°C), are described by Grimaud et al. (1990). These authors modeled the evolution of chemical conditions in Stripa groundwaters by assuming equilibrium for selected mineral-water reactions. JNC adopted this approach to derive "*generic*" (i.e., not site specific) groundwater compositions for the first performance assessment progress report (i.e., the H-3 report; PNC, 1992). We extend this approach in the present study to model the chemistry of groundwaters in the Kurihashi granodiorite, and compare results with the "*real*" groundwater chemistry measured at this site.

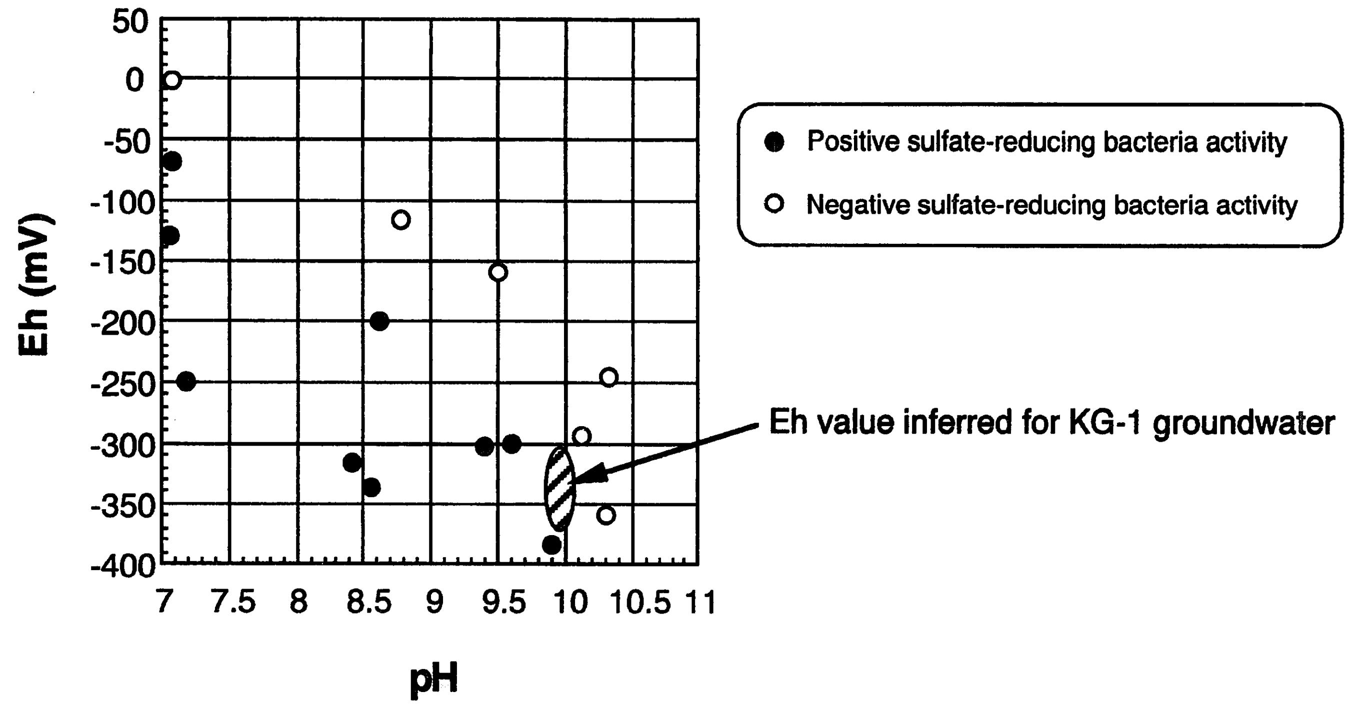

***Figure 15** ; Active range of sulfate reducing bacteria (Desulfovibrio desulfuricans) at 35 ℃ with lactate as an electron donor (from Fukunaga et al., 1995). The area hatched is Eh value inferred for the groundwater of KG-1-2 section based on the measured pH value and the SRB activity.*

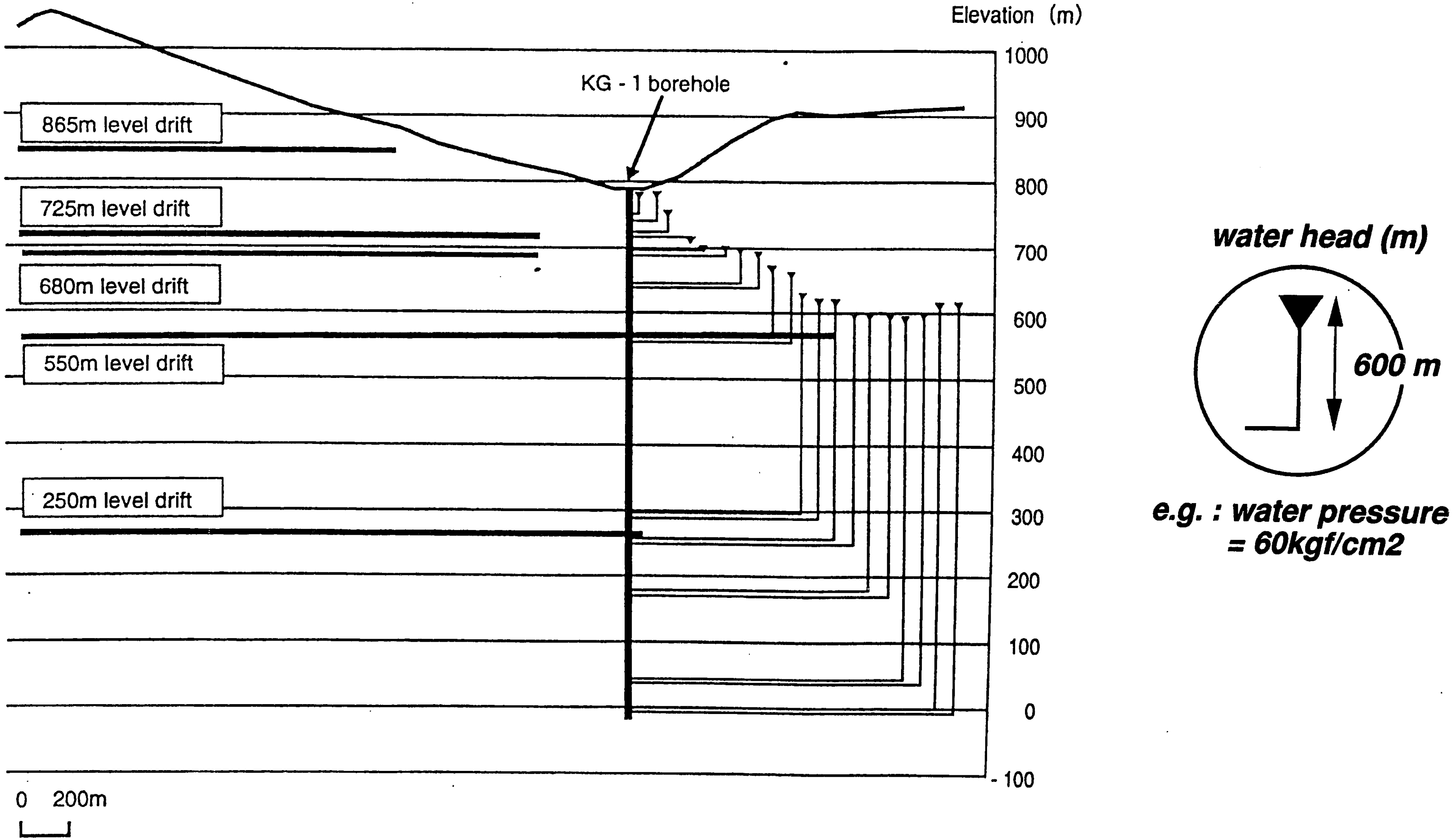

Figure 16 : Distribution of pore water pressure along the depth from the surface at KG-1 borehole

2.5.1 Reference Chemistry of Groundwater in the Kurihashi Granodiorite

A reference groundwater composition was defined for purposes of testing the groundwater evolution model based on observed compositions of groundwaters in the Kurihashi granodiorite. Parameters that were assumed to be controlled by water-rock interactions include physico-chemical parameters (pH, Eh), concentrations of major cations and anions (Na, Ca, K, carbonate, sulfate) and dissolved silica concentrations. The results of continuous monitoring of physico-chemical parameters in the TK-24 borehole, where stable pH and Eh values were determined, were used to select values of these parameters for the reference groundwater (Table 5). The average composition of groundwater samples from the KH-1 borehole (Table 5), which appear to be considerably older than most other groundwaters in the Kurihashi granodiorite, was used to define values of the other parameters in the reference groundwater. The reference groundwater chemistry is given in Table 6. It is similar to a type of groundwater, referred to as FRHP (Fresh-Reducing-High-pH), which appears to be characteristic of many deep subsurface environments in Japan (Yui et al., 1999).

2.5.2 Modeling

2.5.2.1 Conceptual Groundwater Evolution Model

A conceptual groundwater evolution model for the Kamaishi site was developed based on JNC's preliminary conceptual model for the FRHP-type reference groundwater (Yui et al., 1999). A schematic diagram identifying the key processes considered in the model is shown in Figure 17. As can be seen, the model assumes that the primary source of Kamaishi groundwaters is rain water. Carbon dioxide, produced by the decomposition of organic matter, dissolves into these solutions as they infiltrate into the soil zone, and the partial pressure of CO_2(g) therefore increases. The pH, Eh and ion concentrations of the groundwater are then controlled by a reasonable set of mineral-water interactions.

2.5.2.2 Assumptions

The following assumptions and dominant reactions are assumed in the conceptual model (Figure 17):

- rain water; pure water equilibrated with the atmosphere – as a result pH = 5.66, log PCO_2 = -3.5, log PO_2 = -0.7, and

Table 5 : *The reference groundwater chemistry of TK-24 and KH-1 boreholes in the Kurihashi granodiorite*

	TK-24 (Ave.)	KH-1-2 (Ave.)	KH-1-3 (Ave.)	KH-1-4 (Ave.)	KH-1-5 (Ave.)	KH-1 (Ave.)
pH	9.0-9.8	9.30	9.20	9.00	9.30	9.20
pe	-4.6 ~ -5.4	2.88	2.75	2.88	1.86	2.59
Eh (mV)	-240 ~ -320	170	162	170	110	153
H4SiO4 (mol/l)	2.68E-04	2.66E-04	2.57E-04	2.78E-04	4.40E-04	3.10E-04
H4SiO4 (mg/l)	25.77	26.58	24.73	26.70	42.24	29.81
Si (mg/l)	7.54	7.48	7.23	7.81	12.35	8.72
Na (mol/l)	2.41E-04	7.08E-04	6.85E-04	7.99E-04	9.30E-04	7.80E-04
Na (mg/l)	5.55	16.27	15.75	18.37	21.38	17.94
Ca (mol/l)	2.12E-04	7.01E-05	7.01E-05	6.79E-05	1.18E-04	8.15E-05
Ca (mg/l)	8.51	2.81	2.81	2.72	4.73	3.27
K (mol/l)	4.09E-06	8.18E-06	9.46E-06	1.51E-05	1.48E-05	1.19E-05
K (mg/l)	0.16	0.32	0.37	0.59	0.58	0.47
Mg (mol/l)	1.23E-06	4.11E-07	4.11E-07	4.11E-07	4.11E-07	4.11E-07
Mg (mg/l)	0.03	0.01	0.01	0.01	0.01	0.01
Fe (mol/l)	-	-	-	-	-	-
Fe (mg/l)	-	-	-	-	-	-
Al (mol/l)	3.71E-06	3.71E-06	3.71E-06	3.71E-06	3.71E-06	3.71E-06
Al (mg/l)	0.10	0.10	0.10	0.10	0.10	0.10
HCO3- (mol/l)	1.92E-04	4.25E-04	5.02E-04	5.02E-04	4.56E-04	4.72E-04
HCO3- (mg/l)	11.71	25.95	30.65	30.65	27.80	28.76
CO3-- (mol/l)	2.65E-05	6.35E-05	2.58E-05	2.58E-05	5.00E-05	4.13E-05
CO3-- (mg/l)	1.59	3.81	1.55	1.55	3.00	2.48
HCO3- + CO3-- (mol/l)	2.18E-04	4.89E-04	5.28E-04	5.28E-04	5.06E-04	5.13E-04
HCO3- + CO3-- (mg/l)	13.30	29.76	32.20	32.20	30.80	31.24
SO4-- (mol/l)	1.33E-04	1.13E-04	1.14E-04	1.33E-04	2.74E-04	1.59E-04
SO4-- (mg/l)	12.77	10.86	10.91	12.81	26.29	15.22
log PCO2	-4.92 (pH=9.0)	-4.87	-4.70	-4.50	-4.84	-
	-5.72 (pH=9.8)					

Table 6 : Reference groundwater chemistry in the Kurihashi granodiorite for comparison with modeling results

Locality :	*TK-24*	*KH-1* **
Temp. (℃)	16 *	12.5
pH	9.0 - 9.8 *	9.2
Eh (mV)	-240 ~ -320 *	153
Na (mg/l)	5.55	17.94
Si (mg/l)	7.53	8.71
Ca (mg/l)	8.51	3.27
K (mg/l)	0.16	0.47
Mg (mg/l)	0.03	0.01
Al (mg/l)	< 0.10	< 0.10
T.Fe (mg/l)	< 0.02	< 0.02
HCO_3^- (mg/l)	11.71	28.76
CO_3^{2-} (mg/l)	1.59	2.48
SO_4^{2-} (mg/l)	12.77	15.22
Cl^- (mg/l)	2.05	2.22

** : Temp, pH and Eh of TK-24 groundwater were measured by continuous physico-chimical monitoring system. In case of KH-1 groundwater, temp, pH and Eh were measured under contacting atmosphere.*

*** : Chemical composition of KH-1 groundwater is average data of 4 packed-off section (tritium concentration is less than 1 T.U.)*

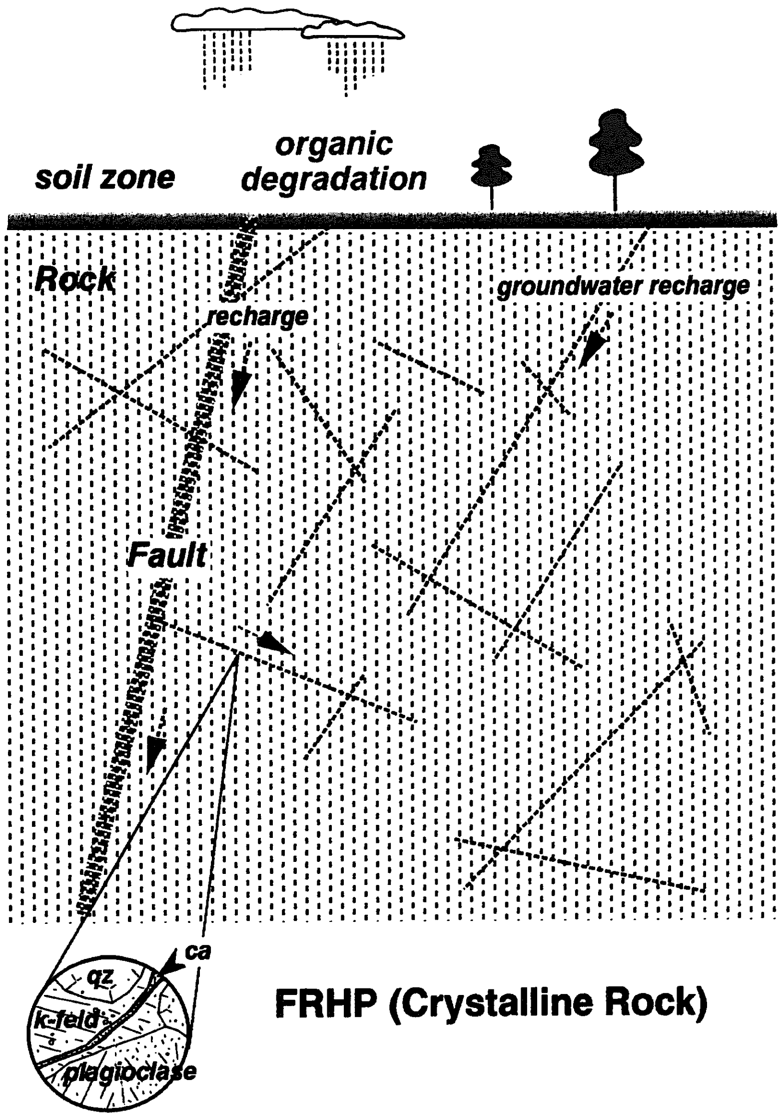

FRHP (Crystalline Rock)

- rain water : equilibrium with atmospher
logPCO2=-3.5, logO2=-0.7

- soil zone : logPCO2=-3.5, -2.0, -1.0

- rock zone : main mineral compositon

rock matrix : quartz, plagioclase, biotite
k-feld, hornblend, chlorite
sericite, sphene, magnetite
epidote,

fracture fillings : calcite, stilbite, quartz
chlorite, laumontite
plagioclase, epidote
hornblend, sericite
prehnite

dissemination : pyrite, pyrrhotite
chalcopyrite

Figure 17 *: Conceptual groundwater evolution model in the Kurihashi granodiorite, assumptions for groundwater modeling in the soil zone and mineralogy in the rock zone.*

· soil zone; soil water – three partial pressures of CO_2 gas (log PCO_2 = -3.0, -2.0, -1.0) are assumed.

The adopted range of $CO_2(g)$ partial pressures is consistent with values observed in natural systems (Stumm and Morgan, 1981). To confirm that this range is also reasonable for conditions at Kamaishi, we sampled surface and soil waters at this site (Figure 18). The soil at Kamaishi is categorized as a brown forest soil or black soil (e.g., Matsumoto, 1989). We calculated $CO_2(g)$ partial pressures in surface waters, soil waters and groundwaters based on the following reaction and corresponding log K value.

$$CO_2(g) + H_2O = H^+ + HCO_3^-, \quad \log K = -7.814 \ (25\,^\circ C : \textit{Johnson et al., 1991})$$

The variation of calculated log PCO_2 values with increasing Na^+ concentration (roughly indicative of increasing water-rock interaction) is shown in Figure 19. As can be seen, the calculated values of log PCO_2 in surface and soil waters vary from -3.0 to -1.0, which is consistent with the range of values assumed in the conceptual model.

· rock zone – "equilibrium minerals" (i.e., minerals that are assumed to achieve equilibrium with the groundwater), and the respective ions whose concentrations are assumed to be fixed by solubility equilibrium, are shown in Figure 20 [note that the thermodynamic database (see below) supporting evaluations of this conceptual model does not include data for zeolites (e.g., laumontite)].

2.5.2.3 Geochemical Code and Thermodynamic Database

We used the PHREEQE geochemical code (Parkhurst et al., 1980) to evaluate the conceptual model discussed above. The thermodynamic database supporting PHREEQE is PNC H3.0 (Yui et al., 1992), which is based on the original PHREEQE database described by Parkhurst et al. (1980) and includes additional and revised data recommended by the OECD/NEA (e.g., Muller, 1985). Dissolution reactions and corresponding log K values for the equilibrium minerals considered in the conceptual model are given in Appendix E. Although the PNC H3.0 database specifies all equilibrium constants at 25°C, reaction enthalpies are unavailable for many aqueous association reactions and mineral-dissolution reactions. To eliminate associated errors in the calculations, the conceptual model is evaluated only for a temperature of 25°C.

Locality : near the surface of KG-1 borehole

physico-chemical parameter measurement
temp : 9.8 ℃ pH : 6.54,
Eh : 394mV, EC : 44.4 μ S/cm

***Figure 18** : Photograph of sampling of soil water around the Kamaishi in-situ tests site*

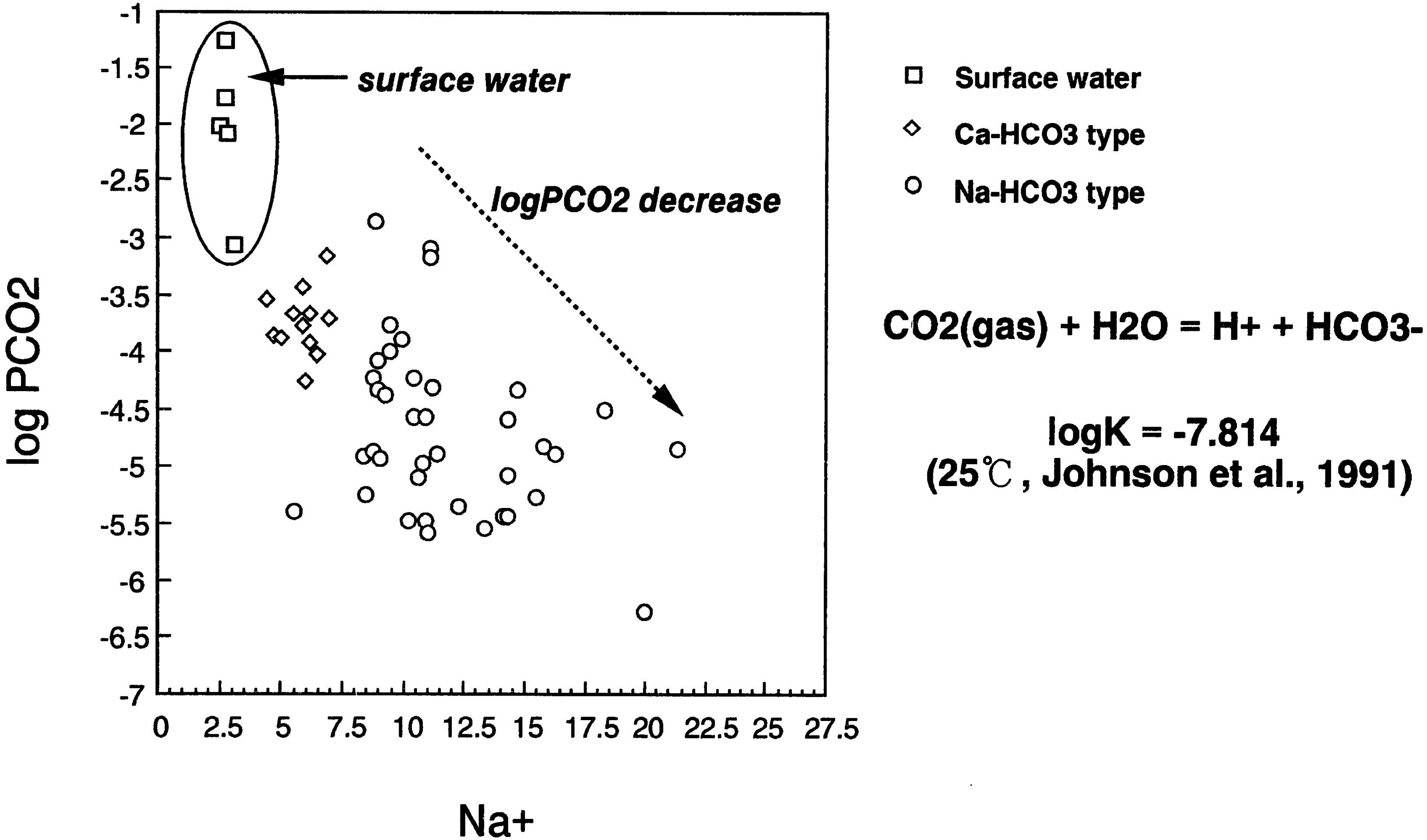

***Figure 19** : Calculated logPCO2 values for the surface waters and groundwaters in the Kurihashi granodiorite with Na+ concentration.*

Figure 20 : *Equilibrium minerals assumed for controlling the each concentration of groundwater in the Kurihashi granodiorite as test cases.*

Rock Zone

- Si : quartz, chalcedony
- Na : albite
- Al : kaolinite
- Ca : anorthite, calcite
- K : k-feldspar
  (orthoclase, microcline)
- Mg : biotite (phlogopite)
- Fe, Eh : magnetite, pyrite
- Sulfate : pyrite
- Carbonate : calcite

2.5.2.4 Calculation Cases

A number of variants based on the conceptual model illustrated in Figure 17 were considered in separate calculation cases, and are summarized below.

- rain water: pure water (pH = 7) equilibrated with the atmosphere
- soil zone: log PCO_2 = -3.0, -2.0, -1.0 (3 cases)
- rock zone: the following combinations (8 cases) of equilibrium minerals for K, Si and Ca concentrations were considered;

Case 1 : orthoclase, quartz, calcite
Case 2 : orthoclase, quartz, anorthite
Case 3 : orthoclase, chalcedony, calcite
Case 4 : orthoclase, chalcedony, anorthite
Case 5 : microcline, quartz, calcite
Case 6 : microcline, quartz, anorthite
Case 7 : microcline, chalcedony, calcite
Case 8 : microcline, chalcedony, anorthite

A number of test cases were then devised based on the above calculation cases to evaluate the effects of varying CO_2(g) partial pressures in the soil zone on dissolved carbonate concentrations in groundwater, and of variations in ionic concentrations in groundwater by mineral-water reactions in the rock zone. The test cases are summarized as follows:

1) Test 1 to Test 8;
- rain water - pure water (pH = 7) equilibrated with the atmosphere,
- soil zone - log PCO_2 = -1.0 (1 case),
- rock zone - Case 1 to Case 8 (8 cases),

2) Test 9 to Test 16;
- rain water - pure water (pH = 7) equilibrated with the atmosphere,
- soil zone - log PCO_2 = -2.0 (1 case),
- rock zone - Case 1 to Case 8 (8 cases),

3) Test 17 to Test 20;
- rain water - pure water (pH = 7) equilibrated with the atmosphere,

- soil zone - log PCO_2 = -3.0 (1 case),
- rock zone - Case 2, Case 4, Case 6 and Case 8 (4 cases),

4) Test 21;
- rain water - pure water (pH = 7) equilibrated with the atmosphere,
- soil zone - log PCO_2 = -2.5 (1 case),
- rock zone - Case 3 (1 case),

5) Test 22;
- rain water - pure water (pH = 7) equilibrated with the atmosphere,
- soil zone - log PCO_2 = -1.8 (1 case),
- rock zone - Case 3 (1 cases), and

6) Test 23;
- rain water - pure water (pH = 7) equilibrated with the atmosphere,
- soil zone - log PCO_2 = -1.5 (1 cases),
- rock zone - Case 3 (1 cases),

2.6 Results

The results of calculations based on the test cases described in Section 2.5.2.4 are documented in Tables 7-1 and 7-2. The effects on groundwater chemistry of reactions in the soil zone and rock zone are summarized below.

2.6.1 Reactions in the Soil Zone

The effects on carbonate concentrations in groundwater resulting from varying partial pressures of CO_2 gas (i.e., log PCO_2 value) in the soil zone are summarized as follows:

A: log PCO_2 = -1.0 (Table 7-1 : Test 1 to Test 8)
The calculated carbonate concentration of groundwater in the rock zone in this case is about 200 mg/L. This is significantly greater than the carbonate concentration (about 30 mg/L) measured in the reference groundwater in the Kurihashi granodiorite.

Table 7-1 : Modeling results by geochemical code PHREEQE (1)

		reference groundwater	Case 1 Test 1	Case 2 Test 2	Case 3 Test 3	Case 4 Test 4	Case 5 Test 5	Case 6 Test 6	Case 7 Test 7	Case 8 Test 8	Case 1 Test 9	Case 2 Test 10	Case 3 Test 11
rain water	pH	-	5.66								5.66		
	pe	-	. 14.95								14.95		
soil zone													
sample:aonoki	pH	6.54	4.41								4.91		
	pe	6.68	14.95								14.95		
	Eh (mV)	394	882								882		
	log PCO2	-2.71	-1.00								-2.00		
	HCO3- (mol/l)	9.08E-05	3.93E-05								1.24E-05		
	HCO3- (mg/l)	5.54	2.40								0.76		
	H2CO3 (mol/l)	8.94E-05	3.43E-03								3.43E-04		
	H2CO3 (mg/l)	5.54	212.35								21.24		
rock zone													
TK-24 borehole	pH	9.0-9.8	9.01	10.14	8.47	10.08	9.02	10.10	8.47	10.08	9.70	10.30	9.26
	pe	-4.6 ~ -5.4	-5.05	-6.36	-4.42	-6.33	-5.06	-6.35	-4.43	-6.33	-5.85	-6.58	-5.33
	Eh (mV)	-240 ~ -320	-298	-375	-261	-373	-299	-375	-261	-373	-345	-388	-315
KH-1 average	H4SiO4 (mol/l)	2.78E-04	1.66E-04	1.66E-04	3.23E-04	3.23E-04	1.66E-04	1.66E-04	3.23E-04	3.23E-04	1.66E-04	1.66E-04	3.24E-04
	H4SiO4 (mg/l)	29.81	15.92	15.92	31.05	31.03	15.92	15.92	31.05	31.03	15.94	15.94	31.08
	Na (mol/l)	7.80E-04	3.78E-03	3.11E-04	3.51E-03	8.64E-05	3.73E-03	3.11E-04	3.47E-03	8.64E-05	7.49E-04	1.91E-04	5.45E-04
	Na (mg/l)	17.94	86.99	7.15	80.62	1.99	85.80	7.15	79.73	1.99	17.22	4.40	12.53
	Ca (mol/l)	8.16E-05	2.94E-05	1.69E-03	9.74E-05	1.89E-03	2.90E-05	1.68E-03	9.63E-05	1.89E-03	5.25E-05	6.00E-04	1.10E-04
	Ca (mg/l)	3.27	1.18	67.57	3.90	75.63	1.16	67.49	3.86	75.63	2.10	24.04	4.39
	K (mol/l)	1.20E-05	7.92E-06	6.51E-07	7.34E-06	1.81E-07	6.49E-05	5.42E-06	6.03E-05	1.51E-06	1.57E-06	4.00E-07	1.14E-06
	K (mg/l)	0.47	0.31	0.03	0.29	0.01	2.54	0.21	2.36	0.06	0.06	0.02	0.04
	Mg (mol/l)	4.11E-07	8.27E-07	5.73E-09	1.03E-05	6.42E-09	3.97E-07	2.83E-09	4.95E-06	3.11E-09	3.06E-08	2.05E-09	2.34E-07
	Mg (mg/l)	0.01	0.02	0.00	0.25	0.00	0.01	0.00	0.12	0.00	0.00	0.00	0.01
	Fe (mol/l)	-	4.88E-05	1.29E-05	5.74E-05	1.36E-05	4.87E-05	1.29E-05	5.74E-05	1.36E-05	2.47E-05	7.02E-06	4.06E-05
	Fe (mg/l)	-	2.73	0.72	3.21	0.76	2.72	0.72	3.21	0.76	1.38	0.39	2.27
	Al (mol/l)	3.71E-06	2.31E-06	2.89E-05	3.35E-07	1.41E-05	2.43E-06	2.89E-05	3.39E-07	1.41E-05	1.10E-05	4.41E-05	2.03E-06
	Al (mg/l)	0.10	0.06	0.78	0.01	0.38	0.07	0.78	0.01	0.38	0.30	1.19	0.05
	HCO3- (mol/l)	4.71E-04	3.28E-03	1.20E-03	3.47E-03	1.19E-03	3.27E-03	1.20E-03	3.47E-03	1.19E-03	3.22E-04	1.25E-04	4.25E-04
	HCO3- (mg/l)	28.76	199.84	73.02	211.67	72.47	199.65	73.02	211.61	72.47	19.62	7.64	25.92
	CO3-- (mol/l)	4.13E-05	1.95E-04	9.14E-04	5.83E-05	8.65E-04	1.98E-04	9.15E-04	5.89E-05	8.65E-04	8.54E-05	1.37E-04	4.07E-05
	CO3-- (mg/l)	2.48	11.69	54.84	3.50	51.92	11.85	54.87	3.54	51.92	5.13	8.24	2.44
	HCO3+CO3 (mol/l)	5.13E-04	3.47E-03	2.11E-03	3.53E-03	2.05E-03	3.47E-03	2.11E-03	3.53E-03	2.05E-03	4.07E-04	2.63E-04	4.66E-04
	HCO3+CO3 (mg/l)	31.24	211.53	127.86	215.17	124.39	211.50	127.89	215.15	124.39	24.75	15.88	28.[illegible]6
	SO4-- (mol/l)	1.33E-04	1.22E-04	1.06E-04	1.21E-04	1.04E-04	1.22E-04	1.06E-04	1.21E-04	1.04E-04	1.23E-04	1.15E-04	1.22E-04
	SO4-- (mg/l)	12.81	11.73	10.16	11.64	10.01	11.73	10.16	11.64	10.01	11.83	11.02	11.72
	log PCO2	-4.53	-3.7103	-5.244	-3.1372	-5.2257	-3.7167	-5.2446	-3.1423	-5.2257	-5.3946	-6.4091	-4.8313
		calculated by pH=9											
	Minerals		orth,qz,cal	orht,qz,an	orth,chal,cal	orth,chal,an	micr,qz,cal	micr,qz,an	micr,chal,cal	micr,chal,an	orth,qz,cal	orht,qz,an	orth,chal,cal

Note : The abbreviations in the above table are as follows ; orth (orthocrase), qz (quartz), cal (calcite), an (anorthite), chal (chalcedony), micr (microcline)

Table 7-2 : *Modeling results by geochemical code PHREEQE (2)*

		Case 4 Test 12	Case 5 Test 13	Case 6 Test 14	Case 7 Test 15	Case 8 Test 16	Case 2 Test 17	Case 4 Test 18	Case 6 Test 19	Case 8 Test 20	Case 3 Test 21	Case3 Test 22	Case 3 Test 23
rain water	pH						5.66				5.66	5.66	5.66
	pe						14.95				14.95	14.95	14.95
soil zone													
	pH						5.41				5.16	4.81	4.66
	pe						14.95				14.95	14.95	14.95
	Eh (mV)						882				882	882	882
	log PCO2						-3.00				-2.50	-1.80	-1.50
	HCO3- (mol/l)						3.91E-06				6.96E-06	1.56E-05	2.21E-05
	HCO3- (mg/l)						0.24				0.42	0.95	1.35
	H2CO3 (mol/l)						3.43E-05				1.08E-04	5.43E-04	1.08E-03
	H2CO3 (mg/l)						2.12				6.71	33.65	67.15
rock zone													
	pH	10.24	9.71	10.32	9.26	10.24	10.35	10.27	10.35	10.27	9.45	9.14	8.91
	pe	-6.51	-5.86	-6.58	-5.34	-6.51	-6.64	-6.55	-6.64	-6.55	-5.56	-5.19	-4.93
	Eh (mV)	-384	-346	-388	-315	-384	-392	-386	392	-386	-328	-306	-291
	H4SiO4 (mol/l)	3.24E-04	1.66E-04	1.66E-04	3.24E-04	3.23E-04	1.66E-04	3.23E-04	1.66E-04	3.23E-04	3.24E-04	3.24E-04	3.23E-04
	H4SiO4 (mg/l)	31.15	15.94	15.94	31.08	31.07	15.94	31.07	15.94	31.07	31.08	31.08	31.07
	Na (mol/l)	5.84E-05	7.41E-04	1.91E-04	5.40E-04	5.84E-05	1.72E-04	5.42E-05	1.72E-04	5.42E-05	3.47E-04	7.26E-04	1.24E-03
	Na (mg/l)	1.34	17.04	4.39	12.41	1.34	3.95	1.25	3.94	1.25	7.98	16.69	28.44
	Ca (mol/l)	8.17E-04	5.21E-05	5.90E-04	1.09E-04	8.16E-04	4.78E-04	6.97E-04	4.77E-04	6.96E-04	1.34E-04	1.02E-04	9.55E-05
	Ca (mg/l)	32.72	2.09	23.64	4.36	32.71	19.14	27.92	19.11	27.91	5.38	4.08	3.83
	K (mol/l)	1.22E-07	1.29E-05	3.32E-06	9.38E-06	1.02E-06	3.59E-07	1.13E-07	2.98E-06	9.42E-07	7.26E-07	1.52E-06	2.59E-06
	K (mg/l)	0.00	0.50	0.13	0.37	0.04	0.01	0.00	0.12	0.04	0.03	0.06	0.10
	Mg (mol/l)	2.78E-09	1.48E-08	1.01E-09	1.14E-07	1.37E-08	1.63E-09	2.38E-09	8.03E-10	1.17E-09	9.45E-08	4.17E-07	1.22E-06
	Mg (mg/l)	0.00	0.00	0.00	0.00	0.00	0.00	0.00	0.00	0.00	0.00	0.01	0.03
	Fe (mol/l)	8.54E-06	2.46E-05	7.01E-06	4.05E-05	8.53E-06	6.01E-06	7.73E-06	6.00E-06	7.73E-06	3.38E-05	4.45E-05	5.04E-05
	Fe (mg/l)	0.48	1.37	0.39	2.26	0.48	0.34	0.43	0.34	0.43	1.88	2.48	2.82
	Al (mol/l)	1.99E-05	1.11E-05	4.41E-05	2.05E-06	1.91E-05	4.86E-05	2.10E-05	4.86E-05	2.10E-05	3.17E-06	1.53E-06	9.11E-07
	Al (mg/l)	0.54	0.30	1.19	0.06	0.51	1.31	0.57	1.31	0.57	0.09	0.04	0.02
	HCO3- (mol/l)	1.26E-04	3.21E-04	1.25E-04	4.24E-04	1.26E-04	1.33E-05	1.36E-05	1.32E-05	1.36E-05	2.19E-04	6.16E-04	1.15E-03
	HCO3- (mg/l)	7.70	19.56	7.64	25.85	7.70	0.81	0.83	0.81	0.83	13.37	37.55	69.97
	CO3-- (mol/l)	1.22E-04	8.61E-05	1.37E-04	4.10E-05	1.22E-04	1.59E-05	1.35E-05	1.59E-05	1.38E-05	3.26E-05	4.47E-05	5.02E-05
	CO3-- (mg/l)	7.30	5.16	8.24	2.46	7.31	0.96	0.81	0.96	0.83	1.96	2.68	3.01
	HCO3+CO3 (mol/l)	2.48E-04	4.07E-04	2.63E-04	4.65E-04	2.48E-04	2.92E-05	2.71E-05	2.92E-05	2.74E-05	2.52E-04	6.60E-04	1.20E-03
	HCO3+CO3 (mg/l)	15.01	24.73	15.88	28.30	15.01	1.77	1.64	1.76	1.66	15.32	40.23	72.98
	SO4-- (mol/l)	1.12E-04	1.23E-04	1.15E-04	1.22E-04	1.12E-04	1.16E-04	1.14E-04	1.16E-04	1.14E-04	1.22E-04	1.22E-04	1.22E-04
	SO4-- (mg/l)	10.79	11.83	11.02	11.72	10.78	11.15	10.91	11.15	10.91	11.69	11.72	11.71
	logPCO2	-6.3449	-5.4006	-6.4095	-4.8369	-6.345	-7.424	-7.342	-7.4246	-7.3421	-5.3127	-4.5479	-4.0521
	Minerals	orht,chal,an	micr,qz,cal	micr,qz,an	micr,chal,cal	micr,chal,an	orth,qz,an	orth,chal,an	micr,qz,an	micr,chal,an	orh,chal,cal	orh,chal,cal	orh,chal,cal

Note : The abbreviations in the above table are as follows ; orth (orthocrase), qz (quartz), cal (calcite), an (anorthite), chal (chalcedony), micr (microcline)

B: log PCO_2 = -3.0 (Table 7-2 : Test 17 to Test 20)

The calculated carbonate concentration of groundwater in the rock zone in this case is about 1 mg/L. This is significantly lower than the carbonate concentration measured in the reference groundwater.

C: log PCO_2 = -2.0 (Table 7-1 and Table 7-2 : Test 9 to Test 16)

The calculated carbonate concentration of groundwater in the rock zone in this case is about 10 mg/L, which is similar to the carbonate concentration measured in the reference groundwater.

As indicated in Table 7-2, the results of calculations for Test cases 21 to 23 (log PCO_2 = -1.5 to -2.5) similarly confirm that an assumed CO_2(g) partial pressure in the soil zone that is most consistent with observed carbonate concentrations in the reference groundwater appears to be about 10^{-2} bar.

2.6.2 Reactions in the Rock Zone

The results of groundwater evolution models considering reactions in the rock zone are summarized in Figures 21 and 22, where it is assumed that CO_2(g) partial pressures in soil solutions equals 10^{-2} bar, consistent with results summarized in the preceding section. We also assume that the redox potential (Eh) and total dissolved sulfate concentrations are controlled by equilibration of the model groundwaters with pyrite. Trial calculations based on an alternative assumption that these solutions equilibrate with magnetite rather than pyrite predict that the redox potential would be oxidizing, which is inconsistent with measured values in samples from the TK-24 borehole (Section 2.3.8). We assume that Mg concentrations are controlled by solubility equilibrium with respect to phlogopite. This is assumed as a matter of convenience because the calculated low solubility of this mineral in Kamaishi groundwaters is consistent with the observation that actual Mg concentrations in these solutions are often below the analytical detection limit (<0.01ppm; Tables 3-1 to 3-3). We acknowledge that more realisitic solubility-limiting phases, such as the smectite clays, may control Mg concentrations in Kamaishi groundwaters, but these phases are not considered here because reliable thermodynamic data for them is lacking. Similarly, because Al concentrations are also consistently lower than detection limits, we assume that Al concentrations are controlled by solubility equilibrium with respect to kaolinite, which appears to be at least partially responsible for controlling Al concentrations in many groundwater systems (e.g., Deutsch, 1997). The effects of other variations in assumed equilibrium mineral assemblages on pH, Eh

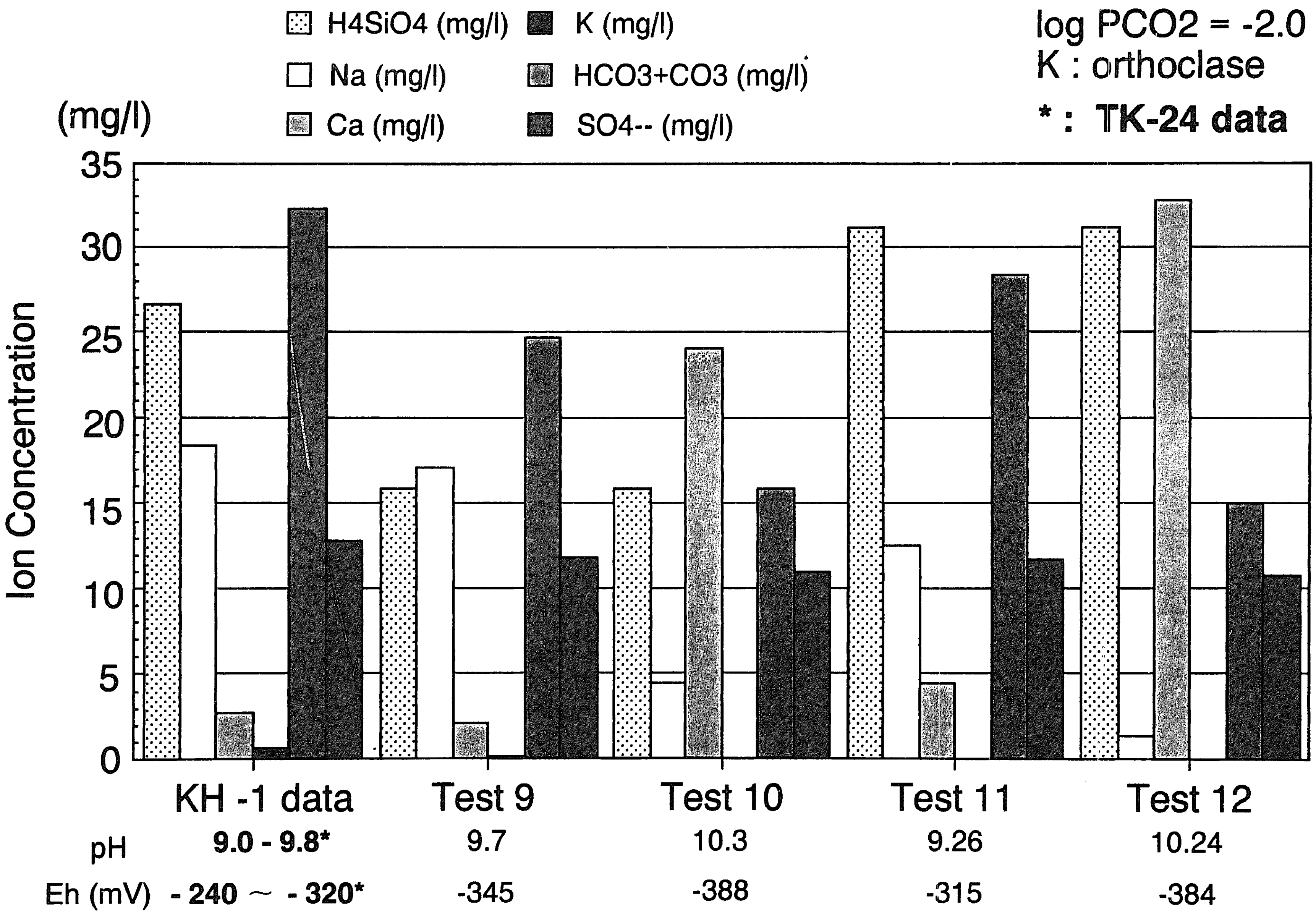

Figure 21 : *Modeling results by geochemical code PHREEQE (Test 9 - Test 12) considering orthoclase as K concentration controlling mineral.*

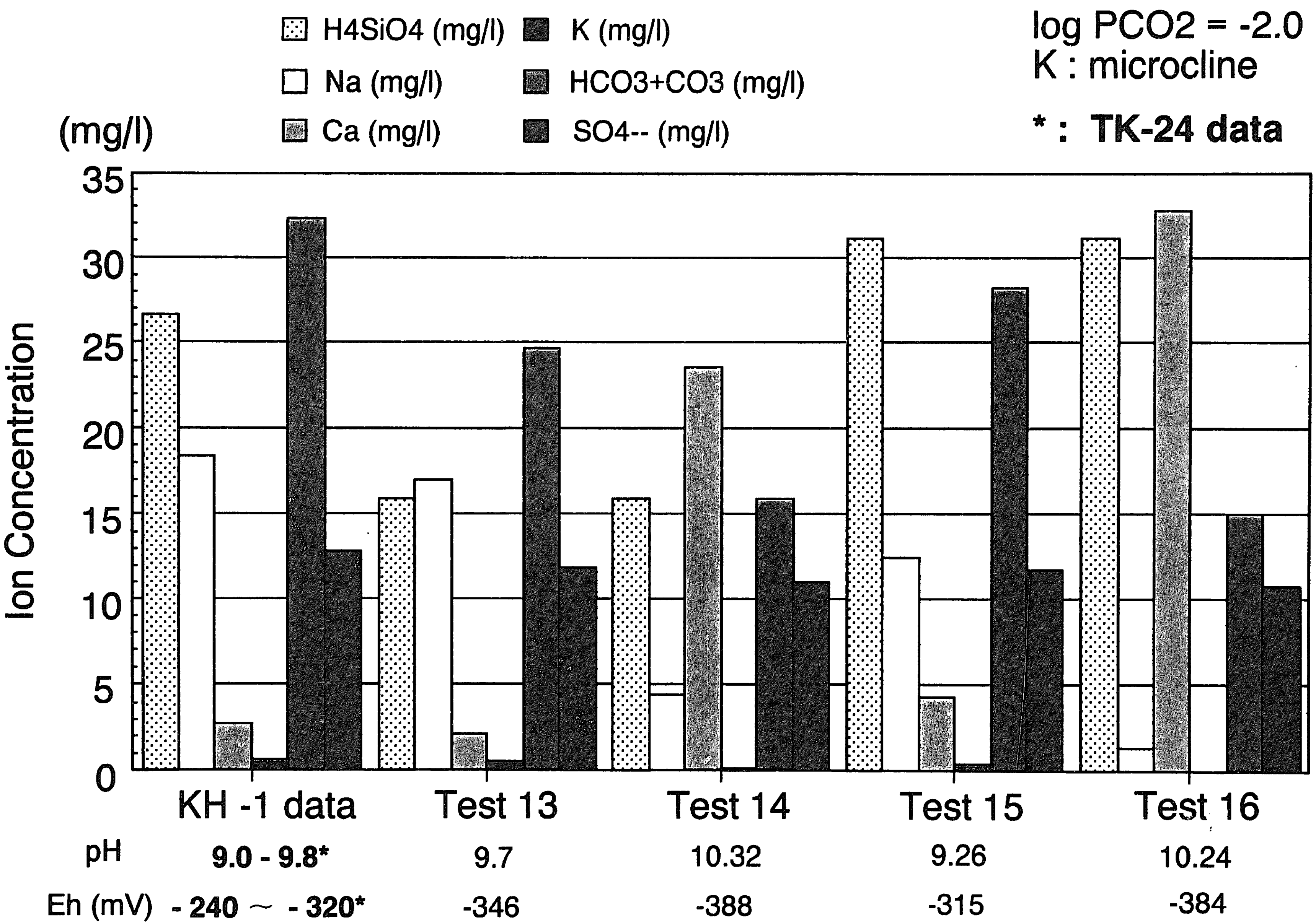

***Figure 22 :** Modeling results by geochemical code PHREEQE (Test 13 - Test 16) considering orthoclase as K concentration controlling mineral.*

and solute concentrations (total dissolved Si, Na, Ca, K, carbonate and sulfate) of groundwaters in the rock zone are summarized below.

A) Solubility equilibrium with orthoclase is assumed to control K^+ concentrations (Tests 9 to 12, Figure 21)

In this case calculated K^+ concentrations in the model groundwater are too low (less than 0.06ppm) in comparison with the reference groundwater (Table 6). Other key results from these test cases are summarized as follows:

- the Si concentration of the reference groundwater is more consistent with solubility control by chalcedony rather than quartz;
- the Ca concentration is more consistent with solubility control by calcite than anorthite;
- the pH and Eh, and Na and CO_3^{2-} concentrations, are most closely approximated in Test 11; and
- sulfate concentrations are reasonably well approximated by all the test cases.

Based on these results, the reference groundwater appears to be best explained by Test 11 (Section 2.5.2.4).

B) Solubility equilibrium with microcline is assumed to control K^+ concentrations (Tests 13 to 16, Figure 22)

In this case calculated K^+ concentrations in the model groundwater (0.04ppm-0.37ppm) are similar to the measured value in the reference groundwater (0.47 ppm). From Test 13 to Test 16, mineral assemblages assumed to control pH, Eh and ion concentrations (except for K concentration) are identical to the assemblages in Tests 9 to 12, respectively. Based on these results, the reference groundwater appears to be best explained overall by Test 15 (which is identical to Test 11, except that microcline rather than orthoclase is assumed to be the solubility-controlling phase for K^+). The PHREEQE input and output file for Test 15 are documented in Appendix F.

2.6.3 Comparison of Modeling Results with the Reference Groundwater

The closest match between model results (Test 15) and the composition of the reference groundwater is summarized in Table 8. As can be seen, the model and reference groundwater chemistry are in good agreement. We reiterate that the modeling has been carried out at 25°C, however, which is slightly higher than the measured groundwater temperature (10 and 16°C,

***Table 8** : Comparison of the modeling result (Test 15) and the measured values selected as reference groundwater chemistry in the Kurihashi granodiorite*

	pH	Eh (mV)	H4SiO4	Na	Ca	K	HCO3- + CO3--	SO4--
Reference groundwater (TK-24,KH-1)	9.0-9.8	-240 ~ -320	3.10E-04 (mol/l)	7.80E-04 (mol/l)	8.15E-05 (mol/l)	1.19E-05 (mol/l)	5.13E-04 (mol/l)	1.59E-04 (mol/l)
			29.81 (mg/l)	17.94 (mg/l)	3.27 (mg/l)	0.47 (mg/l)	31.24 (mg/l)	15.22 (mg/l)
Modeling result (Test 15)	9.26	-315	3.24E-04 (mol/l)	5.40E-04 (mol/l)	1.09E-04 (mol/l)	9.38E-06 (mol/l)	4.65E-04 (mol/l)	1.22E-04 (mol/l)
			31.08 (mg/l)	12.41 (mg/l)	4.36 (mg/l)	0.37 (mg/l)	28.30 (mg/l)	11.72 (mg/l)

- pH and Eh of the reference groundwater are the results of measurement by physico-chemical monitoring system at TK-24 borehole

- Chemical composition of the reference groundwater is average data of 4 packed-off section (tritium concentration is less than 1 T.U.) at KH-1 borehole

Tables 3-1 to 3-3). The effects of such differences in temperature on model results should be evaluated in future work..

2.7 Summary

The results of hydrochemical investigations at the Kamaishi *in-situ* tests site and local equilibrium modeling of groundwater evolution at this site are summarized as follows:

- groundwaters in the Kurihashi granodiorite are meteoric in origin;
- the residence time of the groundwaters are generally less than 40 years, but deeper groundwaters may be considerably older because tritium concentrations in these solutions are below the detection limit, and because preliminary results of radiocarbon dating (of samples from the KH-1 borehole) indicate residence times between 1,450 to 3,030 years BP;
- the pH of the groundwater varies with increasing depth from weakly acid-to-neutral to weakly alkaline;
- redox potentials monitored continuously in groundwaters from the TK-24 borehole using a continuous monitoring system, and inferred from observations of microbial activities in groundwaters sampled from the KG-1-2 interval of the KG-1 borehole, indicate that deep groundwaters in the Kurihashi granodiorite are reducing;
- the evolution of the "real" groundwater chemistry at the Kamaishi site can be approximated with reasonable accuracy using a local-equilibrium model of water-rock interactions, and the following assumptions;
  - log PCO_2 = -2.0 in soil solutions, and
  - equilibrium minerals in the rock zone controlling the concentrations of respective elements in groundwater include chalcedony (Si), albite (Na), kaolinite (Al), calcite (Ca and carbonate), microcline (K) and pyrite (Eh and sulfate), and
- future groundwater chemistry models appropriate for the Kamaishi site should be based on groundwater temperatures actually measured at this site.

3. DISCUSSION ON GROUNDWATER EVOLUTION MODELS

3.1 Executive Summary

The modeling approach and results described in Section 2.5 are considered with regard to the following questions:

- is the proposed model *adequately constrained* by site data ?
- are modeling results and conclusions *consistent* with the site data ?, and
- are modifications needed to improve the modeling approach ?

It is concluded that the modeling study at the Kamaishi *in-situ* tests site is of very high technical quality overall, and that JNC generally is carrying out a sophisticated and comprehensive study of geochemical controls on the chemistry and chemical evolution of groundwater systems. Recommendations to strengthen and improve the Kamaishi study include are summarized below.

- The exact nature of equilibrium in models of groundwater chemistry and evolution must be clearly defined, and should include the concepts of local, partial and metastable equilibrium. Including, or excluding, minerals for consideration in a model on the basis of assumed partial or metastable equilibrium behavior should be supported by referencing relevant laboratory and field studies.
- Stable isotope and tritium data suggest that groundwaters flow relatively rapidly through the Kamaishi site, and that an open-system model for this site may therefore be more appropriate than the closed-system model evaluated in Section 2.5.
- JNC should consider all the groundwaters sampled at the Kamaishi site - not just the older groundwaters sampled in the KH-1 borehole. Although it may reasonable to assume the older groundwaters are the most likely to have attained equilibrium, the younger groundwaters sampled in drifts and other boreholes may also provide valuable clues about irreversible processes taking place at early stages of groundwater evolution.
- JNC should strengthen the assumption that oxidizing conditions in most Kamaishi groundwaters can be traced to difficulties in measuring reliable redox potentials. The results of various international studies, in which this has been convincingly demonstrated in both the laboratory and field, should therefore be discussed.
- Variations in the compositions of groundwaters among samples from individual fractures

intersecting the E.L. 550, E.L. 250m and KD-89 drifts should be evaluated to support the (implied) assumption that samples obtained from the KH-1 borehole are representative of solutions in the Kurihashi granodiorite.

- JNC studies (Osawa et al., 1995), which suggest that Kamaishi groundwaters flow preferentially in fractures, or fractures and adjacent altered-rock zones, should be acknowledged. The possibility that groundwaters flow only in fractures, for example, would suggest that only fracture minerals will affect groundwater evolution. Secondary effects, such as diffusional mixing of solutions in fractures and altered zones may also need to be considered, however.
- More detailed information on the actual mineralogy of the Kamaishi site is needed, including the compositions of plagioclase, sericite, chlorite, biotite, calcite and epidote, and the identities of minerals that may occur in trace amounts (e.g., clays, kaolinite, chalcedony).
- Minerals considered to be heterogeneous equilibrium constraints should be selected from among minerals actually present at Kamaishi. Minerals of igneous or hydrothermal origin should be considered with caution because they are probably unstable at low temperatures (i.e., they should dissolve irreversibly and incongruently). Models indicating that groundwater compositions are supersaturated with respect to Kamaishi minerals should also be revised such that these "metastable" phases are assumed to equilibrate, if precipitation at low temperatures is reasonable.
- A lack of highly reliable thermodynamic data should not necessarily deter choices of equilibrium minerals. Reasonable estimates of the necessary data will greatly improve credibility in the model, provided the uncertain reliability of the data is acknowledged and documented.
- JNC's approach in using a reference groundwater composition as the only criterion by which the validity of equilibrium-based models is tested should be reconsidered. It is recommended that JNC should instead consider the range in groundwater compositions actually measured at Kamaishi. JNC should then evaluate whether alternative models of groundwater evolution are equally valid, given this range.

It is also recommended that a more systematic approach toward developing and testing equilibrium-based groundwater evolution models should be adopted. The approach should include the following steps.

1. obtain *detailed* information on the mineralogy of the site and chemistry of site groundwaters,
2. calculate the saturation index of minerals for which it is reasonable to assume that site

groundwaters are in contact,

3. develop a preliminary reaction-path model of groundwater evolution at the site, using the results of Step 2 to guide initial selection of possible equilibrium phases,
4. evaluate model results for consistency with field observations,
5. if results are inconsistent with site data, modify the reaction-path model by revising one assumption concerning whether a mineral observed at the site should be considered stable, unstable or metastable.
6. iterate steps 4 and 5 until an optimal model is obtained that is consistent with site mineralogy and which best explains observed groundwater compositions.
7. evaluate of the validity of the equilibrium approach by comparing results of the optimized model with site data.

These steps emphasize the iterative use of reaction-path models to raise questions concerning the validity of assumptions in an evolving conceptual model of the system. To carry this procedure out successfully, the modeler must rely on expert judgement to answer these questions.

3.2 Discussion Points

In Section 2.5, the results of testing of equilibrium-based geochemical models for conditions at the Kamaishi site were described. The test procedure includes the following steps:

- development of a qualitative conceptual model of chemical, physical and biological processes controlling groundwater chemistry,
- quantification of the model in terms of representative site-specific reactions, other local-equilibrium constraints, and estimates of groundwater flow properties (e.g., residence times of groundwater in the host rock),
- simulation of the chemical evolution of groundwaters at the site assuming initial and boundary conditions in the quantitative model, and
- evaluation of the validity of the equilibrium basis supporting the model by comparison of simulation results with observed variations in groundwater chemistry.

Application of this procedure using the site-specific data suggests that a "local-equilibrium" model involving heterogeneous equilibrium constraints on the aqueous concentrations of Na, K, Ca, Mg, Fe, Al, Si, S and C successfully simulates the chemical evolution of these parameters as dilute surface waters infiltrate first into a soil zone and then into the Kamaishi granodiorites.

Similar tests using field data from the Tono and Mobara sites have also been carried out (Sasamoto et al., 1999b ; Sasamoto et al., 1999c).

The modeling approach and results described in Section 2.5 are discussed in this section with regard to the following questions:

- is the proposed model *adequately constrained* by site data ?
- are modeling results and conclusions *consistent* with the site data ?, and
- are modifications needed to improve the modeling approach ?

3.3 Discussion

3.3.1 Model Constraints

3.3.1.1 Local Equilibrium

"Local equilibrium" is assumed for Kamaishi groundwaters in Section 2.5, but this term may be too general in meaning to capture the true nature of the model. Local equilibrium refers only to the possibility that for any real system that is in disequilibrium overall, it is possible to find smaller subregions of the system that have locally attained equilibrium (e.g., Anderson and Crerar, 1993). Groundwaters in fractured crystalline rocks, for example, may be in local equilibrium with fracture minerals, but not with minerals in the rock's matrix.

To more accurately characterize this model, the concepts of *partial* and *metastable equilibrium* should be incorporated into its definition. Partial equilibrium refers to the possibility that a given system may appear to be at equilibrium with respect to some processes, but not with others. A groundwater may be in local equilibrium with some minerals, for example, but not all the minerals with which it is in contact. A limited number of such "equilibrium" minerals are assumed in Section 2.5, but other minerals present in fractures, and in altered and unaltered host rocks at Kamaishi, are excluded from consideration. This may be consistent with the concept of partial equilibrium if it is assumed that reactions involving the *"excluded"* minerals do not significantly affect groundwater compositions, possibly because dissolution rates are too slow.

Metastable equilibrium refers to the possibility that a given system may appear to be at equilibrium with respect to some processes, but this is because others are prevented for various reasons from achieving their lowest possible energy states. Groundwaters are often supersaturated with respect to several minerals, for example, because activation energies of corresponding precipitation reactions are too high. The proposed model similarly predicts supersaturation of solutions with respect to several minerals (Appendix F-2), and for this reason and reasons discussed above, it is probably most accurately termed a *metastable-partial-local*-equilibrium model.

These distinctions in terminology are important because determining the validity of equilibrium-based models, the primary objective of this study, depends on how equilibrium is defined. For example, the main conclusion that local equilibrium is an appropriate basis for understanding groundwater chemistry and evolution at Kamaishi must be incorrect because:

- the model assumes that some host-rock minerals (e.g., hornblende, sphene) do not significantly affect groundwater compositions - partial equilibrium may be consistent with this assumption, however - and
- calculated solution compositions are assumed to be metastable with respect to several minerals - metastable equilibrium may, however, be consistent with this assumption.

It is therefore recommended that the descriptions in Section 2.5 should include a more precise definition of equilibrium, and that this definition should encompass the concepts of local, partial and metastable equilibrium. The validity of the model should then be evaluated in relation to the assumed nature of equilibrium in the system being modeled. For example, if certain fracture minerals in the Kurihashi granodiorite are not considered in a test of the model because partial equilibrium is assumed, then plausible reasons for excluding the solids should be documented. Such reasons could include the possibility that dissolution rates are too slow, but this needs to be backed up (if possible) with reference to tangible evidence, such as laboratory investigations of dissolution behavior. If such evidence does not exist, then this should at least be acknowledged. Similarly, equilibrium solution compositions may be supersaturated with respect to various minerals if metastable equilibrium is assumed. If so, credible reasons for metastable behavior should also be identified and supported with reference to relevant laboratory or field studies.

3.3.1.2 Groundwater Chemistry

JNC has carried out an impressive groundwater sampling and analysis study at the Kamaishi site. Over 200 samples of surface waters, groundwaters entering the E.L. 550m, KD-89 and E.L. 250m drifts, and groundwaters in packed-off intervals of the KG-1 and KH-1 boreholes have been collected. A special effort to sample groundwaters in the TK-24 borehole (drilled from the E.L. 550m drift) using a continuous monitoring apparatus is used to determine pH and Eh before the samples are contacted by atmospheric gases. Sampling at Kamaishi started in 1988 : the most recent samples described in Section 2.3.3 are from 1995.

The surface and groundwater samples are analyzed for temperature, pH, Eh, electrical conductivity, dissolved oxygen, dissolved gases and a comprehensive suite of inorganic and organic constituents, micro-organisms, stable isotopes (^{18}O and deuterium) and radioactive isotopes (^{3}H). Care has been taken to distinguish formation waters from drilling fluids by monitoring variations in sample compositions with time. The quality of individual analyses is determined by charge-balance. A difference between total cationic and anionic concentrations of ±0.2 meq/L is taken as the cutoff for an acceptable analysis.

Selection of groundwaters for equilibrium analysis. Tritium concentrations in most groundwaters are greater than 1 Tritium Unit (T.U.), indicating that these solutions are relatively young (< 40 years). Groundwaters sampled only at depths greater than 100 m in the KH-1 borehole have ^{3}H concentrations < 1 T.U., suggesting that only these waters were recharged at Kamaishi more than 40 years ago. In Section 2.5.1, JNC restricts their analysis of the geochemical evolution of groundwaters in this system to the subset of *"old"* groundwaters, and thus only to samples obtained from the KH-1 borehole at depths greater than 100 m.

The reasoning behind this decision is unclear. It is reasonable to assume that the older groundwaters are the most likely to have attained, or closely approached, equilibrium, but the younger groundwaters may also provide valuable clues about irreversible processes during early stages of groundwater evolution. Moreover, however unlikely, it is still possible that the young groundwaters have also equilibrated with Kamaishi host rocks, at least in the sense discussed in Section 3.3.1.1.

It is recommended for these reasons that JNC should provide more convincing arguments for neglecting the young groundwaters in their evaluation. It is also suggested that analysis of the complete Kamaishi groundwater dataset using a reaction-path modeling approach (Section 3.3.3) could provide valuable insights concerning the true evolution of these solutions from initially dilute surface waters - to young groundwaters that are still far from equilibrium - to more mature groundwaters that have closely approached, or achieved, equilibrium. It is also noted that reasonably reliable kinetic data are available for most of the minerals considered in Section 2.5 (testing of equilibrium-based geochemical model), and a kinetic reaction-path model could therefore be developed to categorize characteristics of young and old groundwaters according to their qualitative ages (i.e., less than or greater than 40 years old).

Redox conditions. Almost all the groundwaters, except those sampled in the TK-24 borehole, are oxidizing. For reasons described in Section 2.3.8, this is almost certainly because concentrations of redox-sensitive species in these solutions are extremely low. The groundwaters are thus poorly poised to resist changes in redox potential, which could be caused by inadvertent introduction of atmospheric $O_2(g)$ into groundwater samples during sampling.

Although this is a reasonable explanation, it may be questioned because the vast majority of groundwaters nevertheless appear to be oxidizing, and because oxidizing groundwaters are known to have serious impacts on assessments of repository performance. It is therefore recommended that JNC should strengthen the case that the apparent oxidizing conditions are due to difficulties in measuring reliable redox values. This can be accomplished by citing relevant studies carried out by SKB (Grenthe et al., 1992 ; Nordstrom and Puigdomenech, 1986 ; Wikberg, 1988 and Wikberg, 1987), for example, where the effects of $O_2(g)$ contamination in poorly poised groundwater samples has been convincingly demonstrated.

Representativeness of samples. The Kurihashi granodiorite is inhomogeneous. It consists of unaltered and altered zones, and fractures. Each of these units is characterized by a distinct mineralogy, as described in Section 2.2, but minor variations in the mineralogy of each unit could occur locally. It is also possible that groundwaters may flow preferentially in these units - for example, most easily in fractures, less easily in altered zones, and perhaps not at all in unaltered zones.

These possibilities suggest that if multiple fractures intersect the packed-off sections of the KH-1 borehole, the fluids sampled from these sections will represent a mixture of groundwaters from each fracture, each of which may have different compositions. An implicit assumption in the description in Section 2.5.1 is that these samples are representative of groundwaters in the Kurihashi granodiorite. This may be valid if such differences in individual fracture-water compositions are small.

A test of this assumption could be made by comparing compositions of groundwaters sampled from individual fractures intersecting the E.L. 550, E.L. 250m and KD-89 drifts. If variations in groundwater chemistry among these samples is small, this would strengthen the assumption that groundwaters sampled in the KH-1 borehole are truly representative of solutions in the

Kurihashi granodiorite.

Preferential flow of groundwaters in the Kurihashi granodiorite has already been studied by Osawa et al. (1995), who showed that these solutions probably migrate most readily through fractures because the fracture-fill mineral assemblages are more permeable than the altered and unaltered zones. It is also concluded, however, that fracture groundwaters can migrate into adjacent altered zones. Because the mineralogy of the fractures and altered zones differ in some important respects (e.g., K-feldspar is present in the altered zone but not in fractures), it is possible that the compositions of solutions in the fractures and altered zones may also differ. If so, JNC may need to consider equilibrium conditions in both the fractures and altered zones, as well as mixing of the equilibrated solutions from both these units.

In summary, it is recommended that JNC should:

- evaluate variations in the compositions of groundwaters among samples from individual fractures intersecting the E.L. 550, E.L. 250m and KD-89 drifts to support the assumption that samples obtained from the KH-1 borehole are representative of solutions in the Kurihashi granodiorite, and
- account for differences in mineralogy between fractures and the altered and unaltered zones of the Kurihashi granodiorite and evaluate possible effects on equilibrium groundwater compositions.

If it is impractical to carry out these evaluations, then the question of the *"representativeness"* of groundwater samples should at least be discussed in Section 2.5.1.

3.3.1.3 Mineralogy

The mineralogy of the Kurihashi granodiorite is described in Section 2.2 as follows:

- unaltered zone - quartz, plagioclase, biotite > k-feldspar, hornblende, chlorite > sericite, sphene, magnetite
- altered zone - quartz, plagioclase, chlorite > k-feldspar, hornblende, sericite > calcite, epidote, sphene
- fracture fillings - calcite, stilbite > quartz, chlorite, laumontite > plagioclase, epidote > hornblende, sericite, prehnite

In comparison, the *"equilibrium"* mineralogy giving the best agreement between the *"reference"* groundwater and the modeled groundwater includes chalcedony, albite, kaolinite, calcite, microcline, biotite (phlogopite) and pyrite.

The rationale for selecting this assemblage of equilibrium minerals is unclear, and may be questionable for several reasons.

First, chalcedony and kaolinite apparently do not exist in fractures, or in the altered and unaltered zones of the Kurihashi granodiorite. While it is true that most groundwaters are metastable with respect to quartz, many are also metastable with respect to chalcedony. The generally reasonable agreement between calculated chalcedony solubilities and SiO_2(aq) concentrations actually observed in Kamaishi groundwaters may therefore be fortuitous. This choice would be much more convincing if chalcedony were actually observed at Kamaishi. Similarly, the fact that kaolinite is not present in these rocks should warn against assuming it is an equilibrium phase. Unlike quartz, and in some cases chalcedony, kaolinite is commonly found as a weathering product in low-temperature systems. Its absence at Kamaishi may indicate it is unstable under these conditions.

Second, it is doubtful whether albite, microcline and biotite (phlogopite) can actually achieve stable reversible equilibrium with an aqueous phase at low temperatures. This has never been demonstrated experimentally for a number of reasons, including the possibility that these minerals are stable only at higher temperatures, or because they dissolve non-stoichiometrically (Nordstrom et al., 1990). To improve credibility in the proposed model, it may therefore be necessary to replace these minerals with more suitable phases, which are known to be stable in low-temperature groundwater systems (e.g., Na-, K- and Mg- zeolites).

Third, at least two "equilibrium" minerals (with the exceptions of chalcedony and kaolinite) are found in each of the unaltered, altered or fracture units at Kamaishi:

unaltered zone - albite (plagioclase), microcline (K-feldspar), phlogopite (biotite), pyrite (disseminated)
altered zone - albite (plagioclase), microcline (K-feldspar), calcite
fractures - calcite, albite (plagioclase)

This suggests that the groundwater may have equilibrated with all these units simultaneously. For example, assuming that biotite and pyrite are equilibrium minerals suggests that the groundwater must react with unaltered granodiorite, because this is the only zone in which these minerals are found. Assuming calcite is an equilibrium mineral similarly implies that the groundwater also reacts with the altered zone minerals and fracture minerals.

If this interpretation is correct, it leads to some logical inconsistencies with field observations. For example, because the solution equilibrates with biotite in the unaltered zone, biotite should also be stable in the unaltered zones and fractures, yet this is not what is observed. Similarly, equilibration of the solution with calcite in fractures and the altered zone would imply that calcite is stable in the unaltered zone. Again, this is inconsistent with field observations.

Fourth, many of the minerals in the Kurihashi granodiorite are of igneous origin, or appear to have formed during a period of hydrothermal activity, probably well after the original granodiorite was formed. Igneous minerals may include quartz, plagioclase, biotite, K-feldspar, hornblende, sericite, sphene and magnetite. Hydrothermal minerals may include, depending on the actual temperatures involved, quartz, plagioclase, chlorite, K-feldspar, sericite, calcite and epidote.

It may not be reasonable to consider these minerals as "equilibrium" phases. If they formed as a result of cooling of the original magma generating the Kurihashi granodiorite, or during a later period of hydrothermal activity, then they may be unstable at the lower temperatures presently existing at the Kamaishi site.

Several of the minerals in fractures are reasonable candidates as equilibrium phases in low-temperature weathering environments, however, including:

- stilbite,
- laumontite,
- sericite (illite),

and may also include

- chlorite, and
- prehnite

Its unclear why these low-temperature minerals are not considered as equilibrium phases. In Section 2.5.2.2, it is noted that thermodynamic data are unavailable for laumontite in their thermodynamic database (TDB), and this may also be true for stilbite and prehnite. Thermodynamic data have been estimated for all these minerals, however, and these data could be incorporated into JNC's TDB. This may be preferable to the current approach of ignoring these minerals, because they are known to be present at Kamaishi and because they contain many of the elements being modeled.

Fifth, the mineralogy of the site may not be characterized in sufficient detail to adequately constrain models of groundwater evolution. Albite, for example, is presumably present as a solid-solution component of plagioclase, but there is apparently no evidence that secondary albite actually forms as a result of plagioclase dissolution. Also the term sericite is ambiguous because this mineral refers to fine-grained *"mica"*, which is often muscovite but may also include paragonite and/or illite. It is also unclear whether the site's mineralogy has been investigated in sufficient detail to detect minerals that might occur in very small amounts (e.g., clays, chalcedony, kaolinite), or which would permit evaluation of end-member compositions of solid-solution minerals, such as chlorite, biotite, calcite and epidote.

For all these reasons, it is recommended that JNC should re-consider the choices of equilibrium minerals in the proposed model. The following guidelines are recommended for this purpose:

- the selected minerals should be from among those observed at Kamaishi - minerals that are possibly of igneous or hydrothermal origin should be considered with caution, however, because they may be unstable at low temperatures,
- preferential flow of groundwater in fractures, or in fractures and associated altered-rock zones, should be acknowledged (Section 3.3.1.2 ; Osawa et al., 1995), and minerals in these units should have highest priority as possible equilibrium phases,
- a lack of highly reliable thermodynamic data should not deter choices of equilibrium minerals - even reasonable estimates of the necessary data will greatly improve credibility in the model, provided the uncertain reliability of the data is documented in the report.
- as much detail as possible should be provided on the actual mineralogy of the site, including the compositions of plagioclase, sericite, chlorite, biotite, calcite and epidote, and the identities of minerals that may occur in trace amounts (e.g., clays, kaolinite, chalcedony).

3.3.1.4 Open- versus Closed-System Behavior

Although the hydrogeology of the Kamaishi site is not discussed in detail, oxygen- and hydrogen-isotope data clearly indicate that the groundwaters have a meteoric origin, and tritium data strongly suggest that groundwaters flow relatively quickly through the site. This raises the question whether an open-system model might be more appropriate for conditions at Kamaishi than the closed-system model currently proposed.

Minerals precipitating from an aqueous phase in an open-system model are removed from contact with the fluid, i.e., they are assumed to be left behind with the rock as the fluid continues to migrate. Such minerals remain in contact with the fluid in closed-system models, however, and hence can "back-react" if conditions change accordingly. Calculated solution compositions can vary significantly in open- versus closed-system models in which other conditions are otherwise identical.

It would be of interest to determine if open- rather than closed-system behavior significantly alters the main conclusions described in Section 2.5 for the Kamaishi site. If not, results could be used to answer potential criticisms that the modeling approach may not be appropriate for the apparently open-system conditions at Kamaishi. If so, then the modeling approach may need to be modified to account for open-system behavior.

3.3.2 Consistency of Model Results and Field Data

3.3.2.1 Reference Groundwater

Several levels of abstraction are introduced to derive a *"reference"* groundwater composition, which is assumed to represent the chemistry of solutions in Kurihashi granodiorite. As noted in Section 2.5.1, only groundwaters sampled at depths greater than 100 m in the KH-1 borehole are considered because tritium concentrations in these solutions are low, suggesting they were recharged more than 40 years ago. The average composition is then calculated among all groundwaters sampled from 4 different packer intervals spanning a total borehole length of approximately 454 m. Because Eh measurements in these samples are considered unreliable, a range of Eh values (-0.24 to -0.32 V) and pH values (9.0 to 9.8) measured in samples from the TK-24 borehole are assumed to constrain these parameters in the reference groundwater. The average temperature of solutions sampled in the KH-1 and TK-24 boreholes are 12.5 °C and 16 °C, respectively, but a temperature of 25 °C is assumed for the reference groundwater.

The reasons for choosing a reference solution composition to represent groundwaters in the Kurihashi granodiorite are unclear. Groundwaters in even reasonably homogeneous host rocks typically display a range of compositions due to differences in the residence times of the fluids in the rock, minor variations in the distribution and abundances of primary and secondary (alteration) minerals, mixing of groundwaters, and for other reasons that may be difficult to quantify. Assuming a single reference groundwater composition is therefore inconsistent with the known behavior of most, if not all, natural systems.

This is important because comparison of calculated groundwater compositions with the reference composition is the only criterion adopted in Section 2.6.3 to judge the reliability of the model. The assumption that a single reference composition adequately characterizes groundwaters in the Kurihashi granodiorite, and the abstract nature by which the reference composition is defined, raises questions concerning conclusions that the model is valid because calculated compositions compare favorably with the reference composition. These questions include:

- is it possible that other models might explain groundwater chemistry in the Kurihashi granodiorite equally well, given the actual range in compositions revealed by the sampling and analysis work carried out at Kamaishi?,
- is it possible that alternative reference compositions could be defined, for example following the same procedure as the description in Section 2.5.1 but using newer groundwater analyses determined since 1995, and, if so, would the proposed model still be valid?, and
- is the key conclusion - that a local equilibrium model of groundwater evolution at Kamaishi is valid - conditioned by the manner in which the reference groundwater composition is defined?

An alternative to addressing these questions may be for JNC to re-evaluate whether a reference groundwater composition provides a reasonable test of the validity of groundwater evolution models. JNC could, for example, consider the total range in compositions of groundwaters sampled in the KH-1 borehole. It may also be desirable to consider samples other than just those obtained from KH-1 (Section 2.5.1). Then, JNC should evaluate whether alternative models are also valid in relation to the ranges in groundwater compositions actually observed at Kamaishi. If so, then additional criteria, such as whether minerals considered in the candidate models are reasonable in low-temperature groundwater systems, and uncertainties in associated thermodynamic data, should be carefully evaluated to select the most reasonable model for the Kamaishi site.

3.3.2.2 Equilibrium Mineralogy

The modeling approach is based on calculation of equilibrium groundwater compositions assuming multiple heterogeneous equilibrium constraints among user-specified minerals and corresponding solution constituents. Application of this approach is fundamentally sound, but results appear to be accepted somewhat uncritically with regard to consistency between model results and field observations.

For example, the model for Test 15 (in Section 2.5) includes the following mineral-equilibrium constraints on total aqueous concentrations of solution constituents:

- chalcedony - $SiO_2(aq)$
- albite - Na^+
- kaolinite - Al^{3+}
- calcite - Ca^{2+} and HCO_3^-
- microcline - K^+
- pyrite - SO_4^{2-} and redox potential
- phlogopite - Mg^{2+}

Calculated results compare favorably with the reference groundwater composition, but the groundwater is supersaturated with respect to several minerals (according to PHREEQE output in Appendix F-2), including:

- siderite,
- $Fe(OH)_3(am)$,
- muscovite,
- epidote,
- tremolite,
- andradite,
- "montmoca" (Ca montmorillonite),
- clinoc26 (clinochlore),
- clinoch8 (clinochlore),
- magnesio (?),
- paragonite,
- illitek2 (illite),
- orthoclase,
- annite,
- hematite,
- $Fe_2Si_2O_6$,
- almandine,
- magnetite,
- goethite,
- ferrosil (ferrosilite),
- fayalite, and
- K-feldspar

Several of these minerals are known to coexist with Kurihashi groundwaters, including:

- siderite (possibly as a solid-solution component of "calcite"),
- muscovite, illite and/or paragonite (in sericite)
- epidote,
- clinoc26, clinoch8 (clinochlore components in chlorite solid solution),
- annite (a mica similar in composition to biotite),
- magnetite, and
- K-feldspar,

which raises the question whether they should be considered as equilibrium constraints in addition to, or rather than, the minerals in Test 15.

A systematic, trial-and-error approach is needed to answer such questions. Such an approach has already been adopted in some respects in Section 2.5, considering variations in Test 15 mineralogy, and resultant effects on calculated groundwater compositions. It is recommended that this work should be further extended and refined by:

- restricting choices of possible equilibrium minerals to those actually observed at Kamaishi, particularly in fractures and in altered zones of the host rock,
- eliminating to the extent possible any supersaturation of calculated groundwater compositions with respect to Kamaishi minerals, if precipitation at low temperatures is reasonable, and
- broadening the definition of the reference groundwater composition to be consistent with ranges in constituent concentrations observed at the site (Section 3.3.2.1).

Finally, it should be borne in mind that assuming metastable, partial and/or local equilibrium may not be realistic for this particular system.

3.3.3 Modeling Approach

The modeling approach described in Section 2.5 involves an element of hypothesis testing insofar as alternative assumptions are made that orthoclase, versus microcline, constrain aqueous K concentrations by partial equilibrium. Choices of similar constraints on Si, Na, Al, Ca, Mg, Fe, S and C are made more arbitrarily, however, because corresponding minerals are not consistent overall with the mineralogy of the Kurihashi granodiorite (Section 3.3.1.3), and because alternative hypotheses that include more realistic minerals are untested.

Hypothesis testing is an important step in the process of developing a reliable geochemical model of groundwater evolution. The assumptions in such models are continuously revised as a result of hypothesis testing until the model finally predicts behavior that best explains all the available field data.

This ideal approach is complicated, however, by the common-ion effect. Because groundwater systems are multicomponent, multiphase systems, the equilibrium status (stable, unstable or metastable) of the fluid with respect to a given mineral will depend on its status with respect to all minerals in the system that contain at least one common element. If the fluid is metastable with respect to more than one Al-bearing mineral (laumontite, prehnite, epidote, etc.), for example, assuming that any one of these minerals equilibrates with the fluid will reduce aqueous Al^{3+} activity, and thus the saturation index of all Al-bearing minerals in the system. For this reason it is essential that a highly systematic approach be taken in applying the concept of hypothesis testing to develop a reliable model of groundwater evolution.

It is therefore recommended that JNC should adopt a more interactive, reaction-path modeling approach to guide the process of identifying heterogeneous equilibrium constraints. A reaction-path model is the more general case of a single-point model (which is implemented in PHREEQE and used in Section 2.5). In essence, a reaction-path calculation divides a single-point calculation into a series of steps, each of which describes the state of the system as it evolves toward equilibrium. The final step calculated in a reaction-path model corresponds exactly to the equilibrium state calculated in a single-point model. The advantage of the reaction-path approach, however, is that the evolutionary path taken by a solution as it equilibrates with the host rock is simulated in detail. If evolving solutions become supersaturated with respect to a given mineral, for example, the modeler is forced to decide whether the mineral should be considered stable, or metastable. If a mineral is predicted to remain undersaturated throughout the reaction path, the modeler must also decide whether this is reasonable. Such decisions, made on a mineral-by-mineral basis, provide a framework for systematically building up a model that is consistent with field observations.

3.3.3.1 Example #1 - Test 15 -

An example of this approach is illustrated below using the REACT module of the Geochemist's Workbench (Bethke, 1996). REACT is used in this example to simulate a reaction path corresponding to the Test 15 conceptual model discussed in Section 2.5.

The REACT input script for this example is shown in Appendix G. Thermodynamic data supporting the simulation are taken at face value using a thermodynamic database (thermo.data) consistent with the Debye-Huckel model for calculation of activity coefficients. *It should be cautioned that the present example cannot be compared meaningfully to results discussed in Section 2.5 because several different minerals are considered, and because differences exist in the respective thermodynamic databases.*

Selected results of the REACT calculation are shown in Figures 23 - 25, which illustrate variations in the saturation index (log Q/K) of Na-, Ca- and K-bearing minerals, respectively, versus respective amounts of albite, calcite and microcline reacted. Positive values of the saturation index indicate the mineral is metastable; negative values indicate the mineral is unstable, and equilibrium is indicated when the saturation index equals zero. All Test 15 minerals are considered in this simulation, but to simplify discussion results are considered in detail for only Na, Ca and K. Final equilibrium conditions in the simulated system are summarized in Appendix H.

Considering the case for Ca in detail (Figure 24), it can be seen that calcite equilibrates with the evolving groundwater after about 2 x 10^{-4} mol of this reactant dissolves (continued dissolution of calcite causes an equivalent amount of calcite to precipitate, with the result that the saturation index for this mineral remains equal to zero). The portion of the reaction path between initial equilibration of the solution with calcite and final equilibrium (indicated in this figure by the trend among all supersaturation and undersaturation curves to become horizontal) is characterized by complicated relations involving the saturation index of metastable and unstable Ca-bearing phases. This behavior is due to the fact that these phases contain elements (e.g., Al, Si) whose aqueous concentrations are still evolving as final equilibrium is approached with other minerals in the Test 15 system.

Figures such as Figures 23 - 25 are useful because they offer a framework for evaluating whether model results are consistent with field observations. For example, Figure 23 indicates that the Test 15 groundwater eventually equilibrates with albite, and that this solution is metastable with respect to several Na-bearing clay minerals. Sodium-beidellite, several Na-zeolites and paragonite are predicted to be unstable in this solution. These relations are partially supported by field observations at Kamaishi because albite is present (presumably as plagioclase) in altered and unaltered zones of the Kurihashi granodiorite. The lack of clay minerals at Kamaishi may, however, be inconsistent with the calculated supersaturation of the

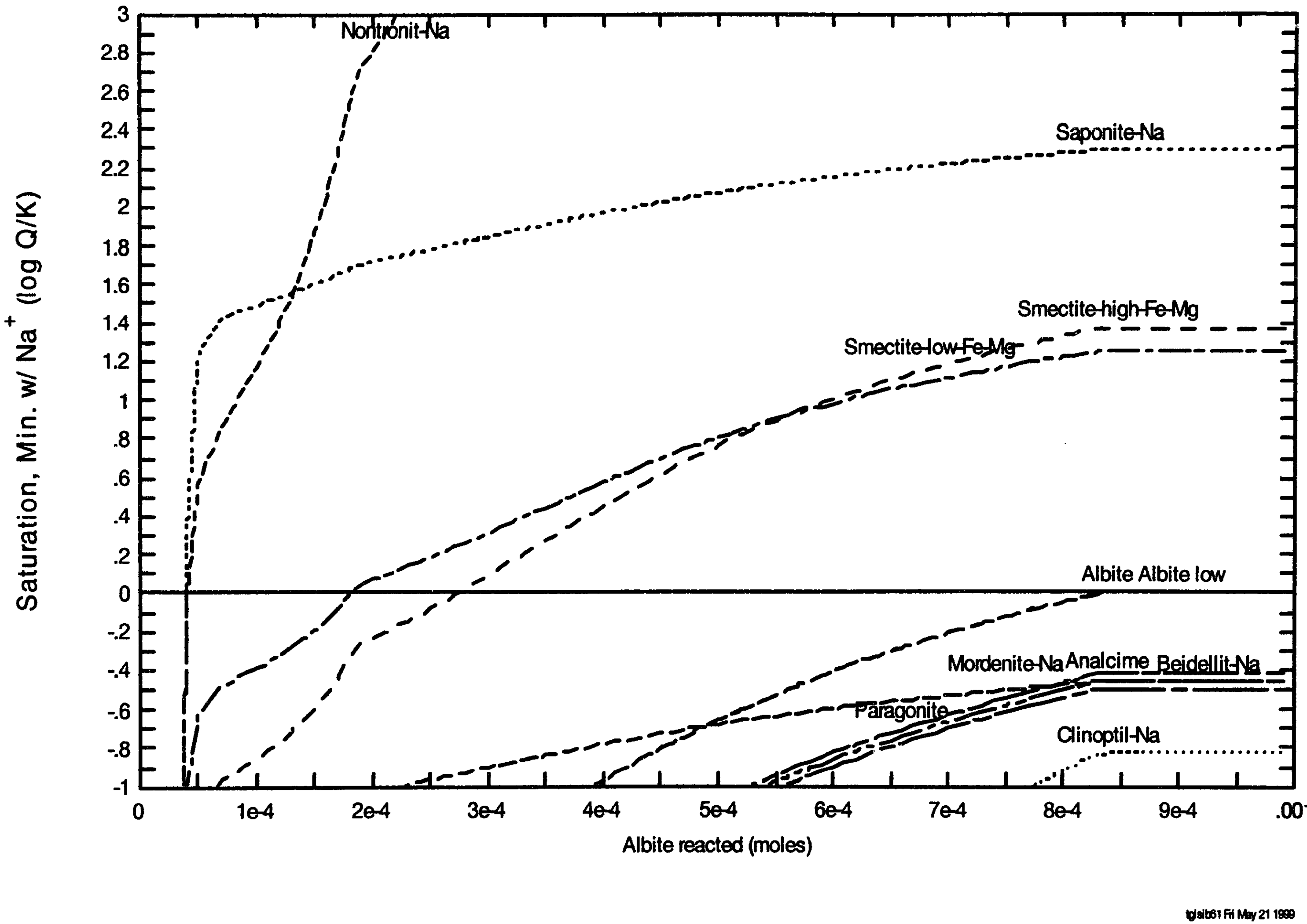

***Figure 23** : Kamaishi reaction-path model : Na. A vertical line shows the saturation index (log Q/K) of Na bearing minerals. A horizontal line shows the amount of albite reacted in this calculation.*

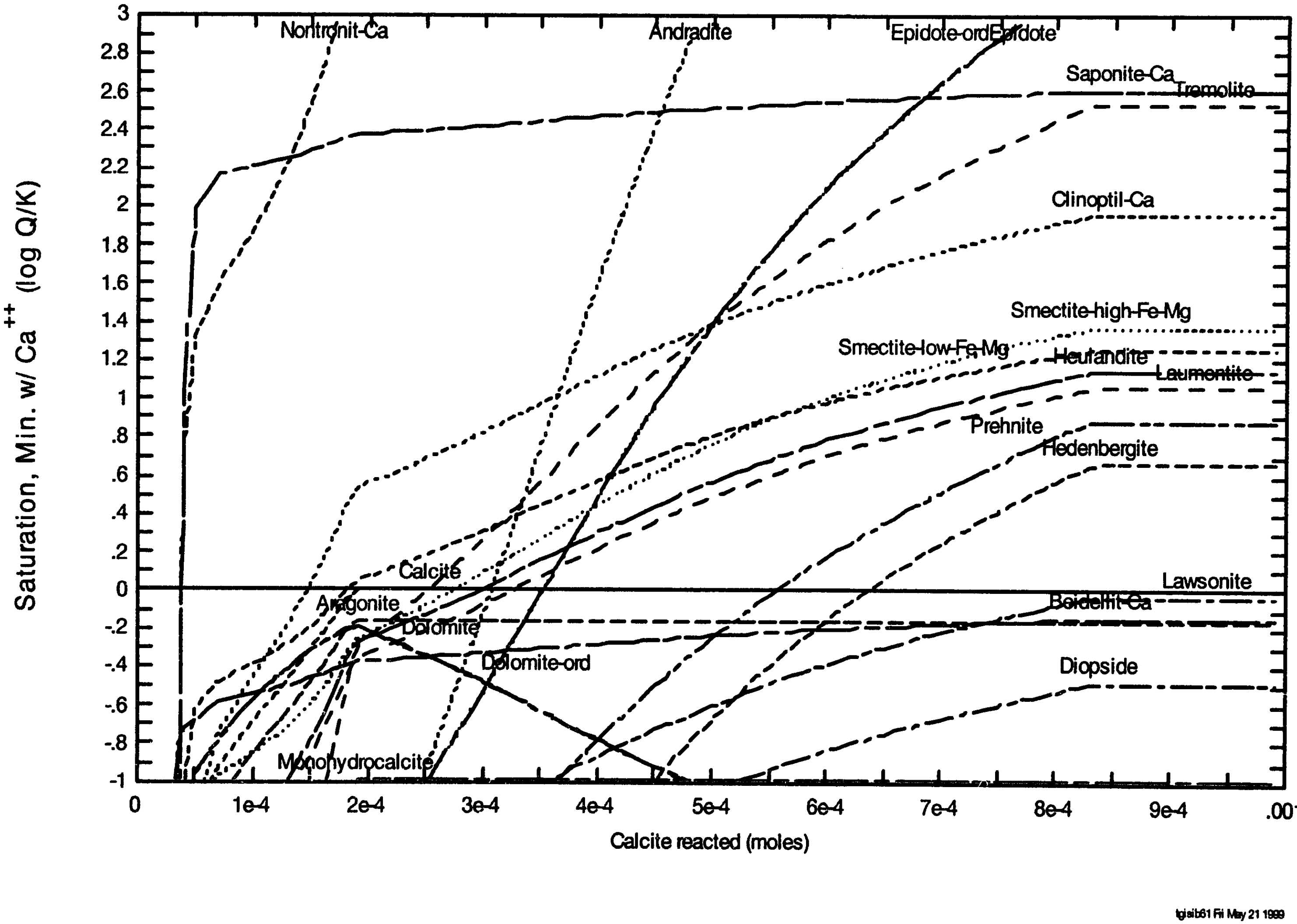

***Figure 24** : Kamaishi reaction-path model : Ca. A vertical line shows the saturation index (log Q/K) of Ca bearing minerals. A horizontal line shows the amount of calcite reacted in this calculation.*

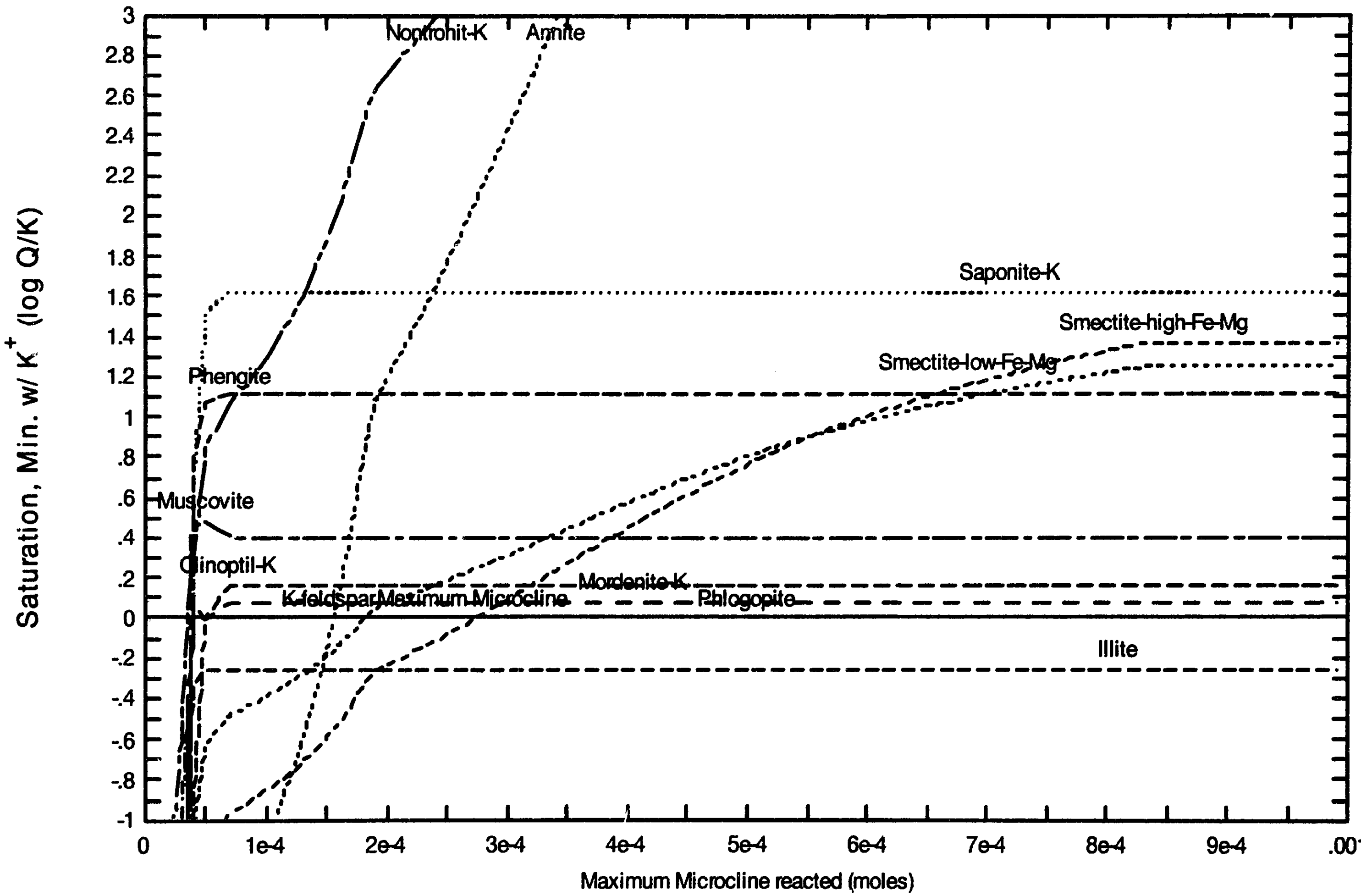

***Figure 25** : Kamaishi reaction-path model : K. A vertical line shows the saturation index (log Q/K) of K bearing minerals. A horizontal line shows the amount of maximum microcline reacted in this calculation.*

groundwater with respect to Na-nontronite, Na-saponite, and the high- and low-Fe-Mg smectites.

Similarly, Figure 24 indicates that the equilibrium groundwater is metastable with respect to laumontite, prehnite, epidote and heulandite, among other minerals, and Figure 25 suggests it is also metastable with respect to muscovite and two K-zeolites (clinoptilolite and mordenite). Both laumontite and prehnite are present in fractures at Kamaishi (Section 2.2). Epidote is also found in these fractures and in altered zones of the Kurihashi granodiorite.

The zeolite heulandite $[(Na,Ca)_2\text{-}3Al_3(Al,Si)_2Si_{13}O_{36} \cdot 12H_2O]$ is compositionally and crystallographically analogous to stilbite $[NaCa_2Al_5Si_{13}O_{36} \cdot 14H_2O]$, an abundant mineral in fractures at Kamaishi, but for which thermodynamic data are presently unavailable in the thermodynamic database supporting these calculations. Muscovite may be present as "sericite" in fractures, and in altered and unaltered portions of the host rock.

3.3.3.2 Example #2 - First Revision of the Test 15 Model -

A modeler evaluating these preliminary results may question whether the Test 15 model should be revised to be more consistent with the mineralogy at the Kamaishi site. One possible modification, for example, is to include laumontite as an equilibrium phase in the model because the predicted supersaturation of the groundwater with respect to laumontite (Figure 24) is inconsistent with the presence of this mineral in fractures. The modeler may also consider the following points:

- although the solution is more supersaturated with respect to epidote than laumontite, it is possible that epidote will not precipitate at low temperatures for kinetic reasons (this assumption should be verified, if possible, by referring to relevant laboratory of field studies), and
- although heulandite may be a reasonable compositional and crystallographic analog for stilbite, it will not be considered in this first revision of the Test 15 model, even though the solution is more supersaturated with respect to heulandite than laumontite (the modeler should, however, consider other sources of thermodynamic data for stilbite that could be added to the thermodynamic database supporting REACT - if none can be found, then simulations using heulandite to approximate stilbite's behavior could be considered in a second revision of the Test 15 model).

The calculated effects on saturation indices shown in Figures 23, 24 and 25 of allowing the

Test 15 groundwater to equilibrate with laumontite are shown in Figures 26, 27 and 28, respectively.

The amount of albite reacted before it equilibrates with the evolving solution (Figure 26) is nearly twice the amount needed in the unrevised Test 15 model (Figure 23). The modified solution composition is still metastable with respect to the same Na-clay minerals, suggesting the revised model may still be inconsistent with field observations indicating that such clays do not exist at Kamaishi.

Laumontite equilibrium strongly reduces supersaturation of the fluid with respect to several minerals (compare Figures 27 and 24). Laumontite stability also causes kaolinite to become unstable, and it is therefore no longer included in the equilibrium assemblage of the revised model (Appendix I). This is consistent with field observations indicating that kaolinite is absent at Kamaishi. Prehnite, however, is predicted to be unstable in this system, which is inconsistent with the observed association of calcite, laumontite and prehnite in Kurihashi fractures. Epidote remains supersaturated in solutions equilibrated with laumontite and calcite. A second revision of the Test 15 model could consider the effects of epidote equilibrium on groundwater evolution.

Calculated saturation indices among K-bearing minerals are not strongly affected when laumontite is included in the Test 15 mineralogy (compare Figures 25 and 28). Dissolved K^+ concentrations are more than doubled in the modified solution (compare Appendices H and I), but are still about a factor of 5 lower than in the reference groundwater. This suggests an additional modification of the Test 15 model could focus on assumptions involving minerals controlling K^+ concentrations.

Figure 29, for example, shows the stability diagram for the Na_2O-Al_2O_3-SiO_2-H_2O system at 25°C, 1 bar, onto which are plotted analyses of surface waters and Kamaishi groundwaters, and the calculated "trace" of the reaction-path calculation considered in example #2. The reaction trace for this example calculation closely approximates the evolution of Kamaishi groundwaters.

3.3.3.3 Recommended Modeling Approach

These examples illustrate a general procedure to systematically develop models of groundwater chemistry and evolution at sites such as Kamaishi:

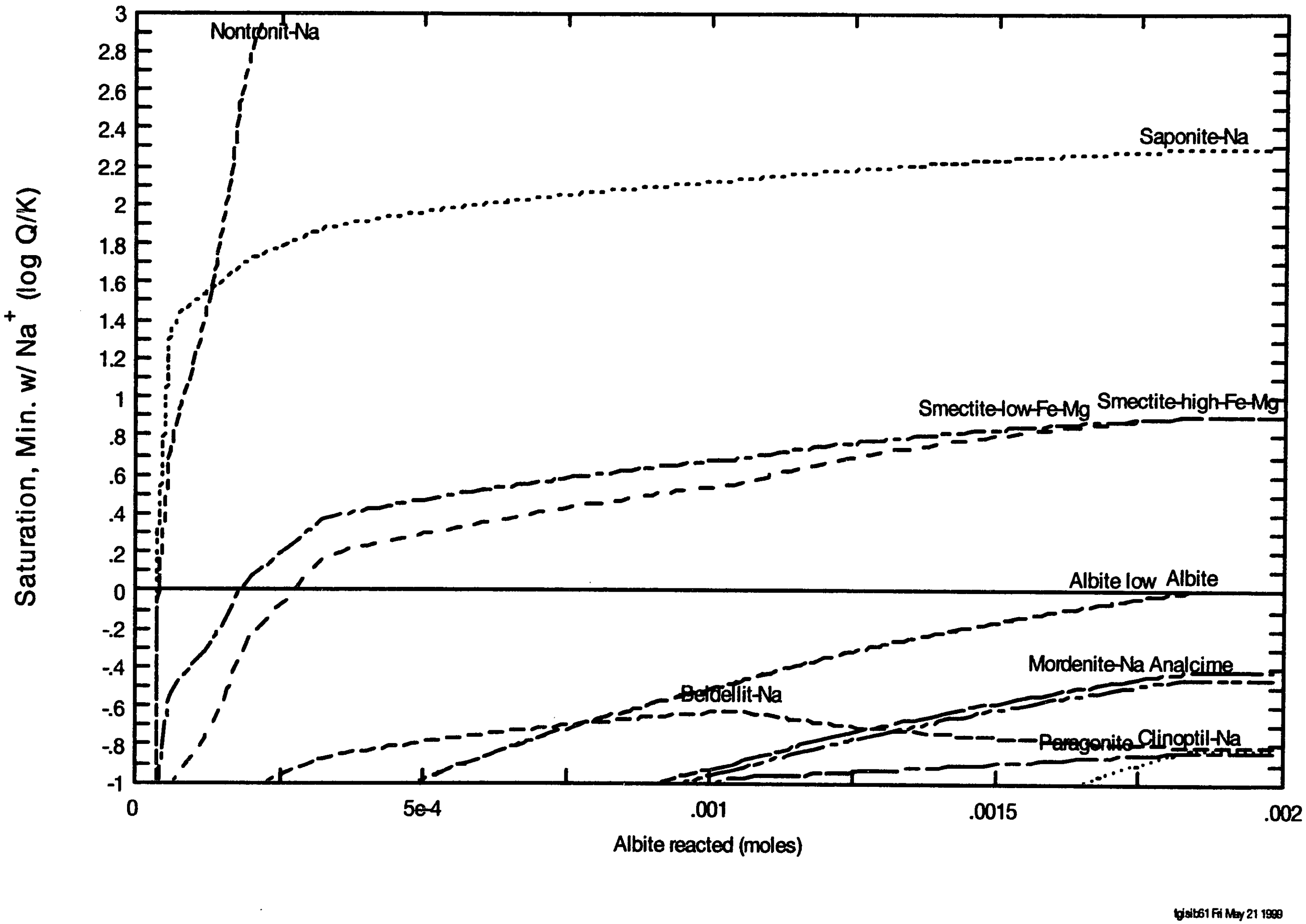

Figure 26 : Modified Kamaishi model : Na. A vertical line shows the saturation index (log Q/K) of Na bearing minerals. A horizontal line shows the amount of albite reacted in this calculation.

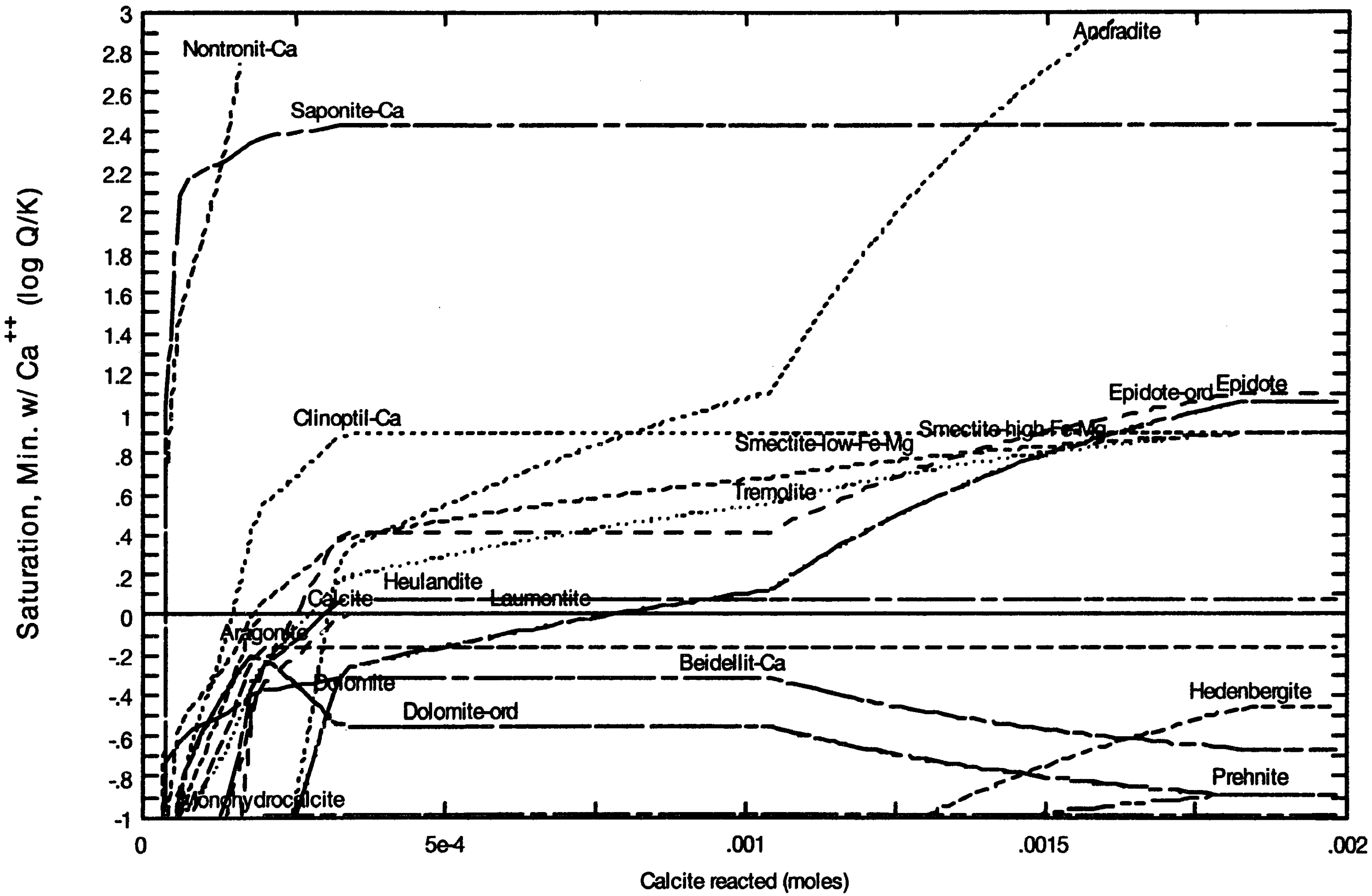

***Figure 27** : Modified Kamaishi model : Ca. A vertical line shows the saturation index (log Q/K) of Ca bearing minerals. A horizontal line shows the amount of calcite reacted in this calculation.*

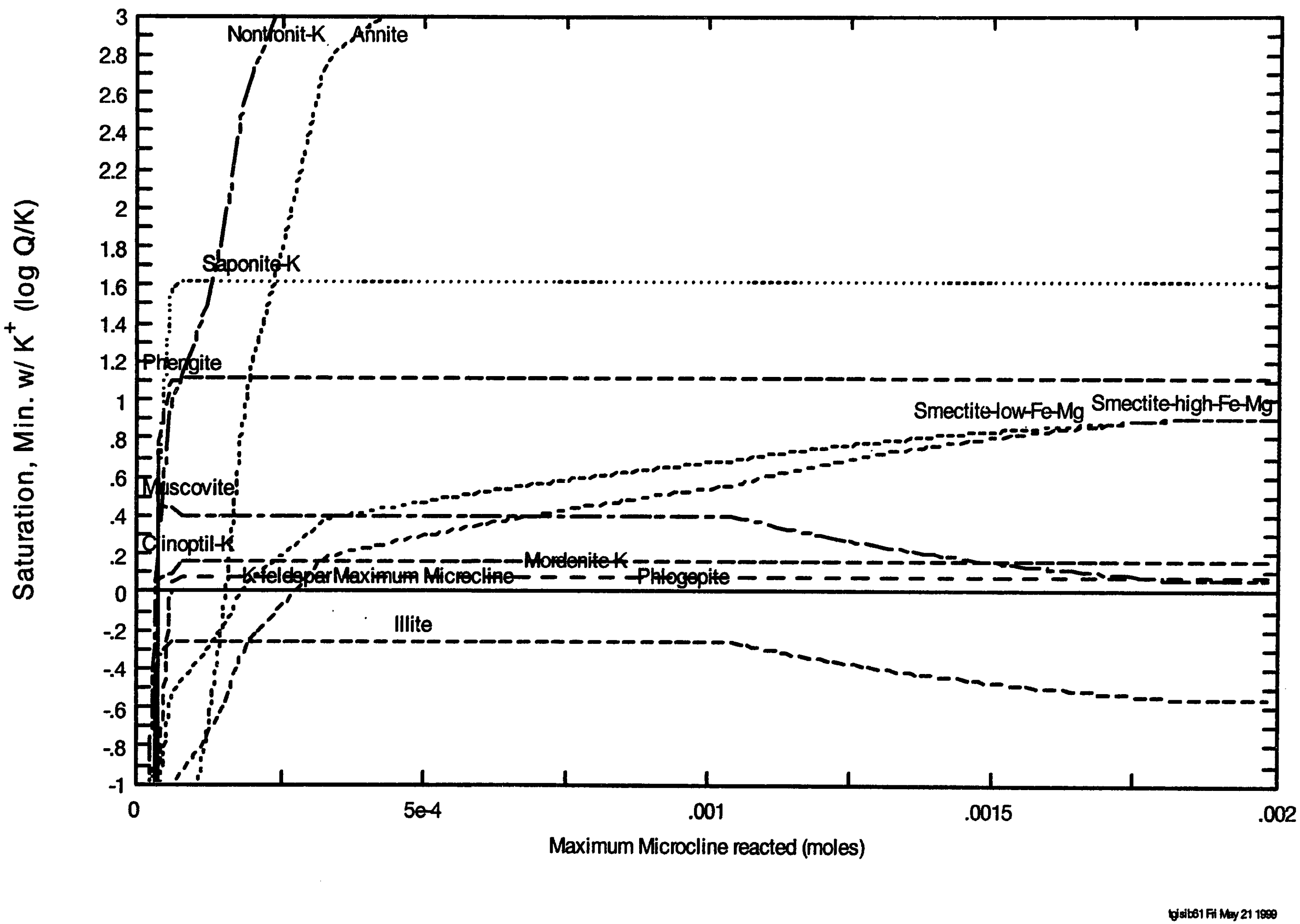

Figure 28 : Modified Kamaishi model : K. A vertical line shows the saturation index (log Q/K) of K bearing minerals. A horizontal line shows the amount of maximum microcline reacted in this calculation.

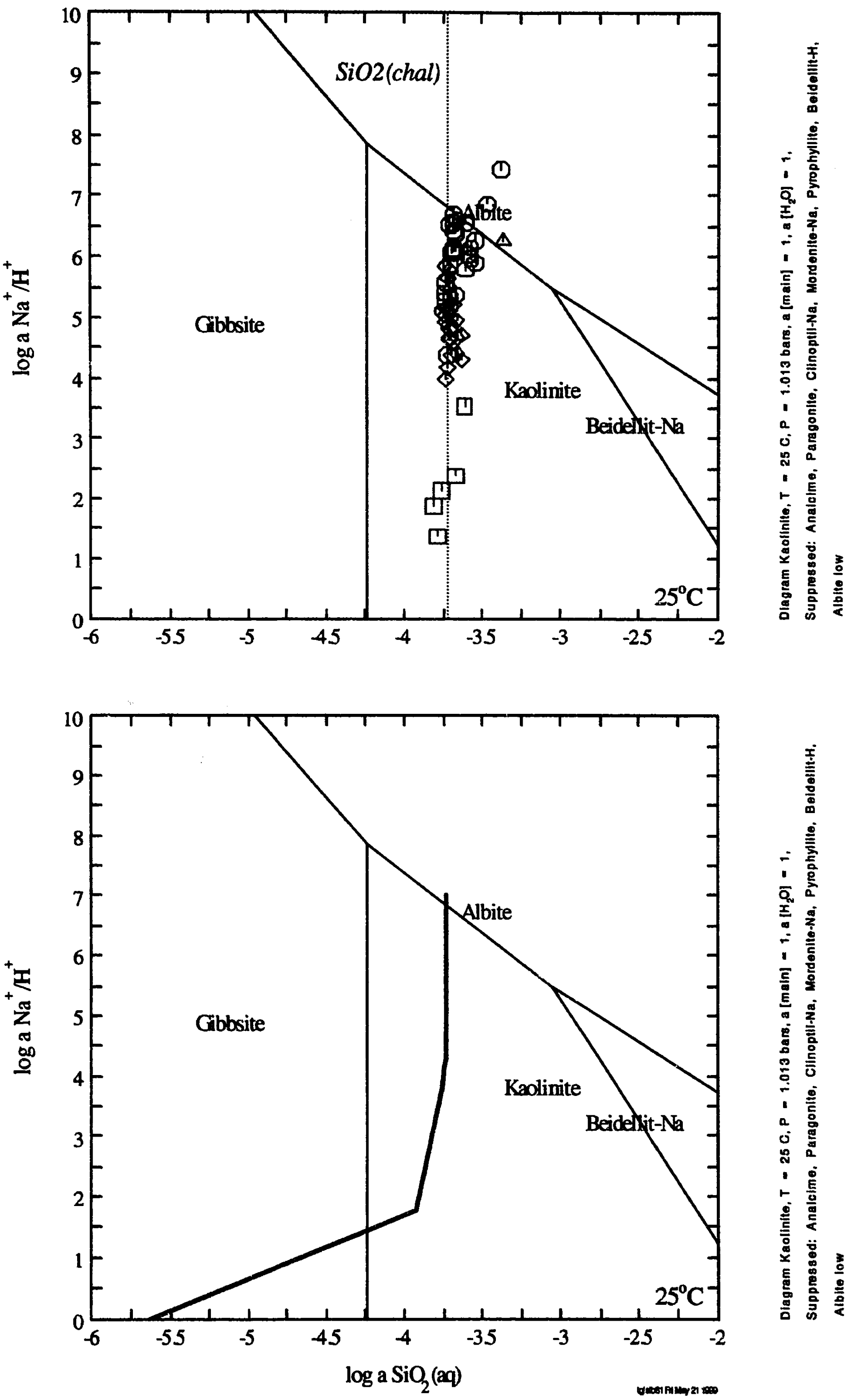

***Figure 29** : Stability diagram for Na2O-Al2O3-SiO2-H2O (above) at 25℃, 1 bar, with plotted surface waters and Kamaishi groundwaters (above), and plotted trace by reaction-path calculation of example #2 (below). Surface waters : square, Groundwaters (diamond : Ca-HCO3 type, circle : Na-HCO3 type, triangle : Na-Ca-SO4 type). The thermodynamic data used are derived from thermo.data of Geochemist's Work Bench. Log K (chal) = -3.7281 (25℃).*

1. obtain detailed information on the mineralogy of the site and chemistry of site groundwaters,
2. calculate the saturation index of minerals for which it is reasonable to assume that site groundwaters are in contact (results are summarized in section 2.3.7.2, for example),
3. develop a preliminary reaction-path model of groundwater evolution at the site, using the results of step 2 to guide initial selection of possible equilibrium phases,
4. evaluate model results for consistency with field observations,
5. if results are inconsistent with site data, modify the reaction-path model by revising one assumption concerning whether a mineral observed at the site should be considered stable, unstable or metastable.
6. iterate steps 4 and 5 until an optimal model is obtained that is consistent with site mineralogy and which best explains observed groundwater compositions (see Section 3.3.2.1).
7. evaluate of the validity of the equilibrium approach (in the sense discussed in Section 3.3.1.1) by comparing results of the optimized model with site data.

These steps emphasize the iterative use of reaction-path models primarily to raise questions concerning the validity of assumptions in an evolving conceptual model of the system. To carry this procedure out successfully, the modeler must rely on expert judgement to answer these questions.

3.4 Recommendations

3.4.1 Conceptual Model

The exact nature of equilibrium in models of groundwater chemistry and evolution must be clearly defined, and should include the concepts of local, partial and metastable equilibrium. Including, or excluding, minerals for consideration in a model on the basis of assumed partial or metastable equilibrium behavior should be supported by referencing relevant laboratory and field studies.

Stable isotope and tritium data suggest that groundwaters flow relatively rapidly through the Kamaishi site, and that an open-system model for this site may therefore be more appropriate than the closed-system model evaluated in Section 2.5. The effects of open-system behavior on conclusions summarized in that section should therefore be evaluated.

3.4.2 Model Constraints : Groundwater Chemistry

JNC should consider all the groundwaters sampled at the Kamaishi site - not just the older groundwaters sampled in the KH-1 borehole. Although it may reasonable to assume the older groundwaters are the most likely to have attained equilibrium, the younger groundwaters sampled in drifts and other boreholes may also provide valuable clues about irreversible processes during early stages of groundwater evolution.

JNC should strengthen their view that the apparent oxidizing conditions in most Kamaishi groundwaters can be traced to difficulties in measuring reliable redox potentials. The results of various international studies, in which this has been convincingly demonstrated in both the laboratory and field,, should therefore be discussed.

Variations in the compositions of groundwaters among samples from individual fractures intersecting the E.L. 550, E.L. 250m and KD-89 drifts should be evaluated to support the (implied) assumption that samples obtained from the KH-1 borehole are representative of solutions in the Kurihashi granodiorite.

JNC studies (Osawa et al., 1995), which suggest that Kamaishi groundwaters flow preferentially in fractures, or fractures and adjacent altered-rock zones, should be acknowledged. The possibility that groundwaters flow only in fractures, for example, would suggest that only fracture minerals will affect groundwater evolution. Secondary effects, such as diffusional mixing of solutions in fractures and altered zones may also need to be considered, however.

3.4.3 Model Constraints : Mineralogy

More detailed information on the actual mineralogy of the Kamaishi site is needed, including the compositions of plagioclase, sericite, chlorite, biotite, calcite and epidote, and the identities of minerals that may occur in trace amounts (e.g., clays, kaolinite, chalcedony).

A lack of highly reliable thermodynamic data should not deter choices of equilibrium minerals. Reasonable estimates of the necessary data will greatly improve credibility in the model, provided the uncertain reliability of the data is acknowledged and documented.

3.4.4 Model Constraints with Field Data : Groundwater Chemistry

JNC's approach in using a reference groundwater composition as the only criterion by which the validity of equilibrium-based models is tested should be reconsidered. It is recommended that JNC should instead consider the range in groundwater compositions actually measured at Kamaishi (see Section 3.4.2). JNC should then evaluate whether alternative models of groundwater evolution are equally valid, given this range.

3.4.5 Model Constraints with Field Data : Mineralogy

Minerals considered to be heterogeneous equilibrium constraints should be selected from among minerals actually present at Kamaishi. Minerals of igneous or hydrothermal origin should be considered with caution because they are probably unstable at low temperatures. Models indicating that groundwater compositions are supersaturated with respect to Kamaishi minerals should also be revised such that these "metastable" phases are assumed to equilibrate, if precipitation at low temperatures is reasonable.

3.4.6 Modeling Approach

A more systematic approach toward developing and testing equilibrium-based groundwater evolution models is recommended. The recommended approach should include the following steps.

1. obtain detailed information on the mineralogy of the site and chemistry of site groundwaters,
2. calculate the saturation index of minerals for which it is reasonable to assume that site groundwaters are in contact,
3. develop a preliminary reaction-path model of groundwater evolution at the site, using the results of step 2 to guide initial selection of possible equilibrium phases,
4. evaluate model results for consistency with field observations,
5. if results are inconsistent with site data, modify the reaction-path model by revising one assumption concerning whether a mineral observed at the site should be considered stable, unstable or metastable.

6. iterate steps 4 and 5 until an optimal model is obtained that is consistent with site mineralogy and which best explains observed groundwater compositions (see Section 3.3.2.1).
7. evaluate of the validity of the equilibrium approach (in the sense discussed in Section 3.3.1.1) by comparing results of the optimized model with site data.

These steps emphasize the iterative use of reaction-path models to raise questions concerning the validity of assumptions in an evolving conceptual model of the system. To carry this procedure out successfully, the modeler must rely on expert judgement to answer these questions.

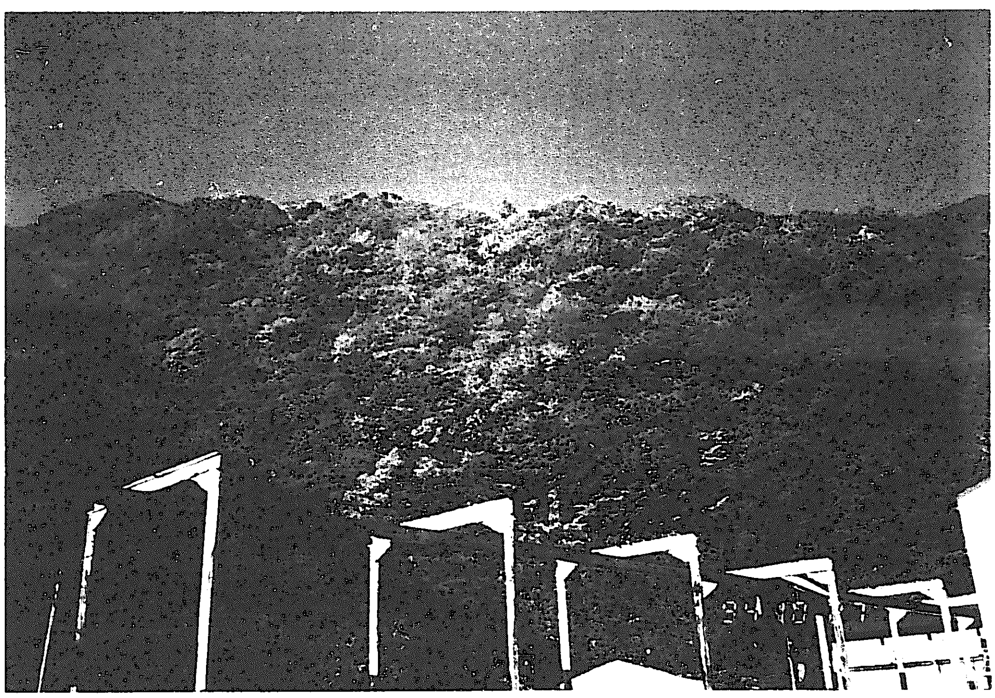

Autumnal tints of Mt Ganidake (at the entrance of E.L.550m drift)
(27 October, 1994)

4. CONCLUSIONS

The results of hydrochemical investigations at the Kamaishi *in-situ* tests site, modeling of groundwater chemistry and evolution at this site by JNC, and discussions of these models with geochemical experts are summarized below.

1) The depth-dependency and evolution of groundwater chemistry at the Kamaishi site have been determined, as has the origin of these solutions and their residence time in the Kurihashi granodiorite.

2) It is possible to interpret the chemistry and chemical evolution of "*real*" groundwaters at Kamaishi using a local-equilibrium model of water-rock interactions that is based on JNC's conceptual groundwater evolution model for the hypothetical FRHP type groundwater.

3) The following issues should be addressed, however, to improve groundwater evolution models appropriate for the Kamaishi site:

- the exact nature of equilibrium in models of groundwater chemistry and evolution must be clearly defined, and should include consideration of the concepts of local, partial and metastable equilibrium;
- it should be determined whether open- or closed-system conditions are most appropriate for the groundwater evolution model;
- more detailed information on the actual mineralogy of the Kamaishi site is needed, including minerals that may occur in trace amounts (e.g., clays, kaolinite, chalcedony);
- minerals that are assumed to be heterogeneous equilibrium constraints in the model should be selected from among minerals actually present at Kamaishi - those of igneous or hydrothermal origin should be considered with caution because they are unstable at low temperature, and should therefore dissolve irreversibly and incongruently;
- a lack of reliable thermodynamic data for key minerals (e.g., clays and zeolites) should not be a reason for excluding them in models of groundwater chemistry and evolution, provided credible estimates of such data are available, and that the uncertain reliability of the data is acknowledged;

- the range in groundwater compositions actually measured at this site should be considered in evaluations of the reliability of the groundwater evolution model, rather than a single composition that is representative of these solutions.
- a more systematic approach (possibly using reaction-path models) is needed to develop and test JNC's equilibrium-based groundwater evolution models.

5. ACKNOWLEDGEMENTS

The authors acknowledge the Nittetsu Mining Co., Ltd and Kamaishi Mining Co., Ltd for field investigations in the Kamaishi Mine and sampling of groundwaters at the Kamaishi *in-situ* tests site, Dr. Michael J Apted (Monitor Scientific, LLC[1]) and Dr. David Savage (Quintessa, Ltd[2].) for discussions of JNC's groundwater evolution models, Nagra reviewers (Dr. Ian G Mckinley, Dr. Urs R Berner, Dr. Michael H Bradbury and Dr. Bart Baeyens) at the H-12 review meeting (6-7 November, 1997 at Tokai) for comments on JNC's approach to groundwater evolution modeling, Mr. Makoto Yoshizoe (Mitsubishi Corp.) and Mr. Atsushi Neyama (Computer Software Development Corp.) for support of contract, Mr. Toshihiro Seo (JNC Tokai Works) for assistance in planning the groundwater sampling strategy and for discussions on thermodynamic interpretations of Kamaishi groundwaters, and staff of JNC's Kamaishi Office (closed March, 1998) and Tono Geoscience Center for carrying out and supporting the fracture mapping work.

[1] *Formerly QuantiSci Inc., Denver, Colorado USA*
[2] *Formerly QuantiSci Ltd., Melton Mowbray UK*

6. REFERENCES

Anderson, G.M. and Crerar, D. A (1993) : *Thermodynamics in Geochemistry*. Oxford Univ. Press, New York, 588 p.

Aoki K, Sasamoto H, Senba T, Amano K, Takahara H, Ohbuchi S and Matsushima E (1997) : Microbial analyses of deep groundwater in fractured granodiorite at the Kamaishi Mine, Japan, Proceedings of the 7th symposium on geo-environments and geo-technics, pp.81-86.

Bethke C (1996) : *Geochemical Reaction Modeling*. Oxford Univ. Press, New York, 397p.

Black W H, Smith H R and Patton F D (1986) : Multiple level groundwater monitoring with the MP system, Proc. NWWA-AGU Conf. on surface and Borehole Geophysical methods and groundwater instrumentation, pp.41-61.

Craig H (1961) : Isotopic variations in meteoric waters, *Science* 133, pp.1702-1703.

Drever J I (1988) : *The geochemistry of natural waters (2nd edition)*, Prentice Hall, ISBN 0-13-351396-3.

Deutsh W J (1997) : *Groundwater geochemistry, fundamentals and applications to contaminatin*, CRC Press LLC, ISBN 0-87371-308-7

Friedman L C, and Erdmann D E (1982) : Quality assurance practices for analyses of water and fluvial sediments (Tech. Water Resources Inc., Book 5, Chapter A6).

Fujita T, Sugita Y, Sato T, Ishikawa H and Mano T (1994) : Plan of coupled thermo-hydro-mechanical experiment at the Kamaishi mine, PNC Technical Report, TN 8020 94-005.

Fukunaga S, Yoshikawa H, Fujiki K and Asano H (1995) : Experimental investigation on the active range of sulfate-reducing bacteria for geological disposal, In: *Scientific Basis for Nuclear Waste Management XVIII*, T. Murakami and R. C. Ewing (eds.), Materials Research Society, Pittsburgh, PA., pp.173-180.

Grenthe I, Stumm W, Laaksoharju M, Nilsson N -C, and Wikberg P (1992) : Redox potentials and redox reactions in deep groundwater systems. *Chem. Geol.*, 98, pp.131-150.

Grimaud D, Beaucaire C and Michard G (1990) : Modelling of the evolution of ground waters in a granite system at low temperature : the Stripa ground waters, Sweden, *Applied Geochemistry*, 5, pp.515-525.

Hamabe S and Kuwata K (1977) : Prospecting at the Kamaishi mine - With particular reference to the related igneous rocks to the mineralization -, *Mining Geology*, 27, pp.73-85 (in Japanese).

IAEA (1986) : Environmental isotope data No.8, Technical Reports Series No.264.

Ii H, Horie Y, Ishii T and Shimada J (1997) : Development of an apparatus to measure groundwater qualities in-situ and to sample groundwater using boreholes, *Environmental Geology*, 32 (1), pp.17-22.

JNC (1999) : Final report of Kamaishi in-situ experiment, JNC Technical Report, TN7410 99-001 (in Japanese with English abstract).

Johnson J W, Oelkers E H, and Helgeson H C (1991) : A software package for calculating the standard molar thermodynamic properties of minerals, gases, aqueous species, and reactions from 1 to 5000 bars and 0 to 1000°C. Geol. Soc. Am. Short-course manual, San Diego, Ca., Oct. 21-24.

Kawano Y and Ueda Y (1969) : K-Ar dating of the igneous rocks in Japan (2) - Granitic rocks in Kitakami massif -, *Assoc.Miner.Petro.Econ*, 53, 143-149 (in Japanese).

Matsubaya O (1985) : Isotope geochemistry of geothermal water 1, *Geothermal energy*, Vol.10, No.2, pp.25-39 (in Japanese).

Matsumoto S (1989) : *Soil formation and soil type*, Kikan Kagaku Sousetsu No.4 (Quarterly publication of chemistry), Chemistry of soil, Chemist, Soc, Japan edit, pp.19-32 (in Japanese).

Muller A B (1985) : NEA compilation of chemical thermodynamic data for minerals associated with granite, OECD/NEA, RWM-5 NEA report.

Nordstrom D K and Puigdomenech I (1986) : Redox chemistry of deep groundwaters in Sweden. SKB TR 86-03. Swedish Nuclear Fuel and Waste Management Co., Stockholm, Sweden.

Nordstrom D K, Plummer L N, Langmuir D, Busenberg E, May H M, Jones B F and Parkhurst D L (1990) : Revised chemical equilibrium data for major water-mineral reactions and their limitations. In: *Chemical Modeling of Aqueous Systems II*, D.C. Melchior and R.L. Bassett (eds.), Am. Chem. Soc. Symp. Ser., 416, pp.399-413.

Osawa H, Sasamoto H, Nohara T, Ota K and Yoshida H (1995) : Development of a conceptual flow-path model of nuclide migration in crystalline rock - A case study at the Kamaishi in-situ test site, Japan. In: *Scientific Basis for Nuclear Waste Management XVIII*, T. Murakami and R. C. Ewing (eds.), Materials Research Society, Pittsburgh, PA., pp.1267-1273.

Ota K, Amano K and Ando T (1998) : In-situ nuclide retardation in a fractured crystalline rock, Kamaishi in-situ test site, In: *Kamaishi international workshop proceedings*, 24-25 Aug.1998 Rikuchu Kaigan Grand Hotel, Kamaishi, Japan, PNC Technical Report TN7413 98-023.

PNC (1992) : Research and development on geological disposal of high-level radioactive waste - First progress report -, PNC Technical Report, TN1410 93-059.

PNC (1998) : Kamaishi international workshop proceedings, 24-25 Aug.1998 Rikuchu Kaigan Grand Hotel, Kamaishi, Japan, PNC Technical Report TN7413 98-023.

Paces T (1972) : Chemical characteristics and equilibration in natural water-felsic rock-CO2 system, *Geochim.Cosmochim.Acta* 36, pp.217-240.

Parkhurst D L, Thorstenson D C, and Plummer L N (1980) : PHREEQE - A computer program for geochemical calculation -, U.S.Geological Survey, Water-Resources Investigations.

Sasamoto H, Kitayama M, Sato T, Yoshida H, Ota K, Nohara T and Takeda S (1993) : Fracture mapping in the E.L.250 meter drift in the Kamaishi Mine, PNC Technical Report KTR 93-02, TN7410 93-032 (in Japanese with English abstract).

Sasamoto H, Seo T, Yui M and Sasaki Y (1996) : Geochemical investigation of groundwater in the Kamaishi In-situ tests site, Japan (Part-1), PNC Technical Report, TN8410 96-203, 59p (in Japanese).

Sasamoto H, Yui M and Hama K (1999a) : Redox conditions in host rocks surrounding a drift in the Kamaishi *in-situ* tests site, Japan, JNC Technical Report, TN8400 99-013, 36p (in Japanese and English).

Sasamoto H, Yui M and Arthur R C (1999b) : Modeling studies of saline type groundwater evolution - A test case for Mobara groundwater chemistry, Japan -, JNC Technical Report (in preparation).

Sasamoto H, Yui M and Arthur R C (1999c) : Status of geochemical modeling of groundwater evolution at the Tono *in-situ* tests site, Japan, JNC Technical Report, TN8400 99-074.

Shimada J, Ishii T, Horie Y and Oike T (1990) : Development of continuous sampling tool of groundwater from deep borehole, Hydrologic experiment center report, University of Tsukuba, vol.14, pp.172-174, ISSN 0385-907X (in Japanese).

Stumm W and Morgan J J (1981) : *Aquatic chemistry (2nd edition)*, Wiley Interscience, ISBN 0-471-09173-1, 780p.

Takeda S and Osawa H (1993) : Current status and future program of In-situ experiments of Kamaishi, Japan, Proceedings of International Symposium on In-situ Experiments at Kamaishi, 11-12 November 1993, Kamaishi.

Westbay Instruments Inc (1992) : An introduction to Westbay's MP system for groundwater monitoring, 20p.

Wikberg P (1987) : The chemistry of deep groundwaters in crystalline rocks. Ph.D. Thesis: Dept. of Inorganic Chemistry, KTH, Stockholm.

Wikberg P (1988) : The natural chemical background conditions in crystalline rocks. In: *Scientific Basis for Nuclear Waste Management XI*, M. J. Apted and R. E. Westerman (eds.), Materials Research Society, Pittsburgh, PA., pp.373-382.

Wolery T J (1983) : EQ3NR, a computer program for geochemical aqueous speciation-solubility calculations, user's guide and documentation, Lawrence Livermore National Laboratory Report UCRL-MA-110662 PT-I, 60p.

Wolery T J : *Private communication*

Yui M, Takeda S, Komuro M, Makino H, Shibutani T, Umeki H, Ishiguro K, Takase K and Neyama A (1992) : Modeling of groundwater evolution for performance assessment of high level radioactive waste isolation, Power Reactor and Nuclear Fuel Development Corporation, Tokai-Mura, Ibaraki, Japan, Technical Report, TN8410 92-166 (in Japanese).

Yui M, Sasamoto H and Arthur R.C. (1999) : Groundwater evolution modeling for the second progress performance assessment (PA) report, Japan, JNC Technical Report, TN8410 99-030.

APPENDIX

Appendix A: Fracture Distribution in the E.L.250m Drift, and Typical Fracture Types in the Kurihashi Granodiorite

[List of Appendix A]

Appendix A-1: Plane view of geological map around *in-situ* tests area in the drift E.L.250m
Fracture mapping was carried out over a section of the drift (440 m in length) that intersects the Kurihashi granodiorite. The mapped section starts at the projection to the drift level of the boundary between Kamaishi City and Toono City, in accordance with an agreement reached between Kamaishi City, Nittetsu Mining Co., Ltd (the owner of the Kamaishi mine) and JNC. Fracture properties and lithology were characterized to aid in the selection of various sites in the E.L.250 m drift for the *in-situ* tests.

All fractures greater than 3m in trace length were mapped and their features (e.g., fracture type, dip-strike, aperture, infilling minerals and alteration pattern) were described. Details of the mapping methodology and results are described by Sasamoto et al. (1993). The main results are summarized as follows:

- the Kurihashi granodiorite contains numerous xenoliths. A number of aplite and lamprophyre dykes are also present;
- a total of 400 fractures were identified, including 100 that are water bearing;
- fracture network systems are common - fracture zones formed by parallel, closely spaced fractures are also observed in several places;
- the average fracture aperture is less than 5mm;
- calcite, quartz, chlorite and epidote are common infilling minerals; and
- fractures with a WNW-ESE to E-W strike and vertical dip are predominant.

Appendix A-2: Fracture distribution of *in-situ* tests area in the drift of E.L.250m.
The photographs in Appendices A-2-1 to A-2-11 document the distribution of fractures in the *in-situ* tests area of the E.L.250 m drift. The yellow horizontal "scan line" shown in these photographs was drawn on the east side of drift wall, 1m above the drift floor. The location from the starting point of this line was marked in 5m increments. The fractures that intersect the scan line were assigned a number (red paint). Note that the photographs in Appendices A-2-1 to A-2-11 cover only the first 175 m of the length of the scan line.

Appendix A-3: Fracture types in the Kurihashi granodiorite (Osawa et al., 1995).
The 400 fractures characterized in the fracture-mapping investigation were categorized based on their fracture-filling mineralogy and alteration characteristics. Type A fractures exhibit a rather simple structure overall and contain fracture-fill minerals. Type B fractures are similar

to Type A fractures, but include an alteration halo extending into the host rock from the fracture plane. Type C fractures are characterized by a fracture zone, consisting of closely spaced sub-parallel fractures, each of which includes fracture filling minerals. Individual fractures in Type C fracture zones commonly exhibit alteration haloes, but some fractures may not exhibit such haloes. Type B fractures are the most common type observed in the fracture mapping area, representing more than 60% of the total number of fractures. Type B fractures were investigated in laboratory experiments to establish a conceptual flow-path model for the Kamaishi site (Osawa et al., 1995; Ota et al., 1998).

Appendix A-4: Magnification photograph around No.58 fracture

This photograph shows a magnified view of Fracture #58 [see Appendix A-2-9(2)], which is a Type C fracture, or fracture zone (see Appendix A-3). The width of the zone is about 1m. The rate of groundwater flow from Fracture #58 into the E.L.250 m drift is relatively high (the location of this fracture is the same as the W3 groundwater sampling point (see Appendix B, photograph 3).

A magnified view of a portion of Fracture #58 is shown in Photograph A-4-1 (upper region of the central photograph, noted as ①). A cataclastic zone is present in the center of the fracture zone, which consists of fragments of cataclastic rock matrix and clay minerals, such as smectite, sericite and chlorite (JNC, 1999). The gray or blackish region between the central cataclastic zone and the unaltered host rock is probably a clay-rich zone.

Photograph A-4-2 shows a magnified view of another part of Fracture #58 (lower part of the central photograph, noted as ②). The photograph shows a cataclastic zone with numerous small fractures. Alteration haloes envelope some of the fractures.

Appendix A-5 : Magnification photograph between No.85 and No.89 fracture

Photograph A-5-1 shows a magnified view of the mapped section between Fracture #85 and Fracture #89. This section, about 4 m in width, is characterized by numerous fractures, each of which includes an alteration halo (Type B fracture). The flow rate of groundwater through the fractures of this section is several hundred ml/minute (sampling points W7 and W8 are located in this region; see Appendix B, photographs 7 and 8).

A magnified view of Fracture #88 is shown in Photograph A-5-2 (noted as ③ in photograph A-5-1). The width of the fracture-filling material is about 10cm. Cataclastics (light-colored material) are evident near the center of the fracture.

[References]

- Osawa H, Sasamoto H, Nohara T, Ota K and Yoshida H (1995) : Development of a conceptual flow-path model of nuclide migration in crystalline rock - A case study at the Kamaishi in-situ test site, Japan. In: Scientific Basis for Nuclear Waste Management X Ⅷ, T.Murakami and R.C.Ewing (eds), Materials Research Society, Pittsburgh, PA., pp.1267-1273.
- Ota K, Amano K and Ando T (1998) : In-situ nuclide retardation in a fractured crystalline rock, Kamaishi in-situ test site. In: Kamaishi international workshop proceedings, 24-25 Aug.1998 Rikuchu Kaigan Grand Hotel, Kamaishi, Japan, PNC Technical Report TN7413 98-023
- Sasamoto H, Kitayama M, Sato T, Yoshida H, Ota K, Nohara T and Takeda S (1993) : Fracture mapping in the E.L.250 meter drift in the Kamaishi Mine, PNC Technical Report KTR 93-02, TN7410 93-032 (in Japanese with English abstract).

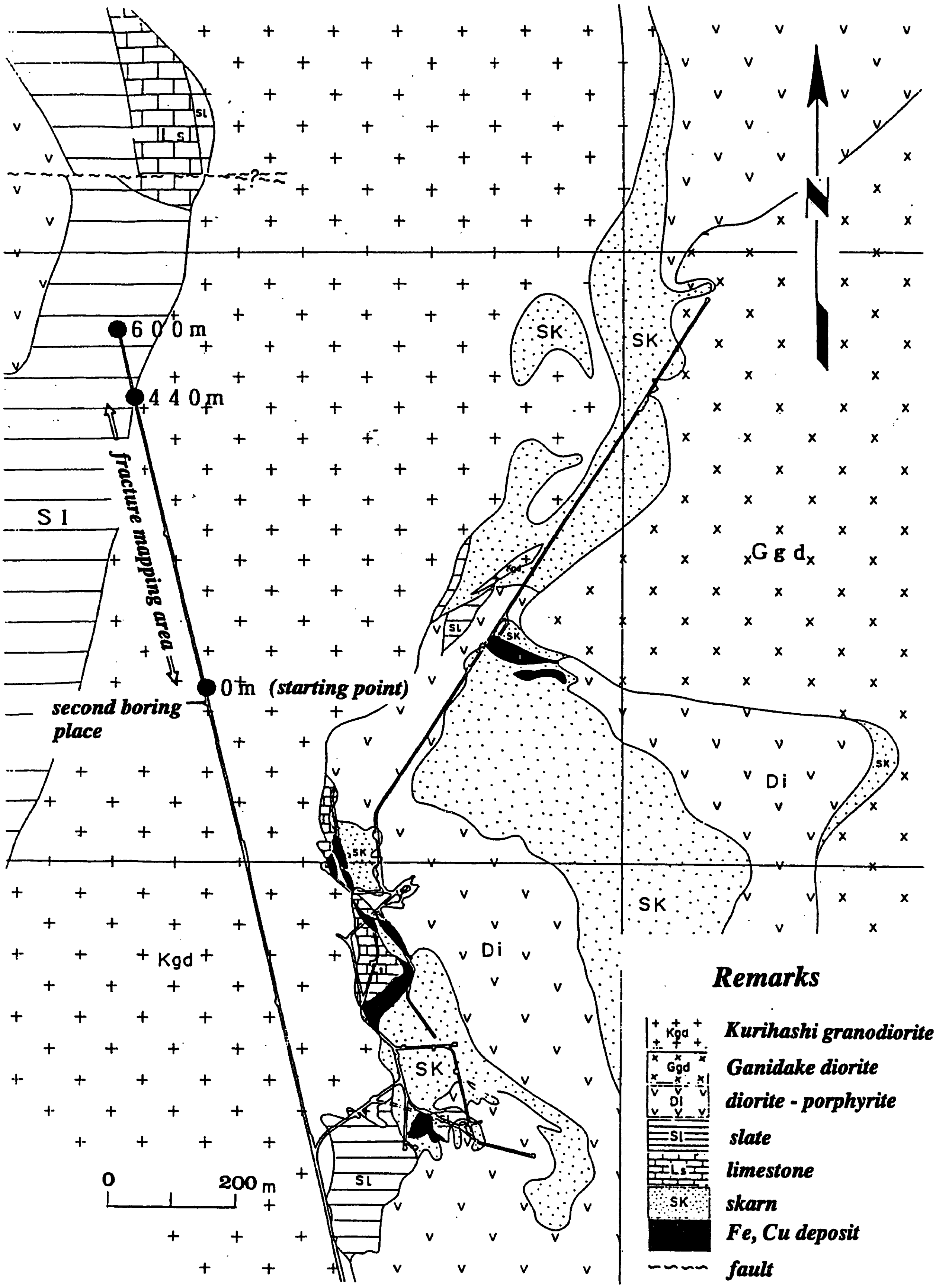

Appendix A-1 : Plane view of geological map around in-situ tests area in the drift E.L.250m

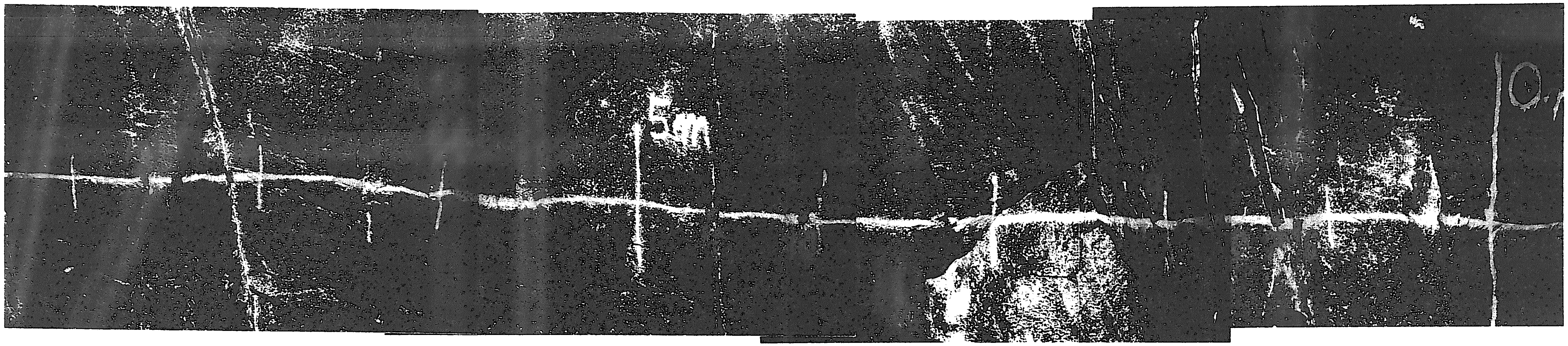

Appendix A-2-1(1) : Fracture distribution of in-situ tests area in the drift E.L.250m (0 to 8m from the starting point of fracture mapping)

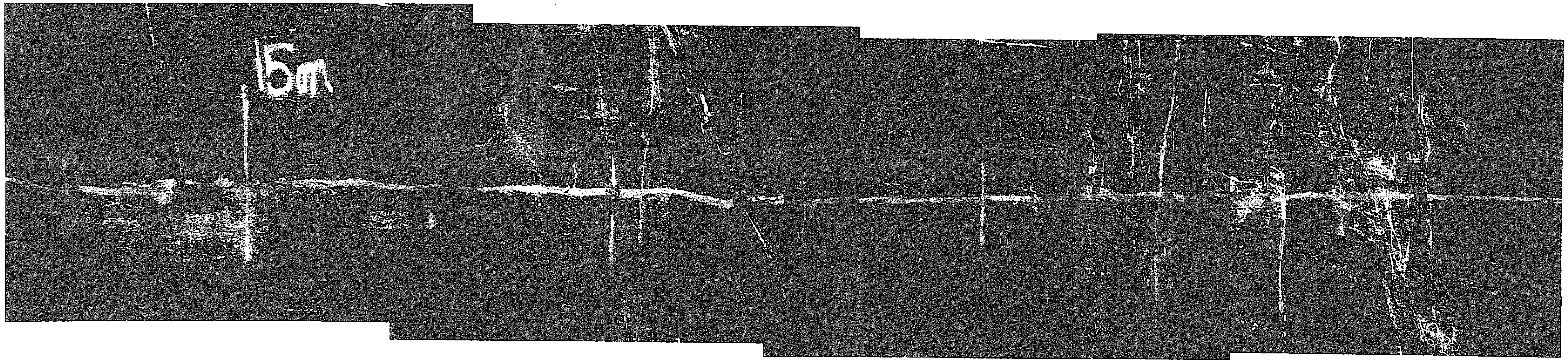

Appendix A-2-1(2) : Fracture distribution of in-situ tests area in the drift E.L.250m (8 to 16m from the starting point of fracture mapping)

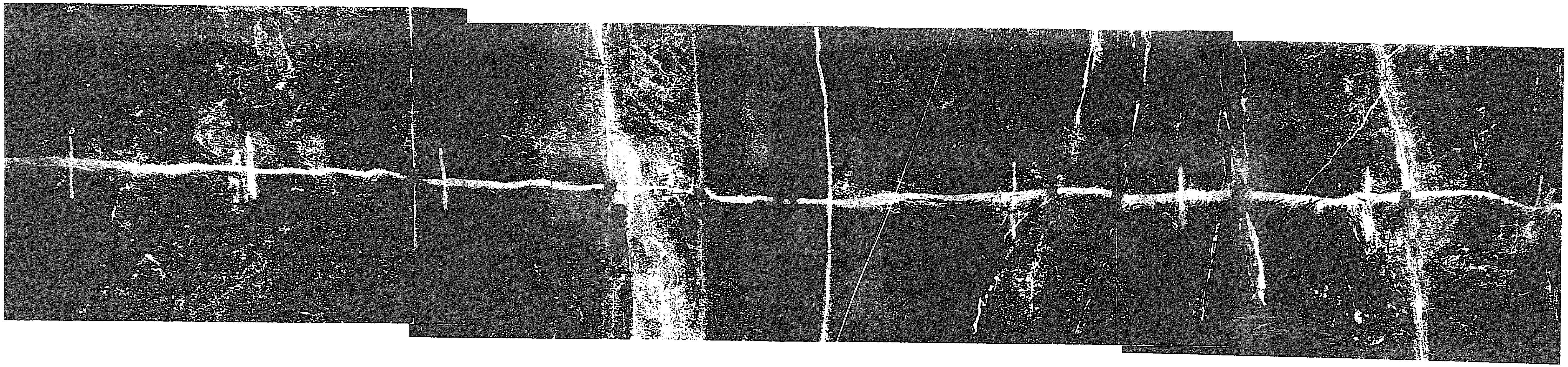

Appendix A-2-2(1) : Fracture distribution of in-situ tests area in the drift E.L.250m (16 to 24m from the starting point of fracture mapping)

Appendix A-2-2(2) : Fracture distribution of in-situ tests area in the drift E.L.250m (24 to 32m from the starting point of fracture mapping)

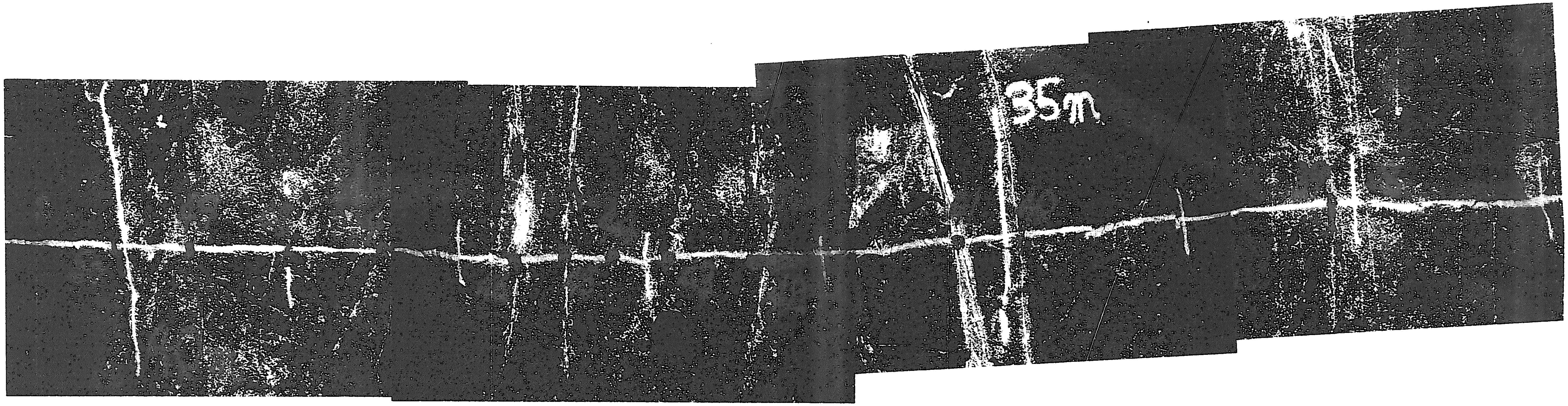

***Appendix A-2-3(1) :** Fracture distribution of in-situ tests area in the drift E.L.250m (32 to 40m from the starting point of fracture mapping)*

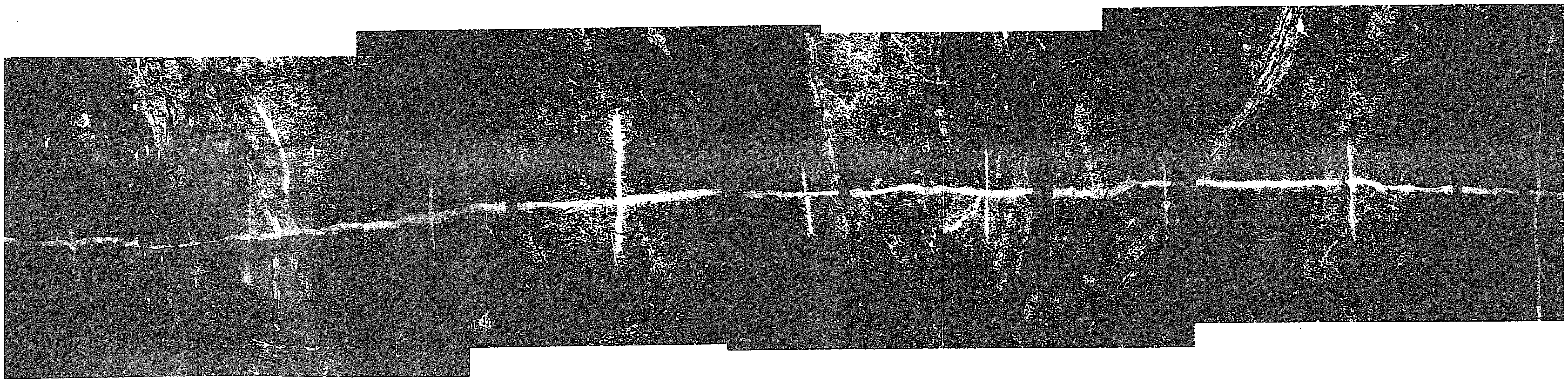

***Appendix A-2-3(2) :** Fracture distribution of in-situ tests area in the drift E.L.250m (40 to 48m from the starting point of fracture mapping)*

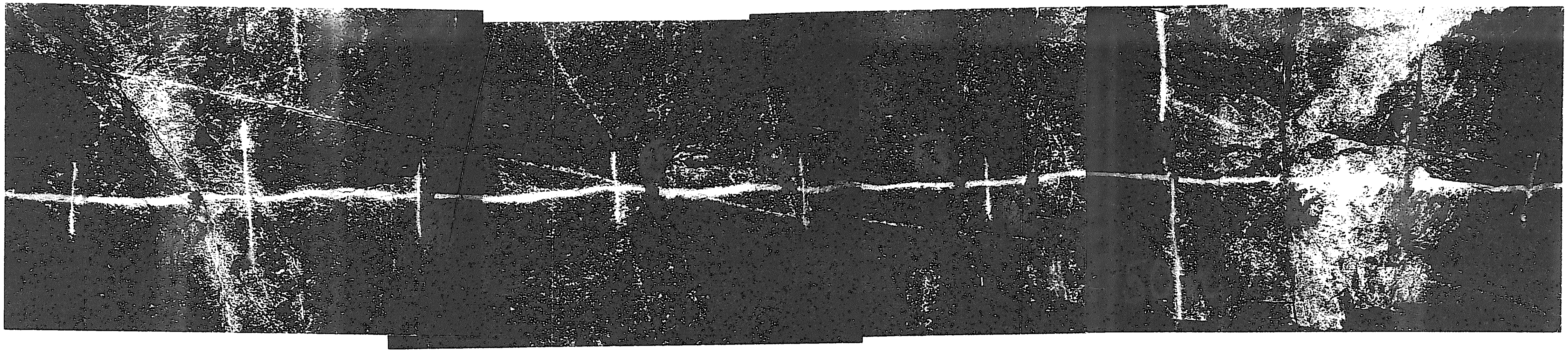

Appendix A-2-4(1) : *Fracture distribution of in-situ tests area in the drift E.L.250m (48 to 56m from the starting point of fracture mapping)*

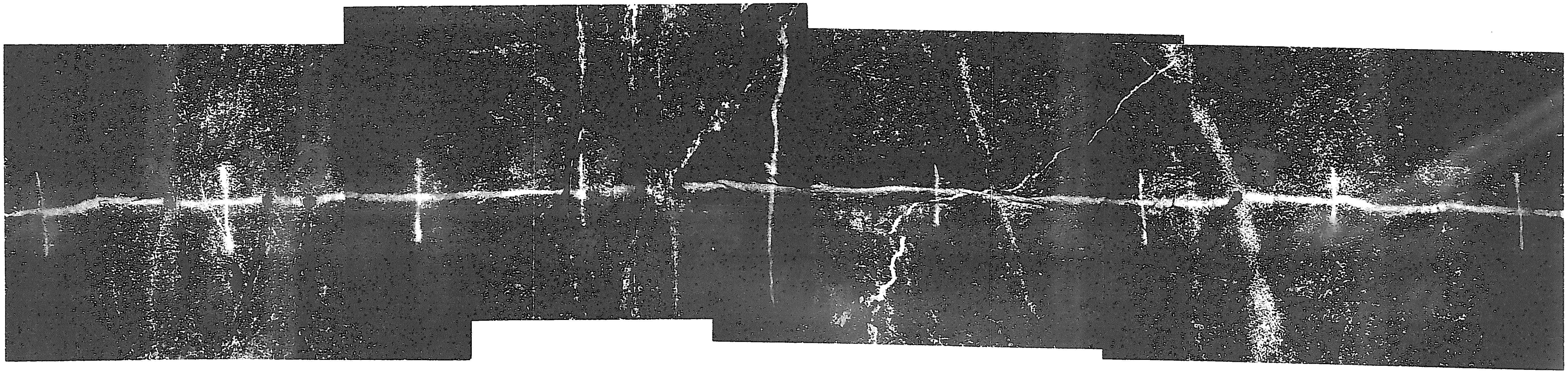

Appendix A-2-4(2) : *Fracture distribution of in-situ tests area in the drift E.L.250m (56 to 64m from the starting point of fracture mapping)*

Appendix A-2-5(1) : Fracture distribution of in-situ tests area in the drift E.L.250m (64 to 72m from the starting point of fracture mapping)

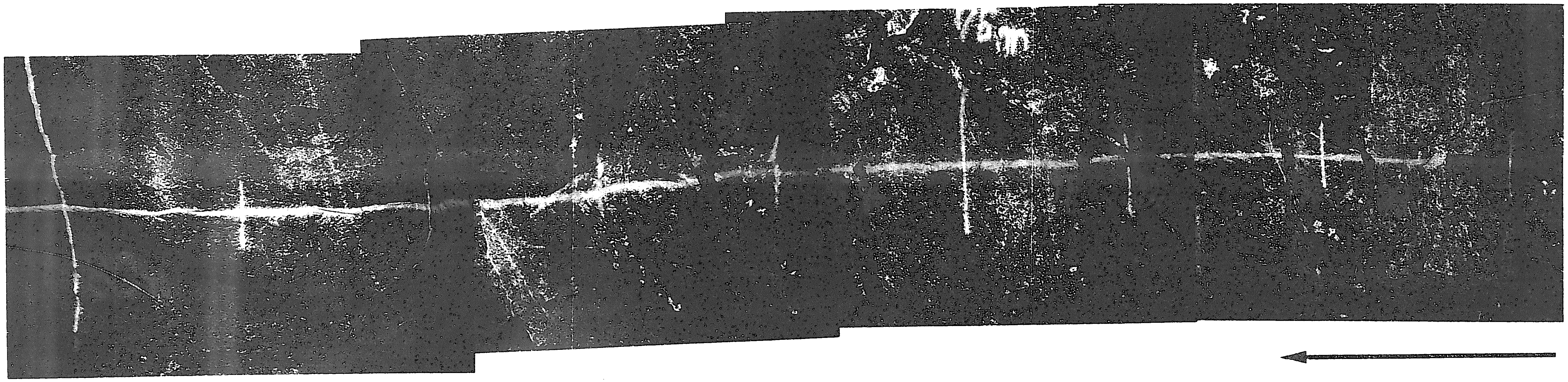

Appendix A-2-5(2) : Fracture distribution of in-situ tests area in the drift E.L.250m (72 to 80m from the starting point of fracture mapping)

Appendix A-2-6(1) : *Fracture distribution of in-situ tests area in the drift E.L.250m (86to 94m from the starting point of fracture mapping)*

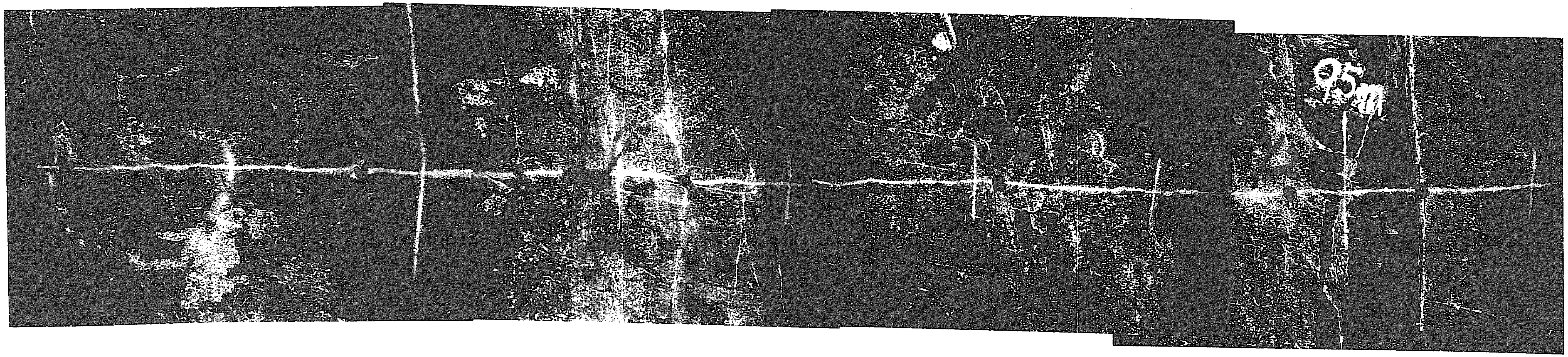

Appendix A-2-6(2) : *Fracture distribution of in-situ tests area in the drift E.L.250m (94 to 102m from the starting point of fracture mapping)*

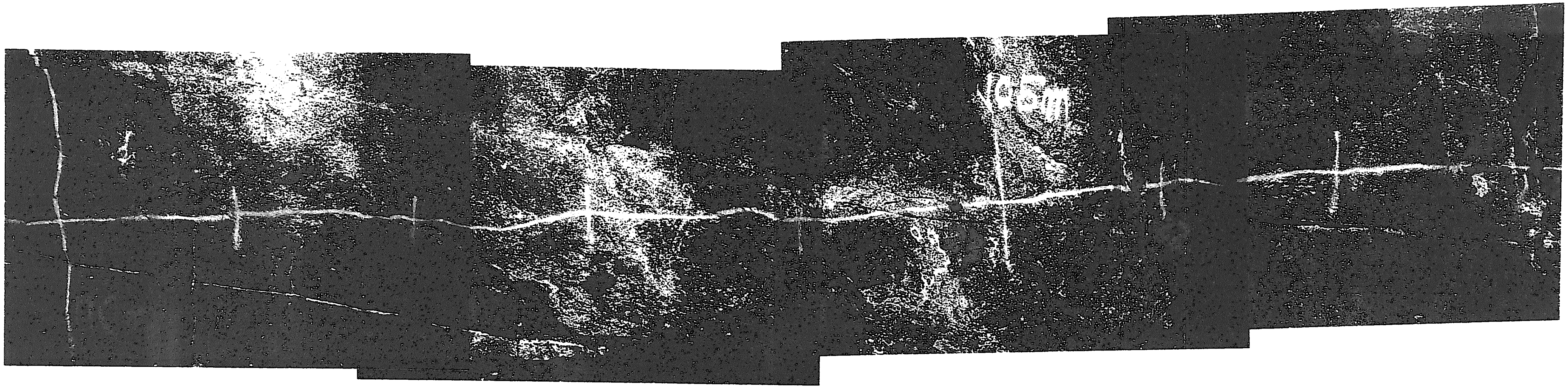

Appendix A-2-7(1) : *Fracture distribution of in-situ tests area in the drift E.L.250m (102 to 110m from the starting point of fracture mapping)*

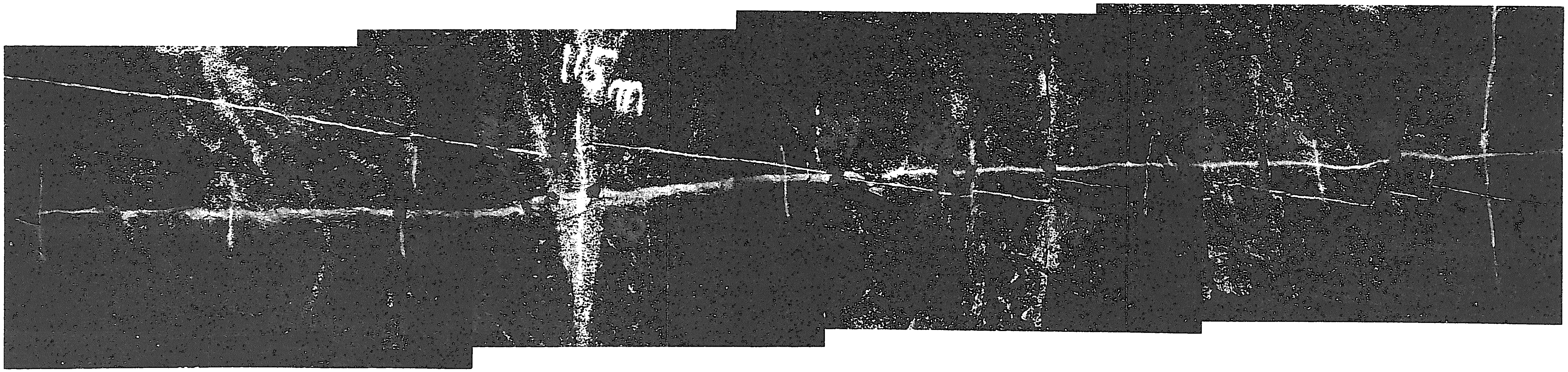

Appendix A-2-7(2) : *Fracture distribution of in-situ tests area in the drift E.L.250m (110 to 118m from the starting point of fracture mapping)*

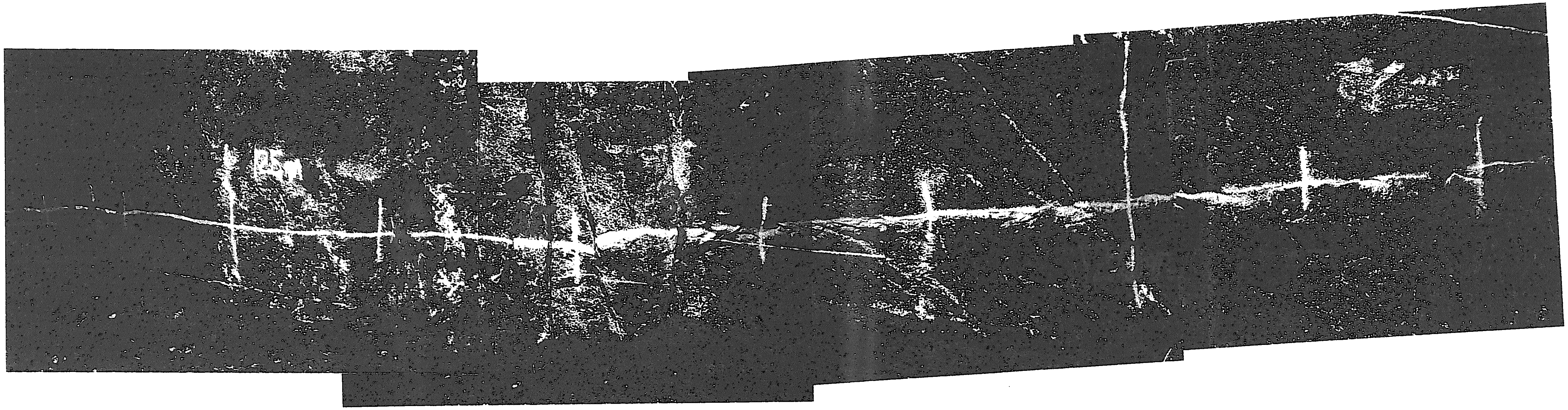

Appendix A-2-8(1) : Fracture distribution of in-situ tests area in the drift E.L.250m (118 to 126m from the starting point of fracture mapping)

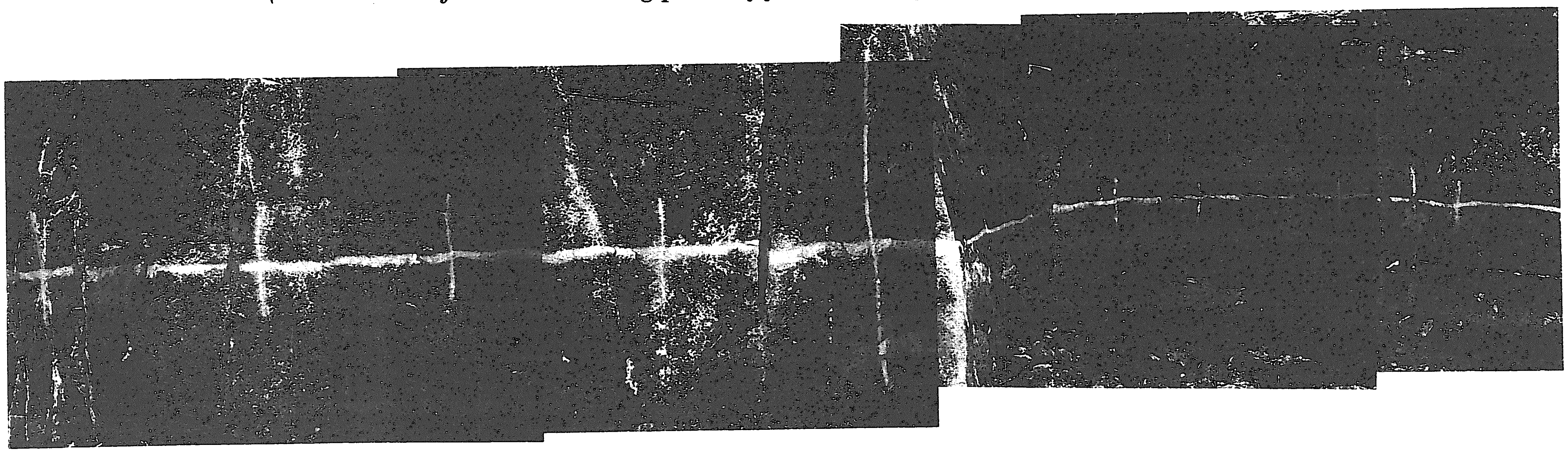

Appendix A-2-8(2) : Fracture distribution of in-situ tests area in the drift E.L.250m (126 to 134m from the starting point of fracture mapping)

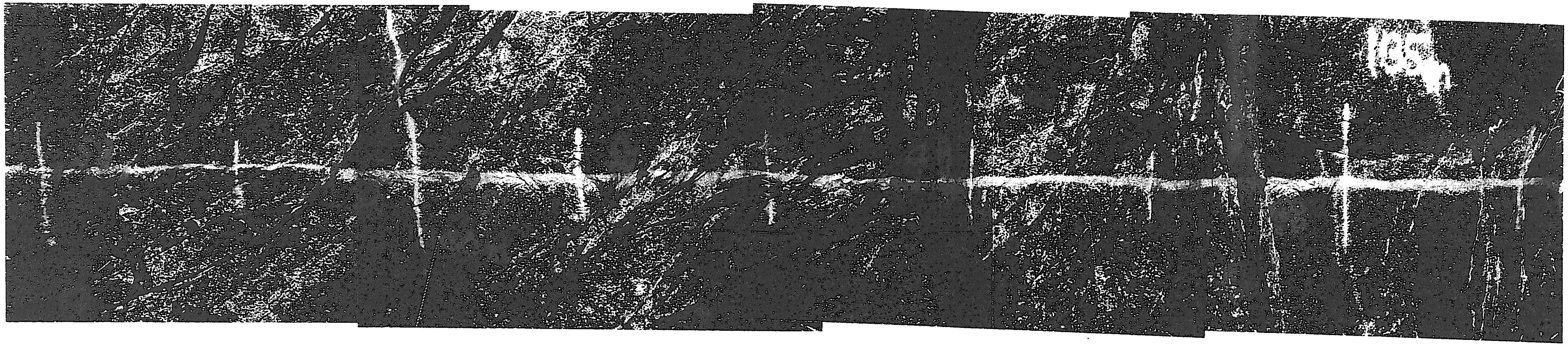

Appendix A-2-9(1) : *Fracture distribution of in-situ tests area in the drift E.L.250m (134 to 142m from the starting point of fracture mapping)*

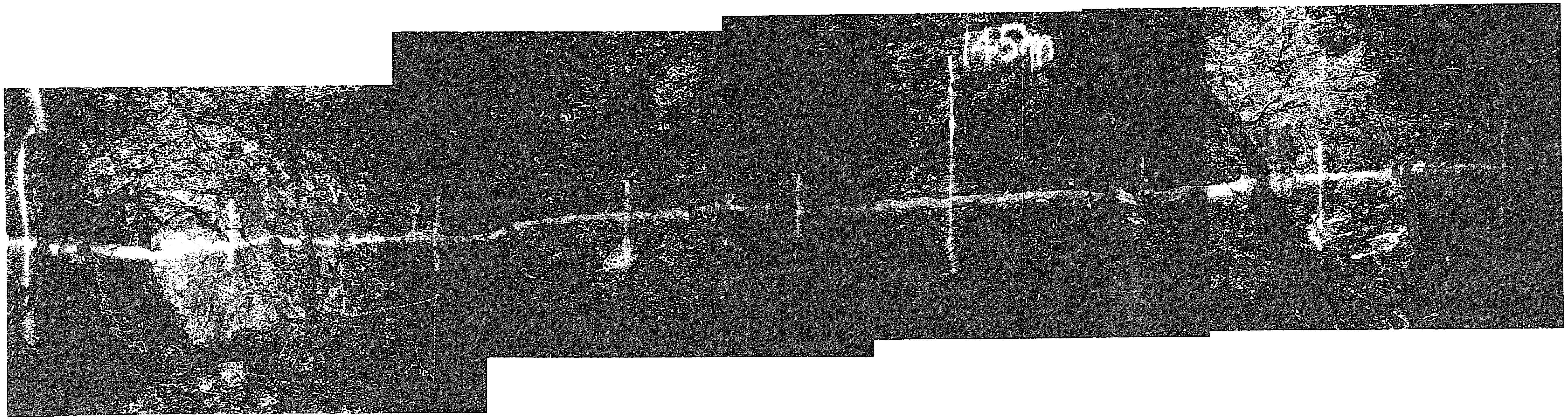

Appendix A-2-9(2) : *Fracture distribution of in-situ tests area in the drift E.L.250m (142 to 150m from the starting point of fracture mapping)*

Appendix A-2-10(1) : Fracture distribution of in-situ tests area in the drift E.L.250m (150 to 157m from the starting point of fracture mapping)

Appendix A-2-10(2) : Fracture distribution of in-situ tests area in the drift E.L.250m (156 to 163m from the starting point of fracture mapping)

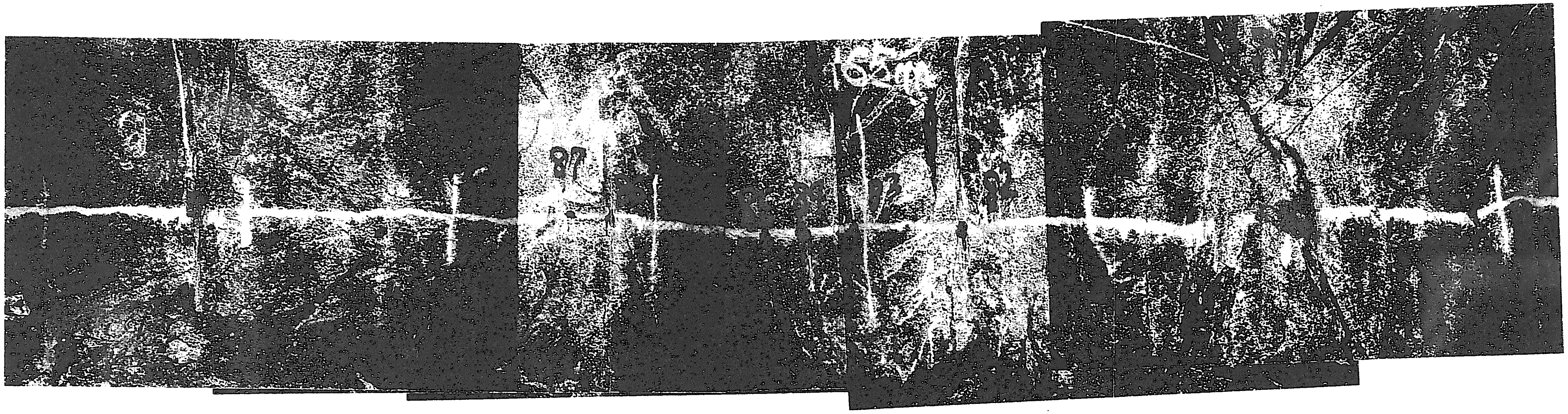

Appendix A-2-11(1) : Fracture distribution of in-situ tests area in the drift E.L.250m (162 to 169m from the starting point of fracture mapping)

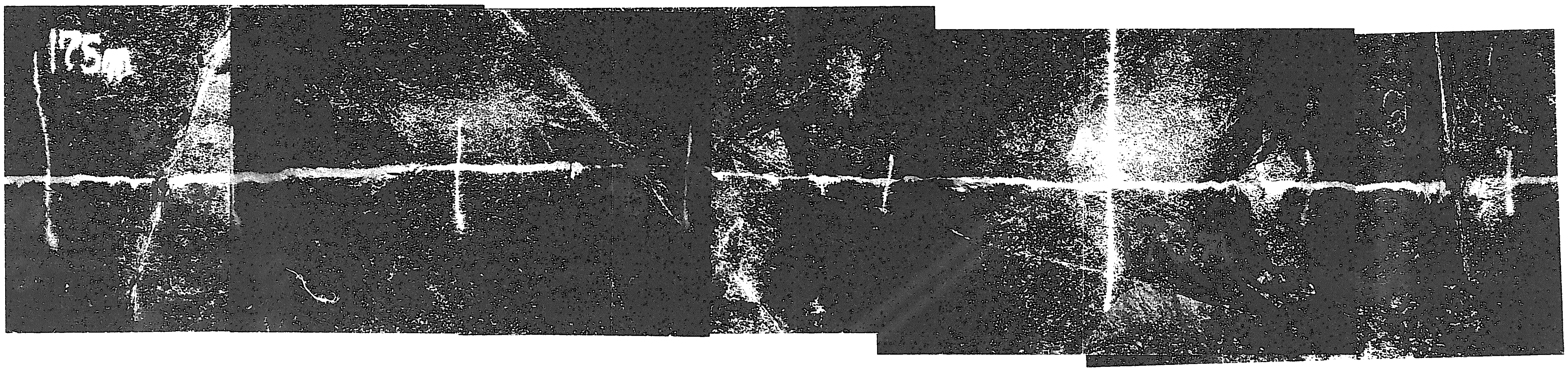

Appendix A-2-11(2) : Fracture distribution of in-situ tests area in the drift E.L.250m (168 to 175m from the starting point of fracture mapping)

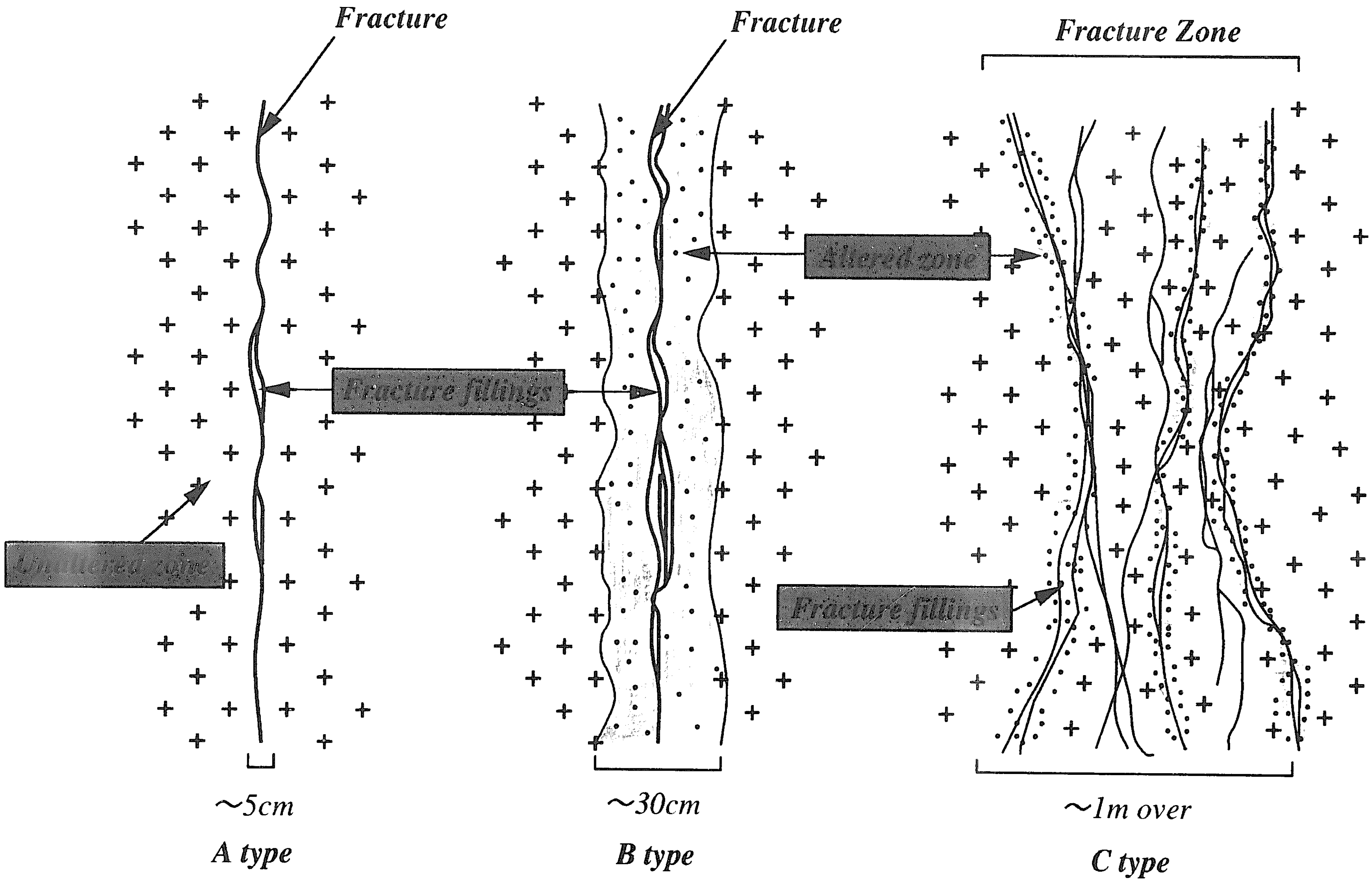

Appendix A-3 *: Fracture types in the Kurihashi granodiorite (Osawa et al., 1995). The fracture types were characterized by considering the existence of fracture fillings and the width of alteration along in the fracture.*

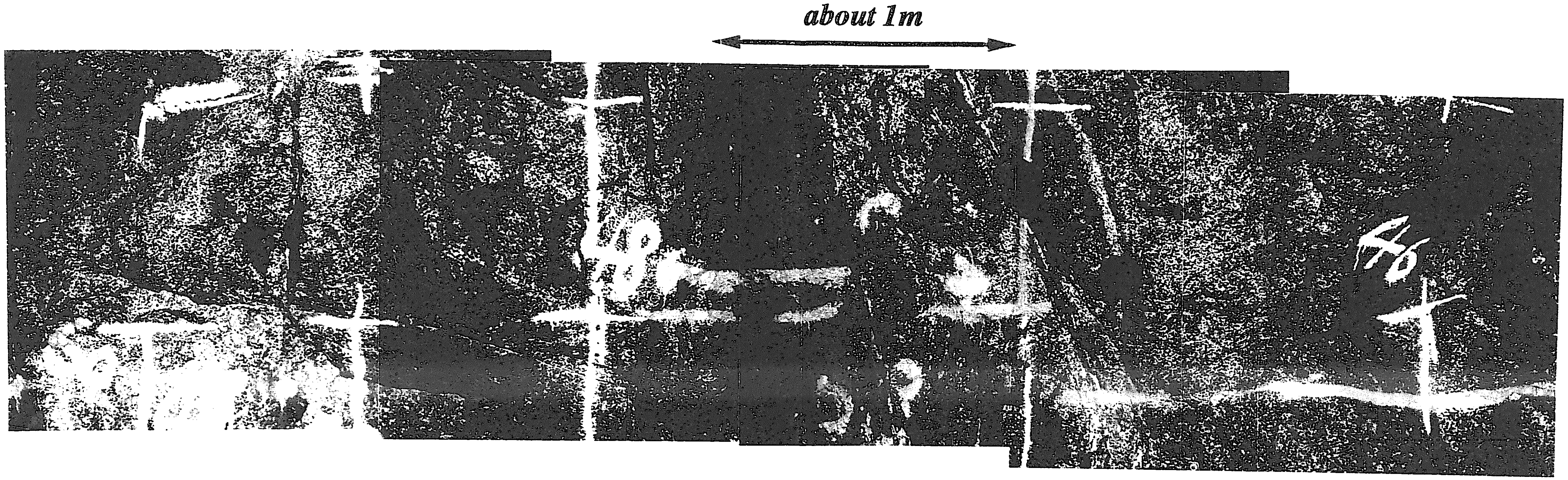

Photograph A-4-1 (noted as ①)

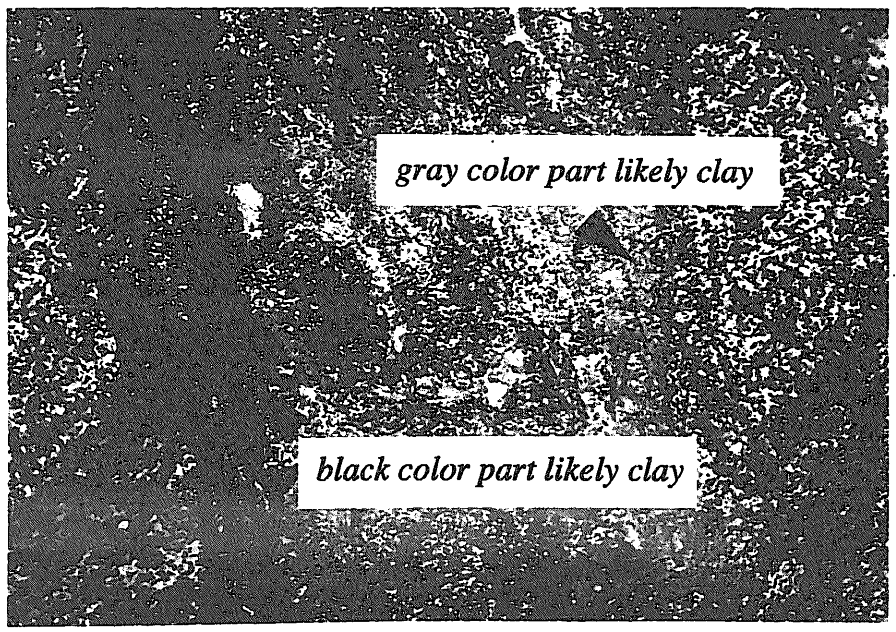

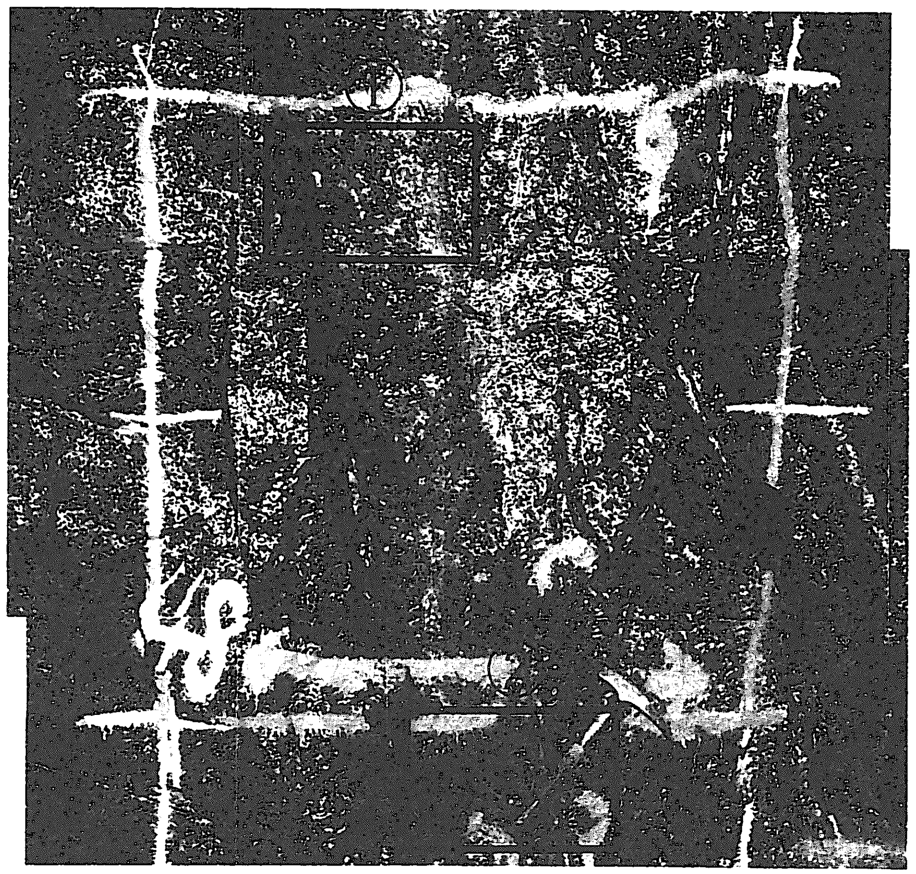

Photograph A-4-2 (noted as ②)

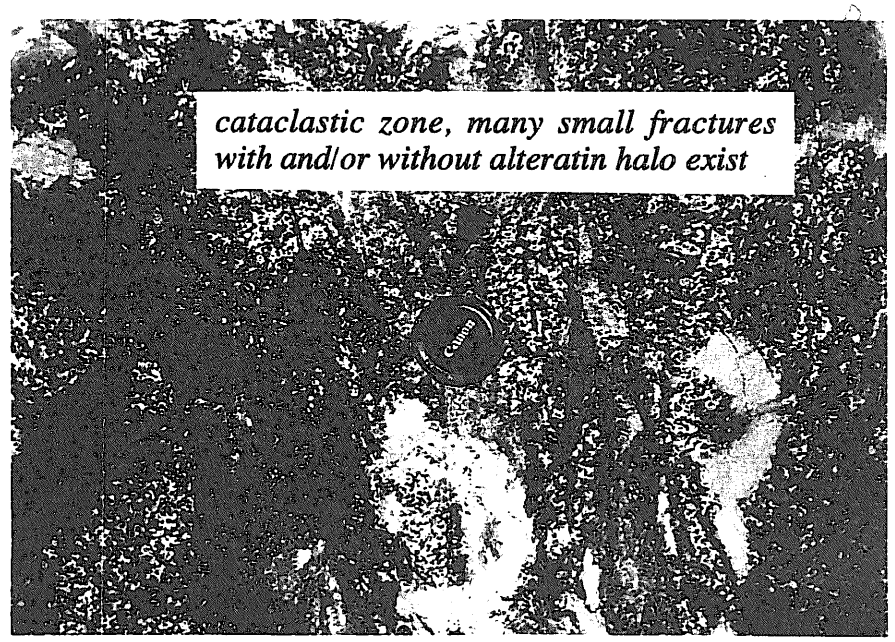

Appendix A-4 : *Magnification photograph around No.58 fracture*

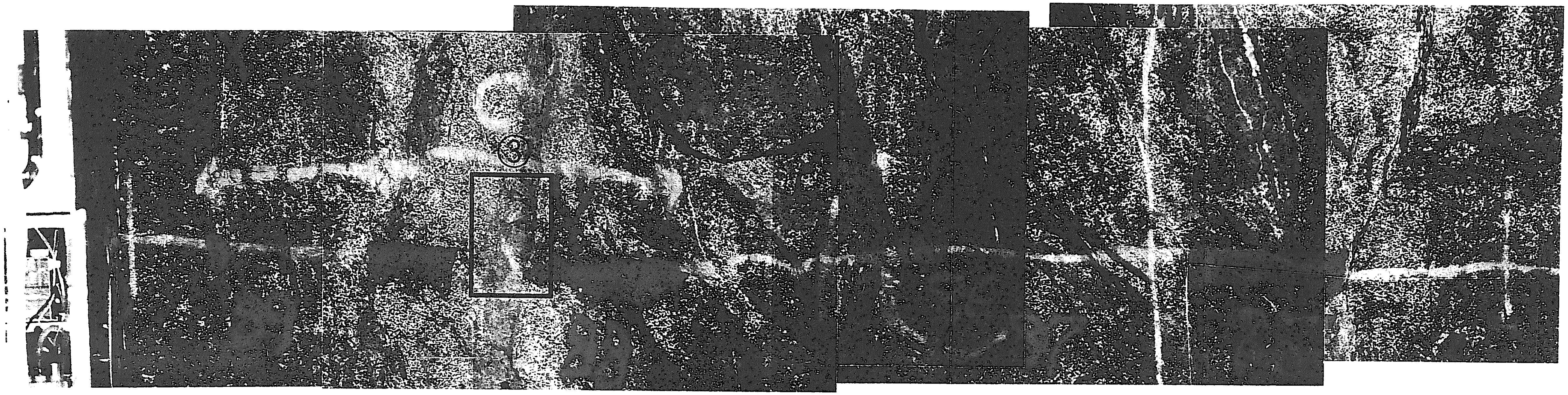

Photograph A-5-1 : *Magnification photograph between No.85 and No.89 fracture*

Photograph A-5-2 : *Magnification photograph of No.89 fracture* ***(noted as ③)***

Appendix A-5 : *Magnification photograph between No.85 and No.89 fracture*

Appendix B: Sampling Locations and Methods

[List of Appendix B]

Appendix B-1: Location of sampling points in the drift E.L.550m

Groundwater sampling stations are plotted on a geological map of the E.L.550m drift. As can be seen, the drift includes two main branches: the NW drift and the NE drift. The KD-89 and KD-90 drifts are also part of the E.L. 550m drift [the KD-90 drift (not indicated in the figure) was extended 50 m to the north of the head of the KD-89 drift in 1990 for tracer injection tests to develop and validate the fracture network model "FracMan", see Uchida and Sawada (1995)]. Groundwater sampling was carried out mainly in the NW drift because it lies within the target host rock (Kurihashi granodiorite) where the Kamaishi *in-situ* tests were carried out. A notation in the figure, such as 88W01, refers to the sampling year (1988), sample type (W = water) and sample number (01). TK-13, TK-14 and TK-6 are boreholes drilled during mining activities at the Kamaishi site. JNC also carried out groundwater sampling in the NE drift to investigate groundwater chemistry in the Ganidake diorite. These solutions are generally richer in sulfate than groundwaters of the Kurihashi granodiorite. Some of the Ganidake groundwaters are Ca-SO_4 type groundwaters. The elevated sulfate concentrations may be due to oxidation of sulfide minerals, which are more abundant in the Ganidake diorite than the Kurihashi granodiorite.

Appendix B-2: Location of sampling points in the drift E.L250m

Groundwater sampling stations are plotted on a geological map of the E.L. 250m drift. The *in-situ* tests area is located near the boundary between Cretaceous sedimentary rocks (slate) and the Kurihashi granodiorte. Small fragments of diorite and slate are present as xenoliths in the Kurihashi granodiorite. There are three boreholes in the test area that were drilled during mining activities at the Kamaishi site. Boreholes W1 (TK-24) and W16 are entirely within the Kurihashi granodiorite. Borehole W-17 (TK-21) penetrates this unit and the slate. Field measurements of Eh using a portable ORP (oxidation-reduction potential) meter indicate that groundwaters flowing into all these boreholes are reducing ($Eh \leq -100mV$ *vs*.SHE, and $pH \approx 9$).

Appendix B-3: Photographs of groundwater sampling points in the drift E.L.250m and sampling method

Detailed results of measurements for physico-chemical parameters of groundwater and groundwater flow rate are documented in PNC (formerly name of JNC) internal technical note (Sasamoto, 1995). Based on this results, the following information is summarized.

Photograph 1: Sampling point W1

The W1 sampling point is a borehole drilled during mining activities at the Kamaishi site. This sampling point is also referred to as the TK-24 borehole (see Appendix B-2), in which continuous monitoring of physico-chemical parameters in groundwaters of the Kurihashi granodiorite was carried out by JNC. The borehole is drilled into the east side of the drift wall. It is about 300m long and is inclined 30° downward from the horizontal. The rate of groundwater flow into the borehole is about 4,000 ml/minute.

Photograph 2: Sampling point W2

This sampling point is located on the ceiling of the E.L.250m drift. The sampling point captures groundwater flowing through a Type A fracture. The flow rate of groundwater in this fracture is about 5 to 9 ml/minute.

Photograph 3: Sampling point W3

The W3 sampling point is located on the ceiling of the E.L.250m drift. Groundwater flowing through a Type C fracture zone is sampled at this site. The groundwater flow rate ranges from 500 to 1,400 ml/minute. The flow rate was observed to increase following drift excavation and/or borehole drilling near the W3 sampling point.

Photograph 4: Sampling point W4

The W4 sampling point is located on the ceiling of the E.L.250m drift. The sampling location captures groundwater flowing through a Type B fracture. The groundwater flow rate is several tens of milliliters per minute. As is the case for the W3 sampling point, the flow rate at W4 was observed to increase following excavation of nearby drifts and/or boreholes.

Photograph 5: Sampling point W5

The W5 sampling point is located on the ceiling of the E.L.250m drift. Groundwater flowing through a Type B fracture is sampled at this location. The flow rate is approximately 100 ml/minute.

Photograph 6: Sampling point W6

The W6 sampling point is located on the west side of the E.L.250m drift. Groundwater flows through a Type B fracture at this location. The groundwater flow rate was observed to decrease to several ml/minute following excavation and drilling activities near this sampling site.

Photograph 7: Sampling point W7

The W7 sampling point is located on the west side of E.L.250m drift. Groundwater flowing through a Type B fracture is sampled at this location. The groundwater flow rate is about 500 ml/minute.

Photograph 8: Sampling point W8
The W8 sampling point is located on the east side of the E.L.250m drift. Groundwater flows through a Type B fracture at this location. The groundwater flow rate was observed to decrease to about 100 ml/minute following excavation and drilling activities near the site.

Photograph 9: Sampling point W9
The W9 sampling point is located on the ceiling of E.L.250m drift. Groundwater flows through a Type A fracture at this location. The groundwater flow rate is several tens of ml/minute.

Photograph 10: Sampling point W10
The W10 sampling point is located on the ceiling of the E.L.250m drift. Groundwater flows through a Type A fracture at this location. The groundwater flow rate is about 50 ml/minute.

Photograph 11: Sampling point W11
The W11 sampling point is located on the ceiling of the E.L.250m drift. Groundwater flows through a Type A fracture at this location. The groundwater flow rate is about 10 ml/minute.

Photograph 12: Sampling point W12
The W12 sampling point is located on the ceiling of the E.L.250m drift. Groundwater flows through a Type A fracture at this location. The groundwater flow rate is about 30 ml/minute.

Photograph 13: Sampling point W13
The W13 sampling point is located on the ceiling of the E.L.250m drift. Groundwater flows through a Type B fracture at this location. The groundwater flow rate is about 30 ml/minute.

Photograph 14: Sampling point W14
The W14 sampling point is located on the ceiling of the E.L.250m drift. Groundwater flows through a Type B fracture at this location. The groundwater flow rate was observed to increase to about 150 ml/min following excavation and/or borehole drilling activities near this site.

Photograph 15: Sampling point W15
The W15 sampling point is located on the ceiling of the E.L.250m drift. Groundwater flows through a Type B fracture at this location. The groundwater flow rate was observed to increase to about 170 ml/minute following excavation and/or borehole drilling activities near this site.

Photograph 16: Sampling point W16

The W16 sampling point is a borehole drilled during previous mining activities at the Kamaishi site. The borehole is drilled from the east face of the E.L.250m drift. It is about 347 m long and is nearly horizontal. The groundwater flow rate is about 4,000 ml/minute.

Photograph 17: Sampling point W17

The W17 sampling point is a borehole drilled during previous mining activities at the Kamaishi site. The borehole is drilled from the west face of the E.L.250m drift. It is about 480m long and is inclined 30° downward from the horizontal. The groundwater flow rate is about 15,000 ml/minute.

Photograph 18: Sampling point W18

The W18 sampling point is located on the ceiling of the E.L.250m drift. Groundwater flows through a Type B fracture at this location. The groundwater flow rate is about 200 ml/minute.

Note: A photograph of the W19 sampling point, which is near the W18 sampling point, is unavailable. The W19 sampling point is located on the ceiling of the E.L.250m drift. Groundwater flows through a Type B fracture at this location. The groundwater flow rate is about 15 ml/minute.

Photograph 19: Groundwater sampling technique (1)

A technique used to sample groundwaters at the Kamaishi *in-situ* tests site is shown in the photograph (W7 sampling point).

Photograph 20: Groundwater sampling technique (2)

A technique used to sample groundwaters at the Kamaishi *in-situ* tests site is shown in the photograph (W8 sampling point).

Photograph 21: Technique for filtering groundwater samples in the field

This photograph shows the method used to filter groundwater samples in the field. The compositions of the filtered samples were later analyzed in the laboratory.

Photograph 22: Rock core sampling technique (1)

This photograph shows the technique and apparatus (a small coring machine) used to obtain in-tact samples of fractured rock.

Photograph 23: Rock core sampling technique (2)

The results of rock-core sampling are shown in this photograph. The left-most cylindrical hole is the result of sampling a Type C fracture. The hole to its right is the result of sampling a Type B fracture.

Photograph 24: Photograph of rock core sample

A core sample obtained using the coring machine in Photograph 22 is shown in this photograph. The core diameter is 10 cm and the core length is about 30 cm. This sample contains an in-tact Type B fracture.

[References]

- Uchida M and Sawada A (1995) : Discrete fracture network modeling for tracer migration experiments at the Kamaishi Mine In: Scientific Basis for Nuclear Waste Management XVIII, T.Murakami and R.C.Ewing (eds), Materials Research Society, Pittsburgh, PA., pp.387-394.
- Sasamoto H (1995) : Monitoring results for physico-chemical parameters of groundwater flowing into existing dirfts (E.L.550 m and E.L.250 m) - Heisei 5 -, PNC Internal Technical Note, A96-3-005 (in Japanese).

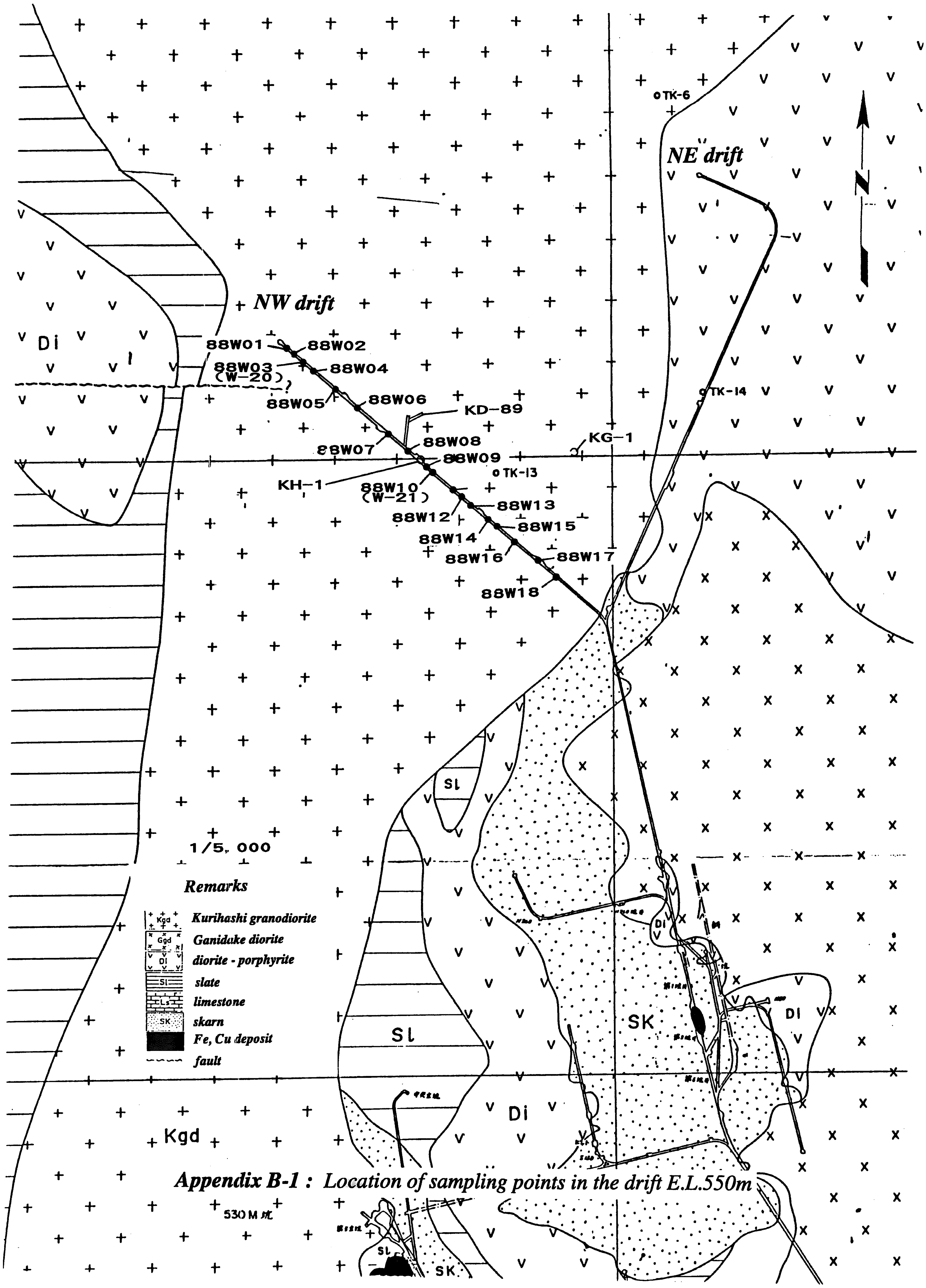

Appendix B-1 : Location of sampling points in the drift E.L.550m

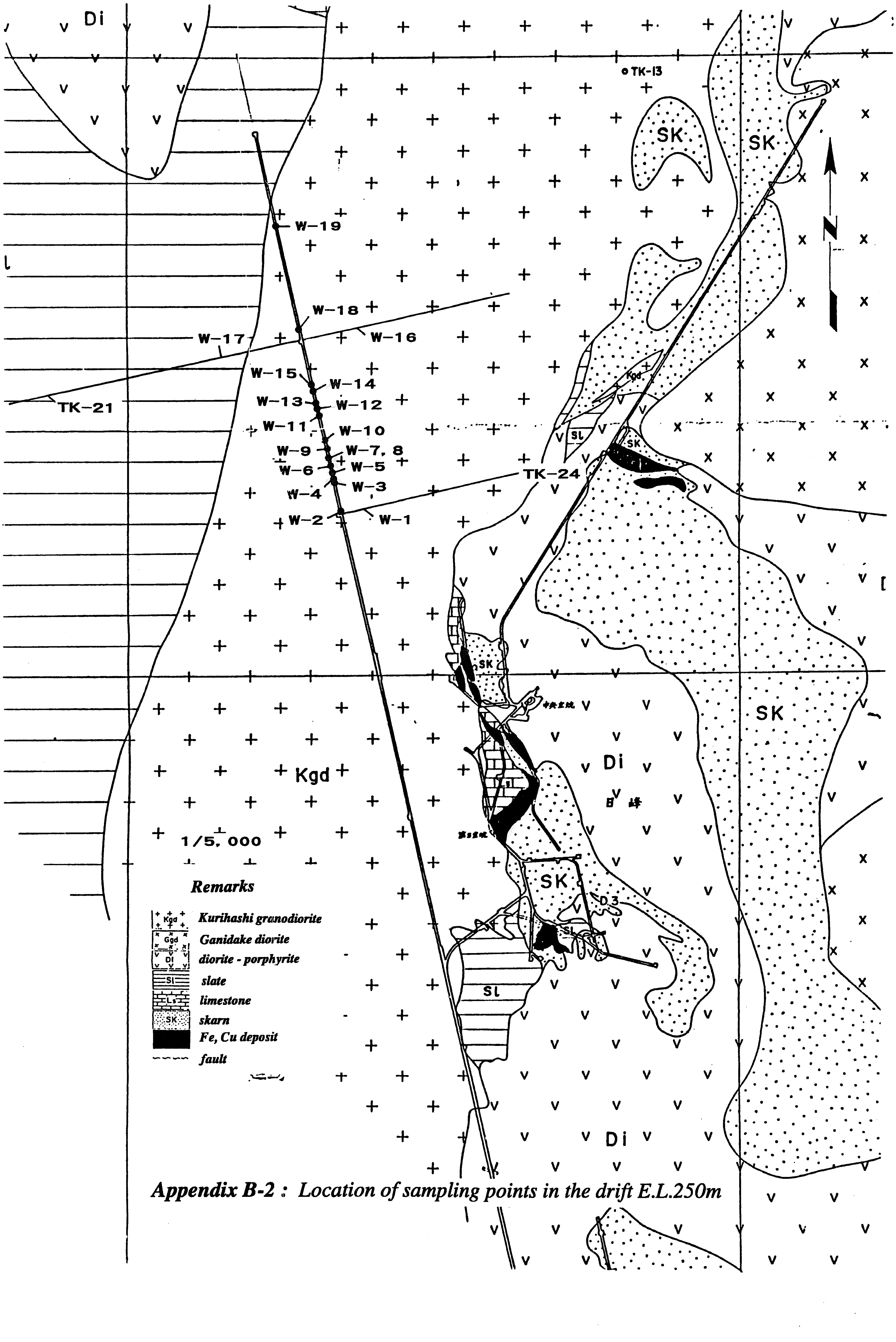

Appendix B-2 : Location of sampling points in the drift E.L.250m

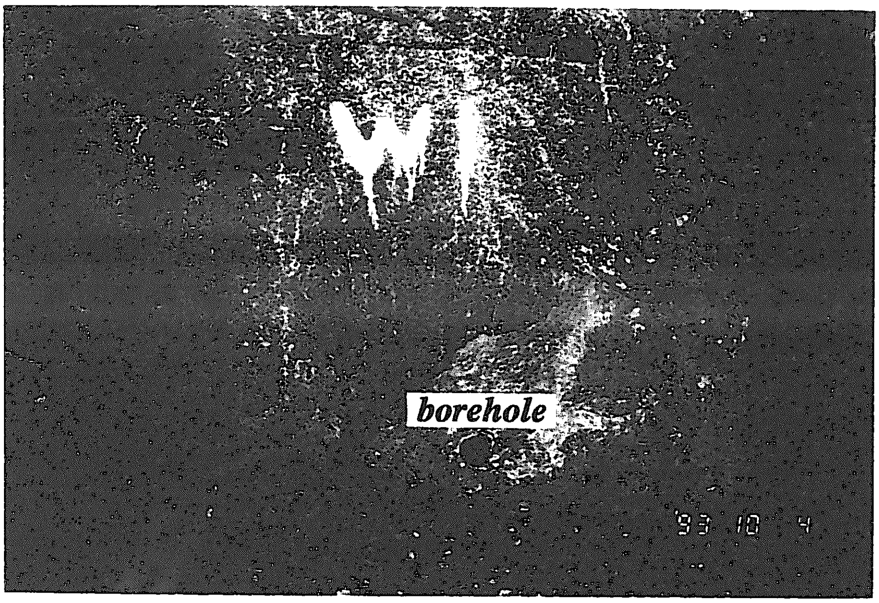

Photograph 1
W1 point

Photograph 2
W2 point

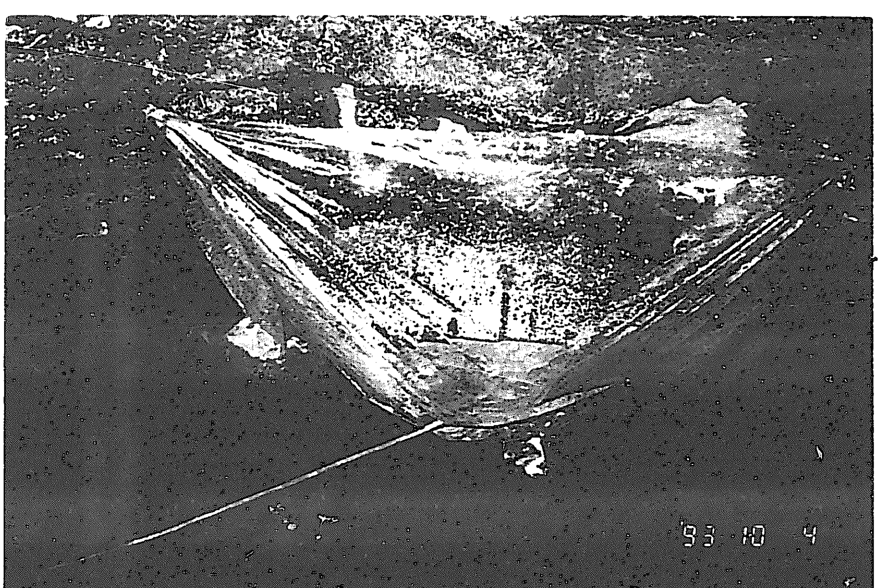

Photograph 3
W3 point

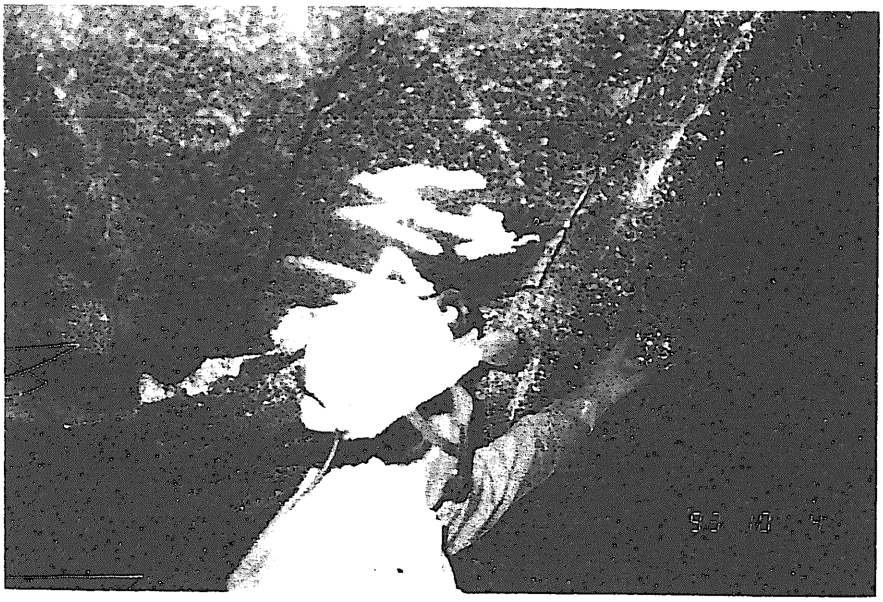

Photograph 4
W4 point

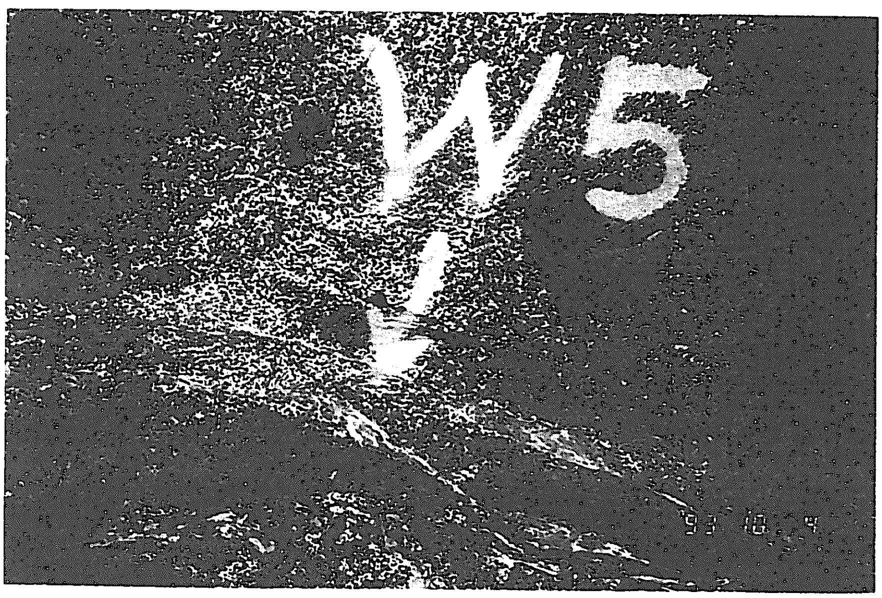

Photograph 5
W5 point

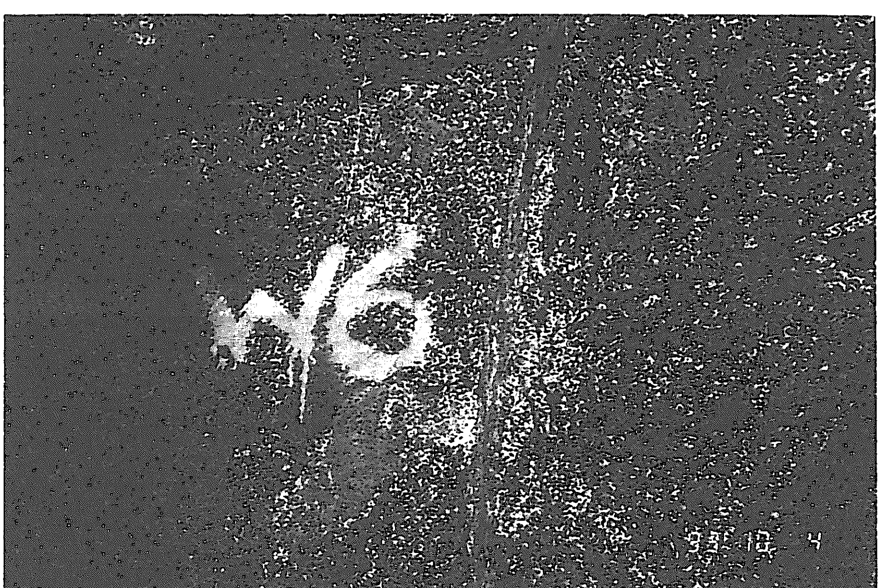

Photograph 6
W6 point

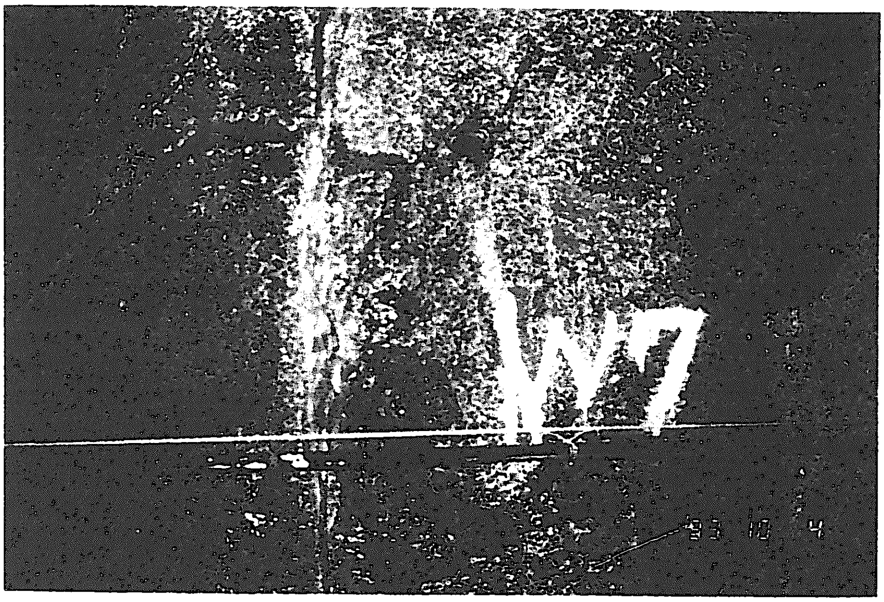

Photograph 7
W7 point

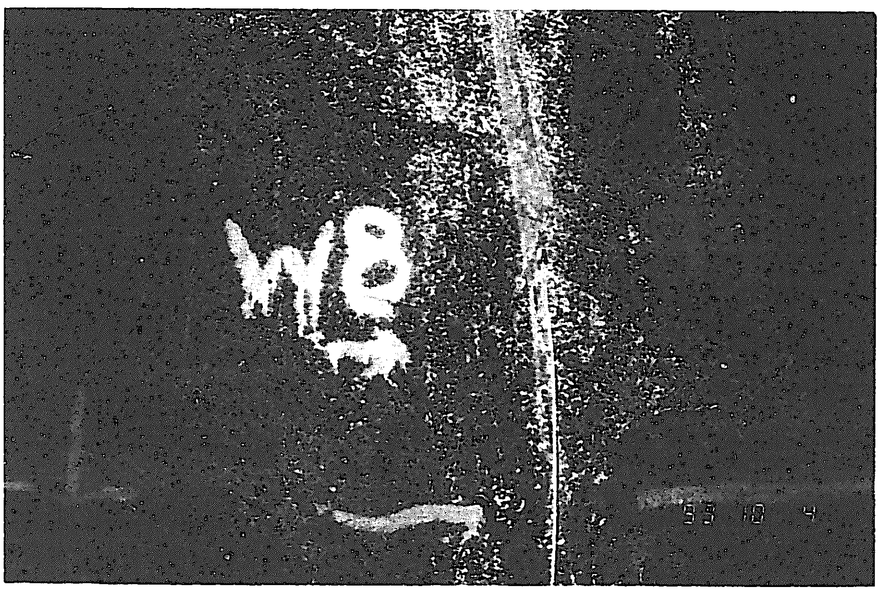

Photograph 8
W8 point

Photograph 9
W9 point

Photograph 10
W10 point

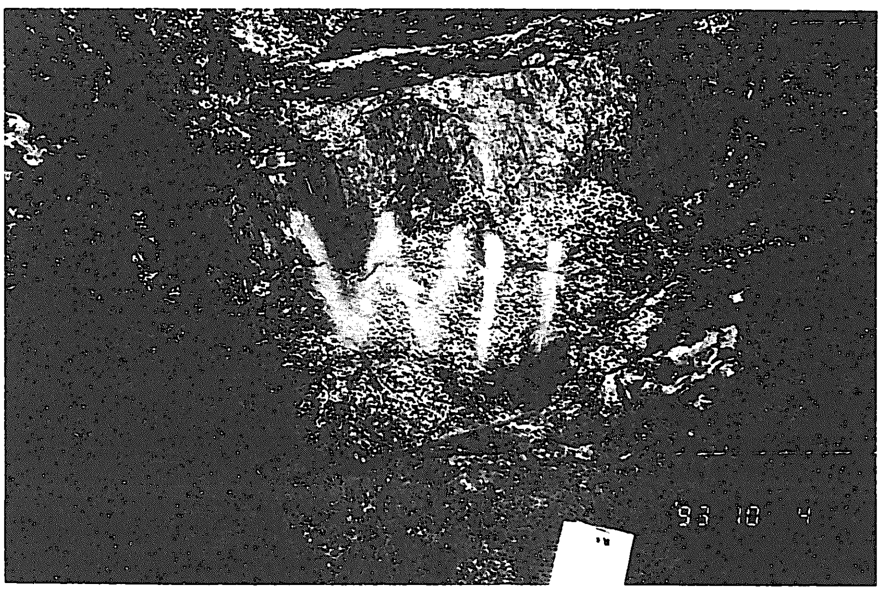

Photograph 11
W11 point

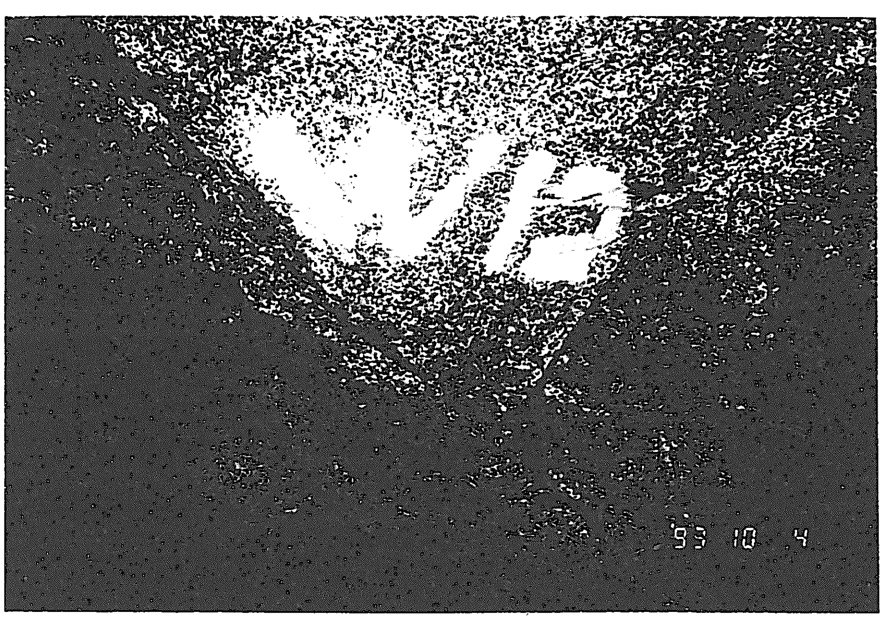

Photograph 12
W12 point

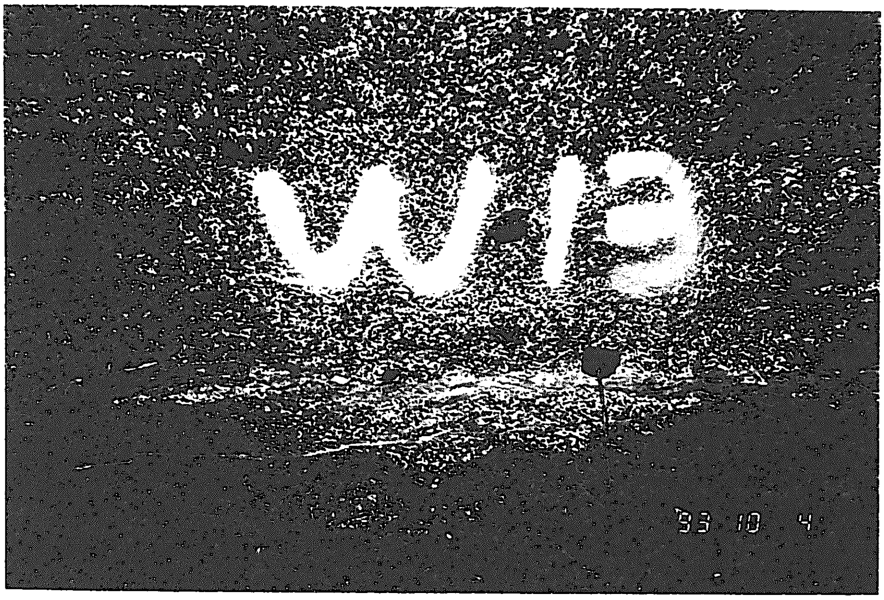

Photograph 13
W13 point

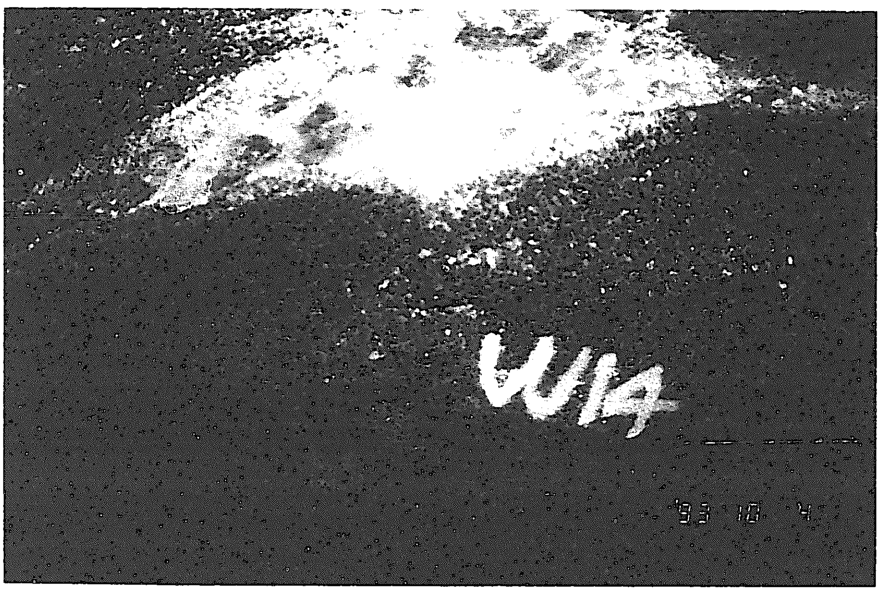

Photograph 14
W14 point

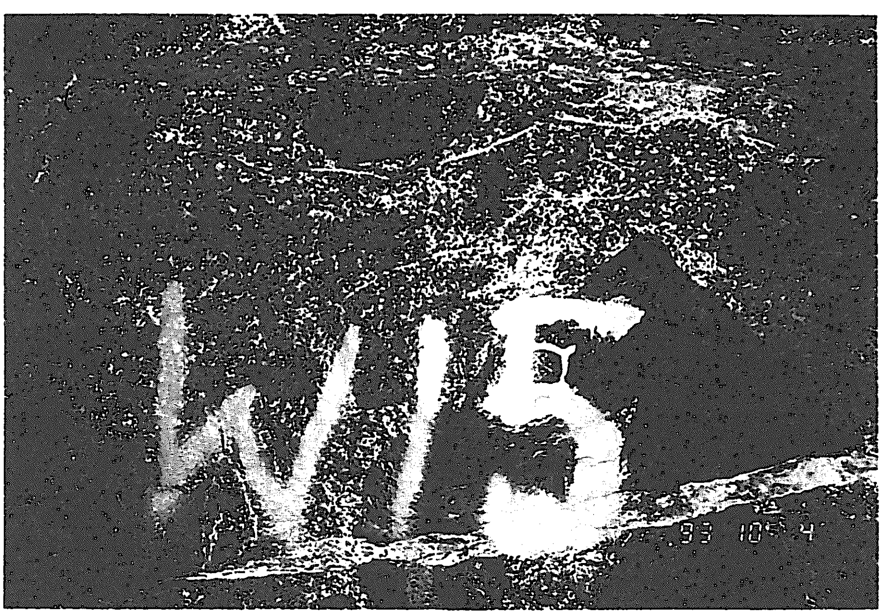

Photograph 15
W15 point

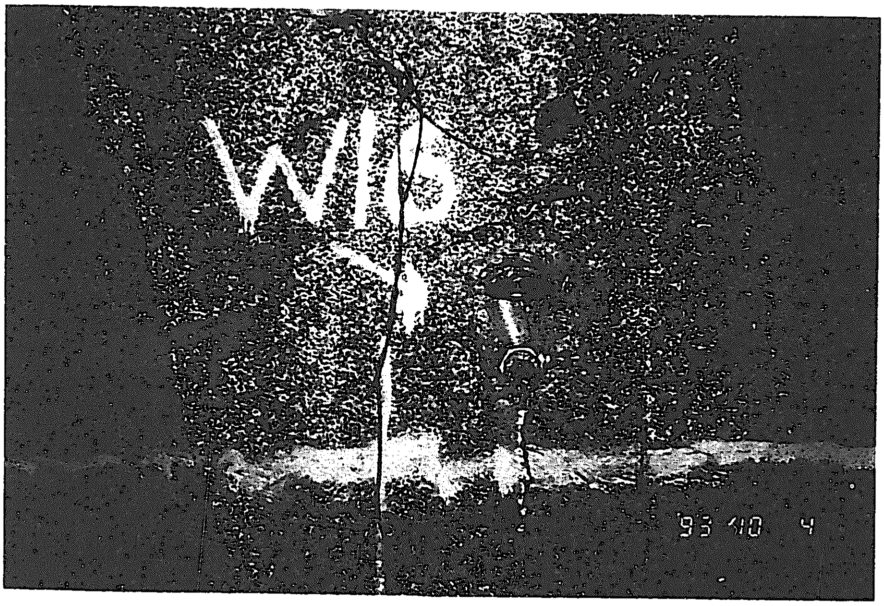

Photograph 16
W16 point

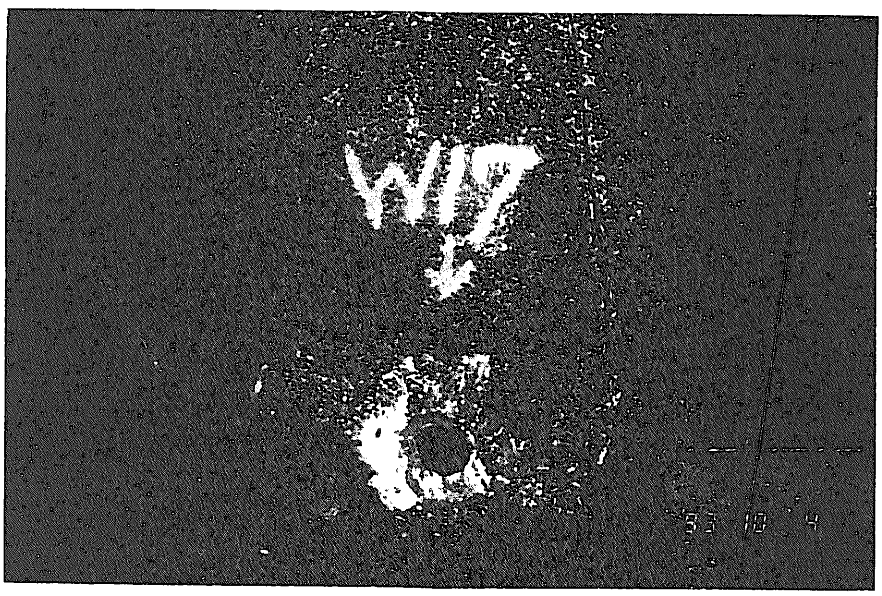

Photograph 17
17 point

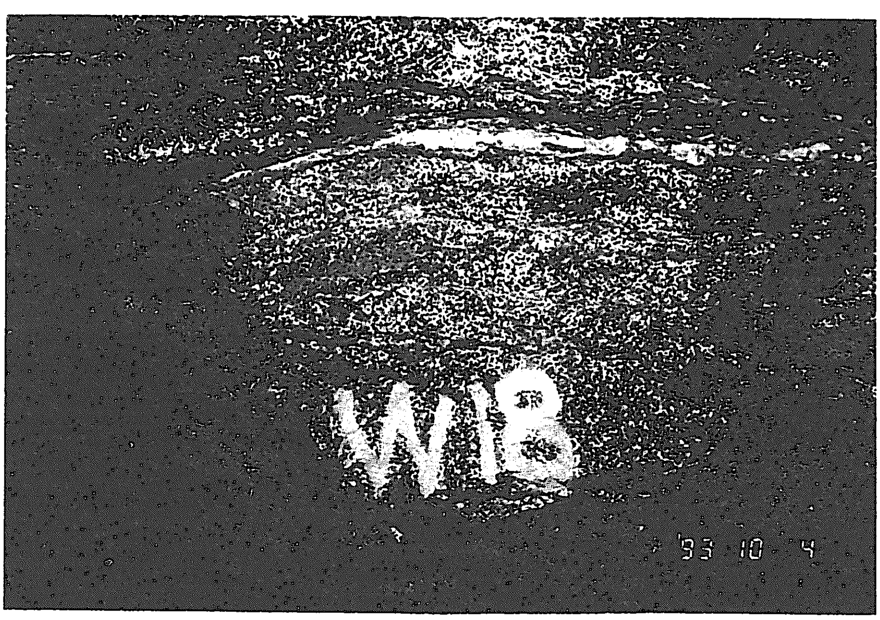

Photograph 18
18 point

Photograph 19
groundwater sampling method (1)

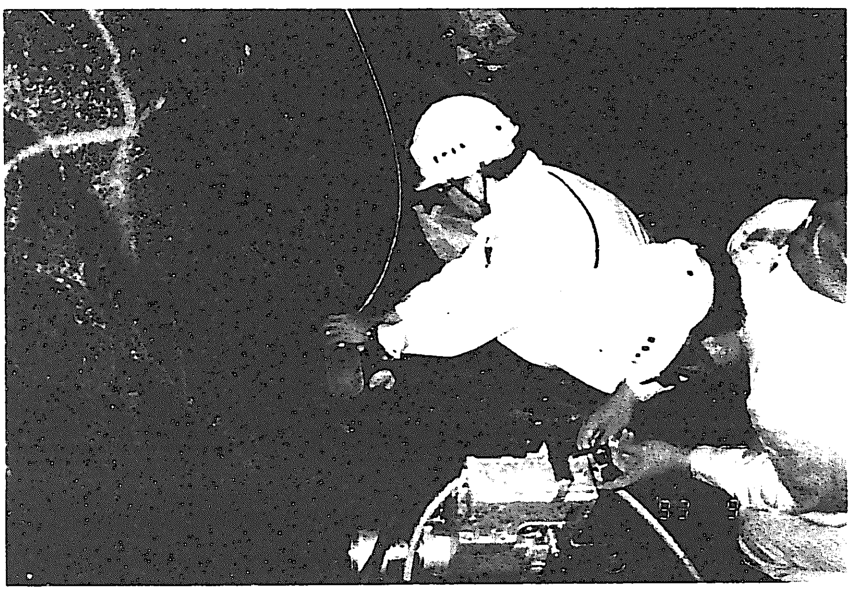

Photograph 20
groundwater sampling method (2)

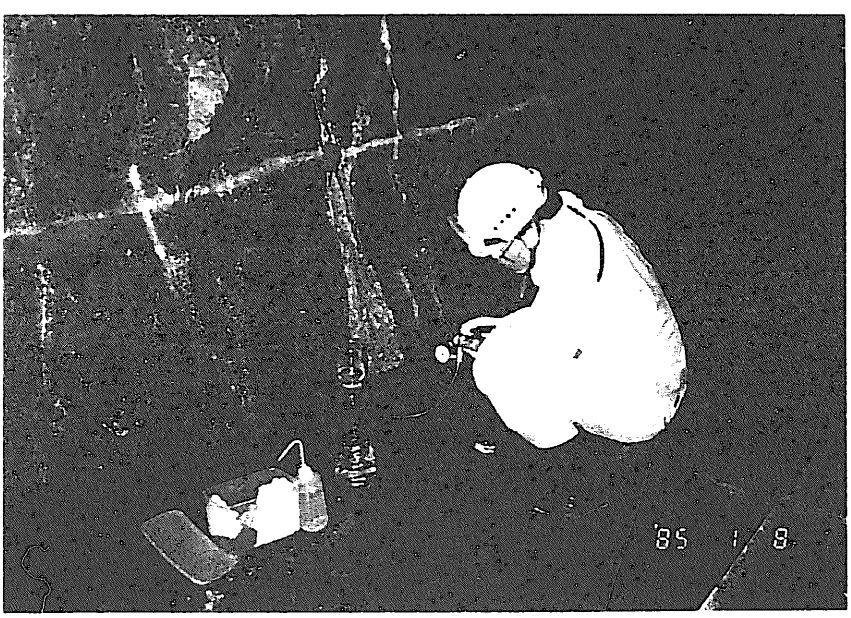

Photograph 21
groundwater percolation at field

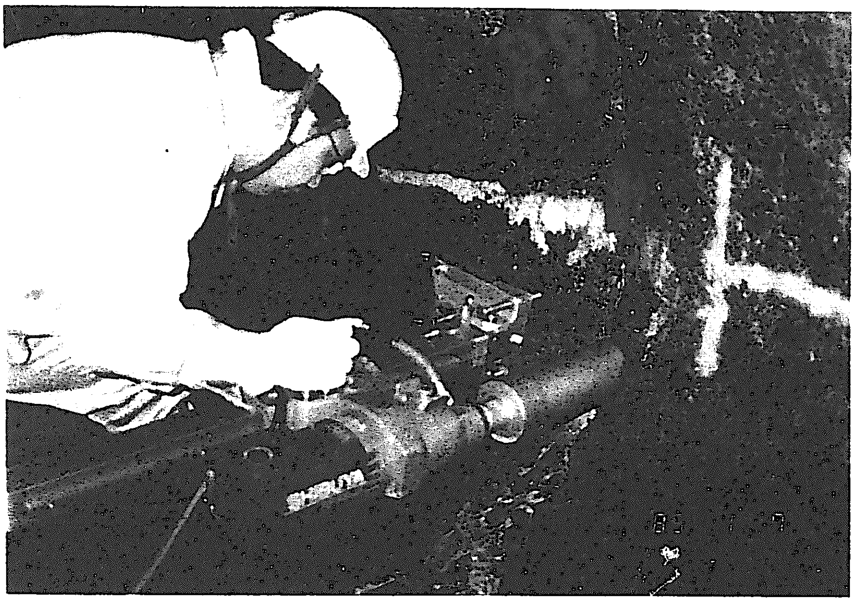

Photograph 22
rock core sampling (1)

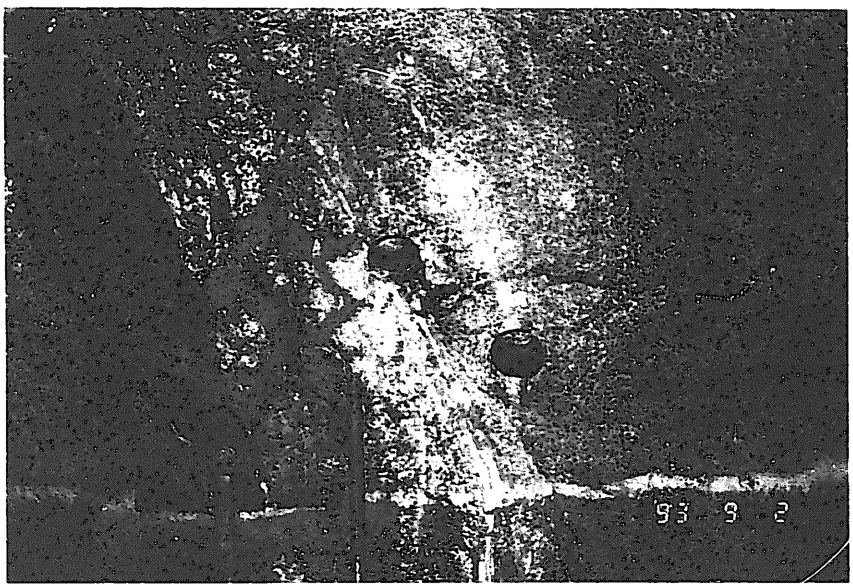

Photograph 23
rock core sampling (2)

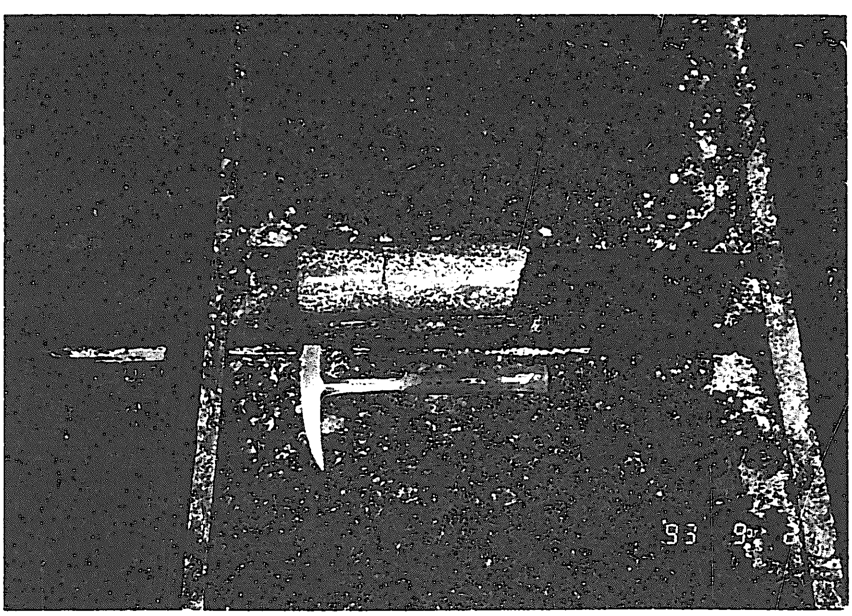

Photograph 24
rock core sample

Appendix C: Description of the MP Groundwater Monitoring System

[List of Appendix C]

Appendix C-1: MP system provided in the KG-1 borehole
The MP system (Westbay Instruments Inc., 1992) is a modular multi-level groundwater monitoring device employing a single, closed access tube with valved ports. The valved ports are used to provide access to several different levels of a drill hole through a single well casing. The modular design permits as many monitoring zones as desired to be established in a borehole. There are two configurations of the MP system: MP 38 and MP 55. The MP 55 system [i.e., with a 2.25-inch (55mm) outer diameter] was installed in the KG-1 borehole. A schematic diagram of this configuration is shown in the figure. The casing components of the system consist of stainless steel.

Appendix C-2: Typical order to clean the borehole and sampling of the groundwater
The figure shows a typical sequence of events involved in drilling and completing a monitoring well (Westbay Instruments Inc., 1992). The events include:

a) migration of drilling fluids into the host rock as the hole is drilled;
b) installation of the packer system, including packer seals;
c) removal, or purging, of drilling fluids by natural groundwater flow or pumping (as for the KG-1 borehole) - formation waters are distinguished from drilling fluids when variations in physico-chemical parameters and the compositions of fluid samples are minimized (Section 2.3.2);
d) groundwater monitoring (the MOSDAX 2350 probe was used in the KG-1 borehole for groundwater sampling and measurements of water pressure).

Appendix C-3: Photographs of KG-1 borehole and the groundwater sampling tool

Photograph 25: Photograph of the head of the KG-1 borehole

Photograph 26: Photograph of the MOSDAX 2350 probe and controller

Photograph 27: Photograph of sampling bottles (500 ml ; two bottles)

[Reference]

- Westbay Instrumets Inc (1992) : An introduction to Westbay's MP system for groundwater monitoring, 20p.

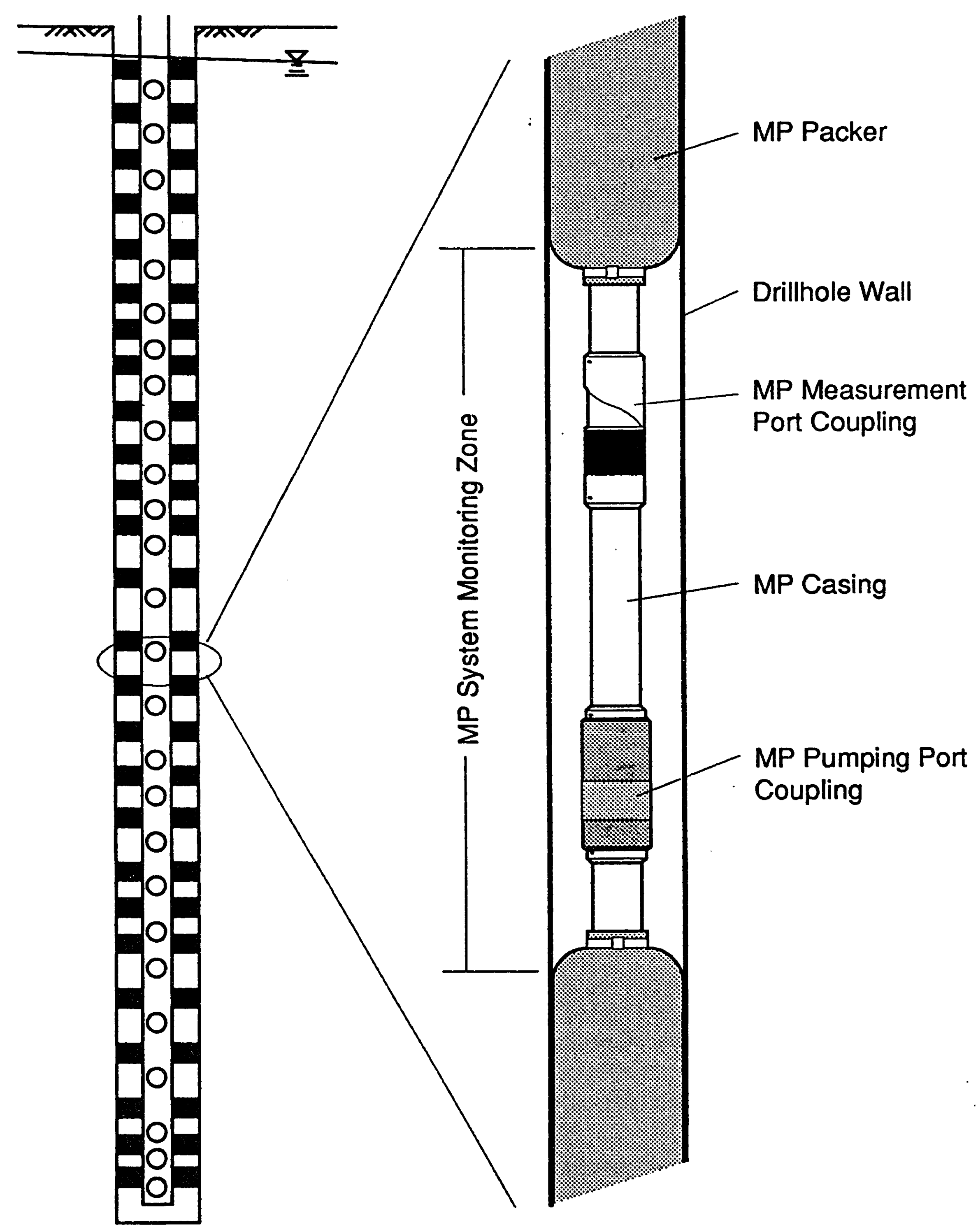

Appendix C-1 : MP system provided in the KG-1 borehole

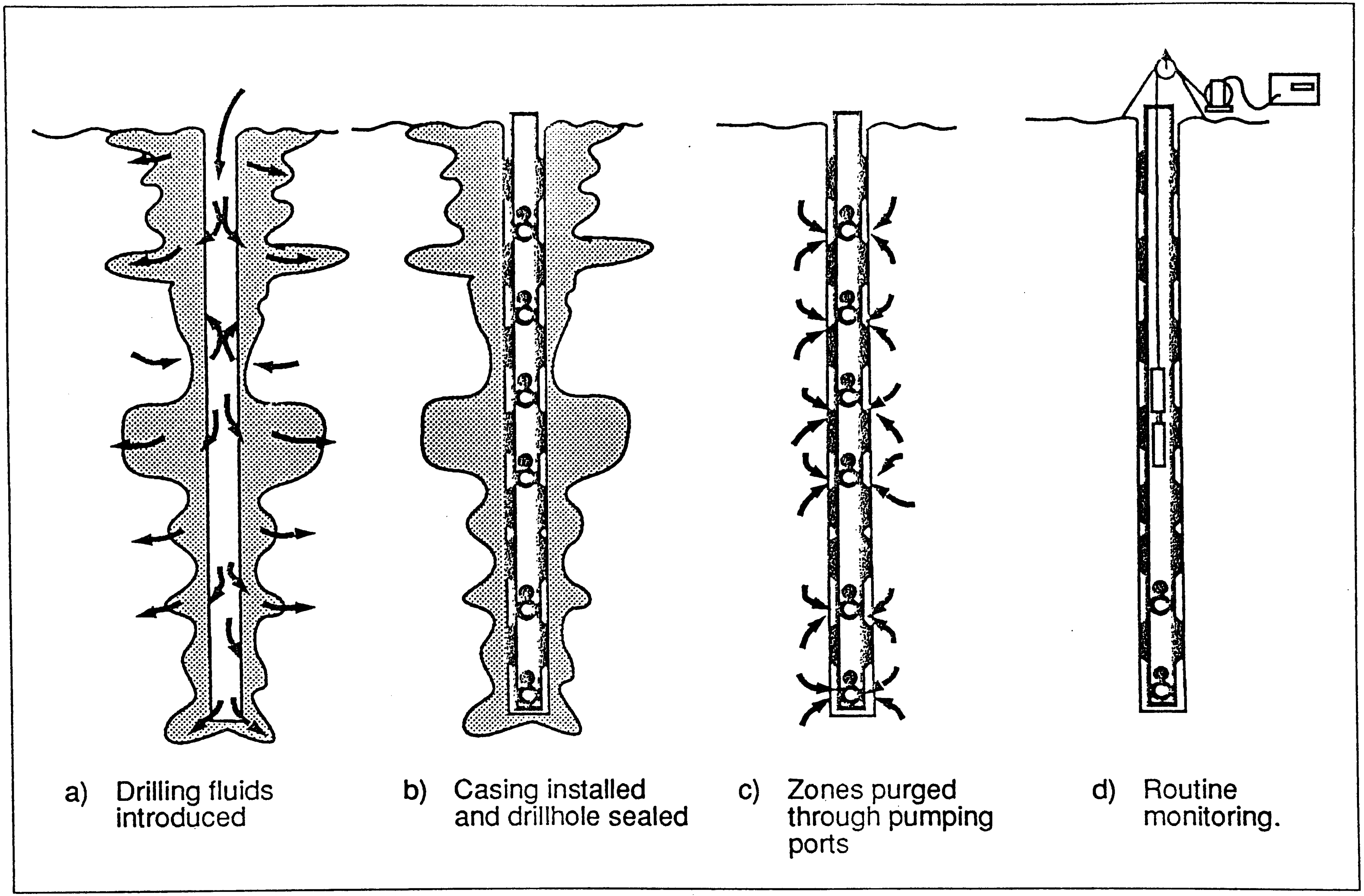

Appendix C-2 : *Typical order to clean the borehole and sampling of the groundwater*

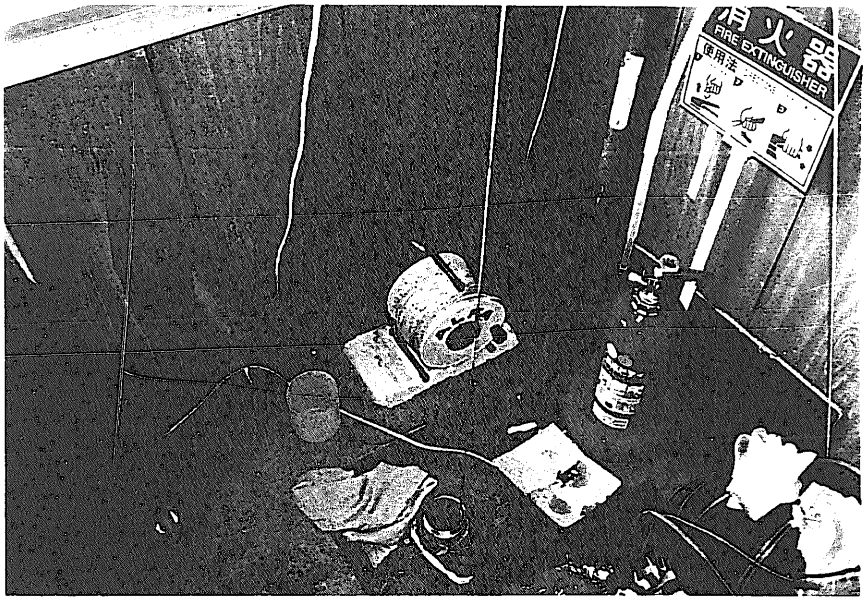

Photograph 25
KG-1 borehole head

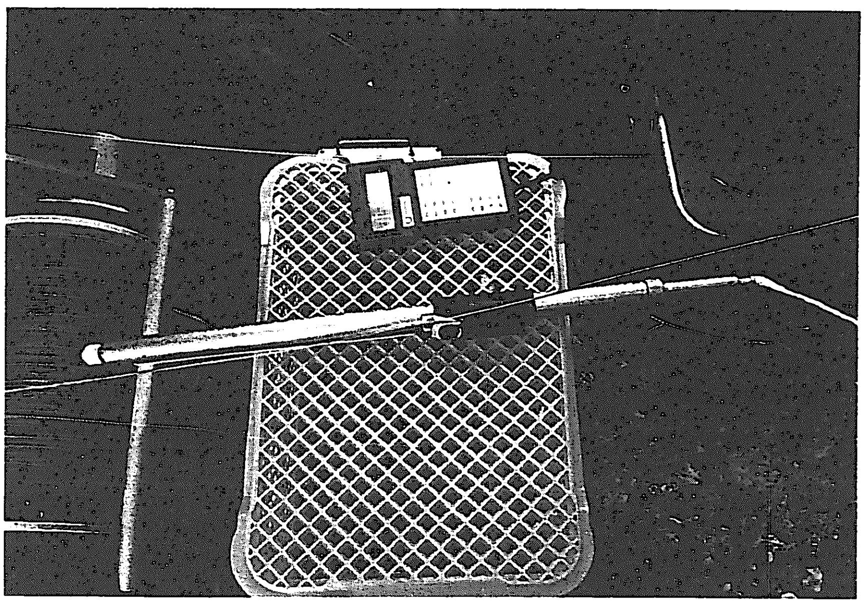

Photograph 26
MOSDAX probe

Photograph 27
sampling bottle

Appendix D: Procedure for Calculating the Activities of Carbonate Species

It is assumed that only hydroxide, carbonate and bicarbonate ions contribute to the alkalinity of groundwater samples. The activities of HCO_3^- and CO_3^{2-} are calculated on the basis of this assumption. The calculation procedure is as follows:

- assume that the total dissolved inorganic carbon concentration is given by the sum of CO_2(aq), HCO_3^- and CO_3^{2-} concentrations;
- note that the activities of these three species depends on the pH of the solution;
- these activities are calculated for each groundwater sample using the table in Appendix D-1 (appropriate for fresh waters, see Horibe et al., 1970), an analysis of the sample's IC (Inorganic Carbon) content and measurements of the sample's pH and temperature;

For example, if we assume that IC = 5.04 (mg/L), temperature = 14°C and pH = 9.6, the activities of carbonate species are calculated using the table in the Appendix D-1 as follows:

$$H_2CO_3 = 0,\ HCO_3^- = 87.5,\ CO_3^{2-} = 12.5$$

$$\text{where, } HCO_3^- = \alpha\ (mg/L),\ CO_3^{2-} = \beta\ (mg/L)$$

$$\alpha : \beta = 87.5 : 12.5$$

$$12.5\,\alpha = 87.5\,\beta,\ \because \alpha = 7\beta$$

$$HCO_3^- : C = 61 : 12 = \alpha : x$$

$$12\,\alpha = 61\,x,\ \because x = 12/61\ \alpha$$

$$CO_3^{2-} : C = 60 : 12 = \beta : \gamma$$

$$12\,\beta = 60\,\gamma,\ \because \gamma = 12/60\,\beta$$

$$x + \gamma = 5.04\ (mg/L)$$

$$12/61\ \alpha + 12/60\,\beta = 5.04$$

$$12/61 \times 7\beta + 12/60\,\beta = 5.04,\ \because \beta = 3.19,\ \alpha = 22.3$$

It is important to note that other aqueous species in natural waters, such as $Al(OH)_4^-$, $Al(OH)_3^0$, $Al(OH)_2^+$, $Fe(OH)_3^-$, and $Fe(OH)_2^0$, silicate, borate and various organic ligands (especially acetate (Pitkanen et al., 1996), may also contribute to the alkalinity. These species react during the alkalinity titration with H^+ ions. However, the concentrations of such species are very low (near the detection limit) in Kamaishi groundwaters compared with the concentrations of the carbonate species. The contribution to the alkalinity of these groundwaters of species other than carbonate species was therefore ignored.

[References]

- Horibe S, Matsuo T, Tsubota H, Kitano Y (1970) : The geochemistry of seawater, Tokai, Univ, publish (in Japanese).
- Pitkanen P, Snellman M, Vuorinen U and Forsman H L (1996) : Geochemical modelling study on the age and evolution of the groundwater at the Romuvaara site, Posiva Report POSIVA 96-06, Posiva Oy, ISBN 951-652-005-7.

Appendix D-1 : Activity of carbonate species under various pH, temperature condition for fresh water (from Horibe et al., 1970)

F : H2CO3, B : HCO3-, C : CO3--

	8°C			10°C			12°C			14°C		
pH	F	B	C	F	B	C	F	B	C	F	B	C
5.0	96.9	3.1	0	96.7	3.3	0	96.6	3.4	0	96.5	3.5	0
5.1	96.2	3.8	0	96.0	4.0	0	95.8	4.2	0	95.7	4.3	0
5.2	95.2	4.8	0	94.9	5.1	0	94.7	5.3	0	94.6	5.4	0
5.3	94.0	6.0	0	93.8	6.2	0	93.5	6.5	0	93.4	6.6	0
5.4	92.5	7.5	0	92.1	7.9	0	91.8	8.2	0	91.5	8.5	0
5.5	91.0	9.0	0	90.5	9.5	0	90.0	10.0	0	89.7	10.3	0
5.6	88.5	11.5	0	88.1	11.9	0	87.8	12.2	0	87.4	12.6	0
5.7	86.0	14.0	0	85.5	14.5	0	85.0	15.0	0	84.5	15.5	0
5.8	83.4	16.6	0	82.7	17.3	0	82.0	18.0	0	81.4	18.6	0
5.9	80.0	20.0	0	78.5	21.5	0	78.5	21.5	0	77.5	22.5	0
6.0	75.8	24.2	0	74.6	25.4	0	73.6	26.4	0	73.0	27.0	0
6.1	71.5	28.5	0	69.5	30.5	0	69.1	30.9	0	68.7	31.3	0
6.2	66.2	33.8	0	64.9	35.1	0	64.2	35.8	0	63.3	36.7	0
6.3	61.5	38.5	0	59.5	40.5	0	58.5	41.5	0	57.5	42.5	0
6.4	55.3	44.7	0	53.8	46.2	0	52.9	47.1	0	51.8	48.2	0
6.5	49.7	50.3	0	43.0	52.0	0	47.0	53.0	0	46.0	54.0	0
6.6	43.9	56.1	0	42.6	57.4	0	41.7	58.3	0	40.5	59.5	0
6.7	38.5	61.5	0	36.8	63.2	0	35.8	64.2	0	35.0	65.0	0
6.8	32.8	67.2	0	31.8	68.2	0	31.1	68.9	0	30.0	70.0	0
6.9	28.0	72.0	0	27.0	73.0	0	26.5	73.5	0	25.5	74.5	0
7.0	23.6	76.4	0	22.7	77.3	0	22.0	78.0	0	21.3	78.7	0
7.1	19.8	80.2	0	19.0	81.0	0	18.2	81.8	0	18.0	82.0	0
7.2	16.4	83.6	0	15.7	84.3	0	15.2	84.8	0	14.7	85.3	0
7.3	13.3	86.7	0	12.8	87.2	0	12.4	87.6	0	12.0	88.0	0
7.4	11.0	89.0	0	10.4	89.6	0	10.1	89.9	0	9.6	90.4	0
7.5	8.8	91.2	0	8.6	91.4	0	8.3	91.6	0.1	8.0	91.9	0.1
7.6	7.3	92.6	0.1	6.9	93.0	0.1	6.7	93.2	0.1	6.4	93.5	0.1
7.7	5.5	94.3	0.2	5.4	94.4	0.2	5.3	94.5	0.2	5.1	94.8	0.1
7.8	4.7	95.1	0.2	4.5	95.3	0.2	4.3	95.5	0.2	4.1	95.7	0.2
7.9	3.7	96.0	0.3	3.6	96.1	0.3	3.5	96.2	0.3	3.4	96.4	0.2
8.0	3.0	96.7	0.3	2.9	96.8	0.3	2.8	96.9	0.3	2.7	97.0	0.3
8.1	2.5	97.1	0.4	2.4	97.2	0.4	2.3	97.3	0.4	2.2	97.4	0.4
8.2	1.9	97.6	0.5	1.9	97.6	0.5	1.8	97.7	0.5	1.7	97.8	0.5
8.3	1.5	97.9	0.6	1.5	97.9	0.7	1.4	97.9	0.7	1.4	97.9	0.7
8.4	1.2	98.1	0.7	1.1	98.1	0.8	1.1	98.1	0.8	1.1	98.0	0.9
8.5	1.0	98.1	0.9	0.9	98.1	1.0	0.9	98.0	1.1	0.8	98.0	1.2
8.6	0.8	98.1	1.1	0.7	98.0	1.3	0.7	98.0	1.3	0.6	98.0	1.4
8.7	0.6	97.9	1.5	0.6	97.8	1.7	0.5	97.8	1.7	0.5	97.7	1.8
8.8	0.4	97.7	1.9	0.4	97.6	2.0	0.4	97.5	2.1	0.4	97.4	2.2
8.9	0.4	97.2	2.4	0.4	97.0	2.6	0.4	97.0	2.6	0.4	96.8	2.8
9.0	0.3	96.7	3.0	0.3	96.6	3.1	0.3	96.5	3.2	0.3	96.3	3.4
9.1	0.3	96.0	3.7	0.2	95.9	3.9	0.2	95.7	4.1	0.3	95.3	4.4
9.2	0.2	95.3	4.5	0.1	95.1	4.8	0.1	94.8	5.1	0.2	94.4	5.4
9.3	0.2	94.2	5.6	0.1	93.8	6.1	0.1	93.5	6.4	0.2	92.9	6.9
9.4	0.1	93.0	6.9	0.1	92.5	7.4	0.1	92.1	7.8	0.1	91.5	8.4
9.5	0.1	90.9	9.0	0	90.6	9.4	0	90.2	9.8	0	89.5	10.5
9.6	0.1	89.4	10.5	0	88.6	11.4	0	88.2	11.8	0	87.5	12.5
9.7	0	86.7	13.3	0	85.9	14.1	0	85.2	14.8	0	84.5	15.5
9.8	0	84.0	16.0	0	83.1	16.9	0	82.3	17.7	0	81.5	18.5
9.9	0	80.5	19.5	0	79.4	20.6	0	78.6	21.4	0	77.5	22.5
10.0	0	76.9	23.1	0	75.7	24.3	0	74.9	25.1	0	73.5	26.5
10.1	0	72.5	27.5	0	71.1	28.9	0	70.2	29.8	0	68.5	31.5
10.2	0	68.0	32.0	0	66.5	33.5	0	65.5	34.5	0	63.5	36.5
10.3	0	52.0	38.0	0	61.0	39.0	0	60.0	40.0	0	57.8	42.2
10.4	0	57.3	42.7	0	55.5	44.5	0	54.2	45.8	0	52.1	47.9

Appendix E: Dissolution Reactions and Equilibrium Constants

We summarize in this appendix equilibrium constants (i.e., log K) at 25°C for dissolution reactions among minerals that could control the chemistry of groundwaters in the Kurihashi granodiorite. The reactions and corresponding equilibrium constants are from Yui et al. (1992), based primarily on the OECD/NEA thermodynamic database (e.g., Muller, 1985) and databases supporting the PHREEQE geochemical software package (Parkhurst et al., 1980).

- **quartz**
  $SiO_2(qz) + 2H_2O = H_4SiO_4(aq)$
  log K = -3.78, (from the OECD/NEA database)
- **chalcedony**
  $SiO_2(chal) + 2H_2O = H_4SiO_4(aq)$
  log K = -3.49, (from the OECD/NEA database)
- **calcite**
  $CaCO_3 = Ca^{2+} + CO_3^{2-}$
  log K = -8.48, (from the original PHREEQE database)
- **anorthite**
  $CaAl_2SiO_2O_8 + 8H^+ = 2Al^{3+} + 2H_4SiO_4(aq) + Ca^{2+}$
  log K = 26.70 (hexagonal), log K = 26.37 (triclinic), (from the OECD/NEA database)
  The data for hexagonal anorthite was used in the present study.
- **albite**
  $NaAlSi_3O_8 + 4H_2O + 4H^+ = Na^+ + Al^{3+} + 3H_4SiO_4(aq)$
  log K = 3.54, (from the OECD/NEA database)
- **kaolinite**
  $Al_2SiO_5(OH)_4 + 7H_2O = 2H^+ + 2H_4SiO_4(aq) + 2Al(OH)_4^-$
  log K = -36.92, (from the OECD/NEA database)
- **phlogopite**
  $KMg_3(Si_3,Al)O_{10}(OH)_2 + 10H^+ = 3Mg^{2+} + Al^{3+} + 3H_4SiO_4(aq) + K^+$
  log K = 36.33, (from the OECD/NEA database)
- **illite**
  illite K3 : $K_3MgAl_9SiO_{14}O_{40}(OH)_8 + 8H_2O + 32H_+ = Mg^{2+} + 9Al^{3+} + 14H_4SiO_4(aq) + 3K^+$
  log K = 67.15, (from the OECD/NEA database)
  illite K2 :$K_2Al_{10}Si_{14}O_{40}(OH)_8 + 8H_2O +32H^+ = 10Al^{3+} + 14H_4SiO_4(aq) + 2K^+$
  log K = 28.54, (from the OECD/NEA database)
- **k-feldspar**
  microcline : $KAlSi_3O_8 + 4H^+ + 4H_2O = Al^{3+} + 3H_4SiO_4(aq) + K^+$
  log K = 1.78, (from the OECD/NEA database)

orthoclase : $KAlSi_3O_8 + 4H^+ + 4H_2O = Al^{3+} + 3H_4SiO_4(aq) + K^+$
log K = 0.86, (from the OECD/NEA database)

- **clinochlore**

clinochlore-26 : $Mg_{26}Fe_8Al_{20}Si_{24}O_{80}(OH)_{64} + 128H^+ = 26Mg^{2+} + 20Al^{3+} + 24H_4SiO_4(aq) + 8Fe^{2+} + 48H_2O$
log K = 447.61, (from the OECD/NEA database)

clinochlore-40 : $Mg_{40}Al_{16}Si_{24}O_{80}(OH)_{64} + 128H^+ = 40Mg^{2+} + 16Al^{3+} + 24H_4SiO_4(aq) + 48H_2O$
log K = 546.83, (from the OECD/NEA database)

clinochlore-8 : $Mg_8Fe_{26}Al_{25}Si_{20}O_{80}(OH)_{64} + 144H^+ + 2e^- = 8Mg^{2+} + 25Al^{3+} + 20H_4SiO_4(aq) + 26Fe^{2+} + 64H_2O$
log K = 178.37, (from the OECD/NEA database)

- **magnetite**

$Fe_3O_4 + 8H^+ + 2e^- = 3Fe^{2+} + 4H_2O$
log K = 30.65, (from the OECD/NEA database)

- **tremolite**

$Ca_2Mg_5Si_8O_{22}(OH)_2 + 8H_2O + 14H^+ = 5Mg^{2+} + 8H_4SiO_4(aq) + 2Ca^{2+}$
log K = 57.70, (from the OECD/NEA database)

- **epidote**

$Ca_2FeAl_2(SiO_4)_3OH + 13H^+ + e^- = 2Al^{3+} + 3H_4SiO_4(aq) + 2Ca^{2+} + 2Fe^{2+} + H_2O$
log K = 45.43, (from the OECD/NEA database)

- **muscovite**

$KAl_3Si_3O_{10}(OH)_2 + 10H^+ = 3Al^{3+} + 3H_4SiO_4(aq) + K^+$
log K = 14.60, (from the OECD/NEA database)

- **pyrite**

$FeS_2 + 8H_2O = 2SO_4^{2-} + Fe^{2+} + 10H^+ + 14e^-$
log K = -85.96, (from the OECD/NEA database)

[References]

・Muller A B (1985) : NEA compilation of chemical thermodynamic data for minerals associated with granite, OECD/NEA, RWN-5 NEA Report

・Parkhurst D L, Thorstenson D C and Plummer L N (1980) : PHREEQE - a computer program for geochemical calculations, U.S.Geological Survey Water-Resources Investigations Report 80-96

Appendix F: Examples of PHREEQE Input and Output Files

[List of Appendix F]

The input file used with PHREEQE to evaluate Test 15, and the corresponding output file, are included in this appendix. The PHREEQE geochemical code calculates aqueous speciation and mass transfer using a Newton-Raphson numerical solution technique based on mass-balance and electrical neutrality constraints (Parkhurst et al., 1980). The code is useful for modeling solution compositions and mineral-fluid equilibria under conditions that are appropriate for natural groundwater systems (i.e., relatively dilute solutions at temperatures less than 100°C). Calculations using PHREEQE were carried out on a DIGITAL ALPHA SERVER 800 5/400.

Appendix F-1: Input file
There are three data blocks in this input file. The first specifies equilibrium reactions between rain water and atmospheric gases. The second refers to equilibrium reactions in the soil zone. The third corresponds to equilibrium reactions in the rock zone.

Appendix F-2: Output file

This output file consists of the following components:

a) INPUT DATA BLOCK; each data block is read from the input file,
b) TOTAL MOLALITIES OF ELEMENTS; refers to total molalities of elements in the aqueous phase,
c) PHASE BOUNDARIES; refers to phases that react with the solution - the term "delta phase" indicates the amount of the phase that is precipitated or dissolved,
d) LOOK MIN IAP: the saturation state of the aqueous solution with respect to the indicated mineral, gas or "fictive" solid (see Parkhurst et al., 1980),
e) DESCRIPTION OF SOLUTION; includes information about the equilibrated aqueous phase (e.g., pH, pe, ionic strength, electrical balance, etc.), and
f) DISTRIBUTION OF SPECIES; the concentration distribution of aqueous species.

The calculation procedure involves the following steps:

1) "rain water" is equilibrated with atmospheric gases [CO_2(g) and O_2(g)] - the equilibrated solution is saved as "SOLUTION 1",
2) SOLUTION 1 reacts with CO_2(g) in the soil zone, where log PCO_2(g) = -2, - this solution is saved as a new "SOLUTION 1", and
3) the new SOLUTION 1 equilibrates with minerals in the rock zone (calcite, albite, chalcedony, kaolinite, microcline, phlogopite and pyrite).

Appendix F-1 : Input File

```
TEST-15 KAMAISHI GROUND WATER MODELLING 97/01/20 by H.Sasamoto
005010100  0 0       0.0
SOLUTION 1
rain water
 0  0 0   7.0        4.0      25.        1.0
MINERALS
CO2 GAS     2        4.00     -1.47     -4.78     1                -3.50!ORIGINAL!
  65      1.000   3      -1.000
 0.10839E+03 0.19851E-01-0.69195E+04-0.40452E+02 0.66937E+06
O2 GAS      1        4.00     -2.96     -1.84     0                -0.70!ORIGINAL!
  62      1.000

END
TEST KAMAISHI GROUND WATER MODELLING 97/01/20
005000100  0 0       0.0
MINERALS
CO2 GAS     2        4.00     -1.47     -4.78     1                -2.00!ORIGINAL!
  65      1.000   3      -1.000
 0.10839E+03 0.19851E-01-0.69195E+04-0.40452E+02 0.66937E+06

END
TEST KAMAISHI GROUND WATER MODELLING 97/01/20
CALCITE     2        4.00     -8.48     -2.30     1                0.000-ORIGINAL-
  15      1.000   4       1.000
-0.17191E+03-0.77993E-01 0.28393E+04 0.71595E+02 0.00000E+00
ALBITE      5        0.00      3.54      0.00     0                0.000- NEA -
   6      1.000  10       1.000  13     3.000   3     -4.000   1     -4.
CHALCEDO    2        0.00     -3.49      4.61     0                0.000- NEA -
  13      1.000   3      -2.000
KAOLINIT    4        0.00    -36.92     49.15     0                0.000-ORIGINAL-
   3     -7.000   1       2.000  13     2.000 183      2.000
MICROCLI    5        0.00      1.78    -12.47     0                0.000- NEA -
  10      1.000  13       3.000   7     1.000   3     -4.000   1     -4.
PHLOGOPI    5        0.00     36.33      0.00     0                0.000- NEA -
   5      3.000  10       1.000  13     3.000   7      1.000   1    -10.
PYRITE      5        0.00    -85.95    131.16     0                0.000- NEA -
  16      2.000   8       1.000   3    -8.000   1     16.000   2     14.

END
```

Appendix F-2 : Output File

```
        DATA READ FROM DISK

ELEMENTS
SPECIES
LOOK MIN
TEST-15 KAMAISHI GROUND WATER MODELLING 97/01/20 by H.Sasamoto
0050101000 0 0          0.00000
SOLUTION 1
rain water
 0  0 0     7.00      4.00      25.0      1.00
MINERALS
CO2 GAS     2       4.0      -1.5      -4.8          1            -3.500
  65   1.00         3  -1.00
  1.0839E+02  1.9851E-02 -6.9195E+03 -4.0452E+01  6.6937E+05
O2 GAS      1       4.0      -3.0      -1.8          0            -0.700
  62   1.00
            0     0.00E+00  0.00E+00  0.00E+00       0             0.000

SOLUTION NUMBER 1
rain water
```

TOTAL MOLALITIES OF ELEMENTS

ELEMENT	MOLALITY	LOG MOLALITY
PURE WATER		

----DESCRIPTION OF SOLUTION----

PH =	7.0000
PE =	4.0000
ACTIVITY H2O =	1.0000
IONIC STRENGTH =	0.0000
TEMPERATURE =	25.0000
ELECTRICAL BALANCE =	-2.0911D-14
THOR =	-1.4159D-25
TOTAL ALKALINITY =	1.0004D-07
ITERATIONS =	5

DISTRIBUTION OF SPECIES

SPECIES	Z	MOLALITY	LOG MOLAL	ACTIVITY	LOG ACT	GAMMA	LOG GAM
1 H+	1.0	1.000E-07	-7.000	1.000E-07	-7.000	9.996E-01	0.000
2 E-	-1.0	1.000E-04	-4.000	1.000E-04	-4.000	1.000E+00	0.000
3 H2O(L)	0.0	1.000E+00	0.000	1.000E+00	0.000	1.000E+00	0.000
61 OH-	-1.0	1.000E-07	-7.000	1.000E-07	-7.000	9.996E-01	0.000
63 H2 AQ	0.0	7.079E-26	-25.150	7.079E-26	-25.150	1.000E+00	0.000

---- LOOK MIN IAP ----

PHASE	LOG IAP	LOG KT	LOG IAP/KT
O2 GAS	-42.0800	-2.9600	-39.1200
H2 GAS	-25.1500	-3.1500	-22.0000

STEP NUMBER

TOTAL MOLALITIES OF ELEMENTS

ELEMENT	MOLALITY	LOG MOLALITY
PURE WATER		

----PHASE BOUNDARIES----

PHASE	DELTA PHASE*	LOG IAP	LOG KT	LOG IAP/KT
CO2 GAS	1.302682D-05	-4.9653	-1.4653	-3.5000
O2 GAS	2.187761D-04	-3.6600	-2.9600	-0.7000

* NEGATIVE DELTA PHASE INDICATES PRECIPITATION
AND POSITIVE DELTA PHASE INDICATES DISSOLUTION.

---- LOOK MIN IAP ----

PHASE	LOG IAP	LOG KT	LOG IAP/KT
CO2 GAS	-4.9653	-1.4653	-3.5000
O2 GAS	-3.6600	-2.9600	-0.7000
H2 GAS	-44.3600	-3.1500	-41.2100
CH4 GAS	-145.4151	-2.8600	-142.5551

TOTAL MOLALITIES OF ELEMENTS

ELEMENT	MOLALITY	LOG MOLALITY
C	1.302682D-05	-4.8852

----DESCRIPTION OF SOLUTION----

PH =	5.6581
PE =	14.9469
ACTIVITY H2O =	1.0000
IONIC STRENGTH =	0.0000
TEMPERATURE =	25.0000
ELECTRICAL BALANCE =	-2.0917D-14
THOR =	9.2721D-04
TOTAL ALKALINITY =	2.2009D-06
ITERATIONS =	49

DISTRIBUTION OF SPECIES

SPECIES	Z	MOLALITY	LOG MOLAL	ACTIVITY	LOG ACT	GAMMA	LOG GAM
1 H+	1.0	2.201E-06	-5.657	2.197E-06	-5.658	9.983E-01	-0.001
2 E-	-1.0	1.130E-15	-14.947	1.130E-15	-14.947	1.000E+00	0.000
3 H2O(L)	0.0	1.000E+00	0.000	1.000E+00	0.000	1.000E+00	0.000

15	C03-2	-2.0	4.712E-11	-10.327	4.680E-11	-10.330	9.931E-01	-0.003
61	OH-	-1.0	4.559E-09	-8.341	4.551E-09	-8.342	9.983E-01	-0.001
62	02 AQ	0.0	2.188E-04	-3.660	2.188E-04	-3.660	1.000E+00	0.000
64	HC03-	-1.0	2.196E-06	-5.658	2.192E-06	-5.659	9.983E-01	-0.001
65	H2C03	0.0	1.083E-05	-4.965	1.083E-05	-4.965	1.000E+00	0.000

```
TEST KAMAISHI GROUND WATER MODELLING 97/01/20
0050001000 0 0          0.00000
MINERALS
C02 GAS    2       4.0       -1.5        -4.8          1              -2.000
 65   1.00        3  -1.00
 1.0839E+02  1.9851E-02 -6.9195E+03 -4.0452E+01  6.6937E+05
           0     0.00E+00  0.00E+00  0.00E+00    0                 0.000
STEP NUMBER
```

TOTAL MOLALITIES OF ELEMENTS

ELEMENT	MOLALITY	LOG MOLALITY
C	1.302682D-05	-4.8852

----PHASE BOUNDARIES----

PHASE	DELTA PHASE*	LOG IAP	LOG KT	LOG IAP/KT
C02 GAS	3.418545D-04	-3.4653	-1.4653	-2.0000

* NEGATIVE DELTA PHASE INDICATES PRECIPITATION
AND POSITIVE DELTA PHASE INDICATES DISSOLUTION.

--- LOOK MIN IAP ---

PHASE	LOG IAP	LOG KT	LOG IAP/KT
C02 GAS	-3.4653	-1.4653	-2.0000
02 GAS	-6.6582	-2.9600	-3.6982
H2 GAS	-42.8609	-3.1500	-39.7109
CH4 GAS	-137.9186	-2.8600	-135.0586

TOTAL MOLALITIES OF ELEMENTS

ELEMENT	MOLALITY	LOG MOLALITY
C	3.548813D-04	-3.4499

----DESCRIPTION OF SOLUTION----

PH =	4.9086
PE =	14.9469
ACTIVITY H20 =	1.0000
IONIC STRENGTH =	0.0000
TEMPERATURE =	25.0000
ELECTRICAL BALANCE =	-2.0921D-14
THOR =	1.4204D-03
TOTAL ALKALINITY =	1.2393D-05
ITERATIONS =	12

DISTRIBUTION OF SPECIES

SPECIES	Z	MOLALITY	LOG MOLAL	ACTIVITY	LOG ACT	GAMMA	LOG GAM
1 H+	1.0	1.239E-05	-4.907	1.234E-05	-4.909	9.959E-01	-0.002
2 E-	-1.0	1.130E-15	-14.947	1.130E-15	-14.947	1.000E+00	0.000
3 H2O(L)	0.0	1.000E+00	0.000	1.000E+00	0.000	1.000E+00	0.000
15 CO3-2	-2.0	4.767E-11	-10.322	4.689E-11	-10.329	9.837E-01	-0.007
61 OH-	-1.0	8.135E-10	-9.090	8.102E-10	-9.091	9.959E-01	-0.002
62 O2 AQ	0.0	2.197E-07	-6.658	2.197E-07	-6.658	1.000E+00	0.000
64 HCO3-	-1.0	1.239E-05	-4.907	1.234E-05	-4.909	9.959E-01	-0.002
65 H2CO3	0.0	3.425E-04	-3.465	3.425E-04	-3.465	1.000E+00	0.000

```
TEST KAMAISHI GROUND WATER MODELLING 97/01/20
0050100000 0 0          0.00000
MINERALS
CALCITE    2       4.0      -8.5       -2.3          1              0.000
  15   1.00        4   1.00
  -1.7191E+02 -7.7993E-02  2.8393E+03  7.1595E+01  0.0000E+00
ALBITE     5      0.00E+00   3.5      0.00E+00     0              0.000
   6   1.00       10   1.00      13   3.00        3  -4.00      1  -4.00
CHALCEDO   2      0.00E+00  -3.5        4.6        0              0.000
  13   1.00        3  -2.00
KAOLINIT   4      0.00E+00  -37.        49.        0              0.000
   3  -7.00        1   2.00      13   2.00      183   2.00
MICROCLI   5      0.00E+00   1.8      -12.         0              0.000
  10   1.00       13   3.00       7   1.00        3  -4.00      1  -4.00
PHLOGOPI   5      0.00E+00   36.      0.00E+00     0              0.000
   5   3.00       10   1.00      13   3.00        7   1.00      1  -10.0
PYRITE     5      0.00E+00  -86.      0.13E+03     0              0.000
  16   2.00        8   1.00       3  -8.00        1   16.0      2   14.0
           0      0.00E+00  0.00E+00  0.00E+00     0              0.000
STEP NUMBER
```

TOTAL MOLALITIES OF ELEMENTS

ELEMENT	MOLALITY	LOG MOLALITY
C	3.548813D-04	-3.4499

----PHASE BOUNDARIES----

PHASE	DELTA PHASE*	LOG IAP	LOG KT	LOG IAP/KT
CALCITE	1.168418D-04	-8.4834	-8.4834	0.0000
ALBITE	5.403479D-04	3.5400	3.5400	0.0000
CHALCEDO	-6.789615D-04	-3.4900	-3.4900	0.0000
KAOLINIT	-2.738381D-04	-36.9200	-36.9200	0.0000
MICROCLI	9.347874D-06	1.7800	1.7800	0.0000
PHLOGOPI	3.963961D-08	36.3300	36.3300	0.0000
PYRITE	6.250408D-05	-85.9500	-85.9500	0.0000

* NEGATIVE DELTA PHASE INDICATES PRECIPITATION
  AND POSITIVE DELTA PHASE INDICATES DISSOLUTION.

---- LOOK MIN IAP ----

PHASE	LOG IAP	LOG KT	LOG IAP/KT

CALCITE	-8.4834	-8.4834	0.0000
ARAGONIT	-8.4834	-8.3387	-0.1447
DOLOMITE	-19.9496	-17.0900	-2.8596
SIDERITE	-8.9125	-10.5700	1.6575
GYPSUM	-8.0097	-4.6039	-3.4058
ANHYDRIT	-8.0096	-4.3800	-3.6296
FEOH3A	4.9671	4.8900	0.0771
GIBBSITE	8.0300	8.7700	-0.7400
KAOLINIT	-36.9200	-36.9200	0.0000
FES PPT	-6.2165	-3.9100	-2.3065
SIL GEL	-3.4900	-2.7000	-0.7900
SIL GLAS	-3.4900	-3.0200	-0.4700
SEP PPT	-43.4367	-37.2100	-6.2267
MACKINIT	-6.2165	-4.6300	-1.5865
MUSCOVIT	17.8400	14.6000	3.2400
CLINOZOI	42.6191	43.6100	-0.9909
EPIDOTE,	52.5882	45.4300	7.1582
TREMOLIT	58.6624	57.7000	0.9624
ANDRADIT	69.0269	55.1000	13.9269
MONTMOCA	50.1396	41.8800	8.2596
ANORTHHE	23.5796	26.7000	-3.1204
ANORTHTR	23.5796	26.3700	-2.7904
LIME, QU	14.4995	32.7000	-18.2005
ILLITEK3	47.5867	67.1500	-19.5633
PHLOGOPI	36.3300	36.3300	0.0000
CLINOC26	488.8367	447.6100	41.2267
MG2SI206	16.0533	23.2600	-7.2067
TALC	20.5900	20.6000	-0.0100
CLINOC40	505.3866	546.8300	-41.4434
SEPIOLIT	25.1266	32.8300	-7.7034
CLINOCH8	592.8432	178.3700	414.4732
MONTMOMG	47.1568	57.0400	-9.8832
MAGNESIO	47.5150	42.8200	4.6950
PERICLAS	11.5167	21.5800	-10.0633
MONTMONA	47.6001	58.5400	-10.9399
PARAGONI	19.6000	18.8700	0.7300
ALBITE	3.5400	3.5400	0.0000
ILLITEK2	39.8801	28.5400	11.3401
MONTMOK	44.0801	57.5100	-13.4299
ALUNITE	-16.7084	1.6100	-18.3184
MICROCLI	1.7800	1.7800	0.0000
ORTHOCLA	1.7800	0.8600	0.9200
ANNITE	43.9913	22.3300	21.6613
HEMATITE	35.9983	22.4000	13.5983
FE2SI206	21.1609	10.6000	10.5609
ALMANDIN	47.8013	33.4100	14.3913
MAGNETIT	50.0687	30.6500	19.4187
PYRRHOTI	-39.8685	-39.7800	-0.0885
GOETHITE	17.9991	11.2900	6.7091
PYRITE	-85.9500	-85.9500	0.0000
TOPAZ, O	12.5700	12.8100	-0.2400
CHALCEDO	-3.4900	-3.4900	0.0000
QUARTZ	-3.4900	-3.7800	0.2900
SILICA H	-7.4187	-2.4700	-4.9487
CO2 GAS	-6.3022	-1.4653	-4.8369
O2 GAS	-70.3651	-2.9600	-67.4051
H2 GAS	-11.0075	-3.1500	-7.8575
H2S GAS	-13.2579	-1.0000	-12.2579
CH4 GAS	-13.3417	-2.8600	-10.4817
FERROSIL	10.5804	7.4200	3.1604
GREENALI	35.2313	22.5900	12.6413
FAYALITE	24.6509	19.0500	5.6009
K-FELDSP	1.7800	0.0830	1.6970
SILI(AM)	-3.4900	-2.7100	-0.7800

TOTAL MOLALITIES OF ELEMENTS

ELEMENT	MOLALITY	LOG MOLALITY

CA	1.168418D-04	-3.9324
MG	1.189188D-07	-6.9247
NA	5.403479D-04	-3.2673
K	9.387513D-06	-5.0274
FE	6.250408D-05	-4.2041
AL	2.059131D-06	-5.6863
SI	4.225684D-04	-3.3741
C	4.717232D-04	-3.3263
S	1.250082D-04	-3.9031

-----DESCRIPTION OF SOLUTION-----

PH =	9.2646
PE =	-5.3359
ACTIVITY H2O =	1.0000
IONIC STRENGTH =	0.0012
TEMPERATURE =	25.0000
ELECTRICAL BALANCE =	5.0037D-14
THOR =	2.7620D-03
TOTAL ALKALINITY =	5.6316D-04
ITERATIONS =	49

DISTRIBUTION OF SPECIES

	SPECIES	Z	MOLALITY	LOG MOLAL	ACTIVITY	LOG ACT	GAMMA	LOG GAM
1	H+	1.0	5.640E-10	-9.249	5.437E-10	-9.265	9.640E-01	-0.016
2	E-	-1.0	2.167E+05	5.336	2.167E+05	5.336	1.000E+00	0.000
3	H2O(L)	0.0	1.000E+00	0.000	1.000E+00	0.000	1.000E+00	0.000
4	CA+2	2.0	1.088E-04	-3.963	9.338E-05	-4.030	8.584E-01	-0.066
5	MG+2	2.0	1.131E-07	-6.947	9.714E-08	-7.013	8.592E-01	-0.066
6	NA+	1.0	5.396E-04	-3.268	5.192E-04	-3.285	9.622E-01	-0.017
7	K+	1.0	9.381E-06	-5.028	9.023E-06	-5.045	9.619E-01	-0.017
8	FE+2	2.0	4.045E-05	-4.393	3.477E-05	-4.459	8.594E-01	-0.066
10	AL+3	3.0	2.396E-20	-19.620	1.722E-20	-19.764	7.187E-01	-0.143
13	H4SIO4(A	0.0	3.235E-04	-3.490	3.236E-04	-3.490	1.000E+00	0.000
15	CO3-2	-2.0	4.098E-05	-4.387	3.518E-05	-4.454	8.586E-01	-0.066
16	SO4-2	-2.0	1.221E-04	-3.913	1.047E-04	-3.980	8.580E-01	-0.067
61	OH-	-1.0	1.912E-05	-4.718	1.839E-05	-4.735	9.618E-01	-0.017
63	H2 AQ	0.0	9.827E-12	-11.008	9.830E-12	-11.007	1.000E+00	0.000
64	HCO3-	-1.0	4.237E-04	-3.373	4.079E-04	-3.389	9.626E-01	-0.017
65	H2CO3	0.0	4.985E-07	-6.302	4.986E-07	-6.302	1.000E+00	0.000
66	CH4 AQ	0.0	4.552E-14	-13.342	4.553E-14	-13.342	1.000E+00	0.000
70	HSO4-	-1.0	5.744E-12	-11.241	5.526E-12	-11.258	9.621E-01	-0.017
71	S-2	-2.0	2.465E-15	-14.608	2.115E-15	-14.675	8.580E-01	-0.066
72	HS-	-1.0	9.876E-12	-11.005	9.499E-12	-11.022	9.618E-01	-0.017
105	CAOH+	1.0	4.505E-08	-7.346	4.334E-08	-7.363	9.621E-01	-0.017
106	CACO3	0.0	5.518E-06	-5.258	5.519E-06	-5.258	1.000E+00	0.000
107	CAHCO3+	1.0	5.049E-07	-6.297	4.860E-07	-6.313	9.626E-01	-0.017
108	CASO4	0.0	1.992E-06	-5.701	1.992E-06	-5.701	1.000E+00	0.000
115	MGOH+	1.0	2.984E-10	-9.525	2.871E-10	-9.542	9.621E-01	-0.017
116	MGCO3	0.0	3.271E-09	-8.485	3.272E-09	-8.485	1.000E+00	0.000
117	MGHCO3+	1.0	4.819E-10	-9.317	4.636E-10	-9.334	9.621E-01	-0.017
118	MGSO4	0.0	1.809E-09	-8.743	1.809E-09	-8.743	1.000E+00	0.000
125	NACO3-	-1.0	3.520E-07	-6.454	3.386E-07	-6.470	9.621E-01	-0.017
126	NAHCO3	0.0	1.194E-07	-6.923	1.194E-07	-6.923	1.000E+00	0.000
127	NASO4-	-1.0	2.833E-07	-6.548	2.726E-07	-6.565	9.621E-01	-0.017
130	KSO4-	-1.0	6.954E-09	-8.158	6.690E-09	-8.175	9.621E-01	-0.017
135	FEOH+	1.0	2.102E-05	-4.677	2.022E-05	-4.694	9.621E-01	-0.017
136	FEOH2	0.0	3.164E-07	-6.500	3.165E-07	-6.500	1.000E+00	0.000
137	FEOH3-	-1.0	2.248E-08	-7.648	2.163E-08	-7.665	9.621E-01	-0.017
138	FESO4	0.0	6.474E-07	-6.189	6.475E-07	-6.189	1.000E+00	0.000
139	FE(HS)2	0.0	2.770E-18	-17.558	2.770E-18	-17.557	1.000E+00	0.000
140	FE(HS)3-	-1.0	2.965E-27	-26.528	2.853E-27	-26.545	9.621E-01	-0.017
145	FE+3	3.0	2.074E-23	-22.683	1.490E-23	-22.827	7.187E-01	-0.143

146	FEOH+2	2.0	2.075E-16	-15.683	1.778E-16	-15.750	8.567E-01	-0.067
147	FEOH2+	1.0	1.125E-10	-9.949	1.083E-10	-9.965	9.621E-01	-0.017
148	FEOH3	0.0	2.339E-09	-8.631	2.340E-09	-8.631	1.000E+00	0.000
149	FEOH4-	-1.0	4.473E-08	-7.349	4.303E-08	-7.366	9.621E-01	-0.017
150	FE2OH2+4	4.0	1.579E-30	-29.801	8.507E-31	-30.070	5.386E-01	-0.269
155	FESO4+	1.0	1.356E-23	-22.868	1.304E-23	-22.885	9.621E-01	-0.017
156	FESO42-	-1.0	4.490E-26	-25.348	4.320E-26	-25.365	9.621E-01	-0.017
180	ALOH+2	2.0	3.784E-16	-15.422	3.241E-16	-15.489	8.567E-01	-0.067
181	ALOH2+	1.0	4.810E-12	-11.318	4.628E-12	-11.335	9.621E-01	-0.017
182	ALOH3	0.0	1.071E-08	-7.970	1.072E-08	-7.970	1.000E+00	0.000
183	ALOH4-	-1.0	2.048E-06	-5.689	1.971E-06	-5.705	9.621E-01	-0.017
184	ALSO4+	1.0	1.963E-21	-20.707	1.889E-21	-20.724	9.621E-01	-0.017
185	ALSO42-	-1.0	1.633E-23	-22.787	1.571E-23	-22.804	9.621E-01	-0.017
217	SI2O2(OH	-1.0	1.590E-06	-5.799	1.530E-06	-5.815	9.621E-01	-0.017
218	SI2O3(OH	-2.0	4.125E-08	-7.385	3.534E-08	-7.452	8.567E-01	-0.067
219	SI3O5(OH	-3.0	9.420E-11	-10.026	6.651E-11	-10.177	7.060E-01	-0.151
220	SI3O6(OH	-3.0	7.483E-12	-11.126	5.283E-12	-11.277	7.060E-01	-0.151
222	SI4O7(OH	-3.0	3.048E-12	-11.516	2.152E-12	-11.667	7.060E-01	-0.151
223	SIO(OH)3	-1.0	9.581E-05	-4.019	9.218E-05	-4.035	9.621E-01	-0.017
224	SIO2(OH)	-2.0	9.235E-09	-8.035	7.911E-09	-8.102	8.567E-01	-0.067
236	H2S(AQ)	0.0	5.520E-14	-13.258	5.521E-14	-13.258	1.000E+00	0.000
237	H2SO3(AQ	0.0	1.978E-25	-24.704	1.979E-25	-24.704	1.000E+00	0.000
239	HS2O3-	-1.0	2.744E-28	-27.562	2.639E-28	-27.578	9.621E-01	-0.017
240	HSO3-	-1.0	5.468E-18	-17.262	5.260E-18	-17.279	9.621E-01	-0.017
243	S2O3-2	-2.0	1.457E-20	-19.837	1.248E-20	-19.904	8.567E-01	-0.067
244	SO3-2	-2.0	6.805E-16	-15.167	5.830E-16	-15.234	8.567E-01	-0.067

Appendix G : React input script for the reaction-path model (Test 15)

```
# React script, created by R.C.Arthur and saved by H.Sasamoto
data = thermo.dat
temperature = 25
swap e- for O2(aq)
1 kg free H2O
Eh = .88
pH = 4.9086
balance on HCO3-
total molality HCO3- = .000355
total mg/kg Na+ = 1e-10
total mg/kg K+ = 1e-10
total mg/kg Ca++ = 1e-10
total mg/kg Mg++ = 1e-10
total mg/kg SiO2(aq) = 1e-10
total mg/kg Al+++ = 1e-10
total mg/kg Cl- = 1e-10
total mg/kg SO4-- = 1e-10
total mg/kg Fe++ = 1e-10
react .001 mol of Albite
react .001 mol of Calcite
react .001 mol of "Maximum Microcline"
react .001 mol of Phlogopite
react .001 mol of Pyrite
suppress Quartz Tridymite Cristobalite Nontronit-Na
suppress Nontronit-Mg Nontronit-K Saponite-Ca Saponite-Mg
suppress Saponite-K Saponite-Na Laumontite Muscovite
suppress Clinoptil-Ca Clinoptil-Na Clinoptil-Mg Clinoptil-K
suppress Heulandite Phengite Talc Tremolite
suppress Saponite-H Antigorite Smectite-low-Fe-Mg Mordenite-K
suppress Andradite Minnesotaite Cronstedt-7A Prehnite
suppress Magnetite Daphnite-14A Ferrite-Ca Ferrite-Mg
suppress Epidote Epidote-ord Annite Greenalite
suppress Smectite-high-Fe-Mg Ripidolit-14A Daphnite-7A Chamosite-7A
suppress Ferrosilite Fayalite Hedenbergite Nontronit-Ca
suppress Goethite FeO(c) Hematite Ripidolit-7A
```

Appendix H : Equilibrium conditions in the reaction-path model for Test 15

```
Step #   100                    Xi = 1.0000
Temperature =  25.0 C           Pressure =  1.013 bars
pH =  9.936                     log f02 =  -71.127
Eh =  -0.4107 volts             pe =  -6.9425
Ionic strength       =          0.001027
Activity of water    =          1.000000
Solvent mass         =          0.999975 kg
Solution mass        =          1.000058 kg
Solution density     =          1.013    g/cm3
Chlorinity           =          0.000000 molal
Dissolved solids     =                84 mg/kg sol'n
```

Reactants	moles remaining	moles reacted	grams reacted	cm3 reacted
Albite	-1.203e-018	0.001000	0.2622	0.1003
Calcite	-1.203e-018	0.001000	0.1001	0.03693
Maximum Microcli	-1.203e-018	0.001000	0.2783	0.1087
Phlogopite	-1.203e-018	0.001000	0.4173	0.1497
Pyrite	-1.203e-018	0.001000	0.1200	0.02394

Minerals in system	moles	log moles	grams	volume (cm3)
Albite	0.0001684	-3.774	0.04416	0.01688
Calcite	0.0009695	-3.013	0.09703	0.03581
Chalcedony	0.001232	-2.910	0.07400	0.02794
K-feldspar	0.0009992	-3.000	0.2781	0.1088
Kaolinite	0.0004075	-3.390	0.1052	0.04056
Phlogopite	0.001000	-3.000	0.4172	0.1497
Pyrite	0.0009999	-3.000	0.1200	0.02394
(total)			1.136	0.4036

Aqueous species	molality	mg/kg sol'n	act. coef.	log act.
Na+	0.0008282	19.04	0.9647	-3.0975
HCO3-	0.0002731	16.66	0.9648	-3.5792
H3SiO4-	0.0002601	24.73	0.9647	-3.6005
SiO2(aq)	0.0001870	11.23	1.0003	-3.7281
CO3--	0.0001190	7.141	0.8664	-3.9867
OH-	9.232e-005	1.570	0.9645	-4.0504
Ca++	2.613e-005	1.047	0.8682	-4.6442
Al(OH)4-	1.730e-005	1.643	0.9647	-4.7776
CaCO3	3.846e-006	0.3849	1.0000	-5.4150
NaH3SiO4	2.827e-006	0.3338	1.0000	-5.5487
K+	8.020e-007	0.03136	0.9643	-6.1116
NaHCO3	2.834e-007	0.02380	1.0000	-6.5477
CaH2SiO4	2.814e-007	0.03775	1.0000	-6.5507
NaCO3-	2.727e-007	0.02263	0.9647	-6.5799
H2SiO4--	1.996e-007	0.01878	0.8658	-6.7625
CaH3SiO4+	1.103e-007	0.01491	0.9647	-6.9730
CaHCO3+	1.033e-007	0.01044	0.9651	-7.0014
SO4--	8.454e-008	0.008120	0.8658	-7.1355
Mg++	7.955e-008	0.001933	0.8706	-7.1595
CO2(aq)	7.086e-008	0.003118	1.0000	-7.1496
HS-	4.483e-008	0.001482	0.9645	-7.3641
NaOH	4.465e-008	0.001786	1.0000	-7.3502
CaOH+	4.160e-008	0.002375	0.9647	-7.3965
Fe++	3.266e-008	0.001824	0.8682	-7.5474
Ca(H3SiO4)2	2.028e-008	0.004671	1.0000	-7.6928
FeOH+	1.681e-008	0.001225	0.9647	-7.7900
FeCO3	1.400e-008	0.001622	1.0000	-7.8537
MgH2SiO4	1.018e-008	0.001205	1.0000	-7.9922

(only species > 1e-8 molal listed)

Mineral saturation states

	log Q/K		log Q/K
Daphnite-14A	12.5848s/sat	Chalcedony	0.0000 sat

Cronstedt-7A	9.4054s/sat	Phlogopite	0.0000 sat
Daphnite-7A	9.2117s/sat	Calcite	0.0000 sat
Minnesotaite	8.1768s/sat	Lawsonite	-0.0361
Nontronit-Ca	7.4420s/sat	Beidellit-Ca	-0.1461
Annite	7.3260s/sat	Aragonite	-0.1649
Nontronit-Na	7.1270s/sat	Antigorite	-0.2443
Nontronit-Mg	7.0454s/sat	Illite	-0.2605
Greenalite	6.9449s/sat	Cristobalite	-0.2793
Magnetite	6.6448s/sat	Mordenite-Na	-0.4189
Nontronit-K	6.4624s/sat	Analcime	-0.4546
Andradite	6.2566s/sat	Beidellit-Na	-0.4611
Hematite	4.5701s/sat	Diopside	-0.4839
Ripidolit-14A	4.5501s/sat	Paragonite	-0.4924
Epidote-ord	3.2225s/sat	Gibbsite	-0.5176
Epidote	3.2225s/sat	Fe(OH)2(ppd)	-0.5231
Saponite-Ca	2.6054s/sat	Beidellit-Mg	-0.5427
Tremolite	2.5272s/sat	Clinoptil-Na	-0.8278
Chamosite-7A	2.4104s/sat	Chrysotile	-0.8652
Saponite-Na	2.2903s/sat	Siderite	-0.9687
Saponite-Mg	2.2088s/sat	Monohydrocalcite	-0.9939
Clinoptil-Ca	1.9530s/sat	Amrph^silica	-1.0145
Fayalite	1.8732s/sat	Pyrophyllite	-1.0869
Goethite	1.8068s/sat	Beidellit-K	-1.1257
Talc	1.6646s/sat	Sanidine high	-1.1992
Saponite-K	1.6256s/sat	Troilite	-1.2120
Smectite-high-Fe	1.3691s/sat	Pyrrhotite	-1.2663
Smectite-low-Fe-	1.2501s/sat	Clinochl-14A	-1.2980
Ferrosilite	1.1810s/sat	Diaspore	-1.3090
Ripidolit-7A	1.1769s/sat	Albite high	-1.3187
Heulandite	1.1373s/sat	Dolomite	-1.6100
Phengite	1.1116s/sat	Dolomite-ord	-1.6100
Saponite-H	1.0636s/sat	Beidellit-H	-1.6984
Laumontite	1.0546s/sat	Ferrite-Ca	-1.7078
FeO(c)	0.9656s/sat	Wustite	-1.7679
Prehnite	0.8808s/sat	Jadeite	-1.8963
Hedenbergite	0.6598s/sat	Wollastonite	-2.1233
Muscovite	0.4041s/sat	Boehmite	-2.1534
Quartz	0.2712s/sat	CaSi205^2H20	-2.1888
Clinoptil-K	0.1640s/sat	Hercynite	-2.2273
Tridymite	0.1054s/sat	Clinozoisite	-2.3141
Mordenite-K	0.0770s/sat	Zoisite	-2.3588
Maximum Microcli	0.0000 sat	Enstatite	-2.4836
Kaolinite	0.0000 sat	Pseudowollastoni	-2.5142
K-feldspar	0.0000 sat	Sepiolite	-2.5192
Albite	0.0000 sat	Fe(OH)3(ppd)	-2.5823
Albite low	0.0000 sat	Grossular	-2.7472
Pyrite	0.0000 sat		

(only minerals with log Q/K > -3 listed)

Gases	fugacity	log fug.
Steam	0.03131	-1.504
CO2(g)	2.008e-006	-5.697
H2(g)	1.028e-006	-5.988
CH4(g)	1.773e-007	-6.751
H2S(g)	4.771e-010	-9.321
S2(g)	4.978e-033	-32.303
O2(g)	7.463e-072	-71.127

		In fluid		Sorbed	
Original basis	total moles	moles	mg/kg	moles	mg/kg
Al+++	0.003000	1.730e-005	0.4668		
Ca++	0.001000	3.053e-005	1.224		
Cl-	2.821e-015	2.821e-015	9.999e-011		
Fe++	0.001000	6.504e-008	0.003632		
H+	-0.01663	-0.0005487	-0.5530		
H2O	55.52	55.51	9.999e+005		
HCO3-	0.001366	0.0003967	24.21		
K+	0.002000	8.020e-007	0.03136		
Mg++	0.003000	9.795e-008	0.002381		
Na+	0.001000	0.0008316	19.12		
O2(aq)	-0.003500	-9.055e-008	-0.002897		

SO4--	0.002000	1.301e-007	0.01249
SiO2(aq)	0.009000	0.0004505	27.07

Elemental composition		In fluid		Sorbed	
	total moles	moles	mg/kg	moles	mg/kg
Aluminum	0.003000	1.730e-005	0.4668		
Calcium	0.001000	3.053e-005	1.224		
Carbon	0.001366	0.0003967	4.765		
Chlorine	2.821e-015	2.821e-015	9.999e-011		
Hydrogen	111.0	111.0	1.119e+005		
Iron	0.001000	6.504e-008	0.003632		
Magnesium	0.003000	9.795e-008	0.002381		
Oxygen	55.54	55.51	8.881e+005		
Potassium	0.002000	8.020e-007	0.03136		
Silicon	0.009000	0.0004505	12.65		
Sodium	0.001000	0.0008316	19.12		
Sulfur	0.002000	1.301e-007	0.004170		

Appendix I : Equilibrium conditions in the revised reaction-path model : Test 15+laumontite

Step #	100	Xi =	1.0000
Temperature =	25.0 C	Pressure =	1.013 bars
pH =	9.772	log f02 =	-71.068
Eh =	-0.4001 volts	pe =	-6.7635
Ionic strength	=	0.002164	
Activity of water	=	1.000000	
Solvent mass	=	0.999920 kg	
Solution mass	=	1.000072 kg	
Solution density	=	1.013 g/cm3	
Chlorinity	=	0.000000 molal	
Dissolved solids	=	152 mg/kg sol'n	

Reactants	moles remaining	moles reacted	grams reacted	cm3 reacted
Albite	-2.406e-018	0.002000	0.5244	0.2005
Calcite	-2.406e-018	0.002000	0.2002	0.07387
Maximum Microcli	-2.406e-018	0.002000	0.5567	0.2175
Phlogopite	-2.406e-018	0.002000	0.8345	0.2993
Pyrite	-2.406e-018	0.002000	0.2399	0.04788

Minerals in system	moles	log moles	grams	volume (cm3)
Albite	0.0001718	-3.765	0.04504	0.01722
Calcite	0.001074	-2.969	0.1074	0.03965
Chalcedony	0.001474	-2.832	0.08856	0.03344
K-feldspar	0.001998	-2.699	0.5562	0.2176
Laumontite	0.0009109	-3.041	0.4285	0.1391
Phlogopite	0.002000	-2.699	0.8345	0.2993
Pyrite	0.002000	-2.699	0.2399	0.04788
(total)			2.300	0.8441

Aqueous species	molality	mg/kg sol'n	act. coef.	log act.
Na+	0.001821	41.85	0.9501	-2.7620
HCO3-	0.0009789	59.72	0.9504	-3.0313
CO3--	0.0003059	18.35	0.8155	-3.6030
SiO2(aq)	0.0001869	11.23	1.0006	-3.7281
H3SiO4-	0.0001809	17.21	0.9501	-3.7647
OH-	6.424e-005	1.092	0.9497	-4.2146
Ca++	1.145e-005	0.4589	0.8190	-5.0279
Al(OH)4-	8.113e-006	0.7707	0.9501	-5.1131
NaH3SiO4	4.194e-006	0.4952	1.0000	-5.3774
CaCO3	3.846e-006	0.3849	1.0000	-5.4150
NaHCO3	2.166e-006	0.1819	1.0000	-5.6644
K+	1.764e-006	0.06895	0.9494	-5.7761
NaCO3-	1.450e-006	0.1204	0.9501	-5.8608
CO2(aq)	3.651e-007	0.01607	1.0000	-6.4376
Mg++	1.791e-007	0.004353	0.8235	-6.8312
CaHCO3+	1.530e-007	0.01546	0.9509	-6.8372
H2SiO4--	9.962e-008	0.009373	0.8143	-7.0909
SO4--	8.586e-008	0.008247	0.8143	-7.1554
NaOH	6.623e-008	0.002649	1.0000	-7.1789
CaH2SiO4	5.461e-008	0.007326	1.0000	-7.2627
HS-	4.831e-008	0.001597	0.9497	-7.3384
CaH3SiO4+	3.172e-008	0.004288	0.9501	-7.5209
MgCO3	3.042e-008	0.002564	1.0000	-7.5169
Fe++	2.873e-008	0.001604	0.8190	-7.6284
FeCO3	2.811e-008	0.003256	1.0000	-7.5511
CaOH+	1.196e-008	0.0006829	0.9501	-7.9444
MgH2SiO4	1.018e-008	0.001205	1.0000	-7.9922

(only species > 1e-8 molal listed)

Mineral saturation states

	log Q/K		log Q/K
Daphnite-14A	10.1953s/sat	Phlogopite	0.0000 sat

Cronstedt-7A	7.7974s/sat	Calcite	0.0000 sat
Minnesotaite	6.9486s/sat	Aragonite	-0.1649
Daphnite-7A	6.8221s/sat	Antigorite	-0.2443
Nontronit-Ca	6.4788s/sat	Cristobalite	-0.2793
Nontronit-Na	6.3379s/sat	Kaolinite	-0.3426
Nontronit-Mg	6.1997s/sat	Mordenite-Na	-0.4189
Annite	6.0978s/sat	Analcime	-0.4546
Greenalite	5.7167s/sat	Hedenbergite	-0.4616
Nontronit-K	5.6732s/sat	Illite	-0.5517
Magnetite	5.4463s/sat	Beidellit-Ca	-0.6627
Hematite	3.7810s/sat	Siderite	-0.6661
Ripidolit-14A	3.3888s/sat	Gibbsite	-0.6889
Andradite	3.3315s/sat	Beidellit-Na	-0.8037
Saponite-Ca	2.4314s/sat	Clinoptil-Na	-0.8278
Saponite-Na	2.2903s/sat	Paragonite	-0.8350
Saponite-Mg	2.1522s/sat	Chrysotile	-0.8652
Talc	1.6646s/sat	Prehnite	-0.8857
Saponite-K	1.6256s/sat	Dolomite	-0.8980
Goethite	1.4122s/sat	Dolomite-ord	-0.8980
Chamosite-7A	1.2491s/sat	Fe(OH)2(ppd)	-0.9325
Phengite	1.1116s/sat	Beidellit-Mg	-0.9418
Tremolite	1.1032s/sat	Monohydrocalcite	-0.9939
Epidote	1.0614s/sat	Amrph^silica	-1.0145
Epidote-ord	1.0614s/sat	Lawsonite	-1.0907
Fayalite	1.0544s/sat	Diopside	-1.1959
Saponite-H	1.0070s/sat	Sanidine high	-1.1992
Smectite-high-Fe	0.9050s/sat	Albite high	-1.3187
Smectite-low-Fe-	0.8998s/sat	Pyrophyllite	-1.4295
Clinoptil-Ca	0.8984s/sat	Pyrrhotite	-1.4310
Ferrosilite	0.7716s/sat	Troilite	-1.4315
FeO(c)	0.5562s/sat	Beidellit-K	-1.4683
Quartz	0.2712s/sat	Diaspore	-1.4803
Clinoptil-K	0.1640s/sat	Clinochl-14A	-1.6405
Tridymite	0.1054s/sat	Jadeite	-1.8963
Heulandite	0.0827s/sat	Beidellit-H	-2.0975
Mordenite-K	0.0770s/sat	Wustite	-2.1540
Muscovite	0.0615s/sat	Boehmite	-2.3247
Ripidolit-7A	0.0156s/sat	Dolomite-dis	-2.4424
Maximum Microcli	0.0000 sat	Enstatite	-2.4836
Albite low	0.0000 sat	Sepiolite	-2.5192
Laumontite	0.0000 sat	Magnesite	-2.5268
Pyrite	0.0000 sat	Wollastonite	-2.8353
K-feldspar	0.0000 sat	CaSi2O5^2H2O	-2.9008
Albite	0.0000 sat	Fe(OH)3(ppd)	-2.9769
Chalcedony	0.0000 sat	Hercynite	-2.9792

(only minerals with log Q/K > -3 listed)

Gases	fugacity	log fug.
Steam	0.03131	-1.504
CO2(g)	1.035e-005	-4.985
H2(g)	9.605e-007	-6.018
CH4(g)	6.953e-007	-6.158
H2S(g)	7.387e-010	-9.132
S2(g)	1.368e-032	-31.864
O2(g)	8.555e-072	-71.068

		In fluid		Sorbed	
Original basis	total moles	moles	mg/kg	moles	mg/kg
Al+++	0.006000	8.113e-006	0.2189		
Ca++	0.002000	1.555e-005	0.6232		
Cl-	2.821e-015	2.821e-015	9.999e-011		
Fe++	0.002000	6.750e-008	0.003769		
H+	-0.03363	-0.0005931	-0.5977		
H2O	55.53	55.50	9.999e+005		
HCO3-	0.002366	0.001293	78.87		
K+	0.004000	1.764e-006	0.06895		
Mg++	0.006000	2.241e-007	0.005446		
Na+	0.002000	0.001828	42.03		
O2(aq)	-0.007000	-9.918e-008	-0.003173		
SO4--	0.004000	1.350e-007	0.01297		
SiO2(aq)	0.01800	0.0003722	22.36		

Elemental composition	total moles	In fluid moles	In fluid mg/kg	Sorbed moles	Sorbed mg/kg
Aluminum	0.006000	8.113e-006	0.2189		
Calcium	0.002000	1.555e-005	0.6232		
Carbon	0.002366	0.001293	15.53		
Chlorine	2.821e-015	2.821e-015	9.999e-011		
Hydrogen	111.0	111.0	1.119e+005		
Iron	0.002000	6.750e-008	0.003769		
Magnesium	0.006000	2.241e-007	0.005446		
Oxygen	55.57	55.51	8.881e+005		
Potassium	0.004000	1.764e-006	0.06895		
Silicon	0.01800	0.0003722	10.45		
Sodium	0.002000	0.001828	42.03		
Sulfur	0.004000	1.350e-007	0.004328		